Alma Mater Studiorum - Università di Bologna

DOTTORATO DI RICERCA IN

PSYCHOLOGY

Ciclo 35

Settore Concorsuale: 11/E1 - PSICOLOGIA GENERALE, PSICOBIOLOGIA E PSICOMETRIA

Settore Scientifico Disciplinare: M-PSI/02 - PSICOBIOLOGIA E PSICOLOGIA FISIOLOGICA

OSCILLATORY MECHANISMS OF CONSCIOUS PERCEPTION AND ATTENTION

Presentata da: Jelena Trajkovic

Coordinatore Dottorato

Elisabetta Crocetti

Supervisore

Vincenzo Romei

Co-supervisore

Giuseppe Di Pellegrino

Esame finale anno 2023

ABSTRACT

Although the prominent role of neural oscillations in perception and cognition has been continuously investigated, some critical questions remain unanswered. My PhD thesis was aimed at addressing some of them.

First, can we dissociate oscillatory underpinnings of perceptual accuracy and subjective awareness? Current work would strongly suggest that this dissociation can be drawn. While the fluctuations in alpha-amplitude decide perceptual bias and metacognitive abilities, the speed of alpha activity (i.e., alpha-frequency) dictates sensory sampling, shaping perceptual accuracy.

Second, how are these oscillatory mechanisms integrated during attention? The obtained results indicate that a top-down visuospatial mechanism modulates neural assemblies in visual areas via oscillatory re-alignment and coherence in the alpha/beta range within the fronto-parietal brain network. These perceptual predictions are reflected in the retinotopically distributed posterior alpha-amplitude, while perceptual accuracy is explained by the higher alpha-frequency at the to-be-attended location. Finally, sensory input, elaborated via fast gamma oscillations, is linked to specific phases of this slower activity via oscillatory nesting, enabling integration of the feedback-modulated oscillatory activity with sensory information.

Third, how can we relate this oscillatory activity to other neural markers of behaviour (i.e., event-related potentials)? The obtained results favour the oscillatory model of ERP genesis, where alpha-frequency shapes the latency of early evoked-potentials, namely P1, with both neural indices being related to perceptual accuracy. On the other hand, alpha-amplitude dictates the amplitude of later P3 evoked-response, whereas both indices shape subjective awareness.

Crucially, by combining different methodological approaches, including neurostimulation (TMS) and neuroimaging (EEG), current work identified these oscillatory-behavior links as causal and not just as co-occurring events. Current work aimed at ameliorating the use of the TMS-EEG approach by explaining inter-individual differences in the stimulation outcomes, which could be proven crucial in the way we design entrainment experiments and interpret the results in both research and clinical settings.

SUMMARY

GENERAL INTRODUCTION

The study of oscillations is one of the most general and multidisciplinary concepts that span mathematics, physics, biology, and computer science. In fact, a repeating pattern of structure in time or space is the most defining characteristic of an oscillator, which governs both the living and non-living universe. Nature itself is oscillatory: as the Earth spins, the sun rises and sets and the days turn into nights. Likewise, ocean tides rise and fall, and the four seasons switch. Therefore, without this periodicity, there is no time that shapes what we define as past, present, and future, and without the periodicity of individual lives, there's no continuity of life on Earth (Buzsáki, 2006).

On the individual level, respiration is also oscillatory, as we resupply our body with oxygen every few seconds, as well as our heart rate or even hormonal states. Crucially, our brain also generates oscillations with the same governing principles as other physical systems. Brain oscillations can compute temporal information over a large variety of time scales, and this computation is the basis of both action and cognition. Therefore, there is currently a wide consensus that neural oscillations are a building block of our mental and motor abilities and are much more than mere background noise, as initially considered. However, cognitive electrophysiology is still far from defining their meaning and role in behavior and cognition. Currently, there is no agreement about some crucial questions: which oscillations, where precisely in the brain, via what mechanism, and to what extent are the cognition, perception, and action defined by these dynamic brain phenomena (Cohen, 2015)?

A large part of the research, and an even bigger part of the debates, has revolved around defining the role of alpha oscillations: the most dominating oscillatory activity pronounced in the posterior cortex, oscillating at a frequency of 7 to 13 cycles per second. These oscillations have been repeatedly associated with visual perception. In fact, although

we experience the external world as continuous and smooth, it has been suggested that the brain processes the world in brief flashes that roughly correspond to the alpha frequency (VanRullen, 2016). However, what we do not know is how they influence perception, with different studies pointing to the relevant role of various parameters of the alpha activity or even other frequency bands, like faster gamma activity. Second, what part of perceptual experience are they influencing, perceptual acuity per se or our subjective perceptual experience? Third, to what extent are they causally shaping our perception, and to what extent do they merely represent an epiphenomenon? Crucially, and most relevant to translational application in a clinical population, how (and to what extent) can we alter the alpha activity to enhance perceptual accuracy?

Attention is also rhythmic, with continuous fluctuations between periods of enhanced and reduced attentional states. Again, it has been noted that alpha oscillations are increased right after the attentional lapse and, importantly, right before the loss of attention happens, thus allowing the prediction of the attentional state. Older theories would suggest that, as increased alpha activity reflects a state of idling, it will increase when we disengage from the attentional task at hand. Modern theories, however, refuted this hypothesis, as there seems to be an increased alpha not only when we are more relaxed but also when we are intentionally ignoring something. These results would suggest alpha to be a mechanism that allows us to actively inhibit irrelevant information, thus shifting all our capacities toward the relevant stimuli. If this were true, how can we reconcile the role of alpha activity in higher-order attention focusing and sensory processing? At first glance, these processes seem almost orthogonal, as the first involves the acuity with which we process sensory input, and the second one is how well we can actively inhibit (unnecessary) sensory information. Are there multiple alpha-mechanisms involved in higher-order cognition and lower-level perception? If so, how do they work in concert to maximize the

efficiency of our conscious experience? Again, can we causally dissociate these distinct roles of alpha activity?

Novel theoretical frameworks, translational computational approaches, and methodological advances are aiding us in proposing more accurate models of oscillatory mechanisms of visual perception and attention, with an ultimate overarching aim of building novel tools to enhance these abilities in clinical populations in need.

NEURAL OSCILLATIONS

What is an oscillation?

An oscillation can be defined as “a rhythmic fluctuation between states of the system” (Cohen, 2015). In the case of neural oscillations, the system is the brain, which in turn is built from diverse subsystems, like visual, auditory, somatosensory, memory systems, etc. The term “state” describes a particular configuration of a system in a given moment, whereas “fluctuations” are the changes in these states over time. In the brain, neurons can fluctuate between the excitatory and inhibitory states. Finally, for a fluctuation to be considered oscillatory in nature, the time that passes between the repeating pattern of these states needs to be constant or, in other words, rhythmic in nature.

Three features can fully describe every oscillation (Figure 1): frequency, amplitude, and phase. Frequency represents the speed of fluctuations, often measured as the number of cycles per second defined as Hertz (Hz). Most neural oscillations involved in perception, cognition, and action range in time scales of milliseconds, from slower oscillatory activity with one cycle per second to fast oscillation going at hundreds of cycles per second. Amplitude refers to the magnitude of change of the oscillation and often is thought to represent the level of activity of the system (i.e., the level of synchronized activity of the adjacent neurons). Phase refers to the momentary state of an oscillator that fluctuates within a cycle, from trough to peaks. These three features are not constant over time but can change in response to a change in the external or internal environment, allowing the system to be flexible. At the same time, if the oscillations become too flexible, they seize to be reliable. In fact, our brain can foretell and prepare for the future via various rhythms it perpetually generates. Thus, neural oscillations balance the optimal ratio between flexibility and rigidity to allow adaptation but also prediction.

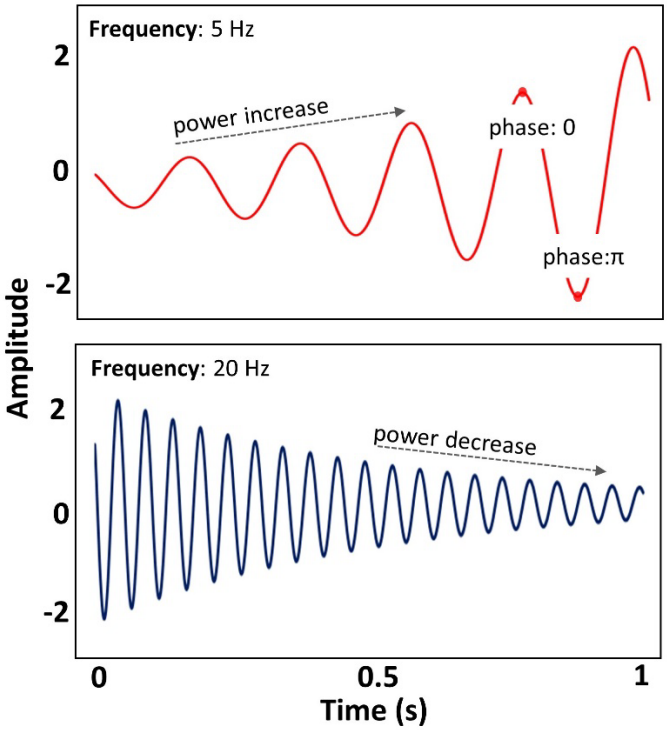

Figure 1. **Two sine-waves illustrating three oscillatory features**

Lastly, different oscillations occur simultaneously in a complex system such as a brain, thus allowing for parallel information transmitting and processing. Likewise, some neural populations are tuned to the specific frequency, thus getting activated only by information of a certain frequency, possibly coordinating a pattern of network activity around the preferred frequency.

How do we measure brain oscillations?

Information exchange between the neurons is happening via electrochemical signals. These neurons can be roughly grouped into excitatory and inhibitory. On the one hand, excitatory neurons activate the neurons to which they are connected, which leads to the triggering of hundreds or thousands Na+ (sodium) channels, depolarizing events that lead to a higher probability of producing action potentials (AP). At the same time, inhibitory neurons de-activate the neurons to which they are connected, leading to hyperpolarizing effects of the action potential of GABAergic synapses, making post-

synaptic neurons less likely to produce APs. These excitatory and inhibitory neurons are highly intertwined and co-dependent. As such, the firing of the excitatory neurons will add up and lead to higher excitation levels. However, as they are also connected to inhibitory neurons, the inhibition will also increase to the point that it will overcome excitation. Thanks to the decrease in excitation and inhibitory neurons inhibiting themselves, inhibition will again decrease, followed by an increase in excitation. This repeating cycle leads to extracellularly recorded fluctuations in the dendritic action potential. As these fluctuations cannot be attributed to a single neuron but rather to the synchronous population of hundreds or even thousands of neurons transmitting electrochemical signals simultaneously, the final outcome has been termed Local Field Potential (LFP) (Postle, 2020). Indeed, this electrical field produced by a large population of neurons working in concert is large enough to be recorded even by electrodes placed further away, even if those electrodes are placed outside the brain (Figure 2). Thanks to this principle, via Electroencephalography (EEG), it is possible to measure electrical brain activity non-invasively by placing the electrodes on the scalp instead inserting them intracranially. Even though LFP recorded by the scalp electrode is an outcome of thousand added up individual events, EEG data has revealed that the large-scale electrical brain activity is indeed predominantly oscillatory, taking the form of a wave-like structure.

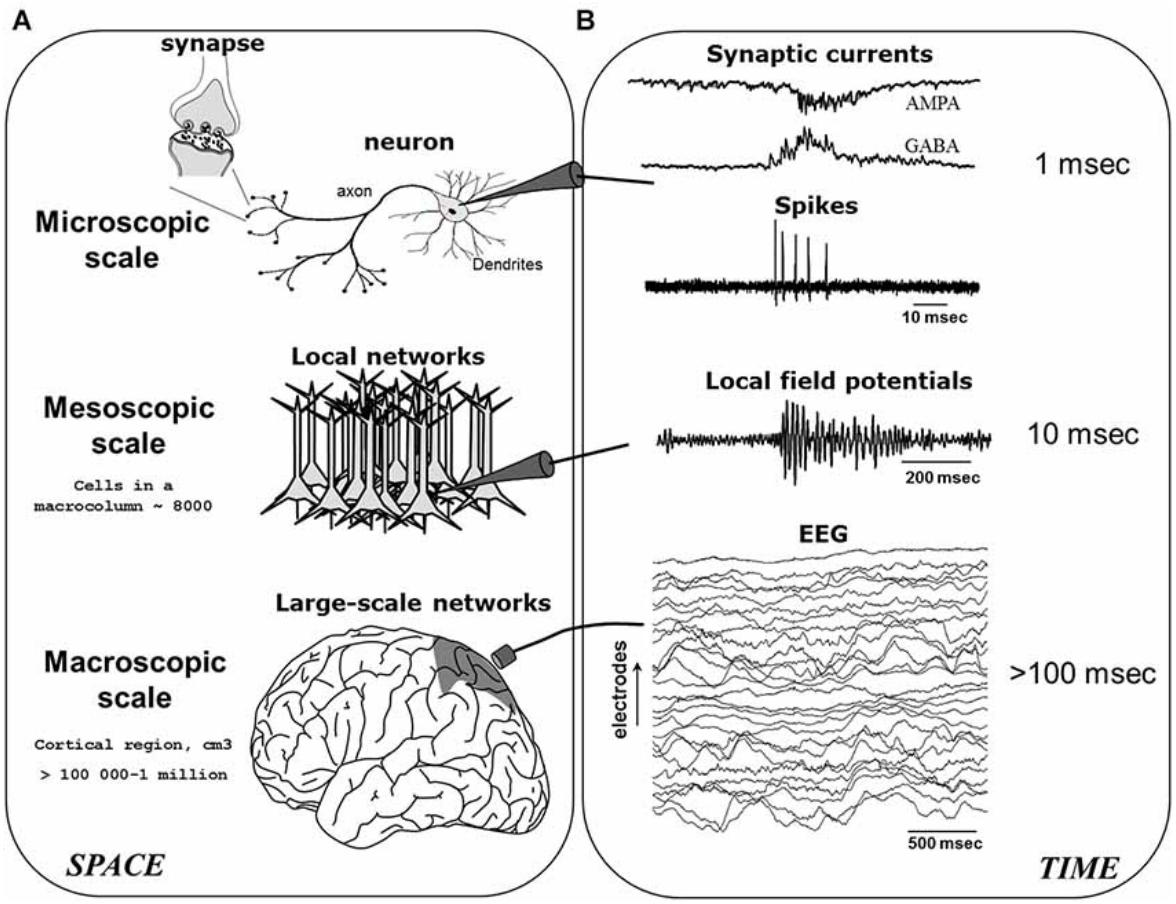

Figure 2. **The generation of electroencephalogram (EEG) neural oscillations.**
EEG signals are generated by the integration of neural activity at multiple spatial (A) and temporal (B) scales.
From *Le Van Quyen, 2011*

However, this interplay between the excitatory and inhibitory neurons is not the only mechanism responsible for generating oscillatory activity. For instance, it has been found that networks of only inhibitory interneurons can provide a means for coherent brain oscillations. Likewise, other mechanisms include synaptic filtering, delayed negative feedback, and electrical coupling, and neural oscillations become evident also in small slices of brain tissue in a petri dish or a simplified computer model of neurons and neural networks. In sum, oscillatory activity seems to arise effortlessly across the wide spectrum of neural architectures (Wang, 2010; Buzsáki et al., 2012).

As already stressed, different oscillatory features tend to change over time, depending on the numbers and types of neurons involved in their creation, the level of

available neurotransmitters, and the sensory (or other) external input. Although there is a broad agreement about the basic mechanism of oscillation genesis (as described above), all the factors that would account for their modulations are still not entirely known. Crucially, the precise functional meaning of these modulations is often still obscure, which will be discussed in detail in the next chapter.

Are neural oscillations functionally significant?

Following their discovery and initial enthusiasm in basic and clinical research, there was a quick loss of interest in probing the functional significance of brain oscillations. It was quickly noted that they tend to fade away when participants open their eyes, revealing low amplitude, desynchronized patterns. This inverse association between cognitive engagement and oscillations strength was further confirmed in anesthesia and epilepsy patients, conditions related to loss of consciousness: at this point, oscillations were considered markers of the 'idling' or even anomalous brain functioning (Senior et al., 2006).

Various methodological and technological developments led to a resurrected interest in the functional significance of brain oscillations in the last few decades. For instance, the emergence of biophysical studies made it possible to observe neural oscillations and create them (Destexhe & Sejnowski, 2003; Hasselmo et al., 2002; Whittington & Traub, 2003). They revealed that even single neurons could resonate and oscillate at multiple frequencies (Llinás, 1988; Traub et al., 2004), strongly suggesting that the precise timing of their activity could represent information processing (Buzsáki & Draguhn, 2004). Likewise, studies also showed that oscillatory patterns during sleep were related to the experiences during the past awake period, leading to the hypothesis that processes like perception, memory, and consciousness can emerge from oscillatory synchrony (Wilson & McNaughton, 1994). Given these findings, oscillations rightfully

regained their status as an important (and necessary) building block of behavior.

As briefly introduced in the previous chapter, neural oscillations occur over a large frequency span. However, they are not randomly distributed nor equally present across various frequencies but rather tend to occur in specific frequency ranges (bands). Specifically, we can distinguish several frequency bands commonly investigated in neuroscience: delta (peak frequency 2 Hz), theta (peak frequency 6 Hz), alpha (peak frequency 10 Hz), beta (peak frequency 30 Hz), and gamma (peak frequency 40 Hz) (Başar et al., 2001; Traub et al., 2004; Varela et al., 2001). Stunningly, these frequency bands seem largely preserved across different species albeit the enormous differences in brain size and development (Figure 3), suggesting that the speed of neural information processing has not substantially changed over thousands of years and across the animal kingdom. From the evolutional standpoint, their consistency loudly speaks in favor of their fundamental role in shaping cognition, perception, and action (Başar et al., 2001; Buzsáki, 2006; Cohen, 2015b).

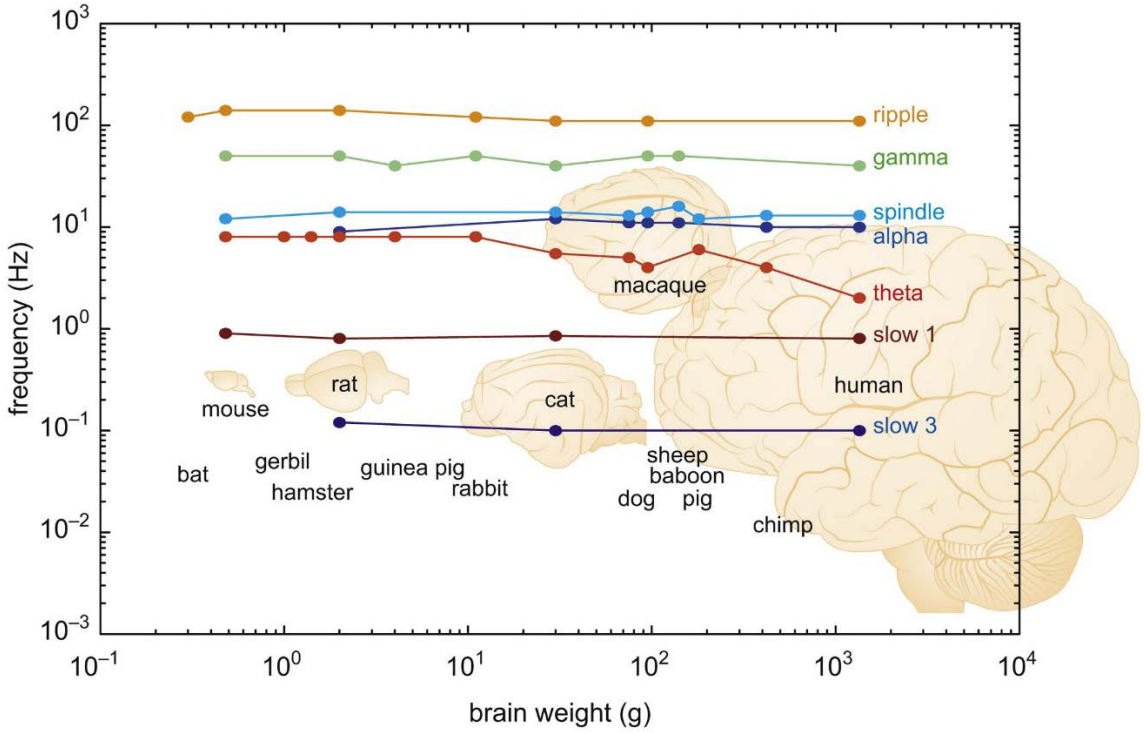

Figure 3. **Preservation of brain rhythms across species.**

Relationship between the brain weight of different mammals and frequency of different brain rhythms on a log-log scale. It can be noted that brain frequencies are invariable despite the changes in brain weight spanning over several orders of magnitude.

From *Buzsáki et al., 2013*.

One of the reasons for this consistency could be that the timing of the environment changes (in terms of physical forces) is stable over time and constant across animal species. Although often neglected, time is a variable that can be considered crucial for information processing and exchange (Cohen, 2011, 2014). Indeed, it has been noted that there is some information contained in the precise timing of the oscillatory activity, both within and across distinct neural regions, that cannot be simply attributed to an individual brain region, suggesting that information is coded via temporal oscillatory schema (Cohen, 2011). This temporal information processing is also energy-efficient, as it allows parallel and rapid information processing in multiple brain networks overlapping across space and time (Akam & Kullmann, 2010). Finally, a direct correspondence can be drawn between the speed of oscillatory activity and coinciding perceptual and cognitive processes. For instance, fast neural processes imply a fast cognitive process, resulting in a swift and

adaptive behavioral response. In sum, oscillations seem like a developed evolutionary tool for estimating time, whereas one of the crucial and most general functional roles of brain oscillations can be argued to be time reconstruction, as well as generating prediction and causality links (Buzsáki, 2006).

Although early research focused on identifying “unique pacemakers”, based on the assumption that distinct frequency bands can be mapped to specific brain areas and well-defined functions (Fernández et al., 1998), the real picture is far more complex, with various frequencies in distributed systems being implicated in the same function (Senior et al., 2006). Indeed, not only are distinct, frequency-specific neural assemblies linked to specific functions, but also long-range oscillatory networks can shape behavior (Buzsáki & Draguhn, 2004). For instance, neurons can aid input selection through their resonant oscillatory features and specific response to distinct input frequencies (Jacobs et al., 2007). These diverse frequency-tuning properties have been proven crucial in organizing network dynamics (Whittington & Traub, 2003). Similarly, oscillatory synchrony between distant neural assemblies can aid their transient intercoupling and subsequent information binding. In turn, this inter-areal facilitated communication can be used to dynamically configure functional oscillatory networks by their anticipatory predictive binding during specific tasks (Buzsáki & Draguhn, 2004; M. Cohen, 2011; Schnitzler & Gross, 2005).

Nonetheless, the general rule, based on timing and conduction constraints of the brain, would be that slower oscillatory activity (such as alpha and theta oscillations) would be able to travel further distances and thus enable long-range communication. On the other hand, faster frequencies are more constricted to local circuits (Moran & Hong, 2011; Schnitzler & Gross, 2005). This co-dependence of large-scale integration and frequency speed has been empirically confirmed in an experiment looking at oscillatory activity during processes involving neural assemblies of varying complexity. While visual

processing in the local network involved gamma activity, synchronization between nearby temporal and parietal assemblies was related to the beta activity. In contrast, long-range synchronization between frontal and parietal networks during a working memory task and mental imagery involved slower theta and alpha activity (von Stein & Sarnthein, 2000).

These findings respect the general functional definitions of the distinct frequency bands. Indeed, gamma oscillatory activity has often been linked to the early sensory response across different modalities but also to a process called binding, defined as the perceptual integration of parts into a gestalt (Rodriguez et al., 1999). However, gamma was also related to various cognitive and sensory processes but also emerged after a simple stimulation of isolated invertebrate ganglia, leading to the hypothesis of gamma activity as a universal code of communication of the Central Nervous System (CNS)(Başar et al., 2001).

As previously stated, beta activity also shows less spread activity with respect to both theta and alpha rhythm. While early research associated beta activity with motor functions and defined it as an index of activation of somatosensory areas (Engel & Fries, 2010), it soon became clear that beta activity has a more general role in the preservation of intended or predicted status quo, with a prominent role in cognitive flexibility and control.

Slower theta oscillations are linked to the hippocampal area, as it represents a dominant rhythm of the hippocampus across different species (Buzsáki, 2006). As such, it is often related to spatial exploration and memory processes. In humans, it has been linked to successful episodic memory retrieval (Nyhus & Curran, 2010; Staudigl et al., 2010), but also with working memory (WM) capacity (Wolinski et al., 2018).

These findings would suggest that low and high-frequency oscillations have some distinct roles in perception and cognition but, at the same time, that there is a significant overlap between them. One of the important oscillatory mechanisms orchestrating this

overlap is cross-frequency coupling, i.e., interactions between the oscillations of different frequencies (Canolty et al., 2006). For instance, in terms of slower or faster theta oscillations, individual theta frequency has been related to WM capacity, with slower theta activity being related to better memory performance. It has been suggested that the coupling between gamma and theta activity may mirror how many memory items can be stored at the same time (Nyhus & Curran, 2010). Thus, this slower theta activity can nest inside more gamma cycles, which would imply more individual memory items (theta-gamma phase coupling theory of WM capacity)(Wolinski et al., 2018).

Taken together, brain oscillations have now consolidated their role as a building block of perception, cognition, and action. Although there are various ways in which they are generated, and an even wider variety of brain oscillations, the key concept that binds them is the concept of time. The instantaneous firing of thousands of adjacent neurons is what generates them, exact frequency tuning and perfectly timed oscillatory synchrony is what enables input selection, and network communication and oscillations is the mechanism that makes possible processing of time and future prediction. Finally, oscillations are the mechanism that paces our perception and temporally and spatially guides our attention, as discussed in later chapters.

Alpha Oscillations

Alpha oscillations were the first oscillatory rhythm to be described; thus, their history closely parallels the history of electrophysiology itself. As with every great discovery, the story of alpha activity involves a series of coincided events and major plot twists. Its revelation can be traced back to a dream: a sister whose brother was a soldier dreamt that he got injured by falling off a horse, thus writing him a worried letter. Strangely, the soldier in question, called Hans Berger, now known as the father of electrophysiology, did indeed fall at roughly the same time when the letter was written.

These events strongly impacted Berger and incited his idea that there must be some communication between the brains via telepathy, devoting the rest of his life to investigating electrical brain activity. Years and numerous experiments later, he concluded that the most prominent electrical activity could be traced back to the posterior part of the brain in an eyes-closed condition (Figure 4), terming it the alpha rhythm (Buzsáki, 2006). Although he did not prove that telepathy via brain communication is possible, his work did create one of the most effective research and clinical tool for investigating quickly changing electrical brain activity, with the alpha activity in the spotlight of these investigations.

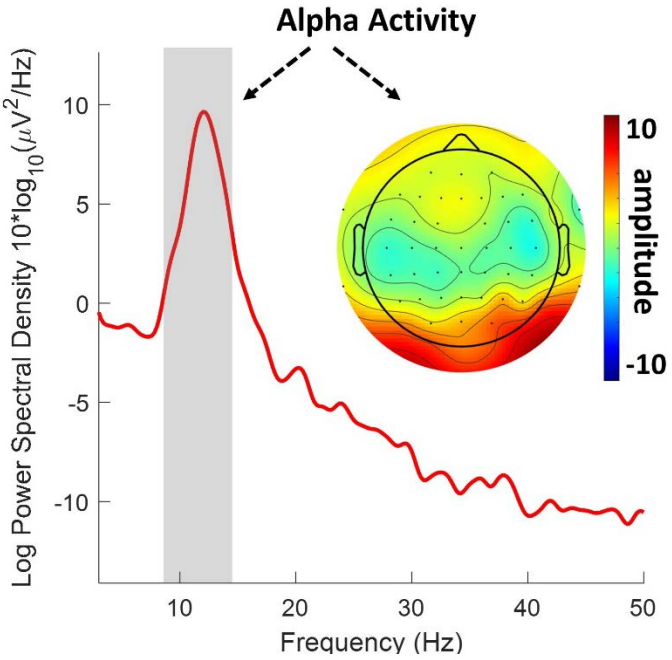

Figure 4. **Frequency characteristics of a single-subject resting-state recording.**

The most prominent feature is the alpha-band activity (highlighted in grey), which is most visible in the posterior cortex, as visible from the topography on the right.

The early enthusiasm for investigating the functional significance of alpha rhythms was short-lasting due to the inability to interfere with the underlying brain mechanisms, thus reducing the utility of alpha activity as a neuroscience tool. Decades later, a special

issue of the International Journal of Psychophysiology announced the “renaissance of alphas,” concluding that “alphas” represent a “universal code and universal operator with major physiological meaning,” intentionally using the plural to highlight the existence of multiple phenomena within the alpha frequency. These claims were backed up by numerous empirical evidence. First, a set of conducted experiments confirmed the functional significance of the spontaneous alpha activity, with pre-stimulus alpha patterns successfully predicting cognitive performance. Second, the authors demonstrated that alpha could not be defined as a pure noise but rather a “signal with quasi=deterministic properties” via chaos theory analysis (Başar et al., 1997). Crucially, neural origins of alpha were demonstrated via cellular recording, with reported action potentials in the alpha range in thalamic neurons, leading to the conclusion that alpha oscillations are related to thalamic pacemakers driving thalamocortical networks (Llinás, 1988; Steriade et al., 1990). This research presented a stepping stone towards a new era in research of the functional meaning of alpha oscillations, linking alpha activity to various cognitive and sensory processes.

For instance, Klimesch established a prominent role of alpha activity in memory. Specifically, between-subject individual differences in alpha speed (frequency) could distinguish between good and bad memory performers, with faster alpha related to better memory. Likewise, different stages of the memory process seem related to different parameters of alpha activity: lower-alpha frequency (8-10 Hz) varied with attentional load, while higher alpha frequency (11-12 Hz) was associated with semantic memory and stimulus characteristics (Klimesch, 1997).

Additionally, alpha-band activity was also related to visuo-verbal information processing, with event-related desynchronization (ERD) in the alpha range (i.e., decrease in alpha power) related to the semantic or numerical task (Pfurtscheller & Klimesch, 1992).

Moreover, alpha ERD was also noticed to systematically vary with attentional load, with a pattern of ERD being more accentuated in the situation of higher attentional demand (Dujardin et al., 1993).

On the other hand, event-related synchronization was related to the state of deactivated cortical areas and localized "cortical idling," defined as a state of the system disengaged from the information processing. In fact, during the visual task where a motor response is not needed, a higher alpha ERS in somatosensory areas was noted. Converging evidence was obtained from motor experiments involving lower (but not upper) extremities, where a selective alpha ERS over the hand area was noted (Pfurtscheller et al., 1996). Finally, alpha ERS was often related to disengagement from an external input while focusing on internal processes. For instance, mental arithmetic operations were related to higher alpha amplitude in parieto-occipital areas (Palva et al., 2005), and similar patterns were also revealed during internal counting, where higher alpha amplitude was noticed during breath-counting, with respect to mind wandering condition (Braboszcz & Delorme, 2011). However, as it would be argued later on, the definition of alpha as a "cortical idling" mechanism could be misleading. Instead "active inhibition" mechanism would be more appropriate, as the alpha mechanism not only enables a passive disengagement but rather active suppression or irrelevant input (Klimesch et al., 2007; Toscani et al., 2010).

This is only a sample of thousands of studies dedicated to affirming the functional role of alpha activity: the even bigger chank of them, described in later chapters, has been devoted to visual perception and attention. Does this mean that our quest for the functional meaning of alpha has come to an end? The answer would be no. Current studies only confirm that a) alpha is not related to one specific function but has a broader role in information processing and cognition, and b) there are several parameters of alpha activity with possibly distinctive roles in perception and cognition. In other words, these studies are

giving us pieces of the puzzle that are still not bound together into a coherent and meaningful image.

VISUAL PERCEPTION

The Visual Pathway

The moment that light meets the retina, an internal surface of the eyes, the process of sight begins. As in the camera, the image on the retina is reversed: objects bellow the centre project to the upper part and vice versa, while objects in the right hemifield fall on the left side of the retina of both eyes (i.e., nasal retina of the right eye and the temporal retina of the left eye). Subsequently, photoreceptors inside the retina would convert input light into neural signals. The first stage of neural computation already takes place at this point. Specifically, bipolar cells will detect light/dark areas on contrasting backgrounds, and retinal ganglion cells, involved in higher-level processing, would respond to differences in light across the receptive fields. The outcome of this processing would be passed on to the brain via optic nerves, which cross at the optic chiasm. From there, the axons of ganglion cells in the nasal retina cross (while those from the temporal retina do not). Hence, objects in the right hemifield are conveyed through the left optic tract and vice versa. From this point, there are various pathways leading to the brain, whereas the most dominant one travels via a processing station termed the lateral geniculate nucleus (LGN), located in the thalamus. When the axons in the optic tract reach the LGN, they terminate in an orderly map of the contralateral hemifield. In other words, objects in the right hemifield fall on the left side of the retina of both eyes and project to the left LGN. In other words, both right and left LGN contain information from both eyes but from one visual field. This information is then segregated in six distinct neuronal layers (three per eye): the upper four layers have smaller cell bodies called parvocellular, which respond to details and colour information. On the other hand, the remaining two layers contain larger cell bodies, termed magnocellular, that would respond to a larger part of the visual filed and movement. Finally, a serious of radiating nerve fibers transmit the information to the primary visual

cortex (V1) in the posterior occipital cortex, with preserved topographical order (Figure 5). Finally, the perception of sight derives from the processing of the V1 and nearby areas (Aine et al., 1996; Zeki, 1993).

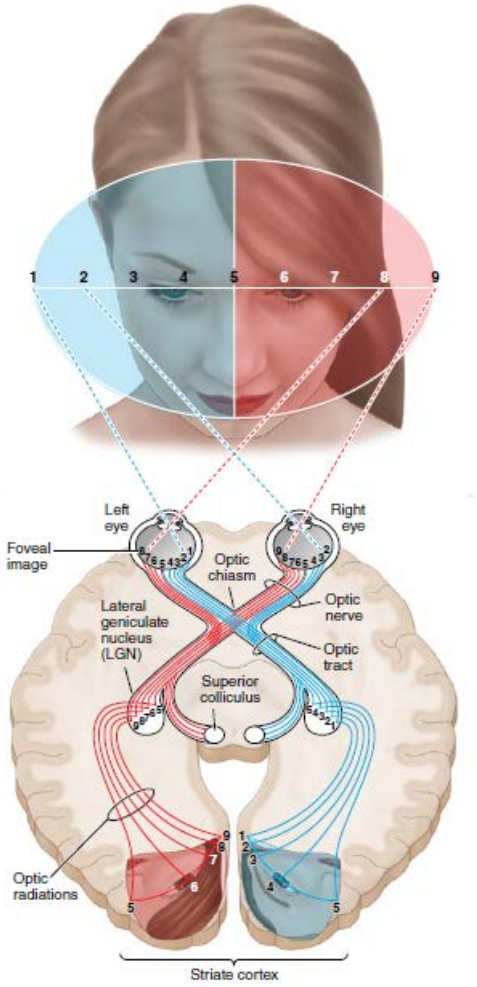

Figure 5. **Visual Pathways**.
Connections from the retina to the primary visual cortex: The Geniculostriate Pathway.
From *Postle, 2015.*

Functional Organization of the Visual System

The visual cortex is a relay station where objects are thoroughly evaluated both within and outside of their visual context. There are cells that react to the edges, curves, and corners of objects for the examination of shape. There are cells that react to both the direction of movement and the direction of movement in reference to the background for the interpretation of movement. There are cells that react to an object's wavelengths in

proportion to wavelengths coming from items nearby and to an average of the wavelengths from objects in other areas of the field of view for the study of colour. Thus, to a certain extent, all these features of the same object are analysed by separate group of cells. Because of this, layer IV of the V1, which is the input layer from the LGN, is one of the most complex structures, divided in different sublayers with distinct connections. For instance, movement information from magnocellular layers of LGN is transmitted to layer IVC_{α}, and then to IVB, which in turn projects to secondary visual cortex (V2 and V5). On the other hand, cells from the parvo- layers of the LGN would project colour information onto layers IVC_{β} and IVA, and then to other layers of the V1 (Daw, 2014).

Although the neurons in V1 are highly specialized for detecting specific features, the occipital areas outside V1 (extrastriate cortex) have receptive fields that are increasingly broader and less spatially organized. A variety of areas in extrastriate cortex are dedicated to processing particular visual characteristics, such as movement (area V5) and colour (area V4). In this case, it seems that the brain developed a “divide and conquer” strategy during orthogenesis. Specifically, this functional division across different areas would ensure that a possible brain lesion would affect only one visual aspect while preserving others (Ward, 2015).

From previously said, it becomes clear that distinct characteristics of the visual stimulus are parallelly process within the visual system. For instance, signals for objects lighter vs. darker than the background would be kept separate throughout various levels of processing (bipolar and ganglion cells, LGN and V1), before being combined for orientation and movement analysis, independently of contrast. Additionally, signals for colour vs. movement remain separate also for V2 and V4/V5 areas. Very likely, parallel processing is also present at higher-cortical levels of analysis (Daw, 2014). The question that, however, emerges is what occurs to these signals as they travel along these parallel

pathways and undergo processing? The answer to this question was brought by the pioneering work of Hubel and Wiesel, crowned by the Nobel Prize in Medicine. Their method of choice was exploring single-neuron response in the visual cortex of cats and monkeys. Thanks to an oriented crevice in the projector slide, they discovered individual neurons that selectively responded to this specific orientation. Subsequently, via systematic manipulations, they discovered distinct neurons in V1 that would respond to different orientations, named simple cells. Their responses were based on the combination of input from LGN independently of stimulus location, thus integrating external input from both eyes (Hubel & Wiesel, 1962). They continue to speculate that responses from simple cells would be combined into complex cells with larger receptive fields, thus requiring stimulation across their entire length. Finally, outside V1 they discovered the existence of orientation-specific hypercomplex cells, that would combine input from different complex cells, and thus be able to construct more complex visual information (Hubel & Wiesel, 1965; Zeki, 1993).

In sum, their research suggests a hierarchical organization within the visual system, where more complex visual characteristics are created by more simple ones (bottom-up processing). However, the opposite is also possible, where more complex representation would shape the response of simple cells. For instance, in the Kanizsa figure, illusory white edges would activate neurons in V2, which would propagate in a feedback manner toward V1 (Kogo & Wagemans, 2013).

Hierarchical organization including bi-directional information streams is also present for several visual pathways leading from extrastriate cortex to non-visual cortical areas: Ventral stream would carry the visual information towards temporal cortices, involved in object recognition, semantics and memory. On the other hand, dorsal stream connects visual areas with parietal regions, thus involved in spatial attention, and visually

guided action (Ward, 2015).

Visual Perception and Brain Oscillations

What we believe we see depends on when we see it: more specifically, it depends on the oscillatory state of the visual cortex at that exact moment. One of the earliest experimental demonstrations of this claim comes from a simple experiment that involved two LED flashes that participants had to define as (a)synchronous. With the aid of EEG, the key manipulation was that these flashes were presented at the peak or trough of the alpha oscillations in the visual cortex. The results showed that participants more often would (correctly) report the flashes as sequential when they were presented during the alpha peak (Figure 6): thus, perception depended on the internal state of the brain, and on the specific alpha phase (Valera et al., 1981). The mechanism would be the following: brief LED flash appears, and its light would activate the receptors in retina, which in turn, via LGN, would activate visual cortex. If this information arrives in visual cortex when the ongoing alpha activity is in a phase of higher excitability, the neurons would be more prone to respond to the arriving information (Cohen, 2015).

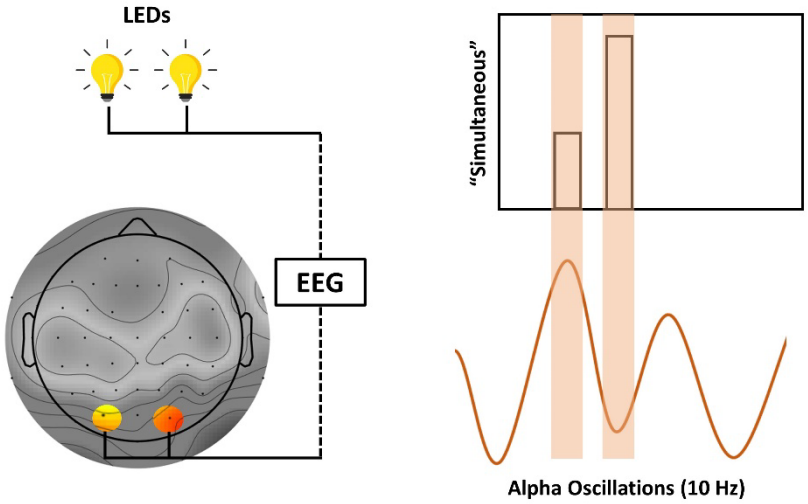

Figure 6. **Graphical presentation of the task and results from Valera et al, 1981.**
In this classical experiment, LED lights were triggered by a specific phase of alpha activity (peak vs trough).Although the timing between the flashes was always constant, participants more often correctly reported the flashes as sequential (vs simultaneous) if they were presented during the alpha peak (vs trough).

Several more recent studies seemed to confirm these results, by investigating trial-based differences in perception in relation to alpha phase (Busch et al., 2009; Busch & VanRullen, 2010; Mathewson et al., 2009; Zazio et al., 2022). In one of these studies, a near-threshold visual stimuli were used, with the prediction that their correct perception would be enabled by the excitatory phase just preceding the stimulus onset. As expected, correct perception depended on the oscillatory phase in the lower alpha and theta band, and these differences could account for the major part of the detection variability (Busch et al., 2009).

Taken together, these results would suggest that, despite our subjective experience of smooth perception, the brain seems to process the perceptual input in brief flashes (cycles), with the phase of ongoing oscillations representing an indicator of an ongoing perceptual cycle (Busch et al., 2009; Busch & VanRullen, 2010). However, this finding is far from robust, with the available evidence pointing to contrasting results, with various empirical and theoretical inconsistencies (Keitel et al., 2022).

Moreover, phase is not the only candidate able to influence perception: as we

suggested previously, oscillations have other properties, such as instantaneous frequency or amplitude, that would also present a possible link to perception. For instance, in a study where peri-threshold stimuli were also used, detected stimuli were related to lower pre-stimulus alpha power, whereas the omitted stimuli were preceded by higher alpha amplitude. Here, alpha power variations were related to an over-all brain excitability level that would explain perceptual variability (Ergenoglu et al., 2004). Similar conclusions were drawn by a study using Transcranial Magnetic Stimulation (TMS) to stimulate the visual cortex and induce phosphenes (illusory visual precepts without the external input), thus allowing to estimate the excitability of the visual cortex at the precise time points. The results showed that the TMS stimulation would evoke phosphenes in case when alpha power in the visual cortex was low, and that identical TMS stimulation would fail to induce phosphenes when alpha power was high, offering direct evidence for the alpha-excitability hypothesis (Romei et al., 2008).

Taken together, here described findings on the role of pre-stimulus alpha power and phase lead to the development of various models sharing the core idea of pulsed-inhibition exerted by oscillatory brain activity in the alpha band (Jensen et al., 2014; Jensen & Mazaheri, 2010; Klimesch et al., 2007; Mathewson et al., 2009). However, it remains unclear whether alpha phase and power would be the same mechanism. Moreover, although these (and many other) studies speak loudly of a role of pre-stimulus alpha power/phase in perception, they do not account for an important possible confound. Specifically, they do not differentiate between perceptual sensitivity per se, and changes in criterion or perceptual awareness. In fact, changes in visual excitability marked by alpha fluctuations could mean that we are seeing better but also that we are prone to reporting seeing something even when the external input is not actually there. This crucial differentiation would be further elaborated in the next chapters.

One of the properties that makes oscillations functionally useful is their non-stationarity, that is, their ability to change according to external and internal demands as to enable the flexibility of the system. This goes not only for the oscillatory power but also its speed, that is, the exact frequency with which they oscillate. Indeed, one of the most robust findings is the frequency fluctuations in the alpha range, named Individual Alpha Frequency (IAF). Berger himself already noticed these shifts, both in terms of inter-individual variability (i.e., variations in cognitive and mental state) but also on the intra-individual level in terms of cognitive abilities.

These initial observations were repeatedly confirmed. For instance, it has been noticed that IAF changes over the life cycle in a similar manner as general cognition, with the fastest alpha during adolescence and a sharp decline in its speed after the third decade. Moreover, at an inter-individual level, faster alpha activity was related to better memory performance and processing abilities (Klimesch, 1999). On the other hand, changes in IAF were also noticed on a within-subject level, as moment-to-moment fluctuations representing the current state. These dynamic changes in IAF could represent an adaptive modulation of activation levels based on sensory input and context (Mierau et al., 2017). Therefore, it could be that each alpha cycle represents a temporal unit to integrate and separate perceptual events, with a tight relation between the IAF and the temporal window of integration. A correlation was indeed found between IAF and the temporal window od the double-flash illusion. In the same participants, the alpha oscillation was subsequently modulated via transcranial Altering Current Stimulation (tACS). If their IAF was slowed-down by 2 Hz, the temporal window of illusion (TWI) was enlarged, and conversely, if IAF was speeded-up by 2 Hz, the integration window shrank., suggesting IAF as a temporal unit of visual processing (Figure 7, Cecere et al., 2015).

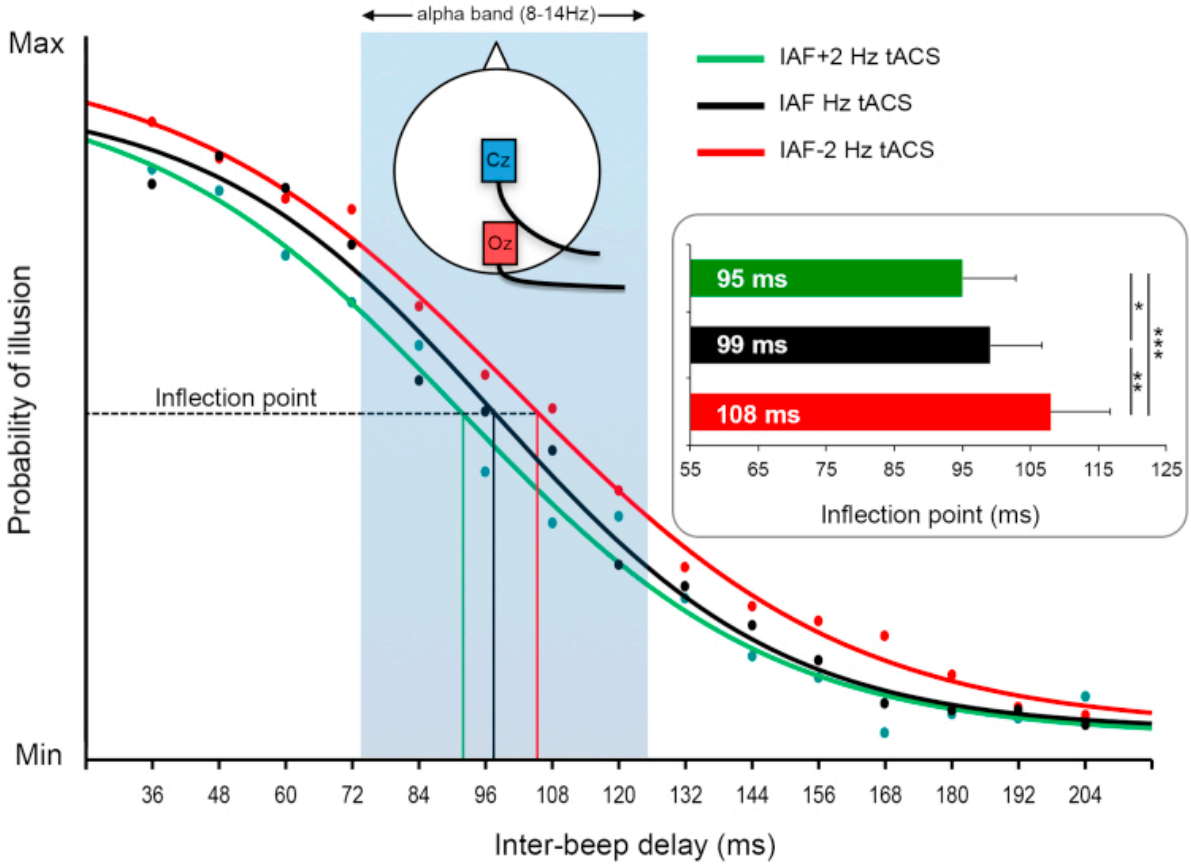

Figure 7. **tACS at different frequencies modulates the size of the temporal Window of Illusion** *(Cecere et al., 2015.).*

The sigmoid fit (with inflection points) of the perceived illusion across participants at different inter-beep delays in different tACS conditions: When IAF was speeded-up (in green), TWI shrank, while when IAF was slowed-down, TWI was enlarged (in red)

From *Cecere et al., 2015.*

These results were confirmed in a study where dynamic IAF changes were evidenced to follow task demands: if the task required temporal integration, IAF in the occipito-temporal cortex would decrease, and the exact opposite happened for the segregation task (Wutz et al., 2018). Apart from the demonstration of the importance of IAF in temporal sampling, this data also demonstrates a top-down mechanism by which the brain controls the temporal resolution of visual processing.

In sum, IAF would represent a useful temporal sampling strategy, thus adjusting the sampling rate as a function of external demands in order to increase performance and optimize representation of sensory information. Importantly, could it be that IAF can also influence spatial sampling abilities within a single temporal window? This question would

be empirically addressed across different studies of the current work.

ATTENTION

Attention: Definition and Pathways

The brain cannot process all of the information it receives: it wouldn't be practical for it to do so, either. Attention represents the mechanism that enables the brain to carefully select information for further processing and discard other unnecessary input. Differently from perception, which is focused on making sense of the external input, attention lies at the crossroad between the external information and internal states, such as expectations or goals. Depending on a specific context, attention can be more influenced by the external environment in a bottom-up manner or more driven by our goals (top-down attention). For instance, one of the most robust findings is that participants are quicker and more accurate in responding to a target when it was quickly preceded by a flash in the same spatial position (bottom-up or exogenous orienting). On the other hand, attention can also be manipulated via task demands, where the participant would be more accurate in detecting all letters if instructed to attend to the whole word, in comparison with a condition where they attend to only a single letter. Most of the time, both forces are at work, and attention can be considered as a cascade of bottom-up and top-down influences which drive the selection (Ward, 2015).

How does this attention spotlight happen? As briefly mentioned in the previous chapter, visual information follows different pathways, one of which is termed the dorsal route, which transmits the information from extrastriate cortices towards parietal lobes and is concerned with locating objects in space and visually-guided action.

The role of the parietal cortex in attention has been affirmed by single-cell studies in monkeys, where a region in the posterior parietal lobe (LIP: Lateral Intraparietal Sulcus) was found to respond to external input but also to elicit saccade movements towards that input. Crucially, it would respond only to abrupt or task-relevant stimuli while ignoring

others, thus having characteristics of both exogenous and endogenous attention. Additionally, these neurons would not only respond to the current eye position but would also support covert orienting, aiding attentional planning in the absence of saccades (Bisley & Goldberg, 2003).

Similar areas were also identified in humans, where a presentation of an arrow, indicating where to orient attention, was followed by activation in the parietal cortex (area similar to LIP), but also frontal cortices (frontal eye filed: FEF). Crucially, these activations were invariant of task instruction to make a saccade, covertly move the attentional spotlight or point to that location, thus reflecting a general attention orienting (Corbetta & Shulman, 2002). Investigating the functional connectivity of this network in a cue-period of covert attention task revealed that the directionality of activation was top-down: from frontal to parietal regions and then to the visual cortex (Astafiev et al., 2003).

Unlike the primary visual cortex, the parietal lobes of both hemispheres represent the full visual field, though in a graded fashion by favoring the contralateral side. For instance, the right parietal role would be maximally responsive for the far-left side of the space, moderately responsive to the center, and minimally responsive for the right visual field: the exact opposite happens for the left parietal cortex. Consequently, a lesion of the parietal region should lead to a failure to attend to the stimuli in the opposite hemisphere (a condition termed hemispatial neglect). However, this phenomenon occurs almost exclusively for lesions of the right hemisphere, thus insinuating a hemispheric asymmetry in spatial attention with a dominant role of the right parietal cortex (Li & Malhotra, 2015).

Attention and Brain Oscillations

As per visual perception, attention is also a rhythmic process, with waxing and waning of attention over time. Although dependent on some internal states, these attentional fluctuations are inevitable when trying to maintain our focus for prolonged

periods of time. As sustained attention is critical in many important jobs (e.g., air traffic control, surgery, negotiation), understanding attention fluctuations and predicting attentional lapses has implications far beyond scientific curiosity.

Attentional fluctuations were also confirmed in the experimental setting. As expected, visual detection is improved for attended stimuli, evidenced by lower threshold values. Interestingly, these attentional benefits were periodic, with fluctuations that would follow the ongoing spontaneous alpha phase, implicating an oscillatory pattern of attentional facilitations (Busch & VanRullen, 2010). These attentional benefits and fluctuations are usually studied via simple but repetitive tasks in which attentional lapses would result in mistakes (Figure 8). The most common finding would be that in a second right before the mistake, there would be a sharp increase in the alpha power (Ergenoglu et al., 2004; Hanslmayr et al., 2007).

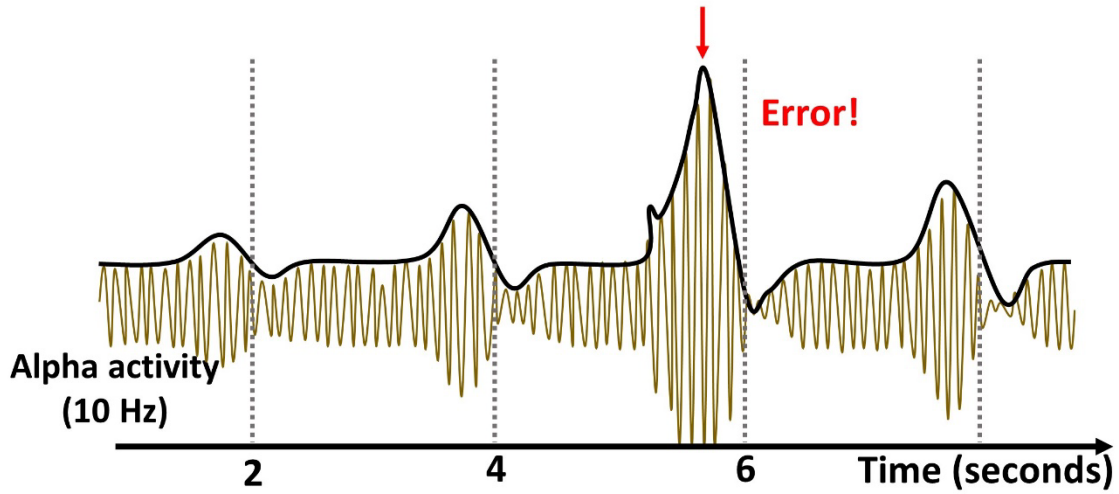

Figure 8. **Changes in alpha power can predict attentional lapses**.
Adapted from *Cohen, 2015.*

Taking into consideration the initial account of alpha amplitude as an oscillatory marker of an "idling" state, could it be that this increment in alpha activity can represent a simple cognitive disengagement? Several studies would strongly argue against this

account. For instance, in a study using audio-visual stimuli with a cue indicating the to-be-attended modality (auditory or visual features), alpha amplitude acted as a dynamic suppression mechanism. Specifically, there was higher posterior alpha amplitude in a preparatory period when auditory features had to be attended and a desynchronization of posterior alpha when the visual features were task-relevant (Foxe et al., 1998). In a similar study using cross-sensory cuing and multimodal attentional task, higher alpha amplitude in the visual cortex for auditory vs. visual features was confirmed, with topographic mapping linking these changes to the inferior parietal cortex, areas known to be implicated in attentional mechanisms (Fu et al., 2001). Therefore, rather than a marker of an idling state, the alpha activity would represent an attentional mechanism, with an increase of alpha activity anticipating irrelevant features and a decrease reflecting active task engagement.

Similar results were obtained using a unisensory approach, where a visual cue was used to mark the attended visual feature, color or motion. The results showed that the locus of alpha modulations was cue-dependent, with increased alpha amplitude near the dorsal visual stream when the color was attended and near the ventral visual stream when the cued feature was motion. As the motion processing is related to the dorsal stream and color to the ventral one, it can be inferred that an increase in alpha amplitude is suppressing the task-irrelevant feature. Taken together, these results confirm the role of alpha activity as a potential attentional suppression mechanism, independent of feature or sensory domain (Snyder & Foxe, 2010).

The role of alpha oscillations as an attentional mechanism was also confirmed in endogenous spatial cueing tasks, where an arrow cue would indicate a to-be-attended stimulus, while stimuli in other spatial locations should be ignored. An increment of parietal alpha power over the hemisphere ipsilateral to the cued location was noted, suggesting the involvement of cortical regions corresponding to the non-cued location,

indicating an active cortical inhibition (Worden et al., 2000). However, if the alpha activity indeed suppresses irrelevant information, alpha modulation should not be present in a task without distractors. This doesn't seem to be the case, with retinotopically organized alpha increases over areas processing unattended space even without distractors, suggesting that alpha activity would be a more general attentional mechanism inhibiting unattended space as to enhance performance (Rihs et al., 2007).

It is worth noting that several studies have also evidenced alpha suppression contralateral to the cued location during shifting of attention, with a diverse time pattern than previously described ipsilateral inhibition, possibly speaking of their differential deployment during anticipatory attention (Rihs et al., 2009). Moreover, apart from alpha suppression contralateral to the attended filed in the posterior cortex, a higher inter-areal phase connectivity between prefrontal regions and these posterior contralateral areas was also evidenced (Sauseng et al., 2005). These results support the hypothesis that alpha suppression signals the attentional shift towards the cued spatial location and that this shift is orchestrated by the prefrontal cortex in a top-down manner. Indeed, the mechanism that involves top-down control from higher-order attentional processes can modify the baseline excitability of the visual cortex. Specifically, visuo-spatial attention directed in the absence of the visual input can enhance the subsequent visual processing at the same spatial location (Figure 9), and these effects can be attributed to the above-mentioned process (Thut et al., 2006).

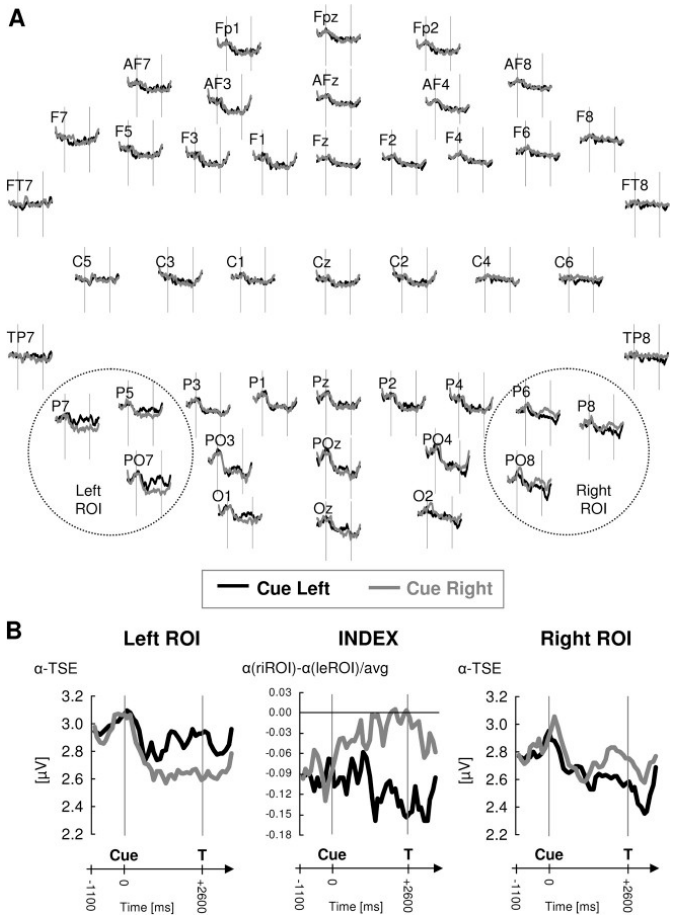

Figure 9 . **Visuospatial attention bias indexed by posterior alpha-amplitude** *(Thut et al., 2006)*

Sustained changes in alpha-amplitude are visible in the cue-target interval, which depended on the cued direction of attention and the side of the recording, with higher ipsilateral and lower alpha contralateral to the cued location. Note that the changes are mostly visible across posterior electrodes.

From *Thut et al., 2006.*

In sum, there seems to be a tight link between changes in the posterior alpha activity, visuospatial attention, and visual processing that is mediated by top-down control: a link that will be explored across different studies of my dissertation.

CONSCIOUSNESS

Perception, Attention, and Consciousness

In every-day life, the processes of perception, attention, and consciousness are constantly working in synchrony to enable a smooth, flowing, and continuous experience of our internal states and external environment. Although crucial for our adaptive functioning, their synergy makes it scientifically challenging to completely dissociate them and study them in isolation.

Curious neurological and neuropsychiatric conditions are what made their distinction visible in the first place. For instance, patients exhibiting blindsight would deny having seen a visual stimulus even though their behavior implies that the stimulus was, in fact, perceived. Specifically, these patients with lesions of the visual cortex would often perform visual detection and discrimination tasks with above-chance accuracy without consciously perceiving those stimuli, thus demonstrating that in some extreme cases, perception and consciousness are indeed dissociable (Weiskrantz, 1996). The exact opposite happens in the case of hallucinations, false memories, and confabulations following different neurological and psychiatric conditions, where there is a conscious experience without the actual environmental input. On the other hand, patients with neglect fail to attend to stimuli on the opposite side of the space (typically in the left hemifield after the right parietal lesion, Figure 10). Here, visual perception is preserved, while one part of the visual field tends to be ignored but processed on the unconscious level (Li & Malhotra, 2015). Even more convincing evidence comes from studies looking at brain activity in some patients in unresponsive states (coma). For instance, when asked to imagine playing tennis or imagine walking through a familiar location in fMRI scanner, activation of brain areas involved in movement and memory was noticed. An identical pattern was also observed in healthy participants, demonstrating that some completely non-

responsive patients are in fact, conscious (Owen et al., 2006).

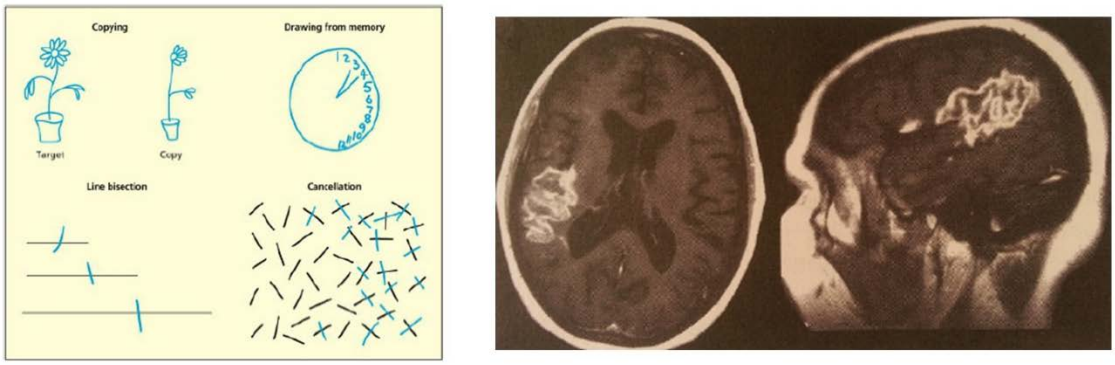

Figure 10. **Neglect: Task performance and brain lesions.**

Left: Typical task performance of neglect patients. It can be noted that, in all the tasks, patients fail to attend the left part of the object and/or visual field.

Right: MR scan of unilateral neglect patient. Bright regions correspond to the lesion, corresponding to the right inferior parietal lobe and superior temporal gyrus.

Adapted from *Postle, 2015.* and *Ward, 2015.*

The question that naturally emerges is which brain regions and circuits are most relevant in consciousness? There is still much debate about what consciousness is in neural terms, with even more disagreement about the brain regions and processes that would determine it.

What is clear, however, is that consciousness cannot be confined to a single brain region. Instead, various cells and pathways seem to be engaged, depending on the type of perception that is involved. For instance, in a recent fMRI study, researchers found out that, compared with healthy individuals, people in minimally conscious states and those under anesthesia have a less dynamic and less complex pattern of coordinating signaling (Demertzi et al., 2019). In other studies, comparing the stimuli that were perceived consciously and the ones that were not in healthy participants, two main activation pattern differences can be noted: higher brain activity in regions involved in perception when the stimuli were consciously processed, followed by a greater spread of this activity in the feedforward manner towards anterior cortex (Dehaene et al., 2006). This propagation towards frontal and parietal lobes gave rise to a theory that awareness of perception arises

from attentional mechanisms, where attentional selection would generate an all-or-nothing outcome (i.e., awareness vs. unawareness) from the continuous flow of information (Rees & Lavie, 2001). However, this theory is still a point of debate, with alternative standpoints claiming that a distinction should be made between the experience of perceiving and the reportability of that experience, where only the reportability would be related to attention. Instead, the experience of perception itself would arise from the interactions withing the perceptual network of the posterior cortex (Block, 2010).

In sum, although intriguing and much discussed and researched, some essential questions about consciousness remain unanswered. This can be attributed to the largely subjective nature of consciousness but also to the difficulties in conducting animal studies in this field. However, new technologies, experiments, and novel theories about what consciousness is and how it is created can push forward our understanding of this phenomenon.

Consciousness and Brain Oscillations

As mentioned in the previous paragraph, there is little doubt that perception, attention, and consciousness work in tight interaction in order to assure a reliable and correct perception with minimal effort. At the same time, previous paragraphs also depicted how both perception and attention are shaped by oscillatory activity. Given these premises, should it be assumed that also consciousness is shaped by oscillatory fluctuations? Moreover, did previously laid out experiments distinguish between perceptual accuracy/attentional selection (i.e., what we see) and perceptual awareness (i.e., what we think we see), and could they offer certainty that this unaccounted variable did not confound their behavioral correlates?

The answer to the first question would be yes. For instance, in a recent sleep study, researchers would wake participants up during the night, while recording EEG. What they

found was the difference in the oscillatory activity right before waking in participants who didn't experience anything and those that were dreaming. The results showed that the participants without conscious experience had a lot of low-frequency posterior activity before waking up, while people that were dreaming had more high-frequency activity, thus showing that the conscious experience can be related to a specific oscillatory pattern (Siclari et al., 2017).

The answer to the second question, for the vast majority of cited studies, would be no. Following the reasoning of the Signal Detection Theory (SDT), a finding that binds the levels of pre-stimulus alpha power and probability of stimulus detection could have diverse origins. For instance, the observed differences can be indeed related to actual changes in sensitivity levels, but the same difference could also derive from the confidence criterion, thus from the fact that subjects are simply more inclined to give a positive response, regardless of the actual perception. In other words, defining conscious awareness in terms of near-threshold stimuli detection is potentially problematic as it is a complex measure that incorporates both the actual perceptual abilities and subjective perceptual experience. In order to distinguish them, two separate measures need to be used, one to quantify perceptual sensitivity and the other to catch subjective awareness (criterion changes or confidence ratings). Recent studies looking at the alpha oscillatory activity and these parameters suggest that alpha amplitude is associated with subjective awareness rather than perceptual accuracy, as initially claimed. For instance, in one of the first studies looking at the role of alpha oscillation in between and within-participants changes in perceptual sensitivity and criterion, a more conservative attitude was associated with higher pre-stimulus alpha power, both within-participants and on single-trial level analysis. On the other hand, alpha power predicted perceptual sensitivity only on the between-subject level, interpreted as the multi-level influence of pre-stimulus alpha activity: participants with an

over-all higher desynchronization of alpha could, in general, demonstrate higher perceptual abilities, while fluctuation on a trial-level would indicate criterion changes (Limbach & Corballis, 2016). More recent research using confidence ratings prompt after stimulus detection was able to draw a clear dissociation between confidence evaluation and discrimination performance. Here, lower pre-stimulus alpha power explained more than 70 percent of confidence variability, with lower parieto-occipital alpha-power leading to higher response confidence. On the other hand, accuracy levels were not associated with pre-stimulus alpha-activity fluctuations (Samaha, Iemi, et al., 2017). Comparable results were also obtained with the perceptual awareness scale, with higher alpha activity leading to lower awareness while not influencing perceptual accuracy (Figure 11, Benwell et al., 2017). These (and other) recent studies would speak in favor of alpha-amplitude having a prominent role in subjective perceptual experience rather than perceptual acuity. Although important, these findings, however, do not clarify what are then the oscillatory correlates of perceptual sensitivity. Additionally, they do not explain if and how these alpha fluctuations involved in perceptual awareness are related to those that determine attentional selection and inhibition.

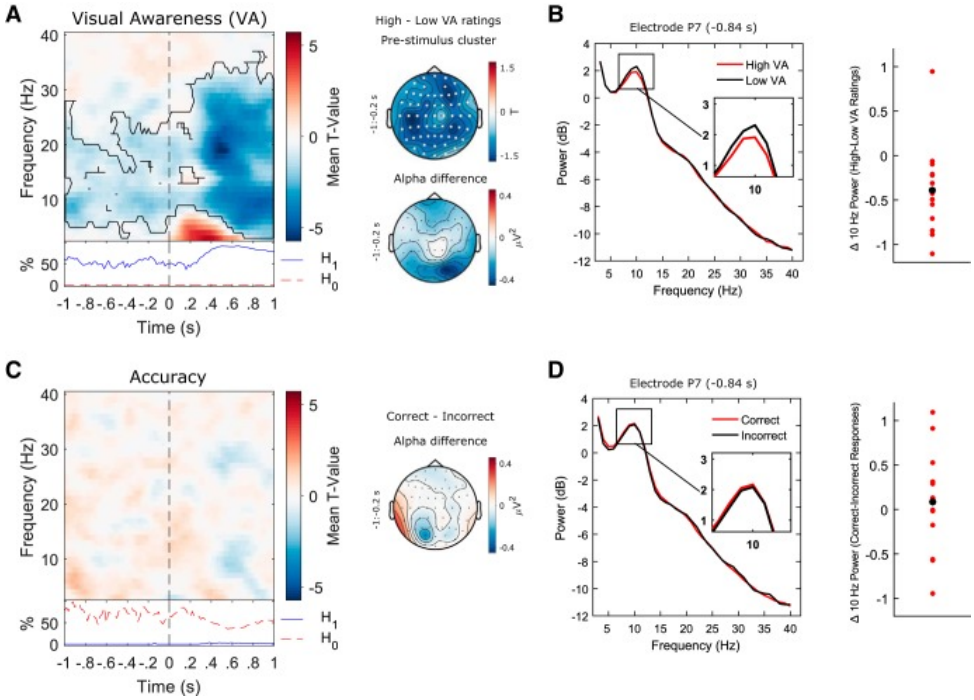

Figure 11. **Relationship between alpha amplitude and perception** *(Benwell et al, 2019).*

Prestimulus alpha-amplitude modulates visual awareness (VA), with lower alpha amplitude for high VA ratings. On the other hand, perceptual accuracy was not affected by pre-stimulus alpha-amplitude changes.

From *Benwell et al, 2017.*

These are some of the core questions that guided my PhD thesis, with a significant part of studies and discussion aimed at addressing these questions and uncovering oscillatory underpinnings of conscious experience.

TMS-EEG METHODS IN THE STUDY OF NEURAL OSCILLATIONS

The Perks of TMS-EEG technique

Transcranial magnetic stimulation (TMS) is one of the most widely used non-invasive brain stimulation techniques that has earned its spot as a crucial tool in neurocognitive research. Its main advantage over neuroimaging methods (e.g., EEG, fMRI, MEG) is the possibility of drawing causal inferences about the brain-behavioral link due to its potential to modulate and interact directly with brain activity. However, if we were to fully exploit its potential in both cognitive and clinical neuroscience, we need to understand the mechanism behind its ability to shape behavior, which is still not fully grasped. One of the ways to gain this direct insight into its mechanism of action is to record the brain activity before, during, and after the TMS, via a concurrent use of one of the neuroimaging techniques. To this aim, the most used neuroimaging technique is certainly EEG, as its widely available due to its low-cost and simplicity in comparison to other techniques and is least technically challenging to combine with TMS (Figure 12).

Figure 12. **A typical TMS-EEG experimental setting.**

As already mentioned, the combined use of TMS with EEG in the last two decades has earned a prominent role in the neuroscientific community, as it aids us in addressing relevant research questions from a new perspective. Specifically, the two techniques complement each other: while TMS provides a causal link between the brain and behavior, a whole-scalp EEG recording offers a direct overview of the TMS-induced effects on the ongoing brain activity that is rarely limited to the stimulation site and is highly dependent on pre-TMS brain states. Therefore, documenting changes in brain activity via EEG combined with TMS can provide key information about brain functioning and dynamics far beyond what is possible by TMS or EEG alone (Miniussi & Thut, 2010).

TMS-EEG technique and Brain Oscillations

Brain oscillation research implementing the TMS-EEG technique could be used via two different approaches. For instance, TMS-EEG approach can explore where, when, and how TMS affects brain excitability and oscillatory activity or even altering behavior

(Miniussi & Thut, 2010). First, it is important to understand that while TMS is without any doubt an “artificial” event, the oscillations induced by a TMS pulse can be considered physiological. This fact has been nicely depicted in a study by Rosanova et al., which showed that, when stimulated, each brain region tends to preserve its natural oscillatory frequency (e.g., alpha activity over occipital cortex, beta over parietal and faster beta/gamma activity over frontal cortex), thus even demonstrating specific oscillatory fingerprints of distinct brain regions (Rosanova et al., 2009). In turn, a single-pulse TMS (sp-TMS) over the visual cortex also demonstrated that TMS-evoked phosphene perception directly depends on pre-stimulus alpha activity (Romei et al., 2008). Moreover, a TMS-EEG approach was also applied to demonstrate how the interference with top-down signals at the higher levels of the functional hierarchy can causally shape the oscillatory activity of visual cortices via cortico-cortical interactions. Specifically, sp-TMS over more anterior areas during visual attention task has been noted to have direct consequences on subsequent alpha oscillatory activity over posterior areas. For instance, in a recent set of TMS-EEG studies exploring the role of FEF in visual attention, a pre-stimulus FEF-TMS lead to changes in the ongoing oscillatory activity of the occipital cortex, but also to the cyclic modulations of visual perception (Veniero et al., 2021).

An alternative, “rhythmic” approach uses TMS-EEG method to interact with the ongoing oscillatory brain activity via multiple pulses applied in phase-alignment with the induced oscillations. For example, when stimulating an area dominantly oscillating at alpha, it could be expected to induce an alpha oscillation by sp-TMS, and to further enhance (entrain) that oscillation with further TMS pulses applied at the same (alpha) frequency in phase with the induced oscillation. A study using rhythmic TMS of an alpha generator at alpha frequency, and concurrent EEG recording, demonstrated that oscillatory entrainment via frequency-tuned TMS is indeed achievable. Therefore, it is possible to

actively manipulate these oscillations and thus draw a conclusion about their role in cognition and perception. For instance, low-frequency stimulation of the motor cortex has been demonstrated to lead to a gradual neural synchronization in the alpha band, which was in turn, inversely correlated with MEPs amplitude (Brignani et al., 2008). A similar study in the visual domain by Romei at al. demonstrated that TMS tuned at IAF shapes perception similarly to spontaneous changes in alpha-actitivy. It was found that alpha TMS diminished perceptual accuracy in the hemifield contralateral to the stimulated hemisphere, and increased accuracy ipsilaterally to it (Romei et al., 2010). In a similar vein, repetitive TMS (rTMS) to the right intraparietal cortex and right FEF was evidenced to disrupt attentional modulations of alpha amplitude in the visual cortex, consequently leading to changes in perceptual accuracy (Capotosto et al., 2012). Together, these results demonstrated a causal implication of the parietal cortex in the attentional control via posterior alpha modulations.

In sum, a TMS-EEG approach has been proven crucial in drawing causal inferences between brain oscillatory activity and behavior, as well as assessing cortical reactivity and within-brain connectivity. Likewise, EEG co-registration during rhythmic TMS stimulation can aid in understanding how oscillations shape different functions. Taking into consideration the multiple benefits of this approach, TMS-EEG technique was method-of-choice for several studies of the current work.

THESIS OUTLINE

Several important points can be deducted from what was previously said. First, neural oscillations (and, more specifically, alpha activity) do seem to have a crucial role in visual perception, attention, and awareness. Second, although often intertwined, these processes can be selectively altered in some neurological and neuropsychiatric cases and thus should be distinguishable in terms of underlying neural mechanisms. Third, research on the oscillatory brain mechanisms in conscious perception and attention often neglects the second point, failing to distinguish and control for the distinct impact of these mechanisms in behavioral measures. Fourth, this neglect can possibly explain the current lack of consensus on the role of different parameters of alpha activity in these mechanisms. Finally, methodological advances in the field of neurosciences have yielded a powerful tool, in terms of the online TMS-EEG approach, that could certainly aid the quest of causally dissociating distinct oscillatory mechanisms.

Given these premises, and via the use of EEG and TMS-EEG methodology, the current thesis aims at describing and dissociating the distinct oscillatory mechanisms underlying visual perception, attention, and awareness.

Study 1 will tackle the boundaries between perceptual accuracy, perceptual awareness, and metacognition. In Experiment 1, EEG will be used during the perceptual task with confidence prompt to explore distinct oscillatory correlates in terms of pre- and post- stimulus oscillatory activity that could explain within- and between- participant variability across these perceptual and cognitive mechanisms. Across Experiments 2 and 3, a rhythmic TMS-EEG (rhTMS-EEG) approach will be applied to manipulate distinct alpha parameters via entrainment protocols, thus causally probing these relations and demonstrating the crucial role of alpha activity in shaping conscious perception.

Study 2 will explore inter-individual differences in the malleability of brain

oscillations via rhTMS. Specifically, starting from the results of Study 1, it was concluded that alpha parameters could influence perceptive and metacognitive abilities and that these parameters can be successfully regulated in order to enhance these abilities, thus serving as a proof-of-principle for the potential use of rhTMS in a clinical setting. However, there were noticeable between-participant differences in the entrainment outcome that subsequently predicted behavioral changes. Therefore, Study 2 will aim at explaining these differences, with the ultimate aim of identifying resting-state neural markers that could predict the entrainment outcome. These results would offer a theoretical model explaining the variance in rhTMS outcomes noticed across different studies and establish an evaluative tool that could pinpoint individuals that would gain the most out of oscillatory entertainment, both in research and clinical settings.

Study 3 aims at describing the relationship between neural oscillations, visual perception and awareness, and event-related potentials (ERPs). Specifically, results described in Study 1 confirmed the crucial role of alpha activity in conscious perception: a role that overlaps with the research exploring ERPs, where earlier components relate to sensory elaboration and later ones to decision making. Therefore, Study 3 will explore and causally probe the oscillatory model of ERP genesis, with the idea that distinct pre-stimulus alpha parameters will differentially shape distinct earlier and later ERPs, with discrete behavioral consequences. These results would shed new light on the relationship between neural oscillations and the genesis and functional significance of evoked components.

Study 4 will explore the relationship between conscious perception, attention, and metacognition. By using an informative cue anticipating the lateralized stimulus presentation, the current study will look at how prior information aids perception and, importantly, what oscillatory mechanisms enable perceptual prediction, accuracy, and

metacognition. Importantly, this study will aim at describing the oscillatory mechanism that would enable the integration of sensory input into our internal representations, but also try to merge these findings with Study 1, thus offering a comprehensive model of perception and attention. The findings of Study 4 could prove crucial for understanding how we reduce sensory ambiguity to maximize the efficiency of our conscious experience, as well as in interpreting the mechanisms of aberrant perceptual experience.

Study 5 will use an sp-TMS to directly emulate the attentional pulse from the anterior attentional network node during a sensory paradigm and thus directly describe and measure the oscillatory mechanisms underlying the interaction between top-down and bottom-up signaling. Therefore, other than alpha parameters explored across previous studies of the thesis, oscillatory feedforward and feedback propagation and integration will be described, as well as the role of gamma activity as the bottom-up mechanism of sensory input processing.

Taken together, these studies have an overarching aim of describing oscillatory mechanisms of attention, perception, and consciousness while at the same time tackling current issues in the field. Specifically, they will try to demonstrate that previous contraddictory findings can be attributed to confounding effects when these distinct mechanisms are not carefully accounted for. Second, it will also try to bridge the gap between studies looking at oscillations and ERPs as predictors of behavior, as here, it is hypothesized that they could present a part of the same mechanism. Third, it will use a TMS-EEG approach, thus enabling active manipulation of oscillatory parameters while having a direct and time-precise overview of the TMS-induced effects on ongoing brain activity.

STUDY 1:
TUNING ALPHA RHYTHMS TO SHAPE CONSCIOUS VISUAL PERCEPTION

Abstract

It is commonly held that what we see and what we believe we see are overlapping phenomena. However, dissociations between sensory events and their subjective interpretation occur in the general population and in clinical disorders, raising the question as to whether perceptual accuracy and its subjective interpretation represent mechanistically dissociable events. Here, we uncover the role that alpha oscillations play in shaping these two indices of human conscious experience. We used electroencephalography (EEG) to measure occipital alpha oscillations during a visual detection task, which were then entrained using rhythmic-TMS. We found that controlling pre-stimulus alpha-frequency by rhythmic-TMS modulated perceptual accuracy but not subjective confidence in it while controlling post-stimulus (but not pre-stimulus) alpha-amplitude modulated how well subjective confidence judgments can distinguish between correct and incorrect decision but not accuracy.

These findings provide the first causal evidence of a double-dissociation between alpha-speed and -amplitude, linking alpha-frequency to spatio-temporal sampling resources and alpha-amplitude to the internal, subjective representation and interpretation of sensory events.

Introduction

The well-known axiom “Seeing is believing” implies that what we see and what we believe we see are largely overlapping phenomena. However, there are many examples of dissociations between sensory events and their subjective interpretation, both in the general population (i.e., false memories, Garry et al., 1996; Hirst et al., 2015) and in subclinical (Fenner et al., 2020; Ferri et al., 2018) and clinical psychiatric populations (e.g., schizophrenia, Köther et al., 2018). A key question, therefore, is whether perceptual accuracy and its subjective interpretation represent mechanistically dissociable events of our conscious experience. And, if so, what their neural underpinnings might be.

Since Hans Berger’s discovery in 1929 of oscillatory patterns around 10 cycles per second in the human brain, namely alpha-oscillations (range 7-13Hz), researchers have long investigated their functional relevance in human perception and cognition. Initially dismissed as a mere reflection of an idling state, a growing body of evidence in the last 15 years has radically changed this view. Influential theories have proposed an active role of alpha-oscillations both in sensory processing and conscious perception (Busch & VanRullen, 2010; Jensen & Mazaheri, 2010; Klimesch et al., 2007; Palva & Palva, 2007; VanRullen, 2016; Wutz et al., 2018; Zazio et al., 2022; Zoefel & VanRullen, 2017). In particular, pre-stimulus alpha-amplitude has been shown to account for a momentary level of cortical excitability with lower and higher amplitude indexing higher and lower cortical excitability, respectively (Romei et al., 2008). This notion has prompted the systematic investigation of its functional correlates. In several studies (Dijk et al., 2008; Ergenoglu et al., 2004; Klimesch et al., 2007), the fate of a peri-threshold visual stimulus was repeatedly linked to the amplitude of pre-stimulus alpha-oscillations. Specifically, low pre-stimulus alpha-amplitude was associated with a higher likelihood of perceiving forthcoming peri-threshold stimuli. Despite the robustness and reliability of these findings, their

interpretation was recently challenged. According to the signal detection theory (SDT) (Green & Swets, 1974), the link between levels of alpha-oscillations and perceptual accuracy in peri-threshold detection tasks may be spurious. Instead, it could be best explained by a change in the internal criterion of the response (and thus dealing with a decision-making process) rather than perceptual accuracy per se, as recently reported (Limbach & Corballis, 2016). Moreover, the momentary level of alpha-amplitude has been shown to best account for the level of subjective confidence levels during a visual discrimination task, without accounting for the level of objective accuracy per se (Benwell et al., 2017; Iemi et al., 2017; Samaha, Iemi, et al., 2017). Therefore, lower levels of alpha-amplitude might account for enhanced proneness to report a visual percept (more liberal criterion), while higher levels of alpha-amplitude might account for reduced proneness to report a visual percept (more conservative criterion), without affecting the level of accuracy of the response.

This new vista on the role of alpha-amplitude in determining perceptual confidence (Iemi & Busch, 2018; Samaha et al., 2020) suggests that alpha-amplitude may not primarily reflect perceptual accuracy but rather a more general mechanism of visual decision-making. However, this leaves open a fundamental question: what are the oscillatory correlates of perceptual accuracy?

Recent reports have highlighted the relevance of alpha-frequency in perceptual sampling, with faster alpha oscillations resulting in higher temporal resolution and more accurate perceptual experience (Cecere et al., 2015; Cooke et al., 2019; Mierau et al., 2017; Migliorati et al., 2020; Minami & Amano, 2017; Wutz et al., 2018), potentially through an increased accumulation of sensory evidence over time. Importantly, we hypothesize here that this higher temporal resolution of visual sampling can successfully translate into higher accuracy in general by allocating more resources to the perceptually relevant

sensory dimension within the same amount of time.

Here, in the first experiment, we have used a visual detection task with spatially lateralized stimuli and electroencephalography (EEG) to directly test the hypotheses that (1) alpha-frequency accounts for objective accuracy (correct vs. erroneous responses and d' measures, Green & Swets, 1974), while (2) alpha-amplitude predicts subjective confidence (low vs. high confidence responses) and/or (3) relates to meta-cognitive abilities, i.e., how well subjective confidence judgments can distinguish between correct and incorrect decisions (as indexed by meta-d' measures, Maniscalco & Lau, 2012).

Crucially, in a second experiment, we used rhythmic Transcranial Magnetic Stimulation (rhythmic-TMS) prior to stimulus onset around individual alpha-frequency (IAF) to entrain pre-stimulus oscillatory activity in the alpha-band towards slower or faster alpha-frequency or higher alpha-amplitudes, in order to influence individual performance towards lower or higher accuracy or to impact individual subjective confidence levels, respectively.

Finally, as stimulus processing has been shown to influence metacognitive abilities (Murphy et al., 2015; Pleskac & Busemeyer, 2010), in a third experiment, we delivered rhythmic-TMS at each participant's own IAF post-stimulus but prior to a subjective confidence prompt to test how increases in post-stimulus alpha-amplitude can modulate their ability to distinguish between correct and incorrect decisions, measured by means of meta-d'.

Methods

Experiment 1.

Participants: 24 healthy volunteers (12 females; mean age= 23.2, SE=2.61) with normal or corrected vision participated in Experiment 1. All participants were recruited at the Centre for Studies and Research in Cognitive Neuroscience in Cesena, Italy. The study was conducted in accordance with the declaration of Helsinki. All participants gave written informed consent to participate in the study, which was approved by the bioethics committee of the University of Bologna.

Stimuli and task procedure. Participants were comfortably seated in front of a CRT monitor (100 Hz refresh rate) at a viewing distance of 57 cm. A PC running E-Prime software (Psychology Software Tools, Inc., USA) controlled stimuli presentation and responses registration. During the main experimental procedure (main task), each trial consisted of a *primary visual detection task*, in which participants responded to visual stimuli displayed on the computer screen, and of a *secondary confidence task*, in which participants rated the level of confidence in their perception on a scale 1 to 4 where 1 = no confidence at all; 2 = little confidence; 3 = moderate confidence and 4 = high confidence. At the beginning of each trial, a white fixation cross was displayed on a grey background. The fixation cross was presented in the center of the screen for 2000 ms and subtended at a visual angle of 0.8°. Afterward, an X (visual angle 2°) was created by rotating the fixation cross by 45 degrees. The cue appeared for a variable time jittered between 2000 and 3000 ms, immediately followed by the primary task stimulus. The stimulus could appear with equal probability on the right or on the left visual field. These stimuli were presented at 4.1°/3.7° eccentricity (horizontal/vertical) in the lower part of the left visual field (LVF) or right visual field (RVF) for 60 ms. The primary task stimulus could be either a catch stimulus or a target stimulus. Catch stimuli consisted of 8x8 black and white checkerboards

(height = 4 cm; width= 4 cm, visual angle = 15.9°). Target stimuli consisted of the same checkerboard containing iso-luminant grey circles, which contrasted the black and white parts of the checkerboard. Participants were prompted to press the spacebar on the keyboard with the right index whenever they detected the circles embedded within the checkerboard. Primary response speed was not stressed over perceptual accuracy, but a time limit of 2000 ms was given. After this primary response, confidence ratings were collected. The Italian version of the question: “How confident are you about your percept?” was presented until participants rated their confidence. Confidence rating was reported on a 4-points Likert scale from “no confidence at all” to “high confidence” by pressing the corresponding number on the keyboard with the left index. Notably, here the confidence reflects the level of subjective certainty in having correctly perceived the stimulus. After the confidence response, a new trial started with the presentation of a new fixation cross. The main task consisted of 5 blocks with 60 trials per block (total trial number = 300) and lasted on average 90 min.

Titration session. Before the main experimental session, in a titration session, iso-luminant circles of 8 different contrast ratios (RGB contrasts on black/white background: 28/227, 32/223, 36/219, 40/215, 44/211, 48/207 and 100/155) were presented along with catch trials (checkerboards without iso-luminant circles) (see Figure 1). In order to account for individual biases that participants may demonstrate in response to catch trials, the false alarm rate was considered, along with target stimuli of different contrast for the calculation of the sigmoid function. For each iso-luminant contrast, individual performance was then entered for the calculation of the sigmoid function.

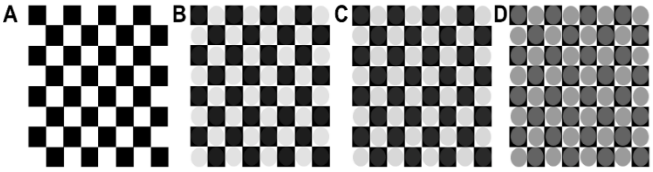

Figure 1. **Samples of stimuli – Different contrasts.**
A. Catch Stimulus ***B.*** Low Contrast Stimulus (RGB contrasts: 30/225) ***C.*** High Contrast Stimulus (RGB contrasts:40/215) ***D.*** Maximum Contrast Stimulus (RGB contrasts:100/155)

Data entered the following formula in order to return the threshold value (y):

$$y = \frac{100}{1 + \mathrm{e}^{-\frac{x-c}{d}}}$$

Where x is the contrast value, c is the inflection point of the curve, and d is the slope of the sigmoid.

The corresponding inflection point was selected as the bias-adjusted threshold to be adopted for stimulus presentation during the experiment. In Experiment 1, the detection performance threshold during the main task (M = 56.9%, SE = 3.69%) was not statistically different form the bias-adjusted threshold (M= 51.58% SE = 0.48%) calculated during the titration session, ($t(24) = 1.68$; $p = .11$; $d = 0.34$). Across participants, the selected luminance contrast ratios during the main task ranged between 20/235 and 50/205 RGB points (M = 32/223; SE = 12).

Psychophysiological recording – paradigm and acquisition. EEG data were collected during the main task in Experiment 1 from 64 Ag/AgCl electrodes (Fp1 , Fp2 , AF3 , AF4 , AF7 , AF8 , F1 , F2 , F3 , F4 , F7 , F8 , FC1 , FC2 , FC3 , FC4 , FC5 , FC6 , FT7 , FT8 , C1 , C2 , C3 , C4 , C5 , C6 , T7 , T8 , CP1 , CP2 , CP3 , CP4 , CP5 , CP6 , TP7 , TP8 , P1 , P2 , P3 , P4 , P5 , P6 , P7 , P8 , PO3 , PO4 , PO7 , PO8 , O1 , O2 , Fpz , AFz , Fz , FCz , Cz , CPz , Pz , POz , Oz) and from the right mastoid with Brain Vision recorder

software (Brain Products, Munich, Germany). The left mastoid was used as a reference, and the ground electrode was placed on the right cheek. The electrooculogram (EOG) was recorded from above and below the left eye and from the outer canthi of both eyes. EEG and EOG were recorded with a band-pass filter of 0.01–100 Hz at a sampling rate of 1000 Hz, which was re-sampled to 500 Hz offline. The impedance of all electrodes was kept below 10 kΩ. EEG data were pre-analyzed using custom-made routines in MatLab R2013b (The Mathworks, Natick, MA, USA). EEG data were re-referenced off-line to the average of all electrodes and filtered with a 0.5–30 Hz pass-band. Epochs were extracted stimulus-locked from -1500 ms to 2500 ms. Artifact-contaminated epochs were excluded using the pop_autorej function in EEGLAB v13.0.1 (Delorme & Makeig, 2004), which first excludes trials with voltage fluctuations larger than 1000 μV, and then excludes trials with data values outside five standard deviations (mean = 9.7% SE = 2.9% of trials removed). Subsequently, EOG artifacts were corrected by a procedure based on a linear regression method (lms_regression function in MatLab R2013b) (Gratton et al., 1983). Because perceptually relevant, pre-stimulus alpha activity shows hemispheric lateralization relative to upcoming stimulus location, for the analyses, we recorded electrode positions as contralateral versus ipsilateral to hemifield of stimulus presentation (resulting in having all contralateral activity on one side, which was conventionally defined to be in the right), i.e., for RVF-stimulus epochs, data from the contralateral (left) electrodes were copied and flipped to right-sided electrodes.

In order to identify the individual alpha-frequency peak during the task, data epochs in the cue-stimulus period (i.e., pre-stimulus alpha from -1000 ms to stimulus presentations, baseline between -1500 and -1000 ms) were analyzed with a fast Fourier transformation (MatLab function spectopo, frequency resolution: 0.166 Hz). Power was calculated separately for each subject and condition and was normalized by z-score decibel

(dB = 10*log10[-power/baseline]) transformation at each frequency. Individual alpha-frequency was defined as the local maximum power within the frequency range 7-13 Hz (i.e., alpha peak). Each subject showed a clear peak within this alpha range. However, a peak in the alpha band was not present at all electrodes. For this reason, power spectra on all parietal-occipital electrodes were visually inspected. Then, the contralateral electrode was selected for analyses where alpha oscillation showed a clear peak (Samaha & Postle, 2015). Homologous electrodes were selected for the analyses in the ipsilateral hemisphere. This procedure identified the following subset of parieto-occipital electrodes that were used separately for each subject and condition to identify alpha-frequency in the cue-stimulus period: contralateral electrodes (P8, PO8, PO4, O2), ipsilateral electrodes (P7, PO7, PO3, O1). Importantly, most of the participants (n=15) showed maximum power over electrode O2.

The amplitude of alpha oscillations was calculated by time-frequency analyses of data epoched from 2000 ms before to 2000 ms after the stimulus presentation. Long epochs prevent that edge artifacts from contaminating time frequency power in the time windows of interest. Spectral EEG activity was assessed by time-frequency decomposition using a complex sinusoidal wavelet convolution procedure (between 2 and 25 cycles per wavelet, linearly increasing across 50 linear-spaced frequencies from 2.0 Hz to 50.0 Hz) with the newtimef function from EEGLAB v13.0.1 and custom routines in MatLab. The resulting power was normalized by decibel (dB = 10*log10[-power/baseline]) transformation at each frequency, using a single trial baseline between -1000 and -500 preceding stimulus onset. This long baseline window was used to increase the signal-to-noise ratio during the baseline period and is frequently applied in time frequency analyses. This procedure was applied separately for each subject and condition. The mean alpha (7-13 Hz) amplitude was computed separately for each condition in the cue-stimulus interval (-500 to 0 ms). In

order to identify electrode clusters for the analyses of alpha-amplitude, we used the same procedure as for alpha-frequency. For alpha-amplitude, the following subsets of posterior contralateral (P2, P4, P8, PO4, PO8, O2) and ipsilateral (P1, P3, P7, PO3, PO7, O1) electrodes were used for the analyses. Importantly, as for alpha-frequency, most of the participants (n=18) showed maximum alpha amplitude over electrode O2.

Statistical Analyses. First, trials were sorted according to objective accuracy (i.e., into correct and error trials). Correct trials consisted of correctly detected target trials (i.e., hits, where participants pressed the spacebar after a target trial) and correctly detected catch trials (i.e., correct rejections, where participants did not press the spacebar after a catch trial). Accordingly, error trials consisted of misses after target trials and false alarms after catch trials. Then we compared participants with high vs. low perceptual sensitivity. Perceptual sensitivity was estimated using the *d'* measure. In signal detection theory (SDT), *d'* reflects a standardized measure of discrimination abilities between the signal and the noise (type I sensitivity). *d'* was calculated as $d' = z(H) - z(FA)$, where z represents the z-scores of Hit rate (i.e., H, the probability of correct reactions on target trials) and false alarms (i.e., FA, the probability of incorrect reactions on catch trials (Green & Swets, 1966)).

Next, we focused on subjective confidence levels during correct trials (i.e., hits and correct rejections). To compare confident vs. non-confident responses, we aggregated high-confident responses and low-confident responses. In this way, correct trials were divided into high confidence (i.e., with a confidence rating of 3 or 4) and low confidence (i.e., with a confidence rating of 1 or 2). Then, we compared participants showing high vs. low confidence or metacognitive performance. For confidence analyses, the mean value of the confidence ratings was calculated for each participant. Instead, metacognitive performance was quantified using the computational method proposed by Maniscalco & Lau

(Maniscalco & Lau, 2012). This method quantifies the efficacy of confidence ratings to discriminate between correct and erroneous responses in an SDT model. The model accounts for the variance in task performance to compute metacognitive sensitivity (type II sensitivity) on subjective confidence rating. This method, previously described in detail and validated, can give a metric (termed *meta-d*') for metacognitive abilities (Barrett et al., 2013; Maniscalco & Lau, 2012). Briefly, the central idea is to link type I and type II SDT models to compute the observed type II sensitivity. *meta-d'* estimates the values, which maximize the fit between the observed type II data and the parameter values of the *d*' type I SDT model. Here, *meta-d*' was calculated with the function fit_meta_d_SSE in MatLab. This function minimizes the sum of squared errors and estimates *meta-d'* using observed type II data and the empirical type I criterion *c'* (Barrett et al., 2013). In this way, *meta-d*' estimates, for instance, the relative likelihood of reporting a high confidence rating after a correct response (Barrett et al., 2013; Maniscalco & Lau, 2012). Higher values of *meta-d*' correspond to participants having better metacognitive abilities.

Within participants, EEG analyses were performed separately for objective accuracy and subjective confidence. For *Objective Accuracy,* we compared alpha activity (both frequency and amplitude) in 2x2 repeated measures ANOVAs with the factors ACCURACY (correct and incorrect) and HEMISPHERE (contralateral and ipsilateral). For Subjective Confidence, analyses were performed on correct trials. The alpha activity was analyzed for the factor CONFIDENCE (high and low confidence) and for the factor HEMISPHERES (contralateral and ipsilateral) in 2x2 repeated measures ANOVAs. Differences between conditions were tested by one or two-tailed t-tests (planned comparisons).

Between participants, EEG analyses were performed on perceptual sensitivity and metacognitive performance. For perceptual sensitivity analyses, we divided participants

into two numerically equivalent groups using the median split of the d' scores (high vs. low d'). As for perceptual sensitivity, we also conducted between-group analysis by dividing participants into two numerically equivalent groups (high vs. low meta d' scores) on a median split basis of the meta-d' scores (i.e., metacognitive performance). Differences between groups were tested by one or two-tailed independent samples t-tests (planned comparisons).

Additionally, to evaluate if the alpha-amplitude and alpha-frequency are independent, we compared them both within- and between- participants. Specifically, , for each participant, we first divided the trials in high and low alpha amplitude, via median-slpit procedure. Next, we calculated alpha-frequency for both types of trials, and compared them via a paird-sample t-test. Finally, we also correlated alpha indices between-subjects, by looking at the possible relationship between alpha-amplitude and frequency for correct trials via Spearman correlation.

Pre-stimulus IAF and resting-state IAF. As we have used resting IAF to target pre-stimulus activity in experiments 2 and 3 (see results sections), we checked for any potential difference between resting-state IAF and pre-stimulus IAF in Experiment 1 to ensure the adequacy of our approach, with the working hypothesis that no significant differences should be observed. In this analysis, resting-state IAF was defined as the maximum local power in the alpha-frequency range during the resting state over a cluster of posterior electrodes (O1,P1,P3,P5,P7,Pz,POz,Oz,PO3,PO7; O2,P2,P4,P6,P8,PO4,PO8), while pre-stimulus IAF was calculated in the same electrode cluster across conditions in a time window between -1000ms and stimulus presentation. The analysis was performed on 22 out of 24 participants as resting EEG was not available for 2 participants. As expected, the two-tailed paired samples t-test showed no differences ($t(21)=0.05$, $p=.968$, $d=.019$) between resting state IAF (M=10.81Hz; SE=0.21Hz) and pre-stimulus IAF (M=10.83Hz;

SE=0.37Hz). Importantly, these results demonstrate that resting-state IAF and pre-stimulus IAF are comparable within the group.

Experiment 2.

Both Experiment 2 and Experiment 3 implemented a rhythmic TMS (rhTMS) entrainment protocol with concurrent EEG recording, whereas the timing of rhTMS pulses differed between the two experiments.

Participants. Fifty-one healthy volunteers (25 females; mean age ± SD = 23.39 ± 2.59 years) took part in Experiment 2. All of them had a normal or corrected-to-normal vision and met TMS safety criteria by self-report. All participants gave written informed consent before taking part in the study, which was conducted in accordance with the Declaration of Helsinki and approved by the local ethics committee. Here, subjects were randomly assigned to one of three groups with distinct stimulation protocols (see next paragraph for details): IAF-1Hz (group 1 = 22.64 ± 2.15, nine females), IAF (group 2 = 23.88 ± 2.15, eight females) and IAF+1Hz (group 3 = 23.88 ± 3.16, eight females), each containing 17 participants.

Stimuli and task procedure. The stimuli and tasks of Experiment 2 corresponded to those described in Experiment 1, with the main difference being the active manipulation of alpha activity via an entrainment protocol.

Entrainment of the intrinsic oscillatory alpha activity was achieved using rhythmic transcranial magnetic stimulation (rhythmic-TMS). Specifically, pre-stimulus alpha activity was fine-tuned relative to individual alpha-frequency using rhythmic five-pulse TMS bursts in which the time lag between pulses was manipulated depending on the group (Cecere et al., 2015; Wolinski et al., 2018). In order to induce changes in the alpha-frequency cycle length, rhythmic-TMS was applied at a slower or faster pace relative to a

participant's individual alpha-frequency. To selectively modulate alpha-amplitude, the frequency of the rhythmic-TMS pulse trains was matched to the intrinsic individual alpha-frequency of the participant, thus enhancing the synchronization of neural firing and phase alignment without influencing the speed of alpha activity. In this way, rhythmic-TMS pulse trains could occur at three different frequencies: at the individual alpha-frequency of the participant to manipulate pre-stimulus alpha-amplitude (IAF group), at 1Hz lower than the individual alpha-frequency (IAF-1Hz group) to slow-down pre-stimulus alpha-frequency; or at 1Hz higher than the individual alpha-frequency (IAF+1Hz group) to speed-up pre-stimulus alpha-frequency. In all groups, the last TMS-pulse coincided with the stimulus appearance.

Biphasic stimulation was applied using a Magstim Rapid Transcranial Magnetic Stimulator via a 70mm figure-of-eight coil (Magstim Company, UK) of maximum field strength ~1.55T. As systematic differences in visual cortex excitability do not seem to be present between the hemispheres (Bestmann et al., 2007; Cattaneo et al., 2009b; Silvanto & Muggleton, 2008), TMS bursts were delivered only to the right occipital site (at O2 electrode position), with the coil surface tangent to the scalp, and the handle oriented perpendicular to the medial plane of the subjects head (latero-medial current direction). Moreover, pulse intensity was kept fixed at 60% of the maximum stimulator output (MSO) (Mevorach et al., 2006; Pitcher et al., 2007; Silvanto et al., 2005), roughly corresponding to previously reported phosphene thresholds (Bolognini et al., 2010; Gerwig et al., 2003; Romei et al., 2009). No subject reported to have perceived phosphenes during the execution of the task. Within-subject sham control stimulation was implemented in order to account for any non-specific rhythmic-TMS effects. To do so, a modified coil was used that provided enough distance from the scalp to ensure the absence of stimulation while at the same time maintaining coil position, as well as tactile and acoustic sensations. Each

participant underwent three consecutive rhythmic-TMS and sham blocks (resulting in a total of 900 active rhythmic-TMS pulses), whereas rhythmic-TMS/sham stimulation block order was randomized. Therefore, the experimental session consisted of 6 blocks with 60 trials per block (total trial number=360) (see also Experiment 1), with short breaks between the blocks (overall average task duration of 50 minutes). The rhythmic-TMS design was in line with current safety guidelines (Rossi et al., 2011, 2021).

Titration session. Titration was run as for Experiment 1. Additionally, in the second experiment, during the titration session, individual alpha peak frequency (defined as the maximum local power in the alpha frequency range) was determined. A total of six minutes resting-state EEG (three minutes with eyes closed and three minutes with eyes open, and with gaze on a fixation cross on the screen) was recorded from 8 Ag/AgCl parieto-occipital electrodes (O1, P3, PO3, PO7; O2, P4, PO4, PO8). Individual alpha frequency peak was calculated from the power spectra of the eyes open condition, applying a Fast Fourier Transformation. In line with Experiment 1 (showing a local alpha power maxima over O2) and previous studies, alpha-frequency was calculated from the O2 electrode (Cecere et al., 2015; Romei et al., 2007), over which rhTMS was subsequently applied (see above). The identified individual alpha-frequency was used to calibrate rhTMS frequency.

EEG recordings –acquisition and processing. EEG data were collected for Experiment 2 as for Experiment 1. However, in Experiment 2, an rhTMS pulse train was applied during EEG recording. The resulting rhTMS artifacts were identified and removed using an open-source EEGLab extension, the TMS-EEG signal analyzer (TESA, Rogasch et al., 2017). First, EEG data were epoched around stimulus onset (between -1500 ms and 2500 ms for Experiment 2 and between -1000 ms and 2000 for Experiment 3, due to differences in stimulation timing), and linear trend from the obtained epochs was removed.

Then rhTMS pulse artifact and peaks of rhTMS-evoked scalp muscle activities were removed (-10ms +10 ms), and cubic interpolation was performed prior to downsampling the data (from 5000 Hz to 1000 Hz). Interpolated data was again removed prior to Individual Component Analysis (ICA). Specifically, a fastICA algorithm was used (pop_tesa_fastica function) to identify individual components representing artifacts, along with automatic component classification (pop_tesa_compselect function), where each component was subsequently manually checked and reclassified when necessary. In this first round of ICA, only components with large amplitude artifacts, such as rhTMS-evoked scalp muscle artifacts, were eliminated. Data were again interpolated prior to applying pass-band (between 1 and 100 Hz) and stop-band (between 48 and 52 Hz) Butterworth filters. Subsequently, interpolated data were again removed prior to the second round of ICA aimed at removing all other artifacts, such as blinks, eye movement, persistent muscle activity, and electrode noise. Then, rhTMS-pulse period was interpolated, and data were re-referenced to the average of all electrodes. Finally, single trials were visually inspected, and those containing residual rhTMS artifacts were removed. The described rhTMS artifact removal procedure was applied to all EEG data, both for active rhTMS and sham stimulation. On average, approximately one-third of all epochs were removed (M = 34.31%, SE = 1.72%) (remaining epochs mean= 236.5 epochs, SE=6.19).

Alpha-frequency and alpha-amplitude were identified in a similar manner as per Experiment 1. Therefore, alpha-frequency was defined as the local maximum power within the frequency 7-13 Hz range in a pre-stimulus period (-650 ms to stimulus presentation). Accordingly, pre-stimulus alpha-amplitude was calculated in the time-frequency data (as for Experiment 1). The time window of analyses corresponded to the stimulation period for both alpha-frequency and -amplitude. Near-stimulation parieto-occipital electrodes in the right hemisphere (PO4, PO8, O2), along with analogous electrodes in the left hemisphere

(PO3, PO7, O1) were used for all of the analyses.

Statistical analyses (behavioral data). Behavioral data were analyzed separately for perceptual sensitivity (d' score) and for confidence (mean of confidence ratings), and metacognitive performance (meta d' score).

All scores were compared between the two HEMIFIELDs (left and right) and two STIMULATION types (active rhythmic-TMS and sham) in three GROUPs of participants (IAF±1Hz, IAF), in 2x2x3 repeated measures mixed-model ANOVAs.

Statistical analyses (EEG data). Electrophysiological data were analyzed separately for pre-stimulus alpha-amplitude and alpha-frequency. Therefore, both parameters of alpha activity were compared between the two HEMISPHERES (left and right parieto-occipital cluster) and the two STIMULATION types (active rhythmic-TMS and sham) in three GROUPs of participants in 2x2x3 repeated measures mixed-model ANOVAs. Differences between conditions were tested by two-tailed t-test (planned comparisons).

Finally, the association between rhythmic-TMS-evoked differences in alpha-frequency in the stimulated (right) hemisphere (computed as a difference in alpha-frequency between active rhythmic-TMS and sham stimulation conditions) and differences in perceptual sensitivity in the opposite (left) hemispace (computed as a difference in d' score between active rhythmic-TMS and sham stimulation conditions) was explored via linear regression.

Experiment 3.

Participants. Seventeen new healthy volunteers (12 females; mean age= 22.47, SE = 0.66) were recruited for Experiment 3.

Stimuli and task procedure. The stimuli and task of Experiment 3 corresponded to those of Experiment 2, with the main difference being the timing of the manipulation of

alpha activity via an entrainment protocol.

Specifically, Experiment 3 aimed at selectively enhancing alpha-amplitude prior to the confidence prompt; therefore, only one entrainment protocol was applied (i.e., stimulation at the exact individual alpha-frequency). While in Experiment 2, the final pulse of the rhTMS-train coincided with stimulus onset, in Experiment 3 final rhTMS pulse coincided with the onset of the confidence prompt.

Stimulation site, coil orientation, stimulation intensity, control conditions, and number of pulses were the same for Experiments 2 and 3.

Titration session. A titration session was conducted as for Experiment 2.

EEG recordings – acquisition and processing. EEG data were recorded, and alpha-frequency and alpha-amplitude were identified as per Experiments 1 and 2, with the only difference being that the analysis window was moved prior to the confidence prompt (850 ms to 1500 ms after stimulus presentation, which corresponded to -650 ms prior to the confidence prompt).

Statistical analyses (behavioral data). Behavioral data were analyzed separately for perceptual sensitivity (d' score) and for confidence (mean of confidence ratings) and metacognitive performance (meta d' score). All scores were compared for the two HEMIFIELDS (left and right) and between different STIMULATION types (active rhythmic-TMS and sham) in a 2x2 repeated measures ANOVA.

Statistical analyses (EEG data). Electrophysiological data were analyzed separately for alpha-amplitude and alpha-frequency. Moreover, differences in alpha-amplitude and alpha-frequency were again compared between the two HEMISPHERES (left and right) and between STIMULATION types (active rhythmic-TMS and sham) in a 2x2 repeated measures ANOVA. Differences between conditions were tested by two-tailed t-test (planned comparisons).

Finally, a linear regression model was used to determine whether rhythmic-TMS-evoked differences in alpha-amplitude in the stimulated (right) hemisphere (computed as a difference in alpha-amplitude between active rhythmic-TMS and sham stimulation conditions) can predict differences in confidence levels in the opposite (left) hemifield (computed as a difference in meta d' scores between active rhythmic-TMS and sham stimulation conditions).

Results

A total of 92 participants took part in three experiments (Figure 1), designed to map pre-stimulus alpha-frequency and alpha-amplitude on objective versus subjective performance measures (EEG Experiment 1) and to test for their causative relationships (TMS-EEG Experiments 2&3).

Alpha-frequency and alpha-amplitude dissociate with respect to objective accuracy, subjective confidence, and metacognitive abilities

In Experiment 1, twenty-four participants performed a visual detection task (Figure 2A) in which lateralized stimuli (8X8 checkerboards) were preceded by a spatially uninformative cue (an X), indicating that a stimulus will be occurring in the lower left- or right-hemifield with 50% probability (chance level). Each black and white checkerboard was flashed for 60ms and could contain iso-luminant grey circles, the contrast of which was set for each individual to their 50% perceptual threshold. Half of the trials were catch trials, i.e. checkerboards without any grey circle embedded in them (see Methods for details).

Participants were instructed to respond whenever they perceived grey circles within the lateralized checkerboards. Following this primary task and about 1.5-2sec post-stimulus, they were prompted to indicate on a scale of 1 to 4 how confident they were of their percept, with 1 representing “no confidence at all”, 2, “little confidence”, 3 “moderate confidence” and 4 “high confidence” (see Figure 2A). EEG signals were concurrently recorded from 64 electrodes while this task was performed (see Methods).

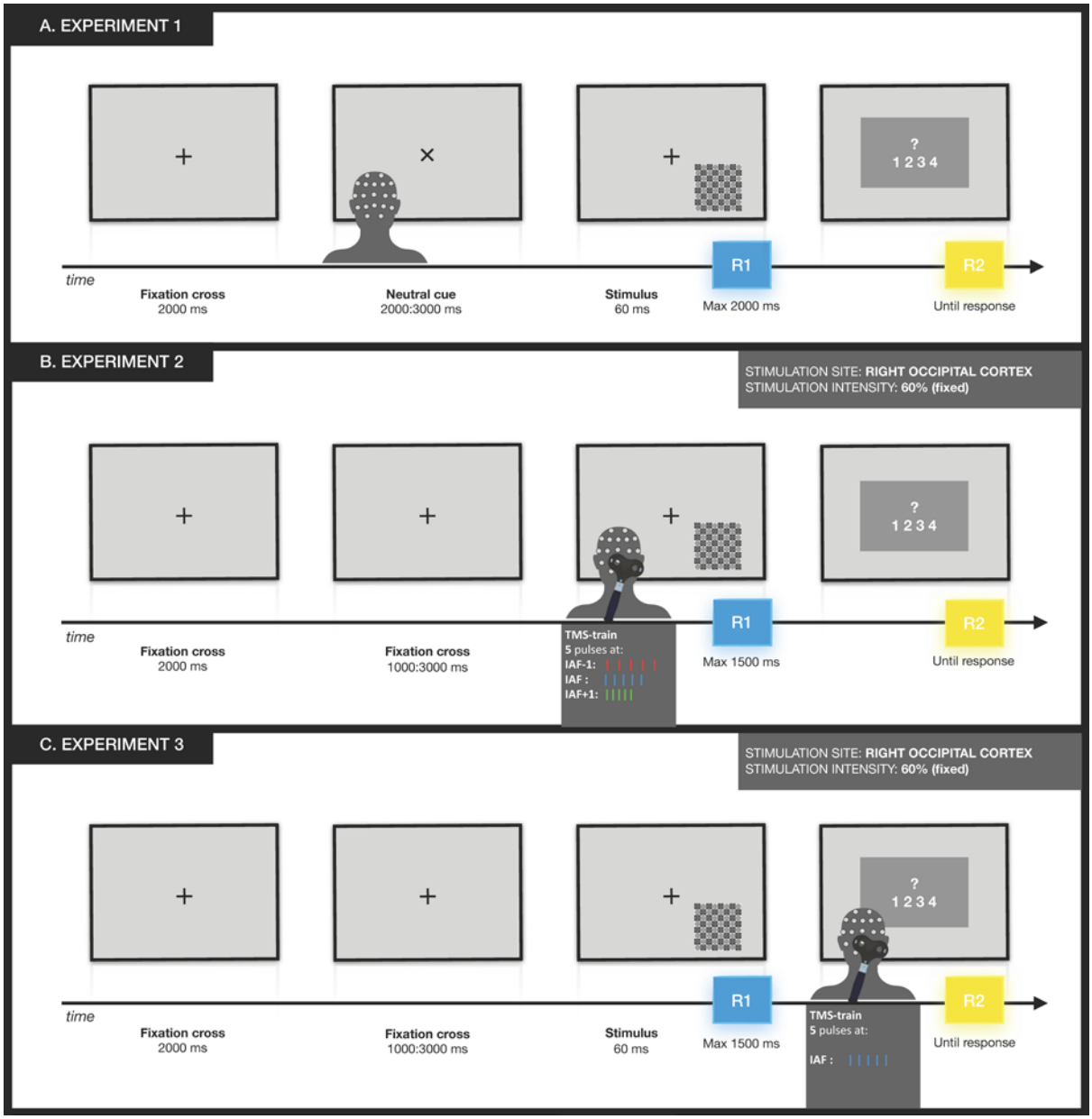

Figure 2. **Experimental design.**

A. Experiment 1. EEG data were collected during a visual detection task. Each trial started with a fixation cross, after which stimuli could randomly appear in the lower left or right visual field. The primary task was to respond (R1) by pressing a space bar if the checkerboard contained grey circles. After this, participants rated their confidence in their first response (R2) on a Likert scale from 1 (no confidence at all) to 4 (high confidence***). B. Experiment 2.*** Participants performed the same visual detection task as in Experiment 1 while undergoing concurrent EEG recording. In addition, 5 rhythmic-TMS pulses were administered before stimulus presentation. Participants were assigned to 3 different groups. For each group, rhythmic-TMS pulses were set at a certain alpha-frequency: individual alpha-frequency (IAF) group (blues bars), slower pace (IAF-1Hz) group (red bars), and faster pace (IAF+1Hz) group (green bars). ***C. Experiment 3.*** Participants performed the same visual detection task while undergoing EEG recordings, as in Experiments 1 and 2. However, rhythmic-TMS pulses were administered before the confidence prompt at each participant's individual alpha-frequency. ms=milliseconds.

Pre-stimulus alpha-frequency and accuracy: We looked at whether correct vs. erroneous responses could be best explained by the frequency of alpha oscillations prior to stimulus presentation rather than by their amplitude. Our analysis of pre-stimulus alpha-

frequency (Figure 3A) showed a significant main effect of ACCURACY (Correct vs. Errors) ($F(1,23)=18.2$, $p<.001$, $\eta_p^2=.442$). This result suggests that individual pre-stimulus alpha-frequency can differentiate between correct and erroneous responses, with faster alpha-frequency predicting correct responses (M=11.45Hz, SE=0.18Hz) and slower alpha-frequency predicting errors (M=11.02Hz, SE=0.18 Hz). Moreover, the effect of alpha-frequency was maximal over the posterior electrodes (Figure 3A), involving left and right sites equally, as no main effect of HEMISPHERE (ipsilateral vs. contralateral to the presented stimulus) ($F(1,23)=1.34$, $p=.259$, $\eta_p^2=.06$), nor a significant interaction of ACCURACYxHEMISPHERE ($F(1,23)=0.33$, $p=.571$, $\eta_p^2=.014$) were found.

We further tested whether pre-stimulus alpha-frequency can predict individual performance across participants as assessed by d', a sensitivity index that takes into account both correct responses and false alarms, and thus – relative to the simple hit rate measure – has the advantage of discounting any potential effect of response bias, with higher values reflecting higher task accuracy (Green & Swets, 1974). Using a median split procedure for d' scores, we divided participants into two numerically equivalent groups (high vs. low d'). In line with our hypothesis, a between-groups analysis of alpha-frequency shows faster pre-stimulus alpha-frequency in the high d' group (11.55Hz, SE=0.22Hz) compared to the low d' group (10.29Hz, SE=0.66Hz) by 1.26Hz: $t(22)=1.832$, $p=.040$, $d=.374$ (one-tailed unpaired two-sample t-test).

By contrast, the analysis of both pre- and post-stimulus alpha-amplitude showed no significant effects on ACCURACY (*all Fs* $(1,23)<3.05$, *all ps*$>.094$, *all* $\eta p^2<.117$), in line with recent reports that alpha-amplitude does not account for objective accuracy (Benwell et al., 2017; Iemi et al., 2017; Samaha, Iemi, et al., 2017).

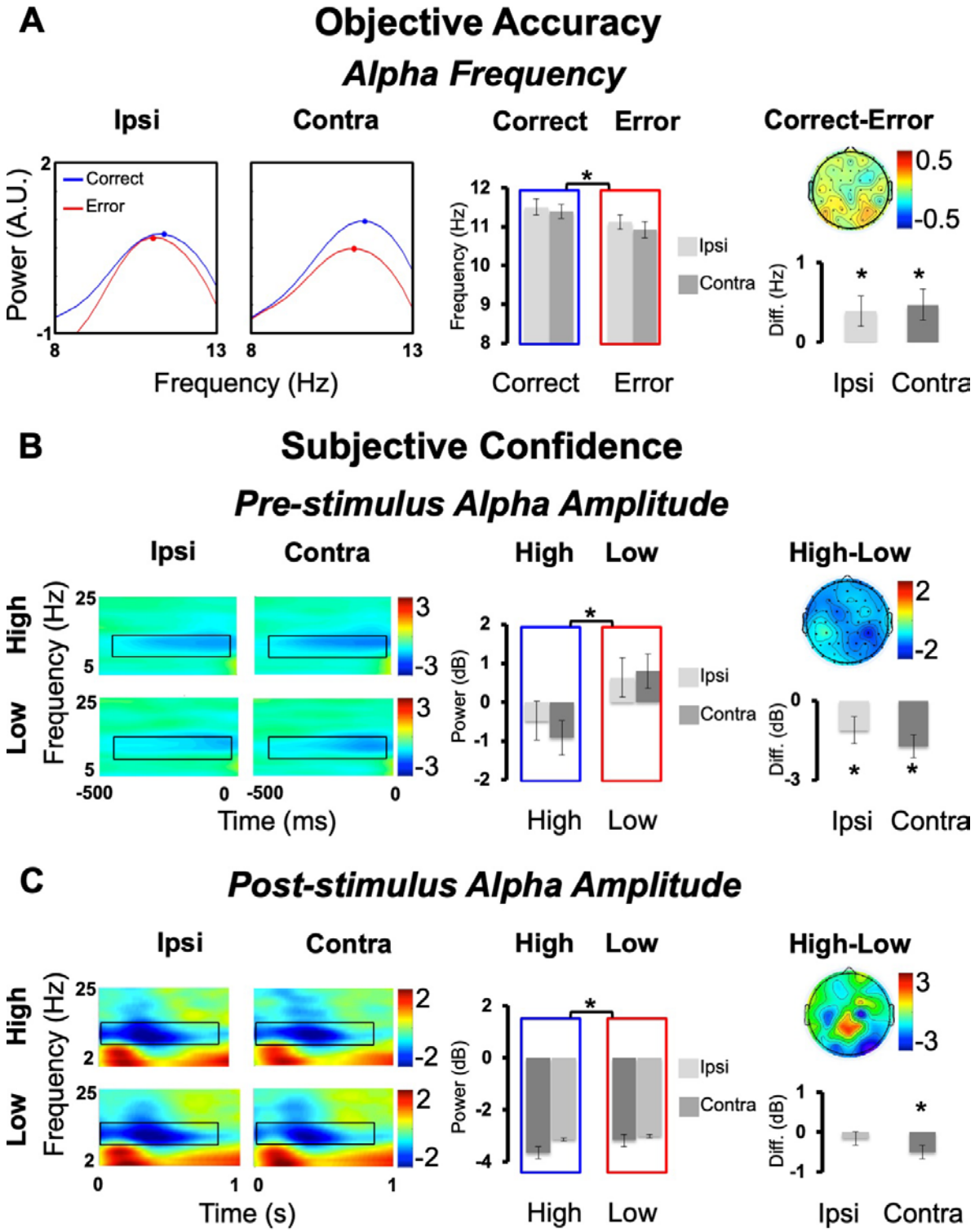

Figure 3. **Results Experiment 1. Alpha-frequency and -amplitude relate to accuracy and confidence.**

A. Objective Accuracy. Averaged alpha-frequency is represented as the z-scored mean power (10*log10[μv2/Hz]) spectrum in the cue-stimulus time period for the contralateral and the ipsilateral electrodes and for Correct and Error trials within the alpha-band. Bar graphs report correct and error trials and the differences in correct/error responses. Topography represents the difference in Correct-Error (electrodes are flipped to represent contralateral activity in the right-hand side and ipsilateral activity in the left-hand side). Subjective Confidence. Pre-stimulus alpha-amplitude **(B)** and post-stimulus alpha-amplitude **(C)** are reported as time-frequency plots. For illustrative purposes we reported data from a cluster of ipsi (P7,PO7,PO3,O1) and contralateral (P8,PO8,PO4,O2) electrodes and for Low and High confident trials. Black boxes denote regions of statistical analyses (alpha-band 7-13Hz). Bar graphs are reported for Low and High confident trials and for the difference in High-Low. Topography represents the difference in High-Low (electrodes are flipped to have contralateral activity in the right-hand side and ipsilateral activity in the left-hand side). Two-tailed t-test statistical

significance is reported (*p<.05). Error bars represent standard error of the mean. A.U.=arbitrary units; Diff=difference; μv=microvolt; Hz=Hertz; ms=milliseconds; dB=decibel.

Pre-stimulus alpha-amplitude and confidence: We then tested whether pre-stimulus alpha-amplitude, rather than alpha-frequency, could account for confidence judgments (Figure 3B). We found a main effect of CONFIDENCE ($F(1,23)=9.03$, $p=.006$, $\eta_p^2=.282$), with desynchronized alpha-amplitude in high confidence trials (-0.699dB, SE=0.409dB) and synchronized alpha-amplitude in low confidence trials (0.719dB, SE=0.251dB), suggesting that alpha-amplitude has a significant impact on perceptual confidence. Moreover, topography (Figure 3B) shows posterior alpha-amplitude modulations with an even distribution across hemispheres, indicating no main effect of HEMISPHERE (ipsilateral vs. contralateral to the presented stimulus) $F(1,23)=0.201$, $p=.658$, $\eta_p^2=.009$), nor a significant interaction CONFIDENCExHEMISPHERE ($F(1,23)=1.323$, $p=.262$, $\eta_p^2=.054$).

For completeness, control analyses performed on pre-stimulus alpha-frequency showed no main effect of CONFIDENCE, nor any interaction with HEMISPHERE (all $Fs(1,23)<0.47$, $ps>.501$, $\eta_p^2<.021$).

Post-stimulus alpha-amplitude, confidence, and meta-d': Because following stimulus presentation, the initial choice on decisions and confidence continue to evolve (Murphy et al., 2015; Pleskac & Busemeyer, 2010), we asked whether subjective confidence judgments are influenced by post-perceptual processes. To this aim, we analyzed alpha-amplitude in a time window after stimulus presentation (0-900ms), corresponding to a post-stimulus time period but before the confidence prompt (Figure 3C). The analysis of post-stimulus alpha-amplitude revealed a main effect of CONFIDENCE ($F(1,23)=4.367$, $p=.048$; $\eta_p^2=.16$), with more desynchronized alpha-amplitude in high confidence trials (-3.41dB, SE=0.38dB) compared to low confidence trials (-3.08db, SE=0.34dB). Moreover,

the analyses showed a main effect of HEMISPHERE ($F(1,23)=5.358$; $p=.03$; $\eta_p^2=.189$) and, most importantly, an interaction CONFIDENCExHEMISPHERE ($F(1,23)=4.347$, $p=.048$, $\eta_p^2=.159$), showing that when looking at post-stimulus alpha-amplitude, the confidence effects are accounted for by the contralateral (high confidence=-3.64dB, SE=0.396dB; low confidence=-3.14dB, SE=0.347dB; $t(23)=2.747$, $p=.011$; $d=.586$) but not the ipsilateral hemisphere (high confidence=-3.17dB, SE=0.387dB; low confidence=-3.01dB, SE=0.349dB; $t(23)=0.906$, $p=.375$, $d=.193$). These findings suggest that post-stimulus alpha-amplitude has a retinotopic distribution being modulated by the stimulus position. Indeed, while the relationship between confidence levels and pre-stimulus alpha-amplitude can be observed for both hemispheres, only contralateral alpha-amplitude accounts for individual confidence levels after stimulus presentation.

We then tested whether post-stimulus alpha-amplitude could specifically account for metacognitive abilities. In other words, we tested how well subjective confidence judgments can distinguish between correct and incorrect decisions by means of meta-d', a measure that quantifies metacognitive performance and that reflects the efficacy of confidence ratings to discriminate objectively correct from erroneous responses (Maniscalco & Lau, 2012). In a between-subject design, by using a median-split procedure, we divided participants with high and low metacognitive abilities. We found that post-stimulus alpha-amplitude in the high meta-d' group was significantly more desynchronized (-4.66dB, SE=0.59dB) relative to the low meta-d' group (-3.26dB, SE=0.39dB; one-tailed unpaired two-sample t-test: $t(22)=1.966$, $p=.031$; $d=.567$), thus supporting the idea that post-stimulus alpha-amplitude can predict metacognitive performance. Moreover, this role seems specific for post-stimulus alpha-amplitude, as pre-stimulus changes of alpha-amplitude could not account for between-subject differences in metacognition ($t(22)=0.929$, $p=.181$, $d=.189$), further supporting this interpretation.

Overall, these EEG results implicate alpha-frequency in the level of objective accuracy, with higher alpha-frequency accounting for higher accuracy but playing no role in determining one's perceptual confidence. Conversely, alpha-amplitude is implicated in perceptual decision confidence but has no role in objective accuracy. In sum, these results point to a functional dissociation of the two oscillatory markers, alpha-frequency and alpha-amplitude, which appear to shape sensory sampling and the subjective readout of this sampling, respectively.

Further support of the independency of the two indices of alpha activity was obtained by their direct comparison. Specifically, there was no significant within-participant difference in alpha-frequency between the low- and high- alpha amplitude trials ($t(23)=0.22$, $p=.827$, $d=.04$), but also there was no significant correlation between alpha-frequency and -amplitude on a between-participant basis (*Spearman* $r = -0.01$, $p = .966$).

Entraining faster vs. slower pre-stimulus alpha oscillations selectively shapes objective accuracy

In Experiment 2, we tested for the causal involvement of alpha-frequency and alpha-amplitude in objective accuracy vs. confidence by using rhythmic-TMS to entrain alpha oscillations while participants performed the same visual task as in Experiment 1 (Figure 2B). In three different experimental groups we recorded EEG activity while concurrently administering 5-pulse rhythmic-TMS trains of fixed-intensity (60% of the maximum stimulator output) to the right occipital cortex (coil placement over O2) prior to stimulus presentation. In the IAF±1Hz groups, rhythmic-TMS-frequency was set at 1Hz faster/slower than the individual participant's alpha-frequency, which should entrain their alpha oscillations towards a faster/slower pace (Cecere et al., 2015; Minami & Amano, 2017), respectively. In the IAF group, the rhythmic-TMS frequency was aligned with the

participant's alpha-frequency. This has been shown to lead to enhanced alpha-amplitude by entrainment (Thut et al., 2011) and should thus have an impact on confidence rather than on accuracy. Together with active rhythmic-TMS, we employed sham stimulation at a matching frequency for every participant in each group to account for any nonspecific effects of rhythmic-TMS.

We looked at the impact of rhythmic-TMS on EEG activity across the three groups (Figure 4). As expected, pre-stimulus alpha-frequency was modulated differently in active rhythmic-TMS versus sham stimulation across the experimental groups, depending on the recording site (STIMULATIONxGROUPxHEMISPHERE interaction: $F(2,48)=4.05$, $p=.024$, $\eta_p^2=.144$). Specifically, stimulating at the lower alpha-frequency slowed down pre-stimulus alpha activity during active rhythmic-TMS (M=9.74Hz, SE=0.20), relative to sham stimulation (M=10.66Hz, SE=0.20), selectively at the (stimulated) right hemisphere ($t(16)=3.98$, $p=.001$, $d=.96$). Conversely, stimulation at the higher alpha-frequency led to faster pre-stimulus alpha activity during active rhythmic-TMS (M=11.11Hz, SE=0.14), relative to sham stimulation (M=10.43Hz, SE=0.31), selectively at the stimulated site ($t(16)=2.19$, $p=.043$, $d=.53$). Finally, stimulation at the exact alpha-frequency did not yield any difference in the pre-stimulus alpha speed ($t(16)=0.13$, $p=.90$, $d=.03$). Moreover, we found that rhythmic-TMS maximally entrained oscillatory activity exactly at the site of stimulation (HEMISPHERExSTIMULATION interaction: $F(1,48)=6.36$, $p=.015$, $\eta_p^2=.117$), and at the entrained rhythm (see Figure 4A).

By contrast, the broadband alpha-amplitude (see Figure 4B) did not differ significantly across the three groups during the entrainment protocol (HEMISPHERExSTIMULATIONxGROUP interaction: $F(2,48)=0.19$, $p=.830$, $\eta_p^2=.008$). However, the entrainment effect on alpha-amplitude (quantified via the difference between active rhythmic-TMS and sham stimulation) was largest at the frequency of stimulation

(FREQUENCYxGROUP interaction: $F(4,96)=5.640$, $p<.001$, $\eta_p^2=.19$).

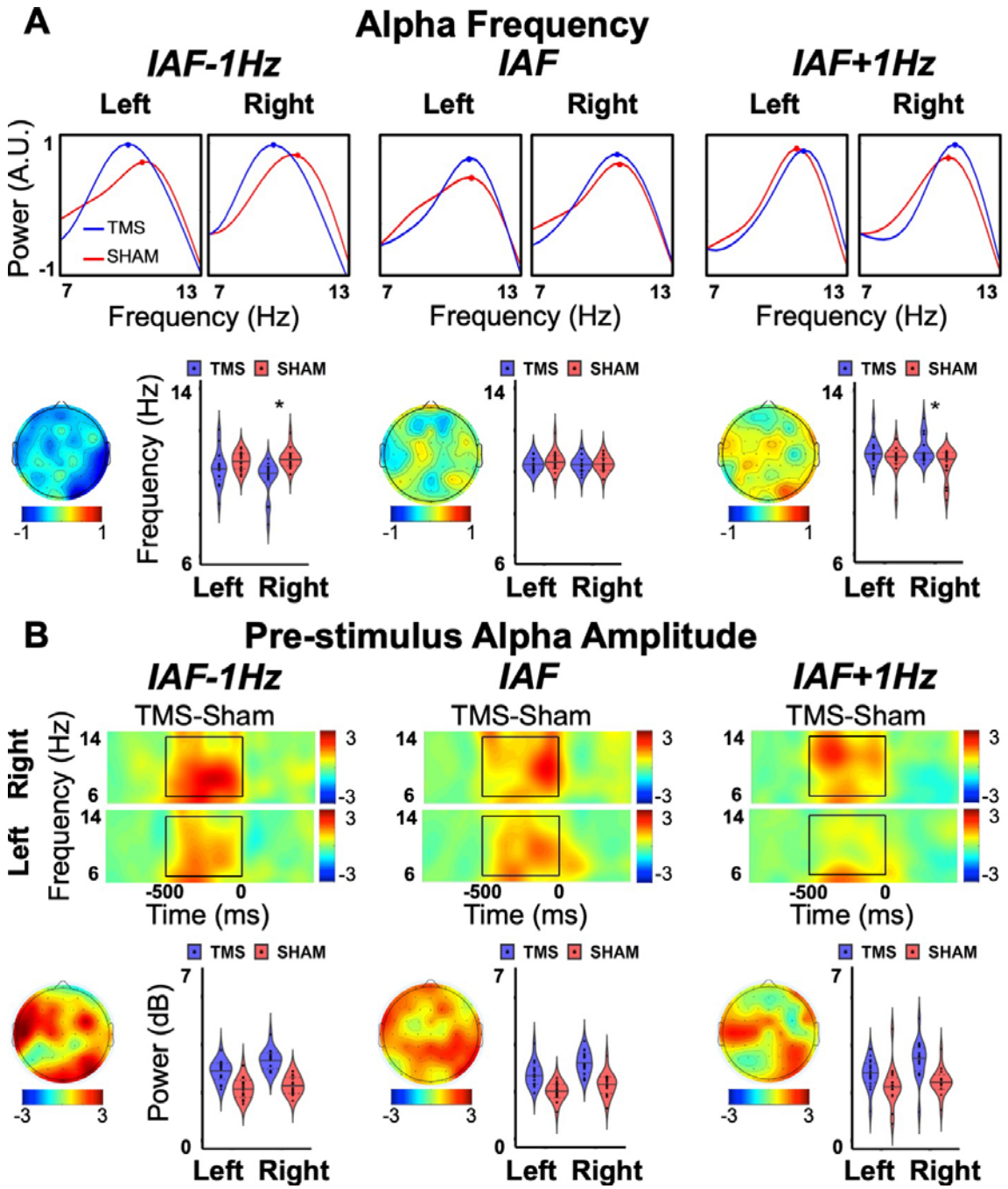

Figure 4. **Results Experiment 2: rhythmic-TMS entrainment modulates EEG alpha-frequency and its amplitude.**

Results are shown for each group performing the task in Experiment 2 under different rhythmic-TMS alpha entrainment protocols (IAF±1Hz, IAF). ***A.*** (Upper) Averaged Alpha-frequency is represented as the z-scored mean power (10*log10[μv2/Hz]) spectrum during rhythmic-TMS in the pre-stimulus time period (-650 0) in the right (stimulated) hemisphere (electrode cluster: O2,PO4,PO8) and left (non-stimulated) hemisphere (electrode cluster: O1,PO3,PO7), for active rhythmic-TMS (TMS) and SHAM-control stimulation. (Lower) Violin plots report peak frequency during TMS and SHAM for each group (IAF±1Hz, IAF) and for the left and right (stimulated) hemisphere. Data are presented as median (full line) ±1 quartile (dashed line). The topography image represents the difference in alpha-frequency between TMS and SHAM stimulation. ***B.*** (Upper) Pre-stimulus alpha-amplitude is presented as time-frequency plots for each group (IAF±1Hz, IAF) of the difference between TMS and SHAM stimulation in the right (stimulated) hemisphere (electrode cluster: O2,PO4,PO8) and in the left (non-stimulated) hemisphere (electrode cluster: O1,PO3,PO7). Black boxes denote regions of statistical analyses (alpha-band 7-13Hz in the pre-stimulus period (-500,0)). (Lower) Violin plots report alpha power during TMS and SHAM for each group, and for the left and right (stimulated) hemisphere. Data are presented as median (full line) ±1 quartile (dashed line). Topography represents the difference in alpha-amplitude between TMS and SHAM stimulation. Two-tailed t-test statistical significance is reported (*p<.05). Error bars represent standard error of the mean. A.U.=arbitrary units;

Diff=difference; μv=microvolt; Hz=Hertz; ms=milliseconds; dB=decibel.

When examining the impact of entrainment on behavior (Figure 5A), we found that speeding up or slowing down alpha oscillations had a direct impact on performance (STIMULATIONxGROUPxHEMIFIELD interaction ($F(1,48)=3.25$, $p=.047$, $\eta p^2=.119$). Specifically, slowing-down pre-stimulus alpha-frequency led to lower d' scores in the active rhythmic-TMS condition (relative to sham stimulation) exclusively in the hemifield contralateral to stimulation ($t(16)=2.67$, $p=.017$, $d=.65$). In contrast, speeding-up pre-stimulus alpha-frequency led to higher d' values during active rhythmic-TMS (relative to sham stimulation), exclusively in the contralateral hemifield ($t(16)=2.52$, $p=.023$, $d=.61$). Finally, entrainment at individual alpha-frequencies did not yield differences in task accuracy, as predicted (all ts$(16)<1.19$, all ps$>.252$, all ds$<.29$). We further tested whether the impact of rhythmic-TMS on EEG oscillatory activity could account for the magnitude of the behavioral modulation induced by the TMS protocol (Figure 5B). To do so, we examined the relationship between sham-corrected performance and sham-corrected entrained frequency across participants (IAF±1Hz groups included). The results reveal that a significant positive relationship exists between the TMS-induced change in oscillatory peak frequency and performance gain ($R^2=0.29$, $p=.001$), further confirming a link between alpha-frequency and performance accuracy.

Our results thus far indicate that pre-stimulus alpha-frequency, but not alpha-amplitude, has a causative role in sampling sensory input, accounting for visual accuracy.

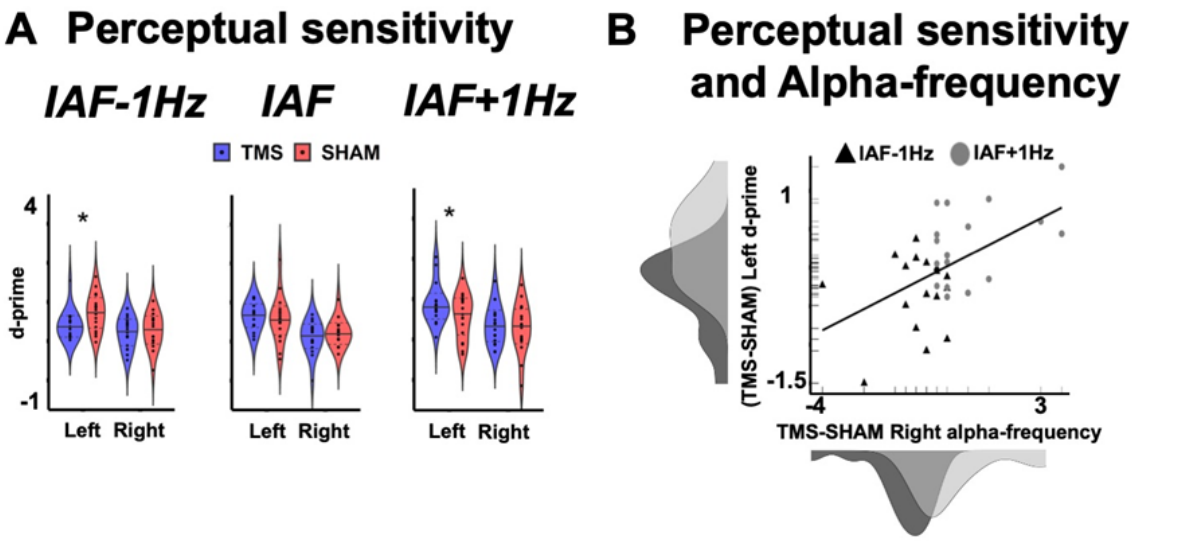

Figure 5. **Results Experiment 2: rhythmic-TMS entrainment causally links alpha speed to perceptual accuracy.**

A. Perceptual sensitivity. Results are presented for three groups of participants (IAF±1Hz and IAF stimulation protocol). Perceptual sensitivity is quantified in d' scores. Violin plots of d' are reported for rhythmic-TMS (TMS) and SHAM-control stimulation, and separately for the left and right hemifields. Data are presented as median (full line) ±1 quartile (dashed line). **B. Perceptual sensitivity and alpha frequency.** Relationship between TMS-induced differences in alpha-frequency in the stimulated (right) hemisphere (computed as a difference in alpha-frequency between TMS and SHAM stimulation) and differences in accuracy in the opposite (left) hemifield (computed as a difference in d' score between TMS and SHAM stimulation), across the slower (IAF-1Hz group, represented as black triangles) and faster rhythmic-TMS groups (IAF+1Hz group, represented as grey circles). Density distributions of the two variables across the two groups are also presented along the corresponding axes. t-test statistical significance is reported (*p<.05).

Alpha-amplitude dynamics shape subjective confidence and metacognition, not accuracy

Another goal of Experiment 2 was to determine whether alpha-amplitude dynamics causally shape subjective representation and interpretation of perceptual performance. However, confidence levels and metacognitive abilities – as measured via confidence mean and meta-d' scores respectively – appeared not to be affected across the three different stimulation protocols nor between the two hemifields, as neither the main effects of GROUP, HEMIFIELD and STIMULATION, nor their interactions, reached significance (all Fs(2,48)< 2.72, all ps>.076, all ηp^2<.102). The short-term nature of entrainment effects might explain these null results, as they are limited to a few hundreds of milliseconds following stimulation (Thut et al., 2011). This is long enough for pre-stimulus TMS entrainment to influence the primary accuracy response, as this was collected immediately

after stimulus presentation. The secondary, higher decision confidence response, however, which was associated with pre-stimulus EEG alpha-amplitude, was collected only 1.5-2 sec post-stimulus (through the confidence prompt) and hence occurred >1 sec after rhythmic-TMS offset (see Figure 2B) when entrainment effects might not be sufficiently sustained anymore. Therefore, in order to further assess the causal role of alpha-amplitude dynamics in perceptual awareness, particularly in metacognitive abilities, we ran a third follow-up experiment aimed at entraining post-stimulus alpha-amplitude in seventeen participants. This group received 5-pulse rhythmic-TMS trains that were tailored to their individual alpha-frequency with pulses applied just before the confidence prompt, i.e., after stimulus presentation (Figure 2C). The aim of this protocol was to enhance alpha-amplitude by rhythmic-TMS without affecting alpha-speed. Importantly, analysis of the alpha-amplitude in the post-stimulus period in Experiment 1 justified the timing of this stimulation, as alpha-amplitude after stimulus presentation (i.e., the time window of stimulation in Experiment 3) was related to subjective confidence (with lower contralateral alpha-amplitude leading to high confidence responses) and metacognitive abilities.

EEG analyses in Experiment 3 revealed a maximal entrainment effect in broadband alpha-amplitude prior to the confidence prompt during active rhythmic-TMS relative to sham stimulation at the stimulated site (HEMISPHERExSTIMULATION interaction: $F(1,16)=6.91$, $p=.002$, $\eta p^2=.302$). Moreover, as expected, the rhythmic-TMS trains at IAF did not have any effect on the alpha frequency measured prior to confidence judgment (all $Fs(1,16)< 0.19$, all $ps>.666$, all $\eta p^2<.012$) (Figure 6). Crucially, this selective modulation of alpha-amplitude right before confidence judgment allowed us to causally test the impact of alpha-amplitude on metacognitive abilities vs. subjective confidence ratings. Our results show clear effects on metacognition, as highlighted by distinct modulations of meta-d' scores, between active rhythmic-TMS and sham stimulation, depending on hemifield

(HEMIFIELDxSTIMULATION interaction: $F(1,16)=4.73$, $p=.045$, $\eta p^2=.228$) (Figure 6C). Specifically, higher alpha-amplitudes prior to the confidence prompt led to lower meta-d' scores during active rhythmic-TMS vs. sham stimulation, exclusively in the contralateral hemifield ($t(16)=2.74$, $p=.014$, $d=.66$). Importantly, these induced changes in post-stimulus alpha-amplitude had a selective impact on metacognitive abilities and not on confidence measures or on perceptual accuracy (*all Fs*$(1,16)<.82$, *all ps*$>.379$, all $\eta_p^2<.049$), thus confirming the role of post-stimulus alpha-amplitude in higher-level post-perceptual decision making.

Finally, we tested whether individual differences in TMS-induced post-stimulus alpha-amplitude modulations could account for the level of metacognitive abilities. To do so, we analyzed the relationship between sham-controlled TMS-induced alpha-amplitude and sham-controlled meta-d' levels for stimuli presented in the contralateral hemifield. We found a significant inverse relationship, confirming that the higher the impact of rhythmic-TMS on alpha-amplitude, the lower the resulting level of metacognition of the individual response ($R^2=0.27$, $p=.032$; *Fig*ure 6D). These results strongly support the role of post-stimulus alpha-amplitude in selectively shaping our metacognitive abilities, with higher post-stimulus alpha-amplitude leading to lower metacognition.

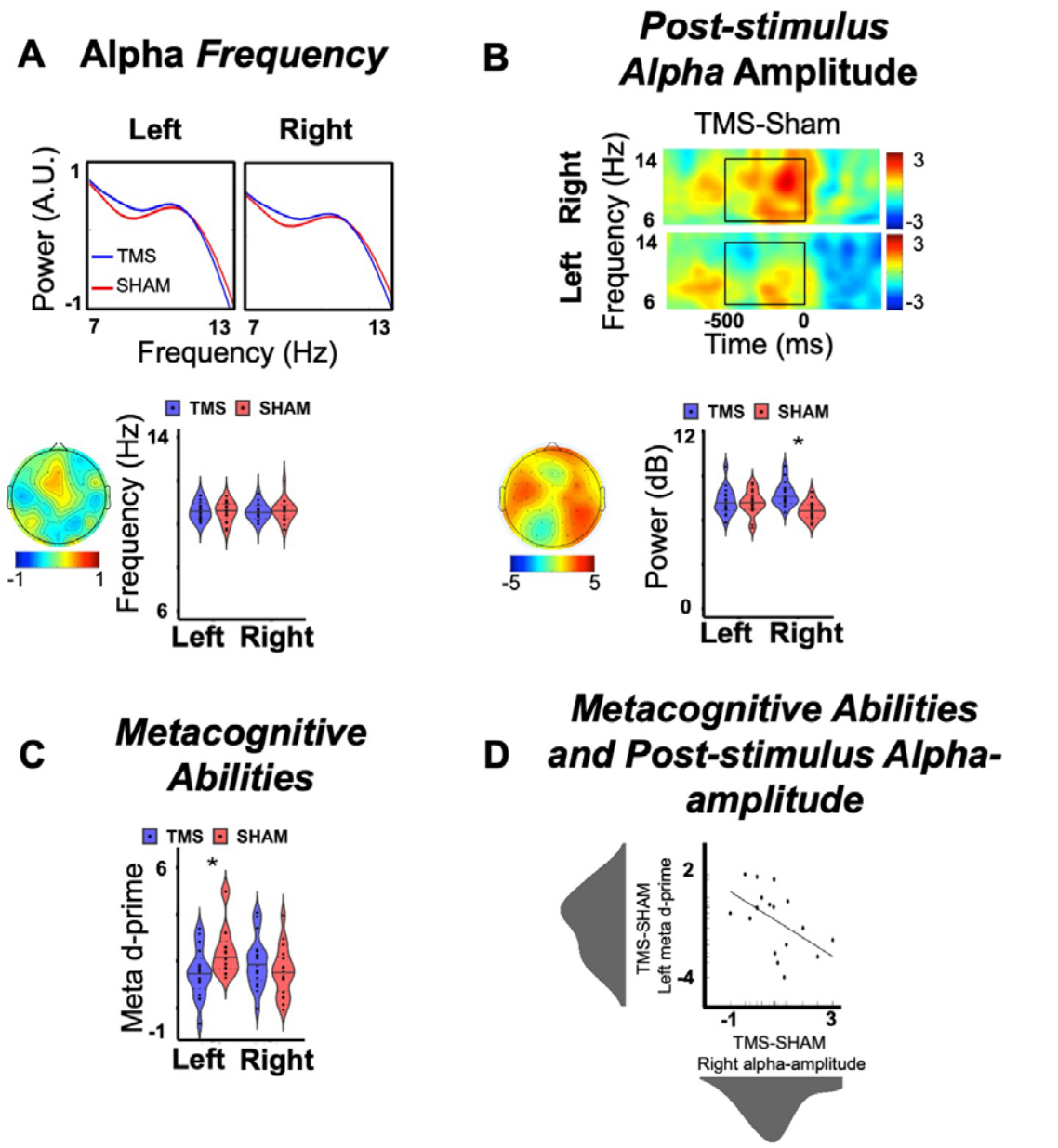

Figure 6. **Results Experiment 3: rhythmic-TMS entrainment causally links post-stimulus alpha-amplitude to metacognitive abilities.**

A. (Upper) Averaged Alpha-frequency is represented as the z-scored mean power (10*log10[μv2/Hz]) spectrum in a pre-confidence time period (850 1500) in the right (stimulated) hemisphere (electrode cluster: O2,PO4,PO8) and in the left (non-stimulated) hemisphere (electrode cluster: O1,PO3,PO7) for rhythmic-TMS and SHAM-control stimulation. (Lower) Violin plots report peak frequency during TMS and SHAM, separately for the left and right (stimulated) hemisphere. Data are presented as median (full line) ±1 quartile (dashed line); Topography represents the difference in alpha-frequency between TMS and SHAM stimulation. **B.** (Upper) Post-stimulus alpha-amplitude reported as a time-frequency plot of the difference between TMS and SHAM stimulation in the right (stimulated) hemisphere (electrode cluster: O2,PO4,PO8) and in the left (non-stimulated) hemisphere (electrode cluster: O1,PO3,PO7). Black boxes denote regions of statistical analyses (alpha-band 7-13Hz in the pre-confidence stimulation period (1000,1500)). (Lower) Violin plots report alpha-power during TMS and SHAM stimulation, and separately for the left and right (stimulated) hemisphere. Data are presented as median (full line) ±1 quartile (dashed line). Topography represents the difference in alpha-amplitude between TMS and SHAM stimulation. **C. Metacognitive Abilities, quantified via meta-d' scores.** Violin plots of meta d' for TMS and SHAM-control stimulation and reported separately for the left and right hemifields. Data are presented as median (full line) ±1 quartile (dashed line). **D. Metacognitive Abilities and Post-stimulus Alpha-amplitude.** Relationship between rhythmic-TMS-evoked differences in alpha-amplitude in the stimulated (right) hemisphere (computed as a difference in alpha-amplitude between TMS and SHAM stimulation) and differences in metacognition in the opposite (left) hemispace (computed as a difference in meta-d' score between TMS and SHAM stimulation). Density distributions of the two variables are also presented along the corresponding axes. Two-tailed t-test statistical significance is reported (*p<.05). A.U.=arbitrary units; μv=microvolt; Hz=Hertz; ms=milliseconds; dB=decibel.

Discussion

Since their discovery, alpha oscillations have been dismissed as mere reflection of a passive idling state. However, a crucial paradigm shift has reversed this long-lasting view in favor of a rather active role played by these oscillations in controlling visual input selection (Hanslmayr et al., 2007). Moreover, in very recent years, this perspective evolved further. The idea that the momentary level of alpha power could predict perceptual performance has been challenged (Limbach & Corballis, 2016). New evidence suggests instead that alpha power modulations reflect the momentary state of the internal decision-making process in performing a given task ranging from conservative (high alpha amplitude values) to liberal choice (low alpha amplitude values) when faced with ambiguous external input.

This new vista has therefore highlighted the need to dissociate the processes that shape perceptual sensitivity from those that shape the subjective interpretation of a sensory event. Here, we disentangle the oscillatory dynamics of these two processes and go beyond a correlative approach. By using an information-based rhythmic-TMS protocol, we demonstrate that distinct markers of alpha activity have a causal role in shaping our conscious perception, a role that goes beyond that of a simple epiphenomenon. By directly manipulating alpha-frequency and -amplitude at the site of stimulation, we were able to dissociate perceptual sensitivity from the subjective representation and interpretation of a sensory event, thus demonstrating their dualistic nature.

The first relevant outcome of our study is based on our EEG findings. These show a double dissociation between pre-stimulus alpha-frequency and alpha-amplitude in terms of their ability to predict objective accuracy versus subjective confidence. Faster alpha oscillations were associated with higher objective accuracy and lower alpha-amplitude with enhanced confidence. The second relevant outcome is that we reveal this relationship

to be causal via the use of brief rhTMS bursts tailored to entrain pre-stimulus alpha activity at the individual endogenous alpha frequency or towards slower vs. faster paces. In line with previous literature, the rhTMS protocol was effective in entraining oscillatory activity recorded over sensors underneath the coil (Albouy et al., 2017; Romei et al., 2016; Thut et al., 2011; Weisz et al., 2014). Specifically, alpha oscillations did align in frequency to the externally imposed rhythm such that faster vs. slower stimulation led to faster vs. slower entrained alpha activity. Moreover, the alpha amplitude was enhanced independently of the chosen alpha frequency of stimulation. Importantly, these entrainment effects had a differential impact on behavior. While slowing-down vs. speeding-up oscillatory alpha activity prior to stimulus presentation led to lower vs. higher task accuracy, respectively, task accuracy was not affected by modulating alpha-amplitude. Conversely, modulation of pre-stimulus alpha-amplitude inversely impacted confidence, but this measure was not affected by changing alpha-frequency. Finally, the impact of stimulation on EEG activity and behavior was topographically and retinotopically specific, with performance being exclusively modulated in the hemifield contralateral to the stimulated site.

Our findings show that the speed of occipital alpha activity has a crucial and selective role in modulating perceptual sensitivity. This adds to previous reports showing that alpha cycles account for sampling sensory information into discrete units/perceptual frames (initially proposed by Varela et al., 2001 and reviewed in VanRullen, 2016). It has been previously reported that the length of an alpha cycle accounts for temporal windows of integration within which an individual is experiencing multisensory illusions (Cecere et al., 2015; Cooke et al., 2019), and accordingly that the individual trial-by-trial variability in frequency can account for the ability to integrate vs. segregate sensory information (Bastiaansen et al., 2020; Samaha & Postle, 2015; Wutz et al., 2018). But why would this effect show even when a sensibly short-lasting stimulus, certainly shorter than one alpha

cycle, is presented, as in our case? With our experimental design (60ms stimulus duration), there is only one chance (sample) to capture the stimulus within an alpha cycle. And what would this tell us about the underlying mechanism? Our data suggest that this sampling is more effective with higher than lower alpha frequencies, even with stimuli as short as 60ms, suggesting that evidence accumulation already starts to differ within one sampling sweep across variations of alpha-frequencies. This can be explained by enhanced processing capacities for shorter than longer cycles because, with the shorter sampling phases, our short-lasting stimulus (60ms) is more likely to be fully comprehended in one perceptual frame. For stimuli of longer durations (e.g., 1000ms), one would expect repeated sampling sweeps to further add to this difference, as more full-sample sweeps can be packed in 1sec at high than low frequencies. In sum, here we claim that in line with existing literature, (Iemi et al., 2019; Samaha & Postle, 2015; Wutz et al., 2018), higher frequencies are expected to aid temporal resolution by creating more sampling frames per second; but our data show that, at the same time, in the context of our specific experiment, higher frequency also means that less time is employed to create a single sampling frame, leading to higher processing capacities. Please note that the role of IAF in having a prominent role in the sensory sampling of short-lasting stimuli has been replicated in a recent study implementing visual detection task with different short-lasting stimuli (Coldea et al., 2022)

Our EEG findings furthermore show an inverse relationship between levels of alpha-amplitude and subjective confidence confirming previous findings (Benwell et al., 2017; Iemi et al., 2017; Samaha, Iemi, et al., 2017). Indeed, pre-stimulus alpha-amplitude has been proposed to relate to internal decision-making variables (Limbach & Corballis, 2016; Samaha, Iemi, et al., 2017) rather than perceptual accuracy per se. Mechanistically, alpha-amplitude modulations have been linked to neural excitability changes that will affect both

signal and noise (Iemi et al., 2017), hence biasing the perceptual report to more subjective (than objective) interpretations of signals (or noise). We propose that this can be equated with the gating of information for conscious access, shaping subjective confidence in the perception of the events (or no-events). Therefore, by dictating enhanced or attenuated neural excitability levels, alpha-amplitude is primarily involved in the generation of decision-making processes without inducing changes in accuracy measures.

Yet, our experimental manipulation by rhythmic-TMS could not verify the existence of a causal link between pre-stimulus alpha-amplitude and confidence. However, several studies have concluded that our sense of confidence is also determined by processes that occur after we make a choice, thus integrating sensory evidence and improving our "metacognitive accuracy," namely the extent to which our confidence is consistent with our probability of being correct (Fleming & Daw, 2017; Murphy et al., 2015; Navajas et al., 2016). Examining post-stimulus alpha-amplitude, Experiments 1 and 3 demonstrate that after lateralized stimuli are presented, perceptually relevant, post-stimulus alpha-amplitude become focused in the hemisphere contralateral to stimulus presentation, with lower alpha-amplitude leading to higher perceptual confidence. Moreover, these levels of post-stimulus alpha desynchronization directly account for metacognitive abilities across participants and can be causally manipulated by rhythmic-TMS. These latter results suggest that post-stimulus alpha modulations may reflect the integration of confidence judgment with the accumulated evidence after stimulus presentation to update and adjust metacognitive decisions (Fleming & Daw, 2017; Murphy et al., 2015). Taken together, these results speak in favor of the relevant role of alpha-amplitude in post-perceptual decision-making. Therefore, it might be possible that pre-stimulus alpha-amplitude dictates the initial level of perceptual bias (effects observed for confidence bilaterally, but not metacognitive effects), that subsequently integrates sensory evidence brought by the

stimulus itself (reflected in hemisphere-specific processes), resulting in a post-perceptual estimation of the performance.

While our experiments show that alpha-frequency and –amplitude, and hence sensitivity and confidence, are dissociable entities, these processes likely work in concert in more ecological situations to maximize the efficiency of our conscious experience. We observed that the entrainment effects on oscillation and perception showed corresponding topographic/retinotopic distributions, with the perception being exclusively modulated in the hemifield contralateral to the stimulated site, suggesting that the oscillatory substrates of effective sampling and subjective confidence could be oriented in space to optimize the allocation of attention resources. Therefore, under controlled conditions (for example, by presenting informative cues (Posner, 1995) or in predictive contexts (Fan et al., 2002) that are associated with spatial priors), one might expect the spatially specific co-occurrence of alpha-frequency and -amplitude modulation that is contralateral to the to-be-attended or expected location (Rihs et al., 2007; Thut et al., 2006). Study 4 of the current work will address this question by looking into the inter-dependency of these two circuits.

In conclusion, our results point to a functional dissociation between the accuracy of what we see and our interpretation of it. We reveal that the sampling of visual information and its subjective interpretation, which are strongly inter-dependent in everyday life, are dissociable in terms of neural mechanisms in oscillatory activity. Specifically, alpha-frequency and -amplitude reflect the activity of these two independent mechanisms that serve complementary functions. Alpha-frequency represents a spatial and temporal sampling mechanism (Haegens et al., 2014; Mierau et al., 2017) that shapes perceptual sensitivity. By contrast, alpha-amplitude dictates more liberal vs. conservative choices in confidence judgments, further modulated with incoming sensory evidence, thus having post-perceptual effect on how these subjective confidence judgments can distinguish

between correct and incorrect decisions (Benwell et al., 2017; Iemi et al., 2017). How these mechanisms interact to give rise to an integrated (or not) sense of our perceptual environment is yet to be addressed. However, we demonstrate that these oscillatory processes can be selectively modulated by non-invasive neurostimulation, offering a foundation for future translational neuroscience approaches and clinical applications.

STUDY 2:
INTER-INDIVIDUAL DIFFERENCES IN THE MALLEABILITY OF BRAIN OSCILLATIONS VIA rhTMS

Abstract

Study 1 demonstrated that alpha parameters can influence perceptual and metacognitive abilities and that these parameters can be successfully regulated via rhTMS. However, there were noticeable between-participant differences in the entrainment outcome that subsequently predicted these behavioral changes. Study 2 aimed to explain these differences by identifying resting-state neural markers that could predict the entrainment outcome. Here we hypothesize that the width of Arnold's tongue, i.e., the frequency offsets that can still lead to entrainment, can be individually modeled for each participant. To this aim, the spectral decomposition of resting-state data was used to extract the spectral curve of alpha activity, serving as a proxy of an individual Arnold tongue. The results showed that the wider the resting-state alpha curve, the higher the entrainment effects during the task when the frequency was shifted toward faster or slower paces. On the contrary, the height of the at-rest alpha curve influenced the entrainment effects selectively during an IAF stimulation, where a higher at-rest spectral curve negatively predicted amplitude-enhancement during entrainment. Possibly, the latter can be explained by a ceiling effect: if, during rest, the targeted neural ensemble is already maximally synchronized in the alpha range, the additional entrainment during the task can have small or null effects. These results not only offer a theoretical model explaining the variance in rhTMS outcomes noticed across different studies but also establish an evaluative tool that could pinpoint individuals that would gain the most out of oscillatory entertainment, both in research and clinical settings.

Introduction

Apart from the novel theoretical insights regarding oscillatory underpinnings of conscious perception, Study 1 has also pointed toward some important aspects regarding the specificity of rhythmic-TMS entrainment protocols (Di Gregorio et al., 2022; Trajkovic et al., 2022). First, it pointed out the importance of individually determined stimulation parameters. Specifically, entrainment protocols can deduce the inter-pulse train interval based on the standard 10 Hz stimulation across all the participants or delivered on individually calibrated frequency, calculated during the resting state or task recording. Previous research would indicate that the modulatory effects are indeed larger if delivered in an individually tailored manner (Coldea et al., 2022; Stecher & Herrmann, 2018). For instance, it was recently shown that attentional bias would be induced only for the IAF stimulation but not IAF +- 2 Hz (Kemmerer et al., 2022). Crucially, the individual approach was also demonstrated to be clinically relevant, as deviations between the IAF and the stimulation frequency predicted NIBS treatment outcomes in depressive patients (Corlier et al., 2019). Importantly, Study 1 demonstrated that the standard 10 Hz stimulation could be inefficient not only because of the lack of precision but also because it can yield distinct consequences based on the IAF of the participant, ranging from lower and higher perceptual acuity for subjects with respectively, higher and lower IAF, or changes in subjective awareness for participants with near-10 Hz IAF (Di Gregorio et al., 2022). Therefore, it is crucial to tailor the rhythmic stimulation protocols to the individual participant or patient across the research and clinical setting.

Second, Study 1 has also shown that there are significant between-participant differences in the entrainment outcome even when the stimulation protocols are individually tailored. Specifically, rhTMS on IAF ± 1 Hz led to speeding-up or slowing-down alpha activity that roughly ranged from 0-2Hz in the actual induced difference across

the participants, while rhTMS on IAF also led to a variable change in alpha-amplitude. Crucially, this variability in entrainment effects correlated with behavioral outcomes, where the more successful entrainment effects led to larger induced behavioral changes (Di Gregorio et al., 2022). How can we explain this variability in the entrainment effects? Does it represent a between-participants random variability, or can we somehow predict it? The potential to identify participants or patients that would better respond to NIBS (Non-Invasive Brain Stimulation) treatments can prove crucial in both research and clinical settings. Therefore, Study 2 aims at explaining these differences by identifying resting-state neural markers that could predict the entrainment outcome. The current theoretical concept of entrainment (the so-called Arnold tongue) predicts the degree of synchronization (entrainment) of an oscillator coupled to a rhythmic driving force, depending on two parameters: the amplitude of the driving force and the driving frequency (Jiménez et al., 2022). With a driving frequency that approaches the intrinsic frequency (here: IAF), entrainment is more likely to occur. On the other hand, frequencies slightly different from IAF (here: IAF – 1Hz and IAF +1Hz) can drive the natural oscillator toward a slower or faster pace, with, however, weaker entrainment effects. However, the model assumes that these variations represent a general rule, therefore, constant across participants. Here we hypothesize that the width and the height of Arnold's tongue, i.e., the frequency offsets that can still lead to entrainment and the baseline amplitude levels, could be individually modeled for each participant, thus allowing the prediction of entrainment effects on an individual level. To this aim, spectral decomposition of resting-state data was used to extract frequency-amplitude curve of alpha activity, that would serve as a proxy of an individual Arnold’s tongue. First, we examined the within-participant consistency of these parameters across different conditions (eyes-open vs eyes-closed resting state). Second, we examined if these parameters could predict entrainment outcomes in Study 1.

Methods

Participants. Data from participants that took part in Experiment 2 and Experiment 3 of Study 1 was also used here in Study 2.

Stimuli and task procedure. EEG data from Experiment 2 and Experiment 3 during the visual discrimination task of Study 1 was also used here in Study 2. Additionally, eyes-opened and eyes-closed resting state data during the EEG recording of the same participants were also used. Specifically, participants were comfortably seated in a dimmed-lit room with their eyes closed (eyes-closed resting state condition) or with a gaze on a fixation cross on a screen while recording their EEG activity for 3 minutes.

Psychophysiological recording – paradigm and acquisition. The EEG recording procedure was the same as in Study 1. Processing of the eyes-open and eyes-closed resting-state data included re-referencing of the signal to the average activity across all electrodes, an offline resampling to 500 Hz, and applying a low-pass (0.5 Hz) and high-pass (50 Hz) filter. Parameters of the alpha activity were then estimated from the O2 electrode, as the rhTMS was applied on this sensor. In order to obtain the local power spectrum, a fast Fourier transformation (FFT) was applied for the alpha range (7-13 Hz), and IAF was estimated as the exact frequency of the local maximum power in the alpha range. Moreover, a Gaussian curve was fitted to the alpha band-limited power spectra, where the amplitude and the width of the curve (defined as the height of the curve's peak and the standard deviation of the Gaussian curve, respectively) were used as a proxy of individuals Arnold tongue. Additionally, to compare alpha synchronization during rest, here defined as a height of the resting-state Gaussian curve of the alpha frequency, with the pre-stimulus alpha-amplitude during visual detection task, we used alpha-amplitude values during the SHAM condition of the task, as obtained in Experiment 1.

Statistical Analyses. To assess the consistency of the alpha parameters across

different conditions, IAF, curve width, and height were compared *between the eyes-open and eyes-closed resting state conditions via* a non-parametric robust correlation estimate (skipped Pearson correlation). The advantage of this correlation coefficient is that it takes into account the presence of bivariate outliers (by excluding them) and, thus is not sensitive to the presence of extreme values in the overall structure of the data (Pernet et al., 2013). Additionally, in order to control for the absence of significant differences between these conditions, paired, two-tailed t-tests were used. Finally, a linear multiple regression analysis was used to test the regression model where different parameters of alpha activity (IAF and curve width and height) would predict entrainment outcomes of Study 1 (defined as the change in frequency or amplitude between the active TMS and SHAM condition). The forward stepwise method was used, starting from the null model and adding each predictor, improving the model the most, one at a time, until the stopping criterion was met.

Results

Inter-condition consistency of resting-state alpha parameters

Previous studies repeatedly demonstrated that there are substantial inter-individual differences in the IAF (Grandy et al., 2013; Mierau et al., 2017), and that these differences could reflect general cognitive abilities (Dickinson et al., 2018; Grandy et al., 2013), memory (Moran et al., 2010) and language processing (Bornkessel et al., 2004), partially explained via genetic variations (Bodenmann et al., 2009; Smit et al., 2006). Based on these results, it has been proposed that at-rest IAF reflects a stable trait, representing a reasonable reference point of NIBS (non-invasive brain stimulation) parameters. Here we aim to further explore this result by comparing different resting-state conditions, such as eyes -open and eyes-closed conditions, as well as parameters that go beyond IAF, like the width and amplitude of the fitted Gaussian to the resting-state power spectrum within the alpha range.

Results obtained here confirm that IAF is indeed stable across the eyes-closed and eyes-open conditions. Specifically, there was no significant difference in IAF across the two conditions (M_{closed}= 10.350; M_{open}= 10.379; t(63) = 0.16, p = .873; d = 0.02), which were also highly correlated (r=.676, CI= [0.494 0.897]). Likewise, the width of the fitted Gaussian curve showed the same trend, thus yielding highly correlated measures (r=.527, CI= [0.339 0.692]), with no differences across the conditions (M_{closed}= 2.027; M_{open}= 2.014; t(63) = 0.40, p = .688; d = 0.05). Additionally, the amplitude of the fitted Gaussian curve was significantly higher for the eyes-closed vs. eyes-open condition (M_{closed}= 11.539; M_{open}= 5.836; t(63) = 0.16, p < .001; d = 1.17), which is expected due to the higher alpha synchronization in the absence of visual stimulation (Pfurtscheller, 1992). Nonetheless, the amplitudes across the two conditions were significantly correlated (r=.377, CI= [0.169 0.578]), with higher alpha synchronization during the eyes-closed condition related to

higher amplitudes during the eyes-open resting state (see Figure 1).

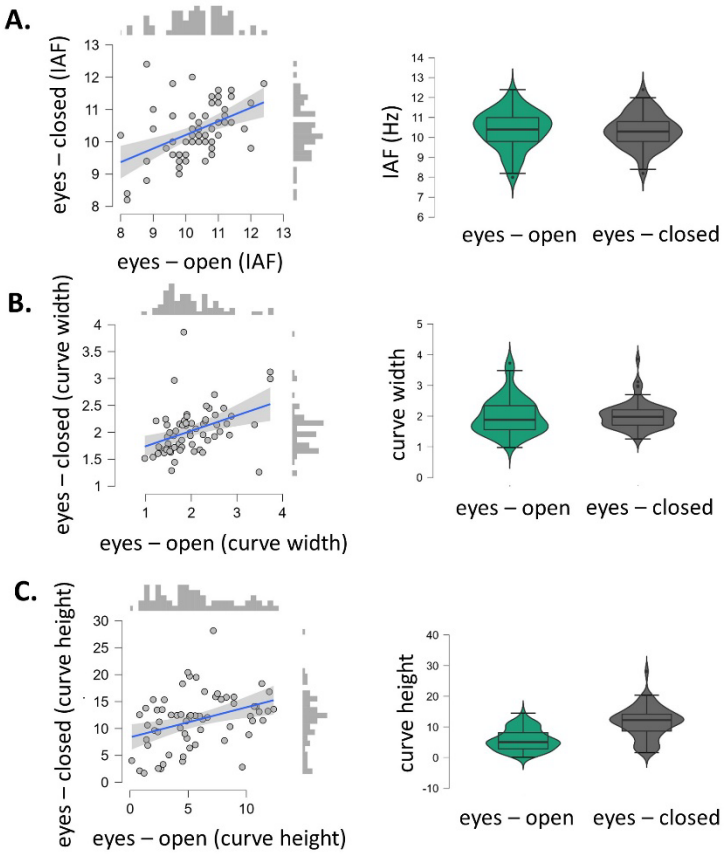

Figure 1. **Consistency of resting-state alpha parameters.**

A. IAF across the eyes-open and eyes-closed resting state. *Left:* Scatter plot with histogram distributions of the IAF (measured in Hz) across eyes-open (x axis) and eyes-closed (y axis) resting state. *Right:* Violin boxplots of the IAF (measured in Hz) across eyes-open and eyes-closed resting state. Middle lines present the median values; the box spans the interquartile range (IQR: from the 25th percentile to the 75th percentile); the whiskers cover 1.5 times the IQR. **B. Curve width across eyes-open and eyes-closed resting state.** *Left:* Scatter plot with histogram distributions of the curve width across eyes-open (x axis) and eyes-closed (y axis) resting state. *Right:* Violin boxplots of the curve widith across eyes-open and eyes-closed resting state. Middle lines present the median values; the box spans the IQR); the whiskers cover the 1.5 times the IQR. **C. Curve height across eyes-open and eyes-closed resting state.** *Left:* Scatter plot with histogram distributions of the curve height across eyes-open (x axis) and eyes-closed (y axis) resting state. *Right:* Violin boxplots of the curve height across eyes-open and eyes-closed resting state. Middle lines present the median values; the box spans the IQR; the whiskers cover the 1.5 times the IQR. Hz = Hertz.

In sum, parameters of alpha activity that could serve to individually calibrate and predict entrainment outcomes seem consistent across different resting-state conditions. Therefore, although these parameters differ across individuals, they seem generally stable within participants across different resting-state conditions. These results are reassuring, as the increased variability across different conditions would question the validity of using

such unstable parameters when selecting the optimal rhTMS target frequency, as well as in predicting entrainment outcomes. The focus of further analysis will be the data obtained during the resting-state eyes-open condition, as it was the condition used in Study 1 to determine stimulation parameters.

The height of the at-rest alpha curve predicts the entrainment effects selectively during an at-peak stimulation (IAF)

Typical entrainment NIBS protocols are focused on increasing alpha-amplitude without inducing changes in alpha-frequency. As previously discussed and as predicted by the Arnolds' tongue, these effects will be maximum for the stimulation on the exact IAF of the participant (Coldea et al., 2022; Di Gregorio et al., 2022; Janssens et al., 2022).

However, could they also depend on individually modeled parameters of the Arnolds' tongue, approximated via fitting of the Gaussian curve to the alpha power spectrum of the participant? Indeed, the results indicate that the height of the Gaussian curve at IAF at-rest could successfully predict the entrainment outcome ($R=0.122$, $\beta=-0.35$, $p= .042$), with higher baseline alpha-peak amplitude leading to lower entrainment effects. On the contrary, the width of the curve and the IAF did not add valuable information to the prediction model of the on-task entrainment outcome ($R<0.034$, $p> .297$): the result that should be expected given that, in this case, there is no deviation from the optimal stimulation frequency (IAF) (see Figure 2).

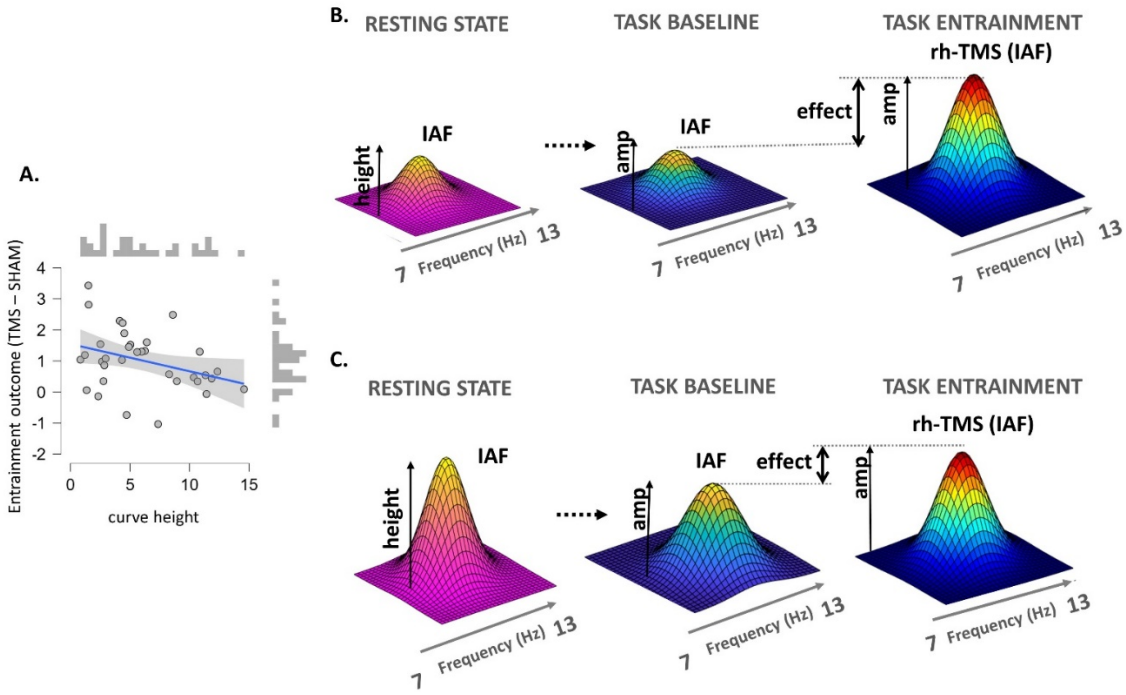

Figure 2. **The height of the at-rest alpha curve predicts the entrainment effects s during an at-peak stimulation (IAF).** **A.** Scatter plot with histogram distributions of the curve height (x axis) as a predictor on on-task entrainment outcome, calculated as a difference of pre-stimulus alpha amplitude during active TMS vs SHAM stimulation (y axis**). B. Model of a participant with lower Gaussian curve during resting state.** It is hypothesized that low-amplitude resting state data would translate into desynchronized (low-amplitude) alpha activity during task, more susceptible to entrainment, evidenced by higher entrainment effects**. C. Model of a participant with higher Gaussian curve during resting state.** It is hypothesized that high-amplitude resting state data would translate into more synchronized (high-amplitude) alpha activity during task. In turn, it is possible that already highly synchronized activity in the alpha range could not be additionally entrained, evidenced by lower entrainment effects. 3D space for Gaussian curves has been used for illustrative purposes.

How could this finding of a more synchronized at-rest alpha having negative effects on at-task entrainment be explained? Possibly, more synchronized alpha during baseline could lead to ceiling effects, where already highly synchronized activity in the alpha range could not be additionally entrained. If that was the case, this high alpha synchronization should be present also during the task, subsequently disabling the maximal entrainment effect when rhTMS occurs. This possibility was tested by comparing resting-state alpha synchronization with pre-stimulus alpha-amplitude during the task in trials without the active rhTMS. Indeed, higher at-rest alpha levels were associated with a lower increase of alpha-amplitude in the pre-stimulus task window (r=-.722, CI= [-0.849 -0.563]) even without stimulation, speaking in favor of a possible ceiling effect stopping alpha from synchronizing further.

The width of the at-rest alpha curve predicts the entrainment effects during an off-peak stimulation (IAF +- 1 Hz)

Although the at-rest IAF can be, at least partially, considered a stable trait, state-dependent alpha-frequency shifts have been well documented. For instance, differences in IAF can drive aspects of visual and temporal processing (Cecere et al., 2015; Coldea et al., 2022; Di Gregorio et al., 2022; Mierau et al., 2017). Therefore, tuning alpha-frequency towards a slower or faster pace is possible via rhTMS and can aid us in understanding the perceptual consequences of such shifts, ultimately leading toward possible therapeutic protocols aimed at enhancing perceptual and temporal sampling in patients.

However, as per stimulation at IAF, even here, there were significant inter-individual differences in the entrainment outcomes, consequently leading to variability in the behavioral effects (Di Gregorio et al., 2022). Here, we aimed to test whether the individual parameters of Arnold's tongue could again aid us in understanding this variability. The results identified the width of the at-rest curve as the most significant predictor of the at-task entrainment outcome towards 1Hz slower or faster pace (R^2=0.463, β=-0.59, p< .001). Specifically, the wider the individual Arnolds' tongue, as approximated via Gaussian fit to the alpha power spectrum, the more successful was the entrainment towards lower or higher frequencies (see Figure 3). Another significant predictor of the model was the IAF (β=-0.38, p= .006), where higher at-rest IAF was more difficult to modulate. Further inspection demonstrated that these differences almost entirely rely on the group where the entrainment aimed at speeding up alpha activity (i.e., the IAF as a predictor remains significant only when including IAF +1 group, β=-0.48, p= .020). Therefore, even in this case, the ceiling effect could play a role: a system tuned at an already high alpha frequency would seem more difficult to further speed-up. Finally, the at-rest height of the alpha curve could not predict the entrainment effects, which is

expected as the stimulation was off-peak, thus not aimed at modulating alpha-amplitude.

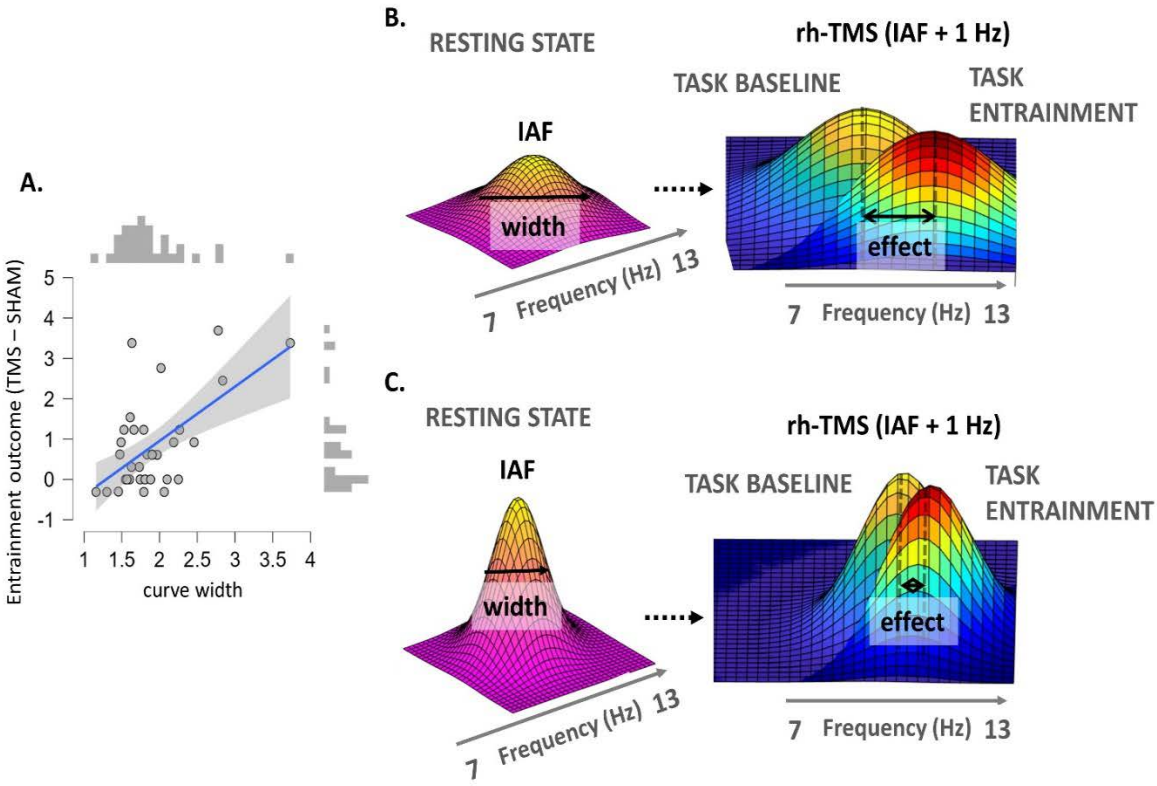

Figure 3. **The width of the at-rest alpha curve predicts the entrainment effects during an off-peak stimulation**

A. Scatter plot with histogram distributions of the curve width (x axis) as a predictor on on-task entrainment outcome, calculated as a difference of pre-stimulus IAF during active TMS vs SHAM stimulation (y axis). **B. Model of a participant with wider Gaussian curve during resting state.** It is hypothesized a wider resting state curve would mean that the alpha-activity of a participant is more susceptible towards off-peak entrainment towards faster or slower alpha pacing, evidenced by higher entrainment effects**. C. Model of a participant with narrower Gaussian curve during resting state.** It is hypothesized a narrow resting state curve would mean that the alpha-activity of a participant is less susceptible towards off-peak entrainment towards faster or slower alpha pacing, evidenced by lower entrainment effects. 3D space for Gaussian curves has been used for illustrative purposes. .

Discussion

In recent years, we have witnessed a sharp rise in the use of a combined TMS-EEG approach, with a grand part of this research dedicated to modulating oscillatory activity via entrainment protocols (Kemmerer et al., 2022; Lin et al., 2021; Miniussi & Thut, 2010). At the same time, not much is known about the parameters that decide the entrainment effects, and that could potentially explain the between-participant variability that is often observed (Janssens et al., 2022).

The rule of thumb is described via Arnold's tongue, whereas the entrainment effects would be largest for the stimulation frequencies closely matching the frequency of the intrinsic oscillator (Jiménez et al., 2022). In terms of entrainment of the alpha frequency, that would mean that the entrainment effects, in terms of the induced increase of the alpha-amplitude, should be largest for the stimulation individually calibrated on the participants' IAF (Janssens et al., 2022; Lin et al., 2021; Trajkovic et al., 2022). Study 1 confirmed this notion while additionally demonstrating that the 1 Hz offsets of the IAF would drive the oscillators towards a slower or faster pace, with distinct behavioral outcomes (Di Gregorio et al., 2022). Nonetheless, a significant inter-individual variability was still observed. The aim of the current study was to explain this variability by hypothesizing that the parameters of Arnold's tongue could be better described on the individual level via Gaussian fitting of the alpha power spectrum (Haegens et al., 2014; Janssens et al., 2022; Van Albada & Robinson, 2013). In other words, the entrainment on the IAF and off-peak frequencies could be better predicted by the intrinsic system parameters shaping the height and the width of the individual spectral curve rather than a general rule applied across the participants. To this aim, we approximated the individual Arnold tongue via Gaussian fitting of the power spectrum in the alpha range during eyes-closed and eyes-open resting state conditions. First, we compared the obtained alpha parameters (IAF, curve width, and

hight) between these two conditions to test their robustness and variability across different cognitive states. Second, we used these parameters to predict entrainment outcomes obtained in Study 1.

First, both the IAF and the width of the fitted Gaussian were highly consistent across the eyes-closed and eyes-open conditions. Likewise, although the curve was higher for the eyes-closed condition, due to the expected higher alpha synchronization in the condition without the visual input (Berger, 1929; D. Cohen, 1968; Pfurtscheller, 1992), the correlation between the two measures remained. Although the fact that the resting-state IAF is an adequate approximation of the on-task entrainment parameters is not a novel finding (Haegens et al., 2014; Janssens et al., 2022), other parameters, such as the width and the height of the Gaussian fit were not previously explored as potential predictors of the entrainment outcomes. Therefore, given their consistency across different experimental conditions, these promising results would encourage their potential use as a valid estimator of the entrainment effects.

Second, entrainment outcomes of the on-task protocol stimulating at at-rest IAF, with the aim of increasing on-task alpha-amplitude, could be best predicted by the height of the at-rest Gaussian curve, i.e., the height of the individual Arnold tongue. Specifically, higher at-rest alpha synchronization would lead to lower entrainment effects in terms of lower alpha-amplitude increase. The most straightforward interpretation of these results would be that the participants that already have highly synchronized alpha activity during rest could experience a ceiling effect during entrainment, where already highly synchronized activity in the alpha range doesn’t have as much space for further entrainment. This interpretation was further confirmed by the additional analysis demonstrating that, even without entrainment, participants that have higher at-rest alpha-amplitude have lower alpha-increase in the pre-stimulus time window during the task. The

practical implication of these results would be that, in order to ensure maximal entrainment effects, the alpha activity of the participant should be desynchronized prior to applying entrainment protocols. For instance, we could expect that highly repetitive and longer task will lead to gradual synchronization of alpha activity (Benwell et al., 2019): thus, we could expect that even entrainment effects would gradually decrease with prolonged task duration, which should be considered when designing entrainment studies.

Third, the width of the individual Arnold tongue successfully predicted entrainment outcomes when stimulating at off-peak frequencies, e.g., when trying to steer alpha activity toward the faster or slower pace. Therefore, participants that have a wider at-rest alpha power spectrum would have more malleable IAF, that could be flexibly tuned towards faster or slower frequencies via rhTMS, subsequently resulting in more accentuated behavioral changes. Although the focus of the current study were the predictors of the entrainment outcome, alpha frequency shifts during the task are present even without entrainment and can be self-regulated and tuned autonomously to adjust to task demands and regulate information processing (Mierau et al., 2017). Therefore, the width of the Gaussian fitting of the at-rest alpha power spectrum could not only predict the flexibility of the IAF when faced with off-peak entrainment, but it might also present a more general marker of the on-task IAF flexibility. In other words, it might represent the ability to regulate the alpha frequency to maximize information processing given the task demands. Future studies should test this hypothesis.

Entrainment effects when stimulating at the off-peak frequencies were also predicted by the at-rest IAF, with higher IAF related to negative entrainment outcomes. Interestingly, the effect was guided by the difficulty of further speeding-up already fast IAF, i.e., the forward shifting of a system that is already working at a maximum speed. As the translational use of entrainment protocols would be to speed up the systems that lack

the appropriate speed and/or flexibility, this particular result should not present an obstacle.

Although the focus of the current study was the entrainment outcome observed via rhTMS in the alpha frequency range, there is no reason to believe that the same parameters would not shape the entrainment outcomes obtained via sensory stimulation or via other NIBS (tACS) or entrainment focused on other oscillatory frequencies. Therefore, future studies should confirm whether the effects obtained here can be generalized across different entrainment approaches and frequencies. Moreover, although here we compare different resting-state conditions, one could argue that the on-task estimation of the IAF and Gaussian fitting would yield more accurate estimates of the entrainment parameters applied during the same task. A previous study comparing on-task and resting-state IAF would argue against this hypothesis, where the resting-state EEG measurements led to more consisting results than task EEG (Janssens et al., 2022), attributed to the difficulty of estimating IAF when alpha is desynchronized during the task. Nonetheless, we cannot exclude the fact that, if possible, on-task estimates would be a more adequate choice. However, if the aim of the clinician or experimenter was to predictively assess the malleability of the participant's system towards the entrainment, the use of resting-state measures would be a more practical choice.

In sum, the current study investigated the predictors of the rhythmic stimulation outcome and demonstrated that not only a careful calibration of the frequency (IAF) but also the width and the height of the individual alpha power spectrum, here defined as individual Arnold tongue, could aid us to understand the variability of the entrainment effects and ultimately seeking the way to enhance them. For instance, these results could aid future research and the way we design entrainment protocols, select participants, and interpret the results, but they also can, at least in part, help us interpret conflicting results and small effect sizes obtained in the past. From the translational perspective, it can guide

future clinical studies in personalizing entrainment protocols and predicting the treatment outcomes, e.g., in NIBS treatment of schizophrenia, depression, and chronic pain (Janssens et al., 2022; Tremblay et al., 2019).

STUDY 3:
PRESTIMULUS ALPHA FREQUENCY AND AMPLITUDE PREDICT THE GENESIS OF P1 LATENCY, AND P3 EVOKED RESPONSE AMPLITUDE

Abstract

Whether prestimulus oscillatory brain activity contributes to the generation of post-stimulus-evoked neural responses has long been debated and empirically investigated, but findings remain inconsistent. Based on recent research that has deepened our understanding of the functional role of prestimulus alpha-frequency and -amplitude in predicting perceptual accuracy and confidence, respectively, we here re-tested the oscillatory model of ERP genesis. By causally manipulating individual prestimulus alpha-frequency and -amplitude, we directly tested for a causal relationship between oscillatory activity in the generation of specific evoked components, namely the C1/P1- and P3-components that have previously been associated more with perceptual accuracy versus awareness. First, the hypothesized relationship was investigated by means of EEG recordings during a perceptual task, where measures of perceptual accuracy and subjective judgments were collected. Second, the hypothesized association was causally probed by means of online rhythmic Transcranial Magnetic Stimulation (rhTMS). A significant negative relationship was found between IAF and P1 latency, with faster pre-stimulus IAF being related to shorter P1 latencies. At the same time, faster IAF and shorter P1 latencies were both associated with higher task accuracy. Crucially, slowing-down IAF via rhTMS significantly delayed P1 latencies in the (same) right hemisphere while speeding up IAF significantly anticipated the same P1 component. On the other hand, a negative relationship was found between alpha- and P3 amplitude, whereas low alpha-amplitude was accompanied by higher P3 responses. At the same time, these lower alphas and higher P3 amplitude led to lower confidence ratings. Finally, induced higher pre-stimulus alpha-amplitude lowered the P3 component. Our results provide fundamental evidence in favor of the oscillatory model of ERP genesis, shedding new light on the relationship between prestimulus oscillations and the genesis of functionally significant evoked components.

Introduction

Intrinsic ongoing brain oscillations represent more than mere background noise. This notion is supported by increasing theoretical and empirical work prompting the idea that oscillatory activity is an important fingerprint of cognitive and perceptual performance (Palva & Palva, 2007). The findings that perceptual performance to a stimulus is influenced by prestimulus oscillations - capturing ongoing activity before any stimulus is presented - is in support of this view (Benwell et al., 2017; Di Gregorio et al., 2022; Iemi et al., 2017; Limbach & Corballis, 2016; Romei et al., 2008, 2010; Samaha et al., 2017). By affirming the functional significance of ongoing (e.g., prestimulus) oscillations that goes beyond "random noise" and thus having a crucial role in the timing of sensory and cognitive processes, it becomes tempting to think that they also play a crucial role in shaping post-stimulus event-related potentials (ERPs) (Klimesch et al., 2007). These observations have cast doubts on the "evoked model" that is based on a strict distinction between ERPs, understood as a stimulus-evoked response of constant latency and polarity, and ongoing electroencephalographic (EEG) oscillations (Klimesch et al., 2004; Mazaheri & Jensen, 2010). The alternative view, known as the "oscillatory model," contradicts complete independence between background EEG activity and ERPs, stating that, at least in part, evoked responses are generated from a reorganization of the ongoing oscillations (Klimesch et al., 2004).

What is the proposed mechanism behind this oscillatory model? Some studies have suggested that, due to the stimulus presentation, oscillations of different frequencies undergo resetting and, as a result, become synchronized in absolute phase, thus generating ERP components (Fuentemilla et al., 2006; Gruber et al., 2005; Hanslmayr et al., 2007; Klimesch et al., 2004; Makeig et al., 2002; Sauseng et al., 2007; Sayers et al., 1974). Indeed, they were able to demonstrate that oscillations across different frequency ranges

sustain a phase reset and become synchronized in a time window within the P1-N1 complex (Gruber et al., 2005; Hanslmayr et al., 2007; Makeig et al., 2002). However, most of the arguments and predictions used to dissociate the evoked and the phase resetting model have been proven inconclusive due to methodological difficulties in clearly dissociating the two proposed models (Klimesch et al., 2007). Therefore, it has been suggested that phase reset represents only one of the possible mechanisms that can explain the association between ongoing oscillatory activity and ERPs (Klimesch et al., 2007). In accordance with this claim, it has been demonstrated that the phase of oscillatory alpha activity could be preserved after stimulus onset with respect to the phase before the stimulus, thus questioning phase-resetting of alpha activity as a primary generator of visual ERPs (Mazaheri & Jensen, 2010). Based on these results, the authors argued that ERPs and ongoing oscillations could represent separate neuronal events, leaving however open the possibility that pre-stimulus alpha oscillations can modulate the generation of ERPs, in line with findings that they can modulate perception (Benwell et al., 2017; Di Gregorio et al., 2022; Iemi et al., 2017; Limbach & Corballis, 2016; Romei et al., 2008, 2010; Samaha et al., 2017).

Although a point of debate now for over two decades, researchers have failed to come to an agreement and demonstrate the exact origins of ERPs (Klimesch et al., 2007). In particular, a long debate has been ongoing regarding the possible association between visually evoked components and ongoing oscillatory activity in the alpha band. Influential theories have proposed an active role of alpha-oscillations in sensory processing, where the neural synchronization in the alpha range would represent a momentary index of visual brain excitability with lower and higher amplitude indexing higher and lower cortical excitability, respectively (Romei et al., 2008). Moreover, this perspective evolved further in recent years. Specifically, in Study 1, we empirically identified the role of distinct

parameters of alpha activity in shaping perceptual accuracy and subjective experience of that accuracy and demonstrated that they could be causally dissociated. Briefly, it was found that controlling alpha-frequency by rhTMS modulated perceptual accuracy but not the subjective confidence in it while enhancing alpha-amplitude reduced confidence but not accuracy. These findings provided the first causal evidence of a double-dissociation between alpha-frequency and -amplitude, linking alpha-frequency to the neural pace of information sampling (Cecere et al., 2015; Cooke et al., 2019; Migliorati et al., 2020; Minami & Amano, 2017; VanRullen, 2016), and alpha-amplitude to the level of neural excitability and conscious access to both signal and noise (Benwell et al., 2017; Iemi et al., 2017; Limbach & Corballis, 2016; Samaha, Iemi, et al., 2017).

Here, we hypothesize that the novel findings on the dissociable role of alpha frequency and amplitude in conscious perception may, at least in part, explain the contradictory results obtained thus far in regard to the oscillatory vs. evoked model of ERP genesis. If different aspects of prestimulus brain oscillations are causally modulating different aspects of perceptual performance such as accuracy and awareness, then entraining these oscillations should also modulate post-stimulus event-related potentials along their functional association with these perceptual performance measures, and in support of an oscillatory model. Specifically, we hypothesize that controlling prestimulus alpha oscillations in their frequency and amplitude through rhTMS will differently affect early and late post-stimulus event-related potential components such as the C1/P1 versus the P300. This is because C1 and P1 are mainly generated in striate and extrastriate visual areas (e.g., Di Russo et al., 2002), should hence more directly reflect the veridical sensory evidence and by extension, be more associated with accuracy. By contrast, the P300 is of a centro-parietal origin and has been related to sensory readout for decision-making (O'Connell et al., 2012), and subjective awareness/ consciousness of a stimulus (Lamy et

al., 2009; Salti et al., 2012) rather than the objective, physically presented evidence (Tagliabue et al., 2019), and hence should be associated more with subjective appraisal of perception.

Given these considerations, we therefore expected that by controlling prestimulus alpha-frequency through rhTMS, we will modulate the efficiency of sensory processing both neurally and in terms of performance (e.g. observe earlier C1/P1-latencies and/or higher C1/P1-amplitudes the faster the prestimulus alpha-frequency, alongside enhanced accuracy). On the other hand, we expected that controlling prestimulus alpha-amplitude through rhTMS would influence the later P3 component (latency or amplitude) as part of a mechanism that shapes subjective stimulus evaluation.

By means of EEG-recording during a perceptual task, we first tested the existence of a relationship between prestimulus alpha-frequency, the C1/ P1-components, and perceptual accuracy on the one hand, and prestimulus alpha-amplitude, P3-component and perceptual confidence on the other hand (Experiment 1). Secondly, non-invasive brain stimulation was used to causally test the oscillatory model of ERPs genesis by directly demonstrating a causal dissociation of different parameters of alpha activity in the genesis of distinct ERP components (Experiment 2).

Methods

Experiment 1.

Participants: Forty-one healthy volunteers with normal or corrected vision participated in Experiment 1 (23 females; mean age ± SE = 23.31 ± 1.66 years), recruited at the Centre for Studies and Research in Cognitive Neuroscience in Cesena, Italy. The study respected the Declaration of Helsinki and was approved by the bioethics committee of the University of Bologna. All participants signed the informed consent to take part in the study.

Stimuli and task procedure. Stimuli and task procedure were the same as per Experiment 1 of Study 1.

Titration session. The titration procedure was already reported in Experiment 1 of Study 1.

Psychophysiological recording – paradigm and acquisition. EEG data were collected as per Experiment 1 of Study 1. EEG data were pre-processed using custom-made routines in MatLab R2013b (The Mathworks, Natick, MA, USA). EEG data were re-referenced off-line to the average of all electrodes and filtered with a 0.5–30 Hz pass-band. After applying a filter, stimulus-locked epochs were extracted (from -1500 ms to 2500 ms after stimulus presentation). Artifact-contaminated trials were excluded via pop_autorej function in EEGLAB v13.0.1 (Delorme & Makeig, 2004), which excludes high-voltage (fluctuations larger than 1000 μV) and trials identified as outliers (trials with data values outside 5 SD). Subsequently, artifacts related to eye movement were corrected via a procedure based on a linear regression method (lms_regression function in MatLab R2013b) (Gratton et al., 1983). As per Study 1, electrode positions were recorded as contralateral versus ipsilateral respect to the hemifield where the stimulus was presented (resulting in all contralateral activity being on one side, which was conventionally defined

to be the right) (Di Gregorio et al., 2022; Trajkovic et al., 2022).

Psychophysiological recording – EEG analyses. Alpha oscillations (frequency and amplitude) were analyzed in a pre-stimulus time window between -400 ms and stimulus presentation in a cluster of contralateral and ipsilateral parieto-occipital electrodes (O1, O2, Po3, Po4, Po7, Po8).

In order to identify the alpha-frequency peaks during the task, a fast Fourier transformation (MatLab function spectopo, frequency resolution: 0.166Hz) was applied. For each participant and condition, power was calculated and normalized by z-score decibel (dB = 10*log10[-power/baseline]) transformation at each frequency. IAF was defined within the contralateral cluster as the local maximum power in the electrode with the largest power within the frequency range 7-13Hz (i.e., alpha peak) (Di Gregorio et al., 2022; Trajkovic et al., 2022).

As per Study 1, alpha-amplitude was calculated via time-frequency analyses of data epoched from 2000ms before to 2000ms after the stimulus onset, with mean alpha (7-13Hz) amplitude computed in the cue-stimulus interval (-400 ms to stimulus presentation). The electrode within the contralateral parieto-occipital cluster with the most negative power was selected for the analyses of alpha-amplitude.

ERP data were analyzed using custom routines in MatLab (Mathworks, Natick, MA) and EEGLAB. In line with previous studies, the P100 amplitude and latency were calculated at the most positive peak in a time window between 70 ms and 130 ms relative to the stimulus onset (Klimesch et al., 2004) and at the same electrode as for the pre-stimulus alpha. The P300 was quantified as the mean amplitude between 100 ms and 500 ms relative to the stimulus onset at a centroparietal electrode (i.e., Cz) (Sannita et al., 2001).

Statistical Analyses. To investigate the possible relationships between inter-subject

differences in alpha oscillatory activity (pre-stimulus IAF and alpha amplitude), ERPs (latency/amplitude of P1 and latency/amplitude of P3), and behavior (task accuracy and confidence), non-parametric robust correlation estimates were used (skipped Pearson correlation). The advantage of this correlation coefficient is that it considers the presence of bivariate outliers (by excluding them) and thus is not sensitive to the presence of extreme values in the overall structure of the data (Pernet et al., 2013).

Experiment 2.

Please note that the experimental procedure (participants and experimental task) is the same as in Experiment 2 of Study 1. However, here the focus of analysis is on the post-stimulus ERPs rather than behavior or pre-stimulus oscillatory activity.

Participants. The same participants that took part in Experiment 2 of Study 1, were here included (N = 51).

Stimuli and task procedure. Task procedure in Experiment 2 was the same as those in Experiment 1, with additional active manipulation of alpha activity via an entrainment protocols.

Entrainment of the alpha activity was achieved using rhTMS. For a complete description, see Experiment 2 of Study 1.

Titration session. Titration was run as for Experiment 1. Additionally, in Experiment 2, individual alpha peak frequency was determined in order to calibrate rhTMS frequency in the same manner as per Experiment 2 of Study 1.

EEG recordings –acquisition and processing. EEG data were collected as in Experiment 1, with the only difference in higher sampling rate applied here (5000Hz instead of 1000 Hz used in Experiment 1), as a higher sampling rate in online TMS-EEG protocols in strongly advised (Veniero et al., 2009).

Additional processing steps included cutting and interpolating (cubic interpolation)

time points around the TMS-pulses, as well as performing Independent Component Analysis (ICA) to deal with potential artifacts. Specifically, a fastICA algorithm is used (pop_tesa_fastica function to identify individual components representing artifacts, as well as automatic component classification (pop_tesa_compselect function)(Rogasch et al., 2017), where each component should be subsequently manually checked and reclassified when necessary (for more details see Trajkovic et al., 2022).

For the subsequent analysis of the ERPs, only correct trials with stimuli contralateral to the stimulation site (stimuli in LVF) were considered. The EEG data were then averaged across trials. Time windows for detecting peak amplitudes and their latencies were the same as per Experiment 1 (60–130 ms for the P1 and 200–400 ms for the P3). Likewise, the electrodes considered for P1 (O2, PO8, and PO4) and P3 (Cz) components were also kept constant across participants and the two experiments.

Statistical Analyses. Differences in ERPs (P1 latency and P3 amplitude) were explored across three experimental GROUPS (IAF-1Hz, IAF, and IAF+1Hz group) and the two STIMULATION protocols (TMS and SHAM stimulation) in 2 × 3 repeated measures mixed-model ANOVAs. Subsequently, specific differences between conditions were tested via two-tailed t-tests (planned comparisons).

Results

Dissociating oscillatory underpinnings and behavioral correlates of the P1 and P3 evoked response

The first goal of this study was to investigate and possibly dissociate the oscillatory underpinnings and behavioral correlates of early (C1/P1) and later (P3) visually evoked responses. To this aim, we measured in a first experiment pre-stimulus alpha oscillatory activity (Figure 1A) and ERPs (Figure 1B) during a visuospatial perception task in which participants were requested to provide accurate responses and confidence ratings (for details, see Methods).

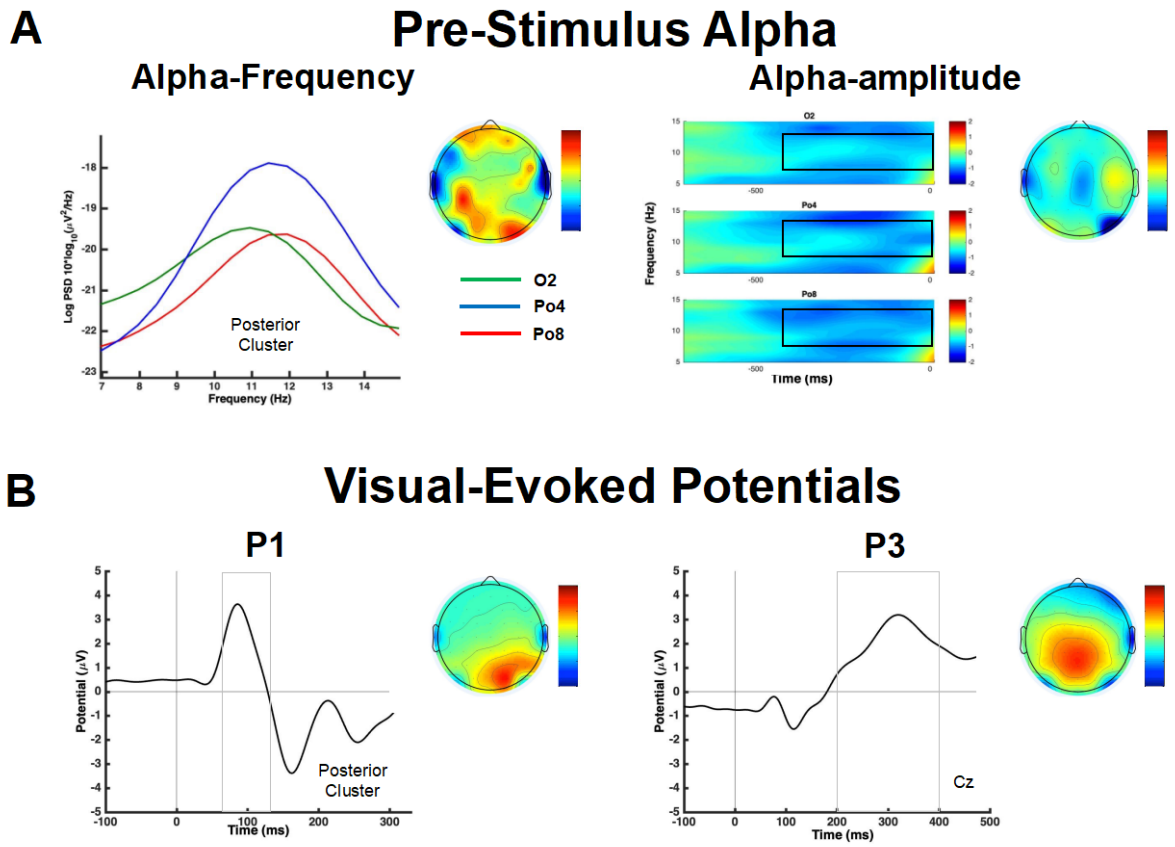

Figure 1. **Prestimulus alpha amplitude and visual evoked potentials.**

A. Pre-stimulus Alpha parameters: On the left column, averaged alpha-frequency is represented as the mean Power Spectral Density (PSD) (10*log10[mv2/Hz]) in the pre-stimulus time period for the contralateral posterior cluster (Po8, Po4, and O2). Topography represents the distribution of the Individual Alpha-frequency peaks. On the right column, Prestimulus alpha amplitude is reported as time-frequency plots in the contralateral posterior cluster. Black boxes denote regions of statistical analyses. Topography represents the distribution of alpha amplitude (electrodes are flipped to have contralateral activity in the right-hand side and ipsilateral activity in the left-hand side). **B Visual-Evoked Potentials:** Grand average stimulus-locked ERP waveforms at Posterior cluster (on the left column) and at electrode Cz (on the right column). Shaded gray bars denote regions of statistical analyses (between 70 and 130 ms for the P1 and between 200 and 400 ms for the P3). Topographies represent the amplitudes of positive peaks in the P1 and P3 time windows (electrodes are flipped to have contralateral activity in the right-hand side and ipsilateral activity in the left-hand side). µv, microvolt; Hz, hertz; ms, milliseconds.

The first important finding is that the pre-stimulus alpha frequency (IAF) negatively correlated with the latency of the P1-evoked response to the presented visual stimulus (r=-0.697, CI= [-0.799 -0.573]). No relationship was found with P1 amplitude (r=-.213, CI= [-0.521 0.103]). In other words, the faster the pre-stimulus IAF, the earlier the P1 of the same amplitude. Crucially, both pre-stimulus alpha frequency and latency of the P1 component seem to be closely related to task outcome. Specifically, faster alpha frequency and earlier P1 latencies were both associated with higher task accuracy as

measured via d-prime score (alpha frequency: r=0.408, CI= [0.135 0.633]; p1 latency: r=-0.309, CI= [-0.561 -0.024]). No relationship was found with P1-amplitude (r=-0.092, CI= [-0.413 0.202). In addition, control analyses confirmed the specificity of these relations, as neither latency nor amplitude of the P3 component was associated with IAF (P3 latency: r=0.104, CI= [-0.251 0.505]; P3 amplitude: r=0.220, CI= [-0.140 0.535]) or task accuracy (P3 latency: r=0.056, CI= [-0.231 0.334]; P3 amplitude: r=0.107, CI= [-0.219 0.437]).

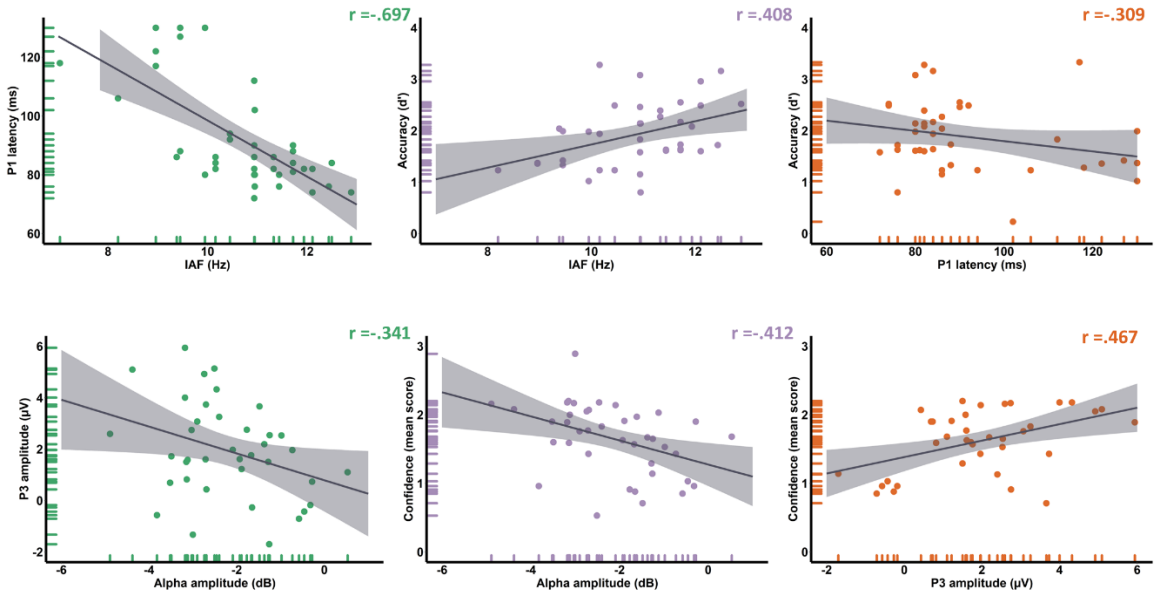

Figure 2. **Results of experiment 1: Dissociating oscillatory underpinnings and behavioural correlates of the P1 and P3 evoked response.**

A. Correlation plots between pre-stimulus alpha activity (IAF, upper plot and alpha-amplitude, lower plot) **and ERPs** (P1 latency, upper plot and P3 amplitude, lower plot). **B. Correlation plots between pre-stimulus alpha activity** (IAF, upper plot and alpha-amplitude, lower plot) **and behavioral outcomes** *(*accuracy, upper plot and confidence, lower plot). **C. Correlation plots between ERPs** (P1 latency, upper plot and P3 amplitude, lower plot) **and behavioral outcomes** (accuracy, upper plot and confidence, lower plot). All correlations presented in the figure were significant as estimated via robust Pearson skipped correlations. Grey shades around the regression line present 95 % confidence interval, as estimated via linear model. ms, milliseconds; Hz, hertz; mv, microvolt; dB, decibel; d', d-prime.

On the other hand, pre-stimulus alpha-amplitude was closely related to the amplitude of the subsequent P3-evoked response. Specifically, lower alpha amplitude prior to the stimulus was associated with higher P3 amplitude (r=-0.341, CI= [-0.575 -0.068]) but did not significantly correlate with the P3 latency (r=.021, CI= [-0.273 0.295]). Furthermore, this lower alpha amplitude and the higher amplitude of the P3 component both predicted perceptual confidence levels (alpha amplitude: r=-0.412, CI= [-0.643 -

0.155]; P3 amplitude: r=0.467, CI= [0.175 0.698]), with lower alpha/higher P3 amplitude being associated with higher confidence ratings. No relationship was observed between confidence ratings and P3 latency (r=0.215, CI= [-0.056 0.497]). Moreover, the P1 evoked response did not seem related to prestimulus alpha-amplitude (P1 latency: r=0.151, CI= [-0.091 0.381]; P1 amplitude: r=0.155, CI= [-0.015 0.489]), and did not exert any effect on confidence ratings (P1 latency: r=-0.026, CI= [-0.430 0.334]; P1 amplitude: r=-0.253, CI= [-0.473 0.139]), thus demonstrating the specificity of the association of alpha-amplitude with the P3-magnitude and confidence measures. For all correlation plots, see Figure 2.

Analyses of C1 were inconclusive (as undetectable in some participants), although our design (with the stimuli consisting of checkerboards) should have allowed for testing C1-responses.

Causally confirming the dissociation between oscillatory underpinnings of the P1 and P3 evoked response

In Experiment 1, we were able to reveal a double-dissociation of oscillatory parameters in the alpha-band (frequency and amplitude, respectively) as to their electrophysiological correlates in the P1 and P3 evoked response components. In Experiment 2, we directly manipulated these pre-stimulus alpha parameters in order to test whether they may causally underlie these subsequent evoked response component effects (namely modulations in P1 latency and P3 amplitude, respectively). Specifically, in three distinct groups of participants, we applied a 5-pulse rhythmic-TMS train of fixed intensity (60% of the maximum stimulator output) to the right posterior cortex prior to stimulus presentation. In the IAF ± 1 Hz groups, the rhTMS frequency was set at 1 Hz slower/faster than the participant's IAF, which should entrain their alpha oscillations toward a slower/faster pace, respectively. In the IAF group, the rhythmic-TMS frequency was

aligned with the participant's IAF, which should lead to enhanced alpha amplitude via entrainment (Miniussi & Thut, 2010). Along with active stimulation, sham stimulation at the matching frequency was also implemented for every participant to account for any nonspecific effects of rhTMS. Experiment 2 of Study 1 reported the electrophysiological results confirming the expected rhTMS outcome during the stimulation itself: IAF was successfully slowed down/ speeded up in IAF-1/IAF+1 group, while there wasn't any modulation of the alpha speed in IAF group. On the other hand, the broadband alpha-amplitude was enhanced across all of the active entrainment protocols, with the maximum entrainment effect at the exact stimulation frequency (Di Gregorio et al., 2022; Trajkovic et al., 2022). In the same study, behavioral outcomes of these entrainment protocols were also reported, linking the changes in IAF and alpha amplitude to perceptual accuracy and confidence (Di Gregorio et al., 2022), which were again confirmed here in Experiment 1. Therefore, the focus of the current analysis will be on the effects of the rhTMS protocols on subsequent ERPs.

Our results showed that the latency of the P1 evoked component in the two hemispheres depended on TMS and SHAM stimulation and the experimental group of the participants (Figure 3, STIMULATIONxGROUP interaction, $F(2,48) = 6.18$; $p = .004$; $\eta p2 = .205$). Further exploration of the data confirmed that slowing-down pre-stimulus alpha-frequency by rhTMS led to longer P1 latencies during active compared to sham stimulation in the stimulated (right) hemisphere ($M_{tms}= 90.23$; $M_{sham}= 84.63$; $t(16) = 2.46$, $p = . 026$; $d = 0.60$). In contrast, speeding-up the right-hemisphere alpha frequency led to shorter P1 latencies during active (vs. sham) stimulation in the same (right) hemisphere ($M_{tms}= 77.67$; $M_{sham}= 84.18$; $t(16) = 2.62$, $p = . 019$; $d = 0.63$). Finally, as hypothesized, inducing higher alpha amplitude in the right hemisphere did not yield any differences in the P1 latency ($M_{tms}= 87.27$; $M_{sham}= 87.23$; $t(16) = 0.15$, $p = . 988$; $d = 0.04$).

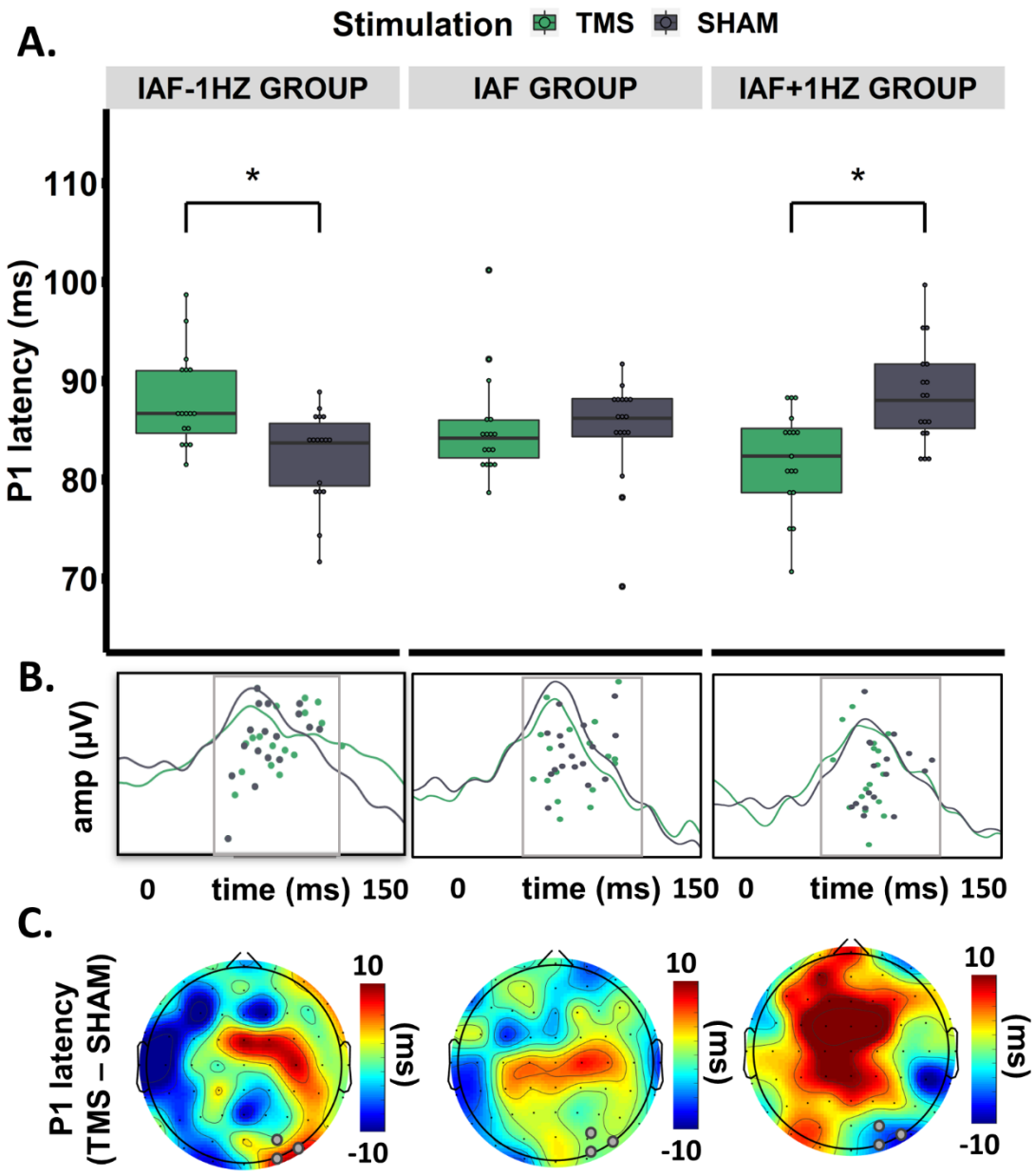

Figure 3. **Results of experiment 2: Rhythmic-TMS entrainment modulates the P1 latency.**

A. Box plots report P1 latency calculated on the near-stimulation posterior cluster (electrodes O2, PO8, PO4), during TMS and SHAM for each group (IAF ± 1 Hz, IAF). Data are presented as median (full line) ± 1 quartile (box limits). **B.** Visual-Evoked Potentials: Grand average stimulus-locked P1 waveform at the near-stimulation posterior cluster (electrodes O2, PO8, PO4) for each group (IAF ± 1 Hz, IAF), separately for TMS (green line) and SHAM (grey line) condition. Shaded gray bars denote regions of statistical analyses (between 70 ms and 130 ms). **C.** Topographies represent the difference in P1 latency between TMS and SHAM stimulations for each group (IAF ± 1 Hz, IAF). Two-tailed t-test statistical significance is reported (*$p < 0.05$). mv, microvolt; Hz, hertz; ms, milliseconds; amp, amplitude.

While the above confirmed that pre-stimulus alpha-frequency, but not alpha-amplitude, has a causative role in the genesis of the P1 component, we also aimed to determine whether modulations of alpha-amplitude in turn, causally shape the amplitude of

the P3 response (Figure 4). Indeed, we found that the P3 amplitude depended on the stimulation protocol across all three groups of participants (STIMULATION effect, $F(2,48) = 10.22$; $p = .002$; $\eta p2 = .176$). Therefore, the induced higher alpha amplitude present in all the groups (Di Gregorio et al., 2022) led to lower P3 amplitude during active (vs. sham) stimulation in the stimulated hemisphere. Descriptively, the difference between the active TMS and SHAM is the highest for IAF group (M_{tms}= 1.945; M_{sham}= 2.595), while differences in IAF-1 and IAF+1 group, although present, are smaller (IAF-1: M_{tms}= 2.569; M_{sham}= 3.163 IAF+1: M_{tms}= 2.656; M_{sham}= 2.984), in accordance with the entrainment effects on alpha amplitude (Di Gregorio et al., 2022).

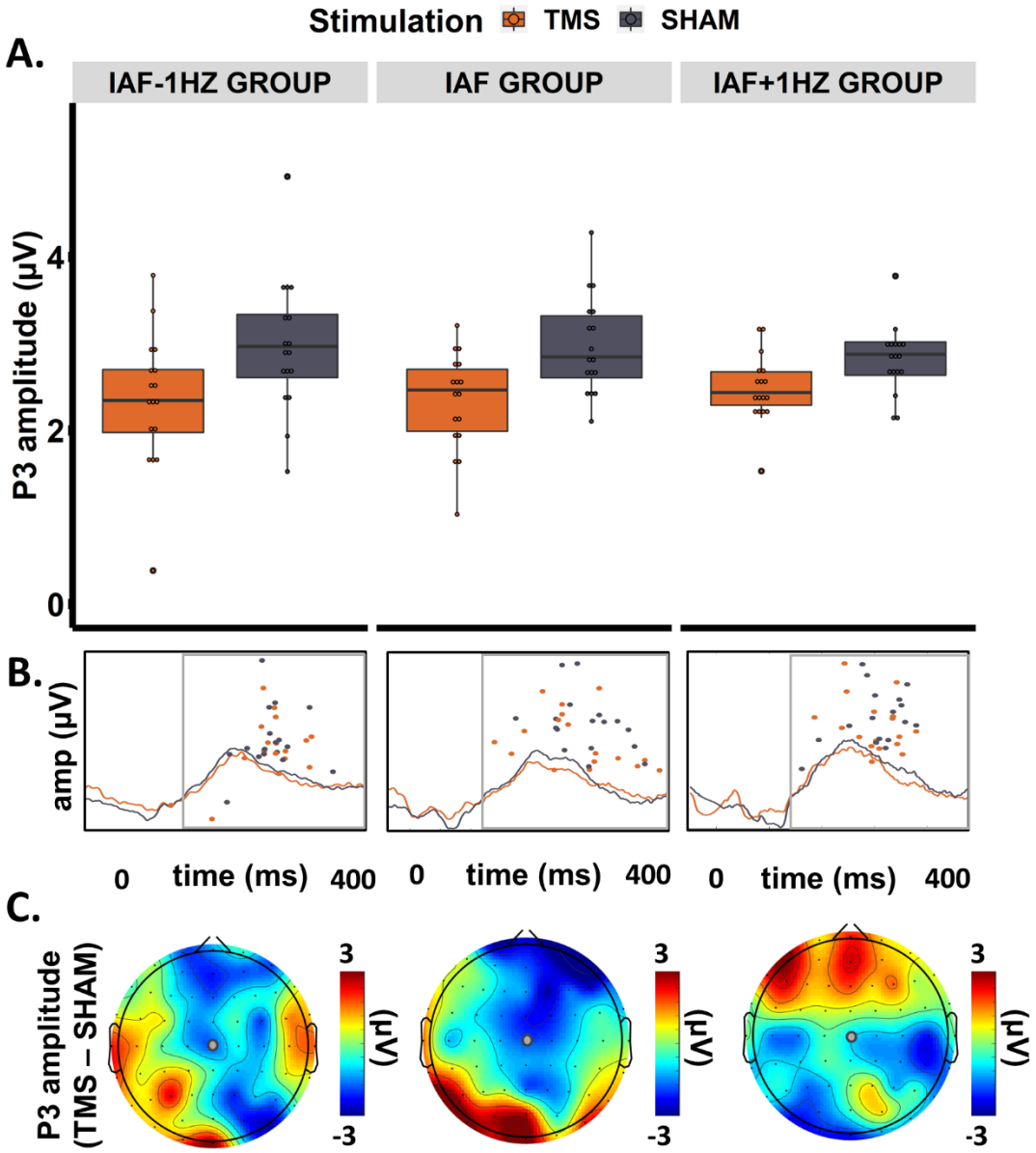

Figure 4. **Results of experiment 2: Rhythmic-TMS entrainment modulates the P3 amplitude.**

A. Box plots report **P3 amplitude** calculated on Cz electrode during TMS and SHAM for each group (IAF ± 1 Hz, IAF). Data are presented as median (full line) ± 1 quartile (box limits). **B. Visual-Evoked Potentials**: Grand average stimulus-locked P3 waveform at Cz electrode for each group (IAF ± 1 Hz, IAF), separately for TMS (green line) and SHAM (grey line) condition. Shaded gray bars denote regions of statistical analyses (between 200 ms and 400 ms). **C.** Topographies represents **the difference in P3 amplitude** between TMS and SHAM stimulations for each group (IAF ± 1 Hz, IAF). Two-tailed t test statistical significance is reported (*p < 0.05). mv, microvolt; Hz, hertz; ms, milliseconds; amp, amplitude.

The obtained results point to a distinct role of alpha frequency and amplitude in shaping evoked responses. While alpha frequency seems to directly determine the exact timing of early P1 component, alpha amplitude selectively shapes later P3 evoked responses.

Discussion

The present findings provide novel insight into the "oscillatory model" of ERP generation, in showing that, at least in part, evoked responses are shaped by the ongoing oscillatory activity (Klimesch et al., 2007). The model directly contradicts the traditional view that holds that event-related potentials reflect evoked responses of fixed latency and polarity that appear superimposed on to the "background noise EEG". Although there is increasing evidence that background EEG is, in fact, task-relevant, this historical gap in the study of evoked responses and functional oscillations has remained wide as ever. Certainly, one of the main reasons explaining this gap today is that a firm, concrete bridge based on empirical findings was proven to be hard to build. Specifically, although the validity of the ERP model was repeatedly questioned by various studies arguing that ERPs are generated by a reset of ongoing oscillations (Fuentemilla et al., 2006; Gruber et al., 2005; Hanslmayr et al., 2007; Klimesch et al., 2004; Makeig et al., 2002; Sauseng et al., 2007; Sayers et al., 1974), actual proof of phase-reset has been proven difficult to find due to various methodological reasons (Sauseng et al., 2007).

By manipulating oscillatory activity via non-invasive neurostimulation protocols, the main goal of this study was to contribute to constructing this bridge by shedding new light on oscillatory mechanisms of ERP genesis. To this aim, an EEG experiment was conducted, where a correlational relationship between different parameters of pre-stimulus alpha oscillations, P1 and P3 evoked components, and behavior was explored. Crucially, an online, rhythmic TMS protocol to change the frequency and/or amplitude of pre-stimulus alpha oscillations in order to observe causal consequences on evoked responses was also used.

The results of the two experiments univocally support the dependence of ERPs on pre-stimulus alpha activity, whereas alpha frequency and amplitude would shape distinct

evoked components. Specifically, faster or slower pre-stimulus alpha activity led to earlier or later P1 components. On the other hand, higher or lower alpha amplitude determined lower or higher P3 amplitude, in line with previous findings (Ergenoglu et al., 2004; Zazio et al., 2022). However, it is probable that the underlying mechanisms guiding the oscillatory influence of alpha activity on earlier versus later ERPs are different (Klimesch et al., 2007). Specifically, the influence of IAF on P1 latency is most likely due to the reorganization of ongoing oscillations via phase-reset. The phase-reset model predicts that the phases of ongoing oscillations would become aligned with the stimulus. Consequently, averaging these phase-locked oscillations across trials would not result in phase cancellation after the stimulus, resulting in the generation of ERP components. Therefore, this account would predict that a reset of an ongoing oscillation would not lead to a power-change, while the generated component would have similar frequency characteristics (Sauseng et al., 2007): in case of alpha activity, phase-reset should generate an early ERP component of the same polarity with an inter-peak latency of one alpha-cycle (~100 ms). First, by using rhTMS with the last pulse coinciding with a stimulus, an alpha phase-reset with stimulus appearance was ascertained. Second, P1 characteristics exactly mirrored the slight changes in alpha frequency, with slower alpha cycles leading to higher P1 latencies, and faster alpha cycles leading to the shorter ones. Third, there was no modulation of the P1 amplitude, in accordance with the phase-reset account.

On the other hand, phase-reset would unlikely explain the influence of increased alpha amplitude on lower P3 component. As the alpha rhythm has much faster fluctuations than the P3 component, the effects should already be visible in earlier ERPs. Instead, it can be better explained by the functional inhibition mechanism (Iemi et al., 2019). Specifically, it is possible that the P3 component is generated when the stimulus reaches conscious awareness, as repeatedly demonstrated (Dehaene & Changeux, 2011; Ergenoglu et al.,

2004; Min & Herrmann, 2007; Sanchez et al., 2020; Zazio et al., 2022), via additive mechanism (Mäkinen et al., 2005; Mazaheri & Jensen, 2006; Shah et al., 2004). Here, the higher pre-stimulus alpha amplitude would mean lower excitability of visual areas, resulting in an inhibitory effect and the attenuation of the amplitude of the additive ERP component. However, it is worth noting that a recent EEG study obtained somewhat contrary results, with pre-stimulus alpha amplitude negatively related to the earlier components, namely the amplitude of C1 and N150, and amplification of late components (from 400-900ms after stimulus onset), explained, respectively, via functional inhibition and baseline-shift mechanism (Iemi et al., 2019). Our study cannot exclude the possibility of an additive mechanism of alpha activity on earlier components, as the current task design did not yield a visible C1 peak. However, across our experiments, P1 amplitude did not relate to the pre-stimulus alpha activity, speaking in favor of the possibility that the inhibition of the additive mechanisms is specific for the conscious perception happening later on. On the other hand, a baseline-shift mechanism cannot explain the inverse relationship between pre-stimulus alpha amplitude and P3, as it would predict the opposite (positive) trend. However, we cannot exclude a baseline-shift-generated component happening 400 ms after stimulus onset, as previously reported (Iemi et al., 2019), but their description is outside of the scope of the current work, limited to the earlier, functionally specific ERPs.

The two alpha oscillatory components investigated (and manipulated) here, along with their ERP dependents, might reflect the activity of two independent mechanisms that serve complementary functions in visual decision-making. Specifically, as demonstrated in Study 1, the speed of pre-stimulus occipital alpha activity has a crucial and selective role in modulating perceptual sensitivity. What is seen here is that induced faster alpha activity is followed by an earlier P1 component, also related to higher perceptual accuracy. At the

same time, the induction of a slower alpha activity has led to the genesis of comparatively late P1 components, which in turn are associated with lower accuracy levels. Much like pre-stimulus IAF, a faster P1 evoked response might represent a resonant (mirrored), the post-hoc neural response of the efficiency of the stimulus processing.

On the other hand, the pre-stimulus alpha amplitude has been proposed to relate to internal decision-making variables that shape conservative (high alpha amplitude values) to liberal response criteria (low alpha amplitude values) rather than perceptual accuracy per se (Benwell et al., 2017; Di Gregorio et al., 2022; Iemi et al., 2017; Samaha et al., 2017). Mechanistically, pre-stimulus alpha-amplitude modulations have been linked to neural excitability changes that will affect both signal and noise, hence biasing the perceptual report to more subjective (than objective) interpretations of signals (or noise). Exactly these modulations of pre-stimulus alpha amplitude would directly influence the amplitude of P3 evoked component, with desynchronized alpha leading to a higher P3 peak that, as demonstrated here, was also selectively related to higher confidence levels. Being one of the most investigated ERP components, there is already ample evidence of various functional roles of the P3 component, ranging from information processing, attentional control, and monitoring, as well as reflecting subjective awareness (Dehaene & Changeux, 2011; Förster et al., 2020; Koivisto et al., 2006; Lamy et al., 2009; Polich, 2007; Rutiku et al., 2015; Salti et al., 2012; Verleger et al., 2005; Volpe et al., 2007). However, there is an ongoing debate about whether the P3 can be modulated by visual awareness (i.e., detection of a peri-threshold stimulus) and/or subjective report and confidence, elicited by thus far contrasting results (Eimer & Mazza, 2005; Lamy et al., 2009; Pitts et al., 2014; Salti et al., 2012). Our result would speak in favor of the latter, as P3 amplitude was positively associated with confidence mean but not detection rate. In line with previous findings associating the P3 component with stimulus relevance (Pitts et al., 2014; Schelonka et al.,

2017; Shafto & Pitts, 2015), attention (Koivisto et al., 2006; Koivisto & Revonsuo, 2008), and confidence (Eimer & Mazza, 2005), it is reasonable to assume that the P3 component reflects a mechanism that shapes our subjective interpretation of events. However, this mechanism is initiated long before the P3 genesis, as already pre-stimulus alpha-activity dictates the level of our initial perpetual bias, shaping both subjective stimulus evaluation and neural evoked response reflected in P3 amplitude.

Although our results indicate that pre-stimulus alpha activity directly influences subsequent ERP components, we can presume that a one-to-one linear relationship is unlikely and overly simplified. Oscillations constantly interact between them (Bonnefond et al., 2017; Palva & Palva, 2012) and are themselves influenced by stimulus presentation and post-stimulus processes: all processes likely to influence ERP genesis itself. Likewise, considering that not only alpha but all EEG oscillations have a common operating principle, that is the control of the timing of the neural activity (Cohen, 2011), we can imagine that task-relevant oscillations will interact and consequently shape task-specific evoked components. For instance, in a memory recognition task, it is reasonable to assume that both hippocampal theta activity, known to influence memory processes and sensory encoding (Herweg et al., 2020), and alpha activity, influencing the processing of sensory-semantic information (Klimesch, 1997, 1999), will interact to give rise to ERPs. Yet, here we provide the first causal demonstration of a linear relationship between different parameters of alpha oscillatory activity and specific evoked components in response to a visual stimulus presentation, able to predict both objective and subjective performance on the task.

In sum, creating a complete model of ERP genesis is outside the scope of the current study: our results simply indicate that IAF and alpha-amplitude represent flexible mechanisms that undergo adaptive changes under specific task demands and directly and

selectively shape the subsequent lower and higher-order evoked responses. By establishing a causal dissociation of IAF in shaping P1 evoked response latency, and alpha amplitude in shaping P3 response, the current research provides fundamental evidence in favor of the "oscillatory model," shedding new light on the relationship between prestimulus oscillations and the genesis and functional significance of evoked components. Moreover, our results confirm previous notions that there could be different mechanisms underlying the oscillatory model (Klimesch et al., 2007): while phase-reset of alpha activity can best explain the genesis of the earlier P1 component, P3 is possibly influenced by the functional-inhibition mechanism. Previous studies that advocated an oscillatory model were based solely on EEG evidence (e.g., (Gruber et al., 2005; Iemi et al., 2019; Mazaheri & Jensen, 2010; Zazio et al., 2022) or theoretical models (Klimesch et al., 2007), thus without a mean to seperate the possibility of overlapping vs. inter-dependent effect. Therefore, the use of information-based TMS has proven crucial in disentangling these two possibilities, thus offering direct, empirical evidence going against the evoked model.

STUDY 4:
TWO OSCILLATORY CORRELATES OF ATTENTION CONTROL IN THE ALPHA BAND WITH DISTINCT CONSEQUENCES ON PERCEPTUAL GAIN AND METACOGNITION

Abstract

Behavioral consequences and neural underpinnings of visuospatial attention have long been investigated. Classical studies using the Posner paradigm have found that visual perception systematically benefits from the use of a spatially informative cue pointing to the to-be-attended spatial location compared to a non-informative cue. Moreover, lateralized alpha-amplitude modulation during visuospatial attention shifts has been suggested to account for such perceptual gain. However, recent studies on spontaneous fluctuations of pre-stimulus alpha-amplitude have challenged this notion. Specifically, these studies showed that spontaneous fluctuations of pre-stimulus alpha-amplitude were associated with the subjective appreciation of stimulus occurrence, while objective accuracy was instead best predicted by the frequency of alpha oscillations, with faster pre-stimulus alpha-frequency accounting for better perceptual performance. Here, by using an informative cue in anticipation of lateralized stimulus presentation, we found that the predictive cue not only modulates preparatory alpha-amplitude but also alpha-frequency in a retinotopic manner. Behaviourally, the cue significantly impacted subjective performance measures (metacognitive abilities, namely meta-d') and objective performance gain (d'). Importantly, alpha-amplitude directly accounted for confidence levels, with ipsilateral synchronization and contralateral desynchronization coding for high-confidence responses. Crucially, the contralateral alpha-amplitude selectively predicted inter-individual differences in metacognitive abilities (meta-d'), thus anticipating decision strategy and not perceptual sensitivity, probably via excitability modulations. Instead, higher perceptual accuracy both within and across participants (d') was associated with faster contralateral alpha-frequency, likely by implementing higher sampling at the attended location. Finally, a successful top-down control seems governed by the frequency-specific oscillatory synchronization between frontal and parieto-occipital sensors in the alpha range. These

findings provide critical new insights into the neural mechanisms of attention control and its perceptual consequences.

Introduction

Conscious perception has become the object of many scientific investigations, and influential theories have proposed it to arise from the recurrent interaction between sensory input and internal predictive representations (Engel et al., 2001). Yet, how sensory input and top-down control interact to give rise to our conscious perceptual experience remains largely unknown.

As mentioned in Study 1, a number of studies have pointed to an active role of pre-stimulus alpha oscillations in sensory processing. They highlighted an inverse link between alpha-amplitude and cortical excitability (Romei et al., 2008), with reduced alpha-amplitude predicting improved performance (Dijk et al., 2008; Hanslmayr et al., 2007). This initial interpretation has been refined though, with new evidence, including Study 1, suggesting that alpha-amplitude covaries with the internal predisposition towards perception leading to more conservative vs. liberal attitudes (low/high confidence in perception associated with low/high cortical excitability and higher/lower alpha-amplitude) (Benwell et al., 2017; Di Gregorio et al., 2022; Iemi et al., 2017; Limbach & Corballis, 2016). A possible mechanistic explanation is that modulation of alpha-amplitude, and hence excitability, affects not only the interpretation of signal but also noise, hence leading to sensory bias. Moreover, Study 1 showed that alpha-amplitude not only accounts for perceptual confidence but that post-stimulus alpha-amplitude predicts subjective metacognitive performance, an index reflecting the efficacy of confidence ratings to discriminate correct from erroneous responses in perceptual tasks, thus suggesting a role of post-stimulus alpha-amplitude in integrating sensory input into the internal representation (Di Gregorio et al., 2022).

What are then the neurophysiological underpinnings of objective performance? Recent studies (Cecere et al., 2015; Mierau et al., 2017; Samaha & Postle, 2015; Wutz et al., 2018) point to a role of alpha-frequency in perceptual sampling, with faster frequency leading to higher sensory resolution. In line with this literature, using rhythmic-TMS to speed up/slow down individual pre-stimulus alpha-frequency (but not alpha-amplitude) results in higher/lower task accuracy, as described in Study 1 (Di Gregorio et al., 2022). These results suggest that the speed of one alpha cycle influences processing abilities, thus dictating the level of perceptual sensitivity, with more effective sensory sampling for faster alpha cycles (Coldea et al., 2022; Di Gregorio et al., 2022).

In sum, there is a growing consensus about the dissociable roles of alpha-frequency and amplitude in shaping sensory input and its subjective interpretation. However, it is hard to imagine that these two mechanisms don't interact in order to optimize the efficiency of our perceptual experience. Attention is certainly one of the crucial mechanisms underlying their interaction, whereas limited resources, in terms of both sensory sampling and sensory bias, are steered towards the to-be-attended spatial location, thus ensuring maximum perceptual efficiency where the relevant stimulus is awaited. Therefore, the interdependency of the circuits of sensory prediction (i.e., alpha-amplitude) and sensory precision (i.e., alpha-frequency) is expected, whereas the conscious perception would result from the continuous attempt to predict the external environment by recurrently updating its internal representation through sensory input integration.

Attentional steering is known to be controlled via a widespread brain network, where feedback signals from frontal brain areas can control the activity of lower-level visual areas (Bichot et al., 2005; Fries et al., 2008). This communication between brain areas is thought to be enabled by the synchronization of neuronal oscillations. This is because the oscillatory properties of the neurons may determine their ability to send and

receive electrical signals, where oscillations in different neuronal sets create rhythmic opportunities during which cells simultaneously increase or decrease their readiness to transfer information (Fries, 2005, 2015; Salinas & Sejnowski, 2001). In the context of visual attention, alpha oscillation could have a prominent role in transmitting these feedback signals via interregional cortico-cortical coupling.

The current study aims at addressing this interdependency between different mechanisms via modulation of the spatial attention prior to the stimulus onset. Specifically, we present a valid cue informing of high (75%) lateralized stimulus occurrence probability. In line with many reports (see also Thut et al, 2006), we expect valid cue to modulate both pre-stimulus alpha-amplitude lateralization and performance. Importantly, we hypothesize that despite their co-occurrence, the alpha amplitude would not directly account for changes in performance but rather for the steering of the decision bias towards attended stimulus via location-specific excitability modulations. Hence, we expect alpha-amplitude changes to account for metacognitive abilities, defined as the extent to which our confidence is consistent with our probability of being correct, already during the pre-stimulus period, as induced by the predictive cue. Enhanced performance should be explained instead by the allocation of sensory resources at the to-be-attended location via faster alpha oscillations. Finally, we expect the successful attentional shifts to be preceded by alpha synchronization between anterior and posterior brain areas.

Methods

Participants: 24 healthy volunteers (12 women; mean age= 23.2, SE = 2.61) were recruited for the study at the Centre for Studies and Research in Cognitive Neuroscience in Cesena, Italy. The same participants also took part in Study 1, involving different task conditions where the informative cue was not present (Di Gregorio et al., 2022). The study was approved beforehand by the bioethics committee of the University of Bologna.

Stimuli and procedure. The Experimental task was controlled via the E-Prime software (Psychology Software Tools, Inc., USA), and stimuli were presented on a CRT monitor (100 Hz refresh rate, 57 cm viewing distance). Each trial of the task involved a primary response on the *visual detection task* of the peri-threshold target stimuli and a *secondary rating of confidence*, in which participants rated the level of confidence on their accuracy on a scale 1 to 4 (1 = no confidence at all; 2 = little confidence; 3 = moderate confidence and 4 = high confidence). Each trial started with a white fixation cross on the center of the screen (duration = 2000 ms; visual angle= 0.8°). Afterward, an informative cue appeared to indicate the spatial position of the following primary task stimulus. The cue was a white arrow (duration = 2000-3000 ms, visual angle = 2°) presented in the center of the screen, which could point either to the left or to the right part of the visual field. In 75% of cued trials, the cue correctly predicted the position of the primary task stimulus (valid cue condition). In the remaining 25% of trials, the cue pointed in the other direction (invalid cue condition).

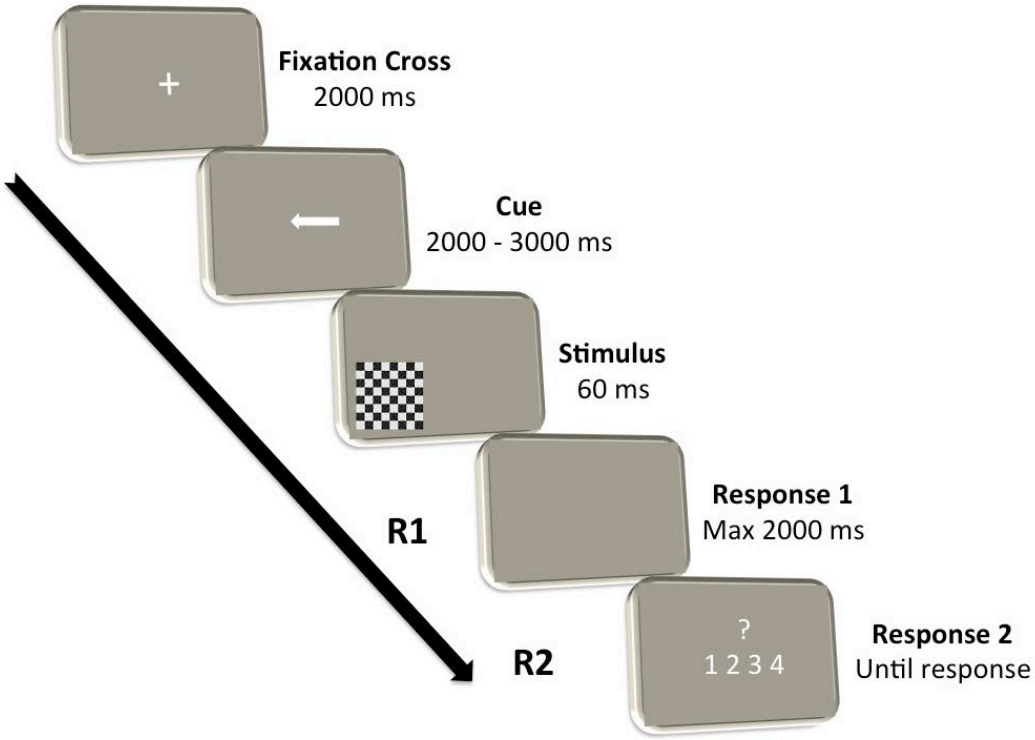

Figure 1. **Trial sequence.**

Each trial started with a fixation cross, then a cue indicates (left or right arrow, valid cue: 75% predictivity) the probability of the position of the forthcoming stimulus (a checkerboard). The primary task was to respond (R1) if the checkerboard contained grey circles. After this primary response, participants rated their confidence (R2) to their first response on a Likert scale from 1 (no confidence at all) to 4 (high confidence). Ms = milliseconds.

The two possible cues (valid and invalid cue) were immediately followed by the primary task stimulus (duration = 60 ms, 4.1°/3.7° eccentricity in the lower part of the left or right visual field), which could be either a catch stimulus or a target stimulus. Stimuli used were the same as in Study 1: 8x8 black and white checkerboards (height = 4 cm; width= 4 cm, visual angle = 15.9°) that could (target stimuli) or not (catch stimuli) contain iso-luminant grey circles (for details, see Study 1). Whenever the participants perceived the circles embedded within the checkerboard stimulus, they were prompted to press the spacebar on the keyboard (Figure 1).

Titration session. Before the main experimental session, in a titration session, the peri-threshold intensity of the iso-luminant circles was identified for every participant (for

details, see Study 1). Obtained threshold values were subsequently used to determine adequate, individually-tailored stimuli for the main experimental task.

Main experiment.

Although response speed for visual detection was never stressed in favor of perceptual accuracy, a time limit of 2000 ms was given. Immediately after the primary task response, a confidence prompt would appear with the Italian translation of the question: "How confident are you about your response?". Confidence rating consisted of a 4-points Likert scale ranging from "no confidence at all" to "high confidence". After the secondary confidence rating, a new trial would start (total trial number= 300).

EEG data.

Psychophysiological recording. EEG data were collected from 64 Ag/AgCl electrodes (Brain Products, Munich, Germany) in the same manner as per Experiment 1 of Study 1.

EEG data were pre-processed using custom-made routines in MatLab R2013b (The Mathworks, Natick, MA, USA). First, EEG data were re-referenced offline to the average of all electrodes and filtered between 0.5–30 Hz. Stimulus-locked epochs were then extracted, from -2000 ms to 2000 ms, with a baseline set -2000 to -1500. Epochs containing artifacts were excluded via a two-fold procedure: first, the pop_autorej function in EEGLAB v13.0.1 (Delorme & Makeig, 2004) was used to exclude trials with high voltage fluctuations (>1000 μV) or containing data values outside five standard deviations. Additionally, we specifically controlled for ocular artifacts by applying artifact rejection on epochs with outlier values over horizontal and vertical EOG (percentage of excluded trials: 6.04%, SE = 0.51%). After artifact rejection, the function lms_regression for automatic EOG correction using Least Mean Squares was applied. The remaining EOG artifacts were corrected by a linear regression method (lms_regression function). Because alpha

suppression is larger contralaterally to stimulus presentation, for the analyses, we compared activities from contralateral and ipsilateral electrodes. To this aim, data epochs for right-presented stimuli were copied and flipped to the right side of the original data, resulting in conventionally defined right-hemisphere activity as contralateral and left-hemisphere activity as ipsilateral to stimulus presentation.

Invalid cue data, representing a residual 25% of trials where the cue incorrectly indicated the position of the forthcoming stimulus (N=75), were not considered in the analyses.

Alpha-frequency. Individual alpha-frequency (IAF) peak during the task was calculated in the cue-stimulus period (i.e., pre-stimulus alpha from -1000 ms to stimulus presentations), by implementing a fast Fourier transformation (MatLab function spectopo, frequency resolution: 0.166 Hz), separately for each condition. IAF was defined as the local maximum power within the frequency range 7-13 Hz. The following subset of posterior parieto-occipital electrodes was used: contralateral electrodes (P8, P6, P4, P2, PO8, PO4, O2), ipsilateral electrodes (P7, P5, P3, P1, PO7, PO3, O1). Although each subject showed a clear peak within this range with maxima over posterior electrodes, the peak itself was not present at all electrodes. For this reason, we visually inspected power spectra on the posterior electrodes and chose for each participant a contralateral electrode with a clear peak of the maximum power (Di Gregorio et al., 2022; Samaha & Postle, 2015; Trajkovic et al., 2022). A homologous electrode was selected for the analyses in the ipsilateral hemisphere.

Alpha-amplitude. Spectral EEG activity was assessed by time-frequency with the newtimef function from EEGLAB v13.0.1 and custom routines in MatLab. Single-trial baseline between 2000 and 1500 preceding stimulus onset was used. The resulting power was normalized by decibel (dB = 10*log10[-power/baseline]).

The same method and subsets of posterior contralateral and ipsilateral electrodes used for alpha-frequency were used for alpha-amplitude analyses, whereas here, for each participant, the contralateral electrode with maximum alpha-suppression was selected, along with its ipsilateral homologous. Therefore, the most negative value (i.e., alpha-amplitude) in the alpha range (7-13 Hz) was computed separately for each condition in the cue-stimulus time period (Samaha, Iemi, et al., 2017). Finally, alpha-amplitude was normalized by subtracting from each electrode used in the analyses the mean of the alpha power over the posterior parieto-occipital electrodes cluster.

WPLI. Phase connectivity was estimated in the sensor space via the weighted phase-lag index (wPLI) (Vinck et al., 2011) between the frontal and parieto-occipital electrodes of both hemispheres. This is a measure of phase lag-based connectivity that accounts for non-zero phase lag/lead relations between two time series signals. Therefore, it is a measure insensitive to volume conduction and noise of a different origin considered optimal for exploratory analysis as it minimizes type-I errors (Cohen, 2015). As a first step, trail number matching was applied (see p. 138), and participants with less than 10 trials for one of the two conditions (correct vs. error trials) were excluded from the analysis ($N_{excluded}$ = 6 participants). To obtain wPLI values, time series data was first transformed into the time-frequency domain via convolution with a family of complex Morlet wavelets (the number of cycles increased from 5 to 18 in logarithmic steps). Therefore, for frequencies ranging from 3 to 30 Hz in 1-Hz steps, first convolution by frequency-domain multiplication was performed, and then the inverse Fourier transformation was taken. Phase was defined as the angle relative to the positive real axis, and phase differences were then computed between all possible pairs of electrodes. Finally, wPLI was calculated as the absolute value of the average sign of phase angle differences, whereas vectors closer to the real axis were de-weighted. Once wPLI values were extracted for every frequency bin (3 to

30 Hz in 1 Hz steps) and epoch, they were averaged to obtain distinct values for each of-interest experimental condition (correct and error trails) in different frequency bands (theta, beta and alpha frequency) in the time-window of interest (-500ms to 0). Subsequently, non-parametric permutation-based analysis (1000 iterations) was performed to compare the connectivity between correct and error trials, and to obtain phase connectivity difference maps of distinct ROIs: fronto-posterior connectivity in the right (stimulated) hemisphere (frontal: AF4, AF8, F2, F4, F6, F8, FC2, FC4, FC6; posterior: Pz POz Oz P2 P4 P6 P8 PO4 PO8 O2), and homologous electrodes of the left hemisphere. Sensor differences with z-values corresponding to $p<0.05$ were retained as significant. The connectivity index of each condition was then estimated using the formula: CI = sig_pos/ sp_total, where sig_pos are connections that are significantly higher for correct vs. error trials, and sp_tot are all possible connections. Furthermore, another permutation test was introduced to calculate the significance threshold for CI. Specifically, wPLI matrices of all ROIs and experimental conditions were randomly permuted and compared 1000 times to obtain the distribution of randomly obtained differences in wPLI. Connectivity indices that exceeded 95% confidence interval were considered statistically significant (connectivity threshold= 0.05).

Behavioral data.

Conditions. Data were sorted according to the cue information (valid vs. invalid cue). D' was computed on this dataset and directly compared to the d' dataset computed in Study 1 on the same group of participants involved in the same task during the presentation of an uninformative (neutral) cue. A direct t-test for d' in the informative vs. uninformative cue conditions was performed to test for the behavioral advantage induced by the informative relative to the uninformative cue condition. Moreover, all trials were sorted according to the primary task response in correct and error trials. Then, in the second step,

we focused on the confidence level after correct trials (i.e., subjective confidence). In order to contrast confident vs. non-confident responses, correct trials were divided in high confident (i.e., confidence ratings 3 and 4) and low confident (i.e., confidence ratings 1 and 2).

D'. Perceptual sensitivity was estimated on the accuracy data using the *d'* measure, considered an unbiased measure of discrimination abilities between the signal and noise in the Signal Detection Theory (Green & Swets, 1974). *D'* was calculated in the same manner as per Study 1.

Meta-d'. Metacognitive performance was quantified using the computational method proposed by Maniscalco & Lau (Maniscalco & Lau, 2012). Here, meta-d' was calculated with the function fit_meta_d_SSE in MatLab., in the same manner as per Study 1.

Statistical Analyses

Behavioral Analyses. Behavioral analyses were performed separately for objective accuracy and subjective confidence, and the performance in the neutral, uninformative condition (see Study 1) vs. informative (valid cue) condition was compared.

Within-participants EEG analysis. As already reported in the literature (Jensen & Mazaheri, 2010; Kelly et al., 2006; Thut et al., 2006), the presentation of an informative cue induces an inter-hemispheric imbalance of alpha-amplitude with larger alpha desynchronization contralateral to the attended location. Thus, in the first step of the analysis, we aimed to replicate this finding by comparing alpha-amplitude in the ipsilateral vs. contralateral cued location. For this analysis, both valid and invalid cue conditions were merged to specifically study the effect of the cue information over inter-hemispheric alpha distribution.

Then, for *Objective Accuracy* we compared alpha activity (both frequency and amplitude) in a 2X2 repeated measures ANOVAs with the factors RESPONSE (Correct trials = 258.8, SE = 4.39; Error trials = 23.04, SE = 3.64) and HEMISPHERE (contralateral and ipsilateral).

For Subjective Confidence, analyses were performed on correct trials (Yeung & Summerfield, 2012). Alpha activity (both amplitude and frequency) was calculated for the factor CONFIDENCE (High confidence trials = 229.7, SE = 9.26, Low confidence trials = 26.5, SE = 5.42) and for the factor HEMISPHERES (contralateral and ipsilateral) in a 2X2 repeated measures ANOVA.

In order to affirm whether trial number influences results of within-participants EEG analyses, a trial number matching procedure between correct and error trials was applied (i.e., accuracy analysis) and between high and low confidence trials (i.e., confidence analysis). Within this procedure, for each participant, the condition with the smaller trial number was identified (trial number = N-inferior) separately for accuracy and confidence. Then, the same number of trials in the other condition (N-superior) was randomly selected. The randomization was repeated N-inferior times, and corresponding EEG data from the N-superior condition were selected and averaged. Finally, EEG data were compared between N-inferior and N-superior conditions.

For all analyses, violations of sphericity were accounted for via Greenhouse–Geisser corrections whenever appropriate (Greenhouse & Geisser, 1959). Differences between conditions were tested by two-tailed t-tests planned comparisons.

Between-participants EEG analysis. Between participants EEG analyses were based on the within-participants results. For perceptual sensitivity analyses, we looked at the relationship between the d' scores and alpha frequency in the contralateral and ipsilateral hemispheres by using non-parametric robust correlation estimates (skipped

Spearman correlations). The advantage of this correlation coefficient is that it takes into account the presence of bivariate outliers (by excluding them) and, thus is not sensitive to the presence of extreme values in the overall structure of the data (Pernet et al., 2013). Similarly, we looked at the relationship between both ipsilateral and contralateral modulations of alpha amplitude and meta-d' scores by using the same correlation estimates.

As a control analysis, we also looked at the relation between alpha-amplitude and d', as well as alpha-frequency and meta-d', where no significant correlation was expected.

Results

Replicating previous findings: informative cues modulate pre-stimulus alpha-amplitude lateralization and enhance perceptual performance

The presentation of an informative cue has often been associated with a mechanism controlling the allocation of attentional resources, namely, the hemispheric asymmetry of alpha-amplitude (Jensen & Mazaheri, 2010; Kelly et al., 2006; Thut et al., 2006). First, here we replicate this robust finding, thus observing that informative cue systematically induces an interhemispheric modulation of alpha amplitude, with significantly higher alpha-amplitude to ipsilateral vs. contralateral cued location ($t(23) = 2.09$, $p = .047$; $d = 0.43$. See Fig. 2A).

Behavioral results for the perceptual task are reported in Table 1. Moreover, previous findings consistently showed that this predictive spatial information carried by the alpha-amplitude modulation enhances perceptual performance at the attended location. Indeed, by directly comparing the behavioral performance for the informative vs. the neutral cue as collected in Study 1, we found that d' values were significantly enhanced when a valid cue was presented (d' = 3.16, SE = 0.16) compared to when an uninformative (neutral) cue was presented, d'= 2.02, SE = 0.13) ($t(23) = 6.34$; $p < .001$; $d = 1.28$, Study 1).

Table 1. **Behavioral results.** Percentages of trials (Mean and standard error into brackets) for hits, false alarms, misses, and correct rejections.

	TARGET	
	Present	Absent
Response	44.53% (1.1%)	2.64% (0.68%)
No Response	5.59% (1.01%)	47.22% (0.72%)

Accordingly, here we observed a significant ACCURACY X HEMISPHERE

interaction for alpha-amplitude ($F(1,23) = 11.43$; $p = .003$; $\eta_p^2 = .332$). In particular, for correct compared to erroneous responses, a suppression of pre-stimulus alpha-amplitude in the contralateral hemisphere ($t(23) = 2.27$; $p = .033$; $d = 0.45$) and a marginally significant synchronization in the ipsilateral hemisphere ($t(23) = 2.01$, $p = .056$; $d = 0.41$) were observed (Figure 2B). However, the same analyses on the alpha-amplitude in the entire parieto-occipital cluster did not show the interaction ACCURACY X HEMISPHERE ($F(1,23) = .374$; $p = .547$; $\eta_p^2 = .016$).

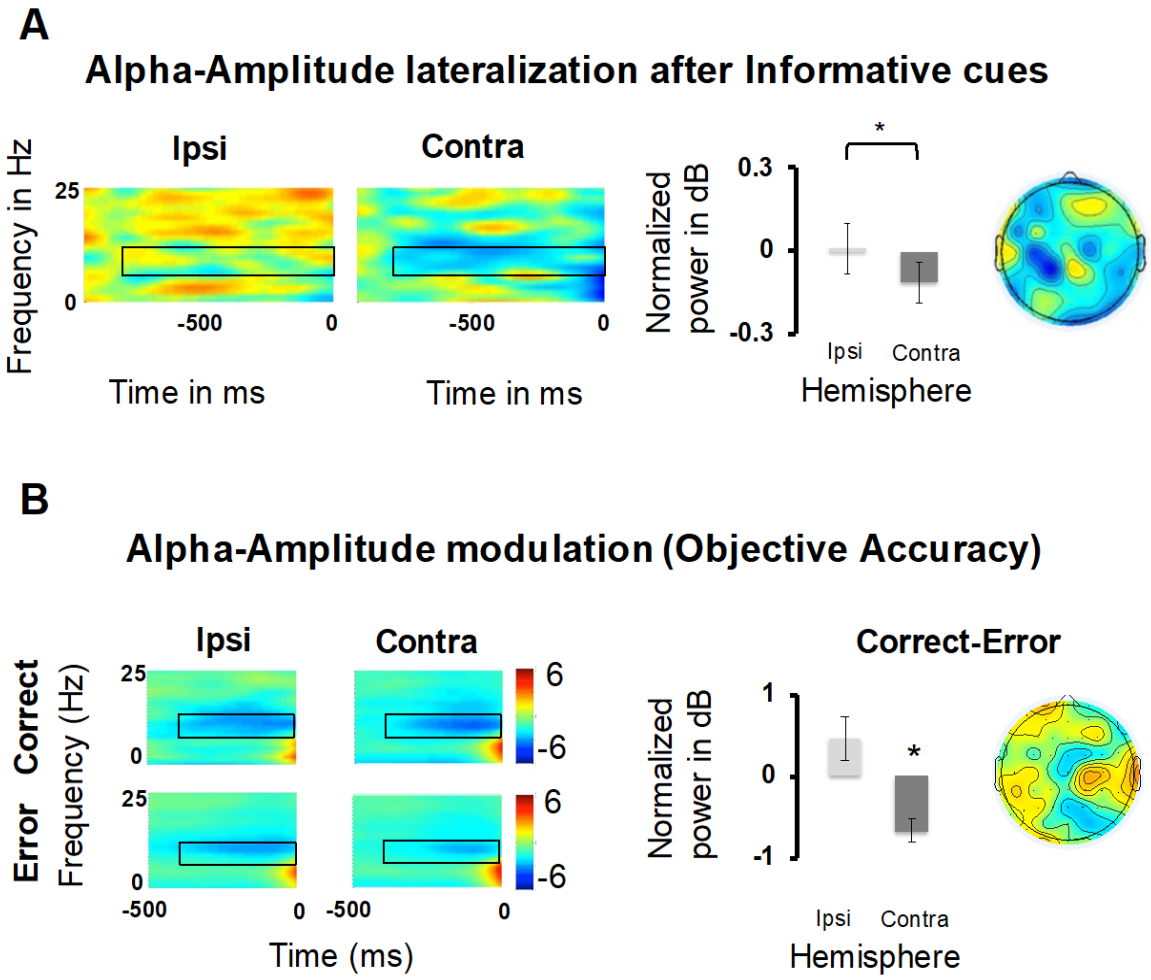

Figure 2. **Alpha amplitude modulations.**

A. Prestimulus alpha-amplitude in the ipsilateral and contralateral hemispheres is reported in the cue-stimulus time period after informative cues as time-frequency plots. For illustrative purposes, we reported data from a cluster of ipsi and contralateral electrodes. Black boxes denote regions of statistical analyses (alpha band 7–13 Hz). Bar graph is reported for normalized power in the ipsi and contralateral hemispheres. Topography represents the alpha-amplitude distribution over electrodes (electrodes are flipped to have contralateral activity in the right-hand side and ipsilateral activity in the left-hand side). **B.** Prestimulus alpha-amplitude in the ipsilateral and contralateral hemispheres is reported in the cue-stimulus time period for correct and error trials. For illustrative purposes, we reported data from a cluster of ipsi and contralateral electrodes. Black boxes denote regions of statistical analyses (alpha band 7–13 Hz). Bar graph is reported for normalized power in the ipsi and contralateral hemispheres for the difference correct-errors. Topography represents the difference between correct and error trials (electrodes are flipped to represent contralateral activity in the right-hand side and ipsilateral activity in the left-hand side). Two- tailed t test statistical significance is reported (*$p < 0.05$). Error bars represent standard error of the mean. Diff, difference; mv, microvolt; Hz, hertz; ms, milliseconds; dB, decibel

The impact of the informative cue on pre-stimulus alpha amplitude lateralization shapes meta-cognition, not performance per se

Therefore, in line with the existing literature, we have shown that the informative

cue modulates pre-stimulus alpha lateralization such that contralateral (vs. ipsilateral) alpha amplitude to the attended stimulus is reduced and that it is associated with perceptual performance.

These findings can be interpreted in a two-fold manner. On the one hand, a traditional and most straightforward interpretation would be that these two measures are directly related and specifically that alpha amplitude lateralization may drive perceptual performance improvement. However, recent findings from our (and other) labs speak against the direct link between alpha amplitude modulations and perceptual sensitivity. Specifically, by use of a neutral cue paradigm in Study 1, we were able to dissociate the impact of pre-stimulus alpha amplitude on confidence response vs. the impact of alpha frequency on perceptual performance. Moreover, we found that following stimulus presentation, post-stimulus alpha amplitude also correlated with meta-d', an index accounting for the level of the individual meta-cognitive ability. These findings suggest that an informative cue may significantly impact alpha amplitude lateralization by anticipating performance strategies and thus shape meta-cognitive abilities before stimulus presentation. Here, we directly tested the hypothesis that the informative cue for valid trials specifically impacts metacognitive abilities, not perceptual sensitivity.

First of all, similar to the d' values, we found that metacognitive performance, measured via meta-d' scores, is significantly higher when an informative valid cue is presented (meta-d' = 3.16, SE = 0.16), compared to the uninformative (neutral) cue (neutral cue, meta-d'= 1.98, SE = 0.20) ($t(23) = 5.08$; $p < .001$; $d = 1.04$, Study 1), thus speaking in favor of the positive impact of the attentional focus on metacognitive abilities of the participant.

Second, in line with recent findings, we found that prestimulus alpha-amplitude can account for an internal predisposition towards stimulus attendance (confidence levels),

with a significant CONFIDENCE X HEMISPHERE interaction $F(1,21) = 19.66$; $p < .001$; $\eta_p^2 = .484$. Specifically, high, relative to low confident trials, were best accounted for not only by an overall alpha suppression, as in our previous study, where attention was not manipulated (see Study 1); here, high confidence responses were preceded by a selective alpha desynchronization contralateral to the to-be-attended hemifield ($t(21) = 2.56$; $p = .018$; $d = 0.54$) along with a significantly higher ipsilateral synchronization ($t(21) = 2.44$; $p = .023$; $d = 0.52$) (Figure 3A). For high confident trials, this resulted in a significant difference between contralateral suppression and ipsilateral synchronization ($t(21) = 2.56$; $p = .018$; $d = 0.54$). Moreover, an opposite pattern was observed for low confident trials (more synchronized activity contralateral and more suppressed activity ipsilateral to the cued location; t(21) = 2.38; p = .027; d = 0.51). Results on trial matching analyses confirmed these findings, with larger alpha-power suppression for high confidence (normalized power = -1.433 db, SE = 0.323 db) relative to low confidence (normalized power = 0.564 db, SE = 0.292 db) trials in the contralateral hemisphere (t(21) = 4.112, p < .001, d =.839). These findings suggest that, in addition to the contralateral alpha desynchronization, an ipsilateral inhibitory process is implemented, able to steer confidence resources away from the to-be-ignored spatial location and towards the cued spatial location in high-confidence trials.

Third, in line with our hypothesis, our findings precisely show that the effect of the informative cue on alpha amplitude modulations can account for individual meta-cognitive abilities already before stimulus presentation. Indeed, between-subject differences in the contralateral pre-stimulus alpha-amplitude were able to explain differences in metacognitive abilities. Specifically, the higher the desynchronization of the alpha amplitude in the contralateral hemisphere, the higher the metacognitive abilities of the participant as measured via meta-d' score (r = -.656, CI = [-0.859 -0.306], Figure 3B). On

the other hand, ipsilateral modulations of alpha amplitude could not account for inter-individual differences in meta-d' (r = -.019, CI = [-0.560 0.253]), speaking in favor of the crucial role of the contralateral hemisphere in shaping metacognitive abilities across participants, as also reported in Study 1. Finally, in line with recent findings, our results confirm that neither contralateral nor ipsilateral modulations of alpha amplitude could directly account for modulations in perceptual accuracy as measured with d' (Contralateral: r = -.001, CI = [-0.532 0.470], Figure 3B; Ipsilateral: r = .261, CI = [-0.203 0.640]).

These findings suggest that, away from the classical interpretation, contralateral modulations of alpha amplitude following informative cue presentation anticipate decision strategy, directly impacting metacognitive abilities and not perceptual sensitivity per se.

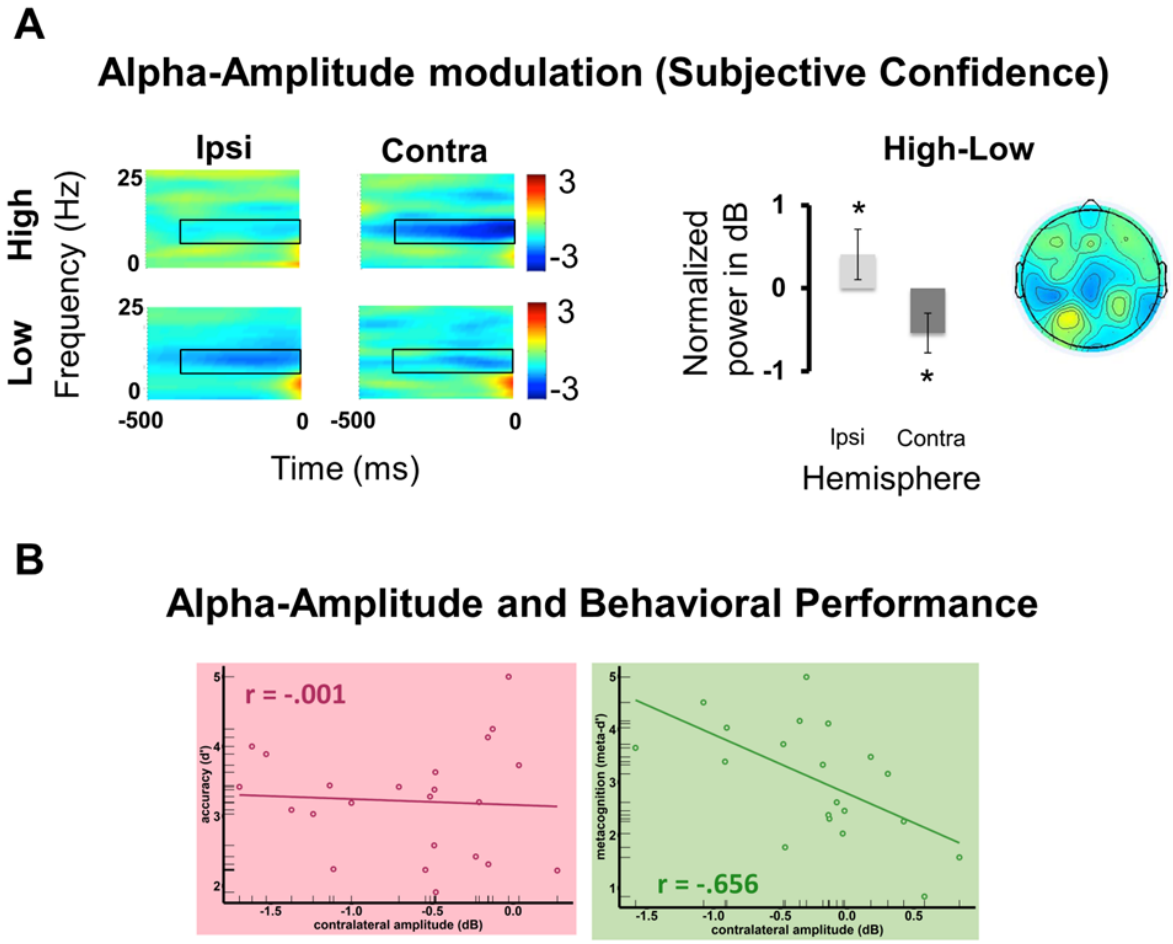

Figure 3. **Alpha amplitude modulations and perception**.

A. Prestimulus alpha-amplitude in the ipsilateral and contralateral hemispheres is reported in the cue-stimulus time period for High and Low confidence trials. For illustrative purposes, we reported data from a cluster of ipsi and contralateral electrodes. Black boxes denote regions of statistical analyses (alpha band 7–13 Hz). Bar graph is reported for normalized power in the ipsi and contralateral hemispheres for the difference High-Low. Topography represents the difference between High and Low confidence trials (electrodes are flipped to represent contralateral activity in the right-hand side and ipsilateral activity in the left-hand side). **B.** Correlation between alpha-amplitude and behavioral performance for accuracy (d' measure) and metacognition (meta-d' measure). Two- tailed t test statistical significance is reported (*$p < 0.05$). Error bars represent standard error of the mean. Diff, difference; mv, microvolt; Hz, hertz; ms, milliseconds; dB, decibel

The impact of informative cue (for valid trials) on contralateral pre-stimulus alpha frequency shapes perceptual sensitivity

According to Study 1, a better candidate to account for changes in perceptual sensitivity is the frequency and not the amplitude of alpha (for a similar account, see also Coldea et al., 2022). Specifically, considering the impact that the informative cue has on perceptual performance at the attended location, being significantly improved, one may expect this effect to be determined by a speeding up of alpha frequency, specifically at

posterior brain areas contralateral to the attended location.

Indeed, informative cue induced an interhemispheric modulation of alpha-frequency, with significantly faster alpha in the contralateral vs. ipsilateral cued location ($t(23) = 2.55$; $p = .018$; $d = 0.52$) (Figure 4A).

Furthermore, results showed that alpha-frequency was able to distinguish between correct and erroneous responses, as we found a main effect of the ACCURACY for alpha-frequency ($F(1,23) = 4.68$; $p = .041$; $\eta_p^2 = .169$). Crucially, a significant ACCURACY X HEMISPHERE interaction ($F(1,23) = 6.63$; $p = .017$; $\eta_p^2 = .224$) pointed to a lateralized effect of alpha-frequency. Specifically, in line with our hypothesis, a speed-up of alpha-frequency could be observed selectively in the hemisphere contralateral to the hemifield where the stimuli were attended for correct responses compared to errors ($t(23) = 3.23$; $p = .004$; $d = 0.69$), but not in the ipsilateral hemisphere ($t(23) = 0.71$; $p = .483$; $d = 0.15$). The difference between the speeded-up contralateral alpha-frequency and ipsilateral alpha-frequency was found to be statistically significant as well ($t(23) = 2.06$; $p = .05$; $d = 0.44$; Figure 4B). Results on trial matching analyses confirmed our findings, with faster alpha-frequency for correct (11.49 Hz, SE = 0.21 Hz) relative to error trials (10.48 Hz, SE = 0.28 Hz) in the contralateral hemisphere $t(23) = 3.552$, $p = .001$, $d = 0.725$. Finally, as an additional control, we analyzed the accuracy effects in the entire cluster for alpha-frequency. The results are again in line with those reported after the electrode selection procedure and trial matching. Indeed, the ANOVA showed a significant interaction ACCURACY X HEMISPHERE $F(1,23) = 4.467$; $p = .046$; $\eta\ 2 = .163$ with faster alpha frequency in the contralateral hemisphere for correct (11.14 Hz, SE = 0.34 Hz) vs. erroneous responses (10.63 Hz, SE = 0.33 Hz) $t(23) = 2.82$, $p = .01$, $d = 0.576$. No accuracy effects emerged in the ipsilateral hemisphere $t(23) = 0.357$, $p = .724$, $d = 0.072$.

Crucially, between-subject differences in accuracy can be explained by the

differences in contralateral speed of alpha activity, but not changes of alpha-amplitude across the two hemispheres (see previous paragraph). Specifically, the faster the contralateral (but not ipsilateral) alpha activity of the participant, the higher the overall task accuracy, as measured via d' score (Contralateral: r = .412, CI = [0.046 0.715]; Ipsilateral: r = .029, CI = [-0.459 0.449]). These effects were specific for d' as pre-stimulus alpha-frequency could not explain inter-individual differences in metacognitive performance (r = .273, CI = [-0.260 0.679), suggesting that alpha-frequency modulation specifically impacts perceptual performance but having no role in determining one individual meta-cognitive ability (Figure 4C).

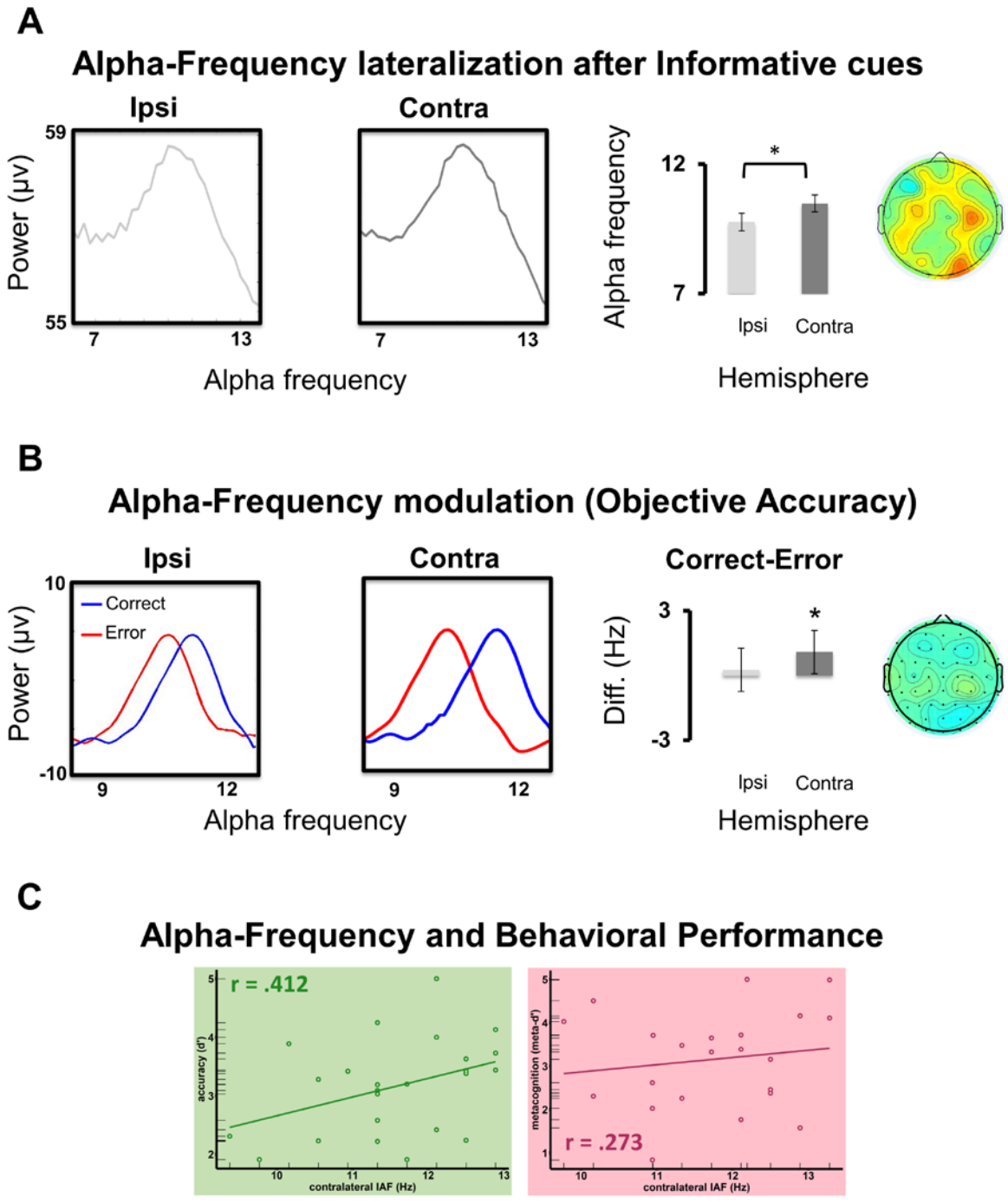

Figure 4. **Alpha frequency modulations and perception.**

A. Prestimulus averaged alpha-frequency (alpha band 7–13 Hz) is represented as the Z-scored mean power (10*log10[mv2/Hz]) spectrum in the cue-stimulus time period in the ipsilateral and contralateral hemispheres after informative cues. For illustrative purposes, we reported data from a cluster of ipsi and contralateral electrodes. Bar graph is reported for alpha-frequency in the ipsi and contralateral hemispheres. Topography represents the alpha-frequency distribution over electrodes (electrodes are flipped to have contralateral activity in the right-hand side and ipsilateral activity in the left-hand side). **B.** Prestimulus averaged alpha-frequency in the cue-stimulus time period for the contralateral and the ipsilateral electrodes and for correct and error trials within the alpha band. For illustrative purposes, we reported data from a cluster of ipsi and contralateral electrodes. Bar graph is reported for normalized power in the ipsi and contralateral hemispheres for the difference Correct-Error. Topography represents the difference between Correct and Error trials (electrodes are flipped to represent contralateral activity in the right-hand side and ipsilateral activity in the left-hand side). **C.** Correlation between alpha-frequency and behavioral performance for accuracy (d' measure) and metacognition (meta-d' measure). Two- tailed t test statistical significance is reported (*$p < 0.05$). Error bars represent standard error of the mean. Diff, difference; mv, microvolt; Hz, hertz; ms, milliseconds; dB, decibel

Higher connectivity in the alpha range between frontal and posterior areas is related to successful attentional control

As seen in previous paragraphs, attentional control would steer both alpha-frequency and alpha-amplitude towards the most likely stimuli location, thus enabling enhanced performance in terms of perceptual accuracy and metacognition. Visual attention is enabled through the fronto-posterior brain network, and the oscillatory synchronization between the nodes of the network could be a key mechanism that would enable their successful information exchange (Fries, 2005, 2015; Salinas & Sejnowski, 2001).

To test this hypothesis, phase-based connectivity between fronto-central and parieto-occipital sensors was calculated separately for correct and error trials in the time window right before the stimulus presentation (-500 ms to 0). Moreover, analysis was conducted separately for each of the frequency bands (theta, alpha, and beta) and for the hemisphere contralateral and ipsilateral to the previously presented cue and the subsequent stimulus location. The results evidenced a significantly higher antero-posterior synchronization in the alpha range for correct responses with respect to errors, speaking in favor of the successful attentional gearing being enabled through long-range oscillatory coherence. Importantly, the effect was frequency-specific, as the synchronization in the theta and beta range was not significantly different between the correct and error trials (see Figure 5).

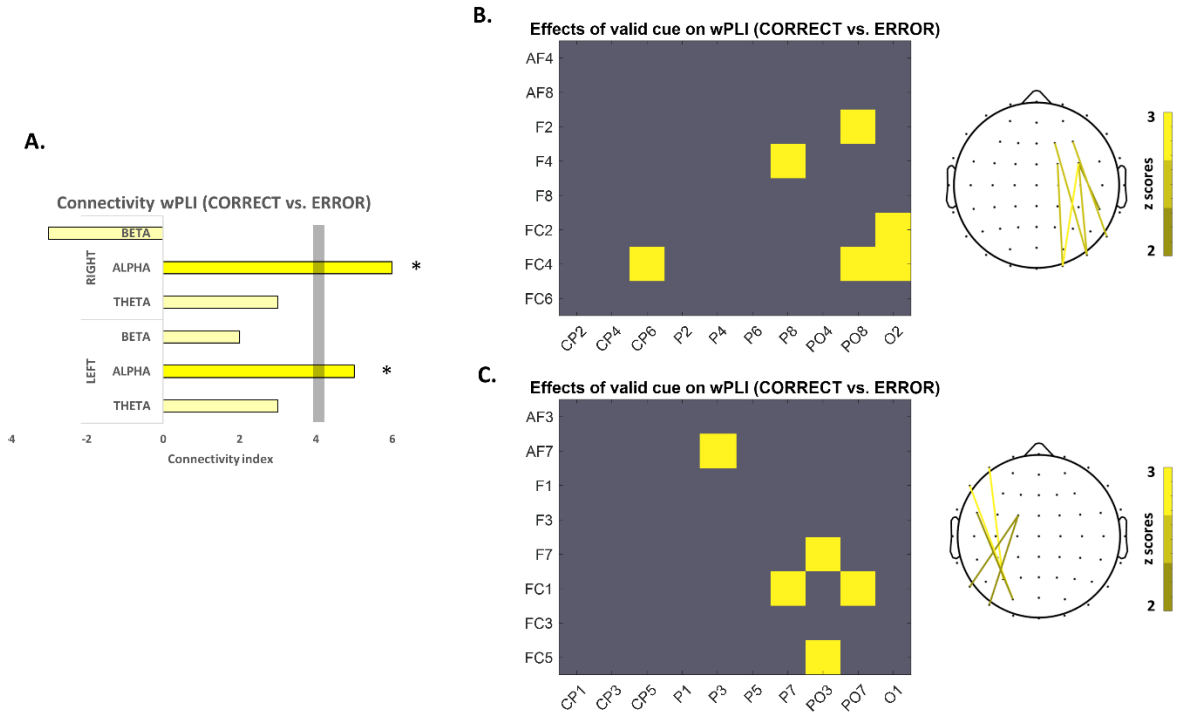

Figure 5. **Changes in interregional coupling between frontal and posterior ROIs when contrasting activity recorded during valid and error trials.**

A. Representation of the connectivity index for each hemisphere (contralateral vs ipsilateral to stimulus) for each frequency band (theta, alpha and beta frequency); the grey vertical bar shows the statistical threshold. Yellow ink indicates increases in interregional coupling for the correct vs. error trials. **B. Connectivity in the hemisphere contralateral to the cue and stimulus.** *Left:* Connectivity matrix measured by the weighted phase lag index (wPLI) across all electrodes included in the regions of interest for the hemisphere contralateral to the cue and stimulus location, in the significant alpha range (7-13 Hz). Yellow ink indicates increases in interregional coupling for the correct vs. error trials. *Right:* Topographical representations of the electrodes showing significantly increased coupling for the correct vs. error trials. **C. Connectivity in the hemisphere ipsilateral to the cue and stimulus.** Connectivity matrix measured by the weighted phase lag index (wPLI) across all electrodes included in the regions of interest for the hemisphere ipsilateral to the cue and stimulus location, in the significant alpha range (7-13 Hz Yellow ink indicates increases in interregional coupling for the correct vs. error trials. *Right:* Topographical representations of the electrodes showing significantly increased coupling for the correct vs. error trials.wPLI = weighted phase-lag index.

Discussion

How does our subjective view match external perceptual information? And how do these mechanisms interact to give rise to an integrated sense of our perceptual environment and even more so when we can predict upcoming sensory information? The present study has been designed to precisely address these crucial questions. By use of a modified Posner paradigm and concurrent EEG recordings, we have tested what neural markers could account for objective accuracy as opposed to subjective confidence. Importantly and differently from previous studies, we addressed these questions in conditions where a clear prediction could be made based on top-down spatial informative cues. The main findings of our study show that spatial cues drive the topographical distributions of both alpha-frequency and -amplitude; however, these alpha parameters are dissociable. In particular, while alpha-amplitude reflects perceptual levels of confidence and metacognition, already before stimulus presentation, alpha-frequency predicts perceptual accuracy and sensitivity.

The link between alpha-amplitude and subjective confidence and metacognition was already reported in previous studies (Benwell et al., 2017; Iemi et al., 2017; Samaha & Postle, 2015). However, in these studies, stimuli are always presented at the same location, with temporal uncertainty as to when stimuli are presented. Participants entertain two alternative hypotheses between one stimulus configuration (e.g., presence: 50% possibility) vs. another stimulus configuration (e.g., absence: 50% possibility) at any given time, thus fluctuating between a more conservative or more liberal attitude towards their internal level of confidence to respond having seen one vs. the other stimulus configuration. Crucially, in our study, in addition to temporal uncertainty, we have provided predictable lateralized contextual information, which was not assessed in previous research (Benwell et al., 2017; Di Gregorio et al., 2022; Iemi et al., 2017; Samaha & Postle, 2015).

What happens when the contextual information provided allows for likely

predictions of the to-be-attended location? Here we found that retinotopically-organized alpha-amplitude still accounts for the level of confidence reported by the participants. However, the process through which this mechanism is achieved relies more tightly on the predictive level of the contextual information provided. In particular, the contralateral hemisphere shows an alpha-amplitude desynchronization accounting for a higher level of confidence, along with synchronization of alpha-amplitude in the ipsilateral hemisphere. An inverse relationship was found for low confident trials. Ipsilateral synchronization (together with contralateral desynchronization) to high-confidence trials reflects the informed hypothesis not to attend (or actively inhibit) irrelevant information that may be presented ipsilaterally, favoring contralateral sensory processing (Thut et al., 2006). Contralateral synchronization (together with ipsilateral desynchronization) to low-confidence trials reflects a failure to allocate resources according to the predictive hypothesis. Analyses performed on metacognitive abilities confirmed these results at the between-subject level, where contralateral changes of pre-stimulus alpha-amplitude selectively accounted for the metacognitive abilities of participants but not their perceptual sensitivity. Here, metacognition can be defined as the ability to assess the accuracy of our internal perceptual states, thus representing a post-perceptual decision-making process rather than subjective perceptual bias.

In Study 1, under uninformative cue conditions, pre-stimulus alpha amplitude accounted for confidence levels but not the metacognitive performance, and only post-stimulus alpha amplitude accounted for metacognitive performance. This finding was interpreted as the result of sensory input updating the internal representation of the stimulus once the stimulus was presented. Here, under informative cue conditions, we found that contralateral pre-stimulus alpha-amplitude accounted for metacognitive abilities already before the stimulus was presented. Thus, the informative condition was used to

anticipate stimulus appearance at the cued location so as to maximize performance and minimize the error, in line with a predictive coding account (Friston & Kiebel, 2009).

In accordance with the results from Study 1, even here, alpha-frequency consistently accounted for objective accuracy such that faster alpha-frequency best accounts for better performance. Importantly, depending on the predictability of the location of the forthcoming stimulus, alpha-frequency can be modulated evenly (as shown previously) or at the predicted location, as demonstrated here, by enhancing sampling resources at the to-be-attended location and thus maximizing in the latter case the possibility to correctly report the presence of a target. Importantly, these effects can be observed at a between-subject level, where perceptual sensitivity, as measured via d', is directly and selectively related to the contralateral speed of alpha-activity, such that the faster the alpha frequency at the to-be-attended location, the higher the d'. Therefore, our capacity to sample information over time is limited by the characteristics of the circuitry of neural ensembles in a range of oscillatory cycles within the alpha band. Such limited resources can be allocated according to the attended quality of the stimulus, such as its occurrence in space. Being such resources limited, the more one can predict the exact location of the forthcoming stimulus, the higher will be the resource allocation at that particular point in space where a higher sampling rate within the alpha band will be observed. Recent evidence goes well in line with the current interpretation, demonstrating flexible retinotopically-organized changes of alpha-frequency during temporal processing and spatial attention deployment. Specifically, in a recent study, stimuli integration vs. segregation was related to slower vs. faster alpha frequency contralateral to an attended location, thus confirming the role of alpha frequency as a general sampling mechanism strategically tuned by the deployment of spatial attention (Wutz et al., 2018).

Under the unpredictive conditions of Study 1, we have found a dissociation

between alpha-frequency and amplitude in explaining accuracy and confidence, respectively (Di Gregorio et al., 2022). Here, however, alpha-amplitude seems to account for accuracy when contextual information provides predictable cues as to where the visual stimulus will be presented. The finding of alpha-amplitude modulations observed here to predict the level of objective accuracy is in line with a wealth of literature (Kelly et al., 2006; Rihs et al., 2009; Sauseng et al., 2007; Snyder & Foxe, 2010; Worden et al., 2000). This mechanism has been proposed to represent a top-down control process (Capotosto et al., 2012; Marshall et al., 2015) able to allocate limited attentional resources towards the to-be-attended location, thus actively ignoring irrelevant spatial locations (Jensen & Mazaheri, 2010). Moreover, the role of this controlled deployment of attentive resources has been suggested to reflect biasing signaling toward the forthcoming stimulus (Landau, 2018; Landau & Fries, 2012; Re et al., 2019). However, whether alpha-amplitude reflects an expression of perceptual confidence per se or can also directly account for objective accuracy remained a matter of debate (Linkenkaer-Hansen et al., 2004; Rajagovindan & Ding, 2011). Our data is in line with recent evidence proposing that pre-stimulus alpha-amplitude encodes biases of upcoming sensory decisions induced by top-down predictions (Mayer et al., 2016). How can we then explain the fact that alpha-amplitude also accounts for objective accuracy? Our data show that alpha-amplitude does encode biases of upcoming sensory predictions based on top-down prediction, but crucially, the predictability of the contextual information will render the bias as predictive as the effective sensory occurrence itself, resulting in a substantially overlapping measure. Yet, the critical point we clarify here for the first time is that it rather reflects the level of top-down induced bias and not the level of accuracy per se. Said otherwise: highly predictable target locations will enforce top-down predicting indices (alpha-amplitude) accounting for a high level of confidence, thus highly overlapping with the level of accuracy. This bias

organizes sensory resources towards the most plausible prediction by modulating, in turn, oscillatory alpha-frequency. Indeed, what more directly allows for a crosscheck of sensory accuracy is subtended by the spatial allocation of sensory sampling, namely the speed up of alpha-frequency. To sum up: lateralization of pre-stimulus alpha-amplitude accounts for metacognitive abilities already before stimulus presentation but not for the enhanced stimulus sensitivity. The latter can be best explained by the allocation of sensory sampling exclusively at the to-be-attended location, namely a speeding up of alpha oscillation allowing for a higher sampling rate.

Importantly, our results indicate that this spatial allocation is enabled via long-range frequency-specific oscillatory coherence in the alpha range, in accordance with previous findings and prominent theories (Fries, 2005, 2015; Salinas & Sejnowski, 2001; Sauseng et al., 2005). Specifically, attention seems to exert control via synchronization of the phases of high excitability between the frontal cortex and visual areas involved in the attended space, thus enabling resource allocation.

Our conscious experience is the result of a complex interaction between functional circuits coding for different aspects of our perceptual experience. Alpha-frequency samples information over time, with each alpha cycle representing a moment of sensory update. Alpha-amplitude matches this incoming information with expected outcomes, resulting in what we could call the best guessing of the world given the information at hand and the richness of our interpretative and predictive history. Therefore, “the present now” could be defined at any given time by the impact of previous information (de Lange et al., 2013) in predicting the occurrence of the forthcoming event (Ho et al., 2019) and the allocation of sensory resources in space and time. This, in turn, would update the strength of our predictive model to confirm or confute the tested hypotheses, in line with recent proposals (Alamia & VanRullen, 2019; Clark, 2013; Daunizeau et al., 2010; Friston, 2019; Kersten et

al., 2004; Ma et al., 2006).

Such a mechanism would represent a highly adaptive heuristic tool we have developed. It allows rapid adjustment of sensory selection based on sensory income feeding into previous knowledge to maximize the use of sensory resources, which ultimately leads to maximal efficiency with minimal homeostatic energy dispersion (Friston, 2009, 2010).

In conclusion, we show here that modulation of alpha-amplitude in space allocates faster sampling capacity (faster alpha-frequency) exclusively at the attended location in order to match what we think we see with what is most likely to be out there, thus maximizing the efficiency of our conscious experience.

STUDY 5:
FEEDBACK AND FEEDFORWARD MECHANISMS OF VISUAL PROCESSING

Abstract

Flexible and adaptive visual processing is enabled through the dynamic interplay between the feedback (top-down) and feedforward (bottom-up) information exchange, presumably brought about by oscillatory brain activity. While the feedback influences do predominate in slower alpha and beta frequencies, activity along feedforward projections is in the faster gamma band. By emulating top-down signals through a single transcranial impulse over a higher-order attention area and careful manipulation of the bottom-up information signaling (through the presentation of moving concentric gratings), the current study aimed at causally testing the oscillatory mechanisms underlying feedforward and feedback interactions in perception. Specifically, in an online TMS-EEG protocol, the strength of sensory input was manipulated while emulating feedback signals by a single TMS pulse over the Frontal Eye Field (right-FEF) in comparison to a control TMS site (right-M1 foot area). As expected, sensory input in the absence of FEF-TMS increased bottom-up gamma activity in posterior brain areas (feedforward mechanism processes). FEF-TMS (vs control stimulation) replicated previous findings of a phase-realignment of beta-band activity over remote posterior occipital sites, as well as higher fronto-posterior phase-connectivity (feedback processes), both for the stimulus present and absent conditions. Crucially, when testing the interaction between bottom-up and top-down processes for the combination of FEF-TMS and sensory input, we observed an increased nesting of the bottom-up gamma activity in the lower beta-band cycles. Therefore, the current study confirmed by a causal probe phase-to-power coupling as an oscillatory mechanism of feedback influences onto feedforward signals, offering novel insights into the neural underpinnings of the interplay between top-down (attentional) control and sensory input.

Introduction

Flexible and adaptive perception is made possible by sensory input and its top-down (e.g., predictive) regulation. This involves a wide-spread brain network in which top-down signals influence lower-level visual areas (Bichot et al., 2005; Fries et al., 2008). For instance, if the task requires preferential processing of visual stimuli at a specific spatial location, top-down visuo-spatial attentional signals will modulate neural assemblies in visual areas to enable enhanced processing of information in the attentional spotlight (Carrasco, 2011). The need for task-related resource allocations will engage complex brain networks (Corbetta & Shulman, 2002), among which the Frontal Eye Field (FEF) is a key area (Barceló et al., 2000). Specifically, non-human primate work has demonstrated that task-related attentional signals generated in the FEF exert a top-down influence on visual areas (Buschman & Miller, 2007; Gregoriou et al., 2009, 2012) and that micro-stimulation of FEF yields attention-like effects on the visual system (Moore & Fallah, 2004). Similarly, causal involvement of the FEF in attentional control has been demonstrated in human participants, whereby the activation of FEF by means of non-invasive brain stimulation causes changes in visual cortex activity (Ruff et al., 2006; Silvanto et al., 2006; Taylor et al., 2007) and perception (Chica et al., 2014; Grosbras & Paus, 2002, 2003).

At the same time, brain oscillations have been identified as a crucial mechanism in visual perception and attention, whereas oscillatory synchronization in specific frequency bands both within and between brain regions would facilitate visual processing and attentional control (Lobier et al., 2018; Michalareas et al., 2016; Miller & Buschman, 2013). For instance, it has been noted that task conditions emphasizing feed-forward processing are related to high-frequency synchronization, whilst task-emphasized feedback processing reveals stronger signaling at lower frequencies (Buschman & Miller, 2007; von Stein & Sarnthein, 2000). This has been confirmed by non-human studies demonstrating

that pathways and layers involved in feedback and feedforward signaling show stronger synchronization at, respectively, lower and higher frequencies (Bastos et al., 2012). Similar to the macaque anatomical hierarchy, recent evidence also found inter-arial rhythmic influences in human visual cortex, with the influences along feedback projections predominated in the slower alpha-beta band, whereas influences along feedforward projections predominating in the faster gamma band (Michalareas et al., 2016). Indeed, multiple studies suggest that sensory input processing in primary visual cortices is related to evoked gamma activity (Brunet et al., 2014; Martinovic & Busch, 2011; Siegel et al., 2007; Zaehle et al., 2009). Gamma modulations have been observed for low-level physical features, such as stimulus size and spatial location (i.e., higher gamma activity for central and bigger visual stimuli) (Busch et al., 2004). Crucially, cognitive effects on gamma activity have been also observed, with higher gamma activity for the attended stimuli, along with a gradual decrease of gamma from more to less feature-similar distractors (Herrmann et al., 1999; Herrmann & Mecklinger, 2001), revealing an early interaction between bottom-up and top-down processes.

These frequency-specific hierarchical pathways seem to be present even across attentional networks, thus not only limited to visual cortices (Siegel et al., 2008). For instance, a recent rhythmic TMS study found that beta-frequency stimulation at parietal cortices disrupts top-down attention, while gamma frequency TMS on the same areas disrupts bottom-up (stimulus-driven) attentional process (Riddle et al., 2019). Additionally, non-invasive stimulation of the FEF area seems to cause an instantaneous phase reorganization of the beta oscillatory activity over occipital areas. Therefore, this top-down control is enabled by the frequency-specific oscillatory phase re-alignment between distant brain areas, that would in turn synchronize the periods of high excitability between them, resulting in perfectly timed enhanced excitability of sensory cortex to external input

(Veniero et al., 2021). Taken together, these findings suggest that the activity associated with the sensory input processed and feedforwarded through fast gamma oscillatory activity, while the top-down mechanisms from higher-order areas would be implemented in the beta oscillatory bands. In line with this notion, gamma band activity has been reported to be phase-locked to slower oscillations, with gamma bursts being nested within specific phases of the slower frequency. It has been suggested that, in this manner, these different frequency oscillations would interact to spatially and temporally coordinate neural communication across large-scale cognitive and perceptual networks (Bonnefond et al., 2017; Jensen et al., 2014b). Therefore, the phase-locking of gamma activity to the beta oscillations could organize the neural code by enabling the fine balance between the two streams, and therefore ensuring optimal performance.

The aim of the current project was to causally test the mechanism of the feedforward and feedback interactions underlying perception based on the cross-frequency coupling. Specifically, in an online TMS-EEG protocol, the strength and timing of sensory input will be manipulated while simultaneously controlling its interaction with feedback signals, emulated by a FEF TMS-pulse.

Methods

Participants

A total of thirty participants took part in the study (18 females; mean age ± SE = 24.6 ± 4.11 years). The College of Science and Engineering's Ethical Committee authorized all protocols, and they were carried out in conformity with their ethical TMS requirements (University of Glasgow). All subjects provided written, fully informed consent to take part in the study. Likewise, all participants included in the study reported no contraindication to TMS, or any neurological or psychiatric symptomatology.

Stimuli and task procedure

Main Experimental Task. Participants were comfortably seated at a viewing distance of 57 cm from an LCD monitor (144 Hz refresh rate), placing their chin on a chinrest to maintain a steady head position. The main experimental session consisted of two conditions: while EEG was continuously recorded during a visual discrimination task, TMS was applied to the right Frontal Eye Field or the control area (right M1-foot area) in four separate task blocks (2 blocks per stimulation, pseudorandomized as two consecutive blocks would not have the same-site stimulation).

A behavioral visual discrimination task was created in Matlab (Psychtoolbox-3). In both stimulation conditions, the task structure, the number of pulses, and pulse timing were kept constant, with the only difference being the stimulation site. Specifically, each trial began with a black fixation cross, which, after 1500ms, would become red to anticipate that the stimulus would shortly appear. After 500ms, a continuous circular sine grating contracting inwards could appear for 5 seconds. The participant's task was to press the button whenever they noticed a glitch in the movement of the grating while always keeping their eyes on the fixation cross. In the jittered time period between 1 and 4 s after stimulus appearance, a TMS pulse could be delivered on one of the two stimulation sites (depending

on the experimental block), which in some trials was immediately followed by the glitch in the grating movement. The duration of the glitch was individualized for each participant, with a separate titration session (see next section). On the other hand, some trials consisted of the sine-grating only, the TMS-pulse not followed by the glitch, or the glitch in the stimulus movement without the TMS-pulse. Finally, there were trials with (and without) TMS pulse where the sine-grating was not presented. In sum, the task consisted of 640 trials of a total duration of about 90 minutes (see Figure 1B for the details on the trial structure and number).

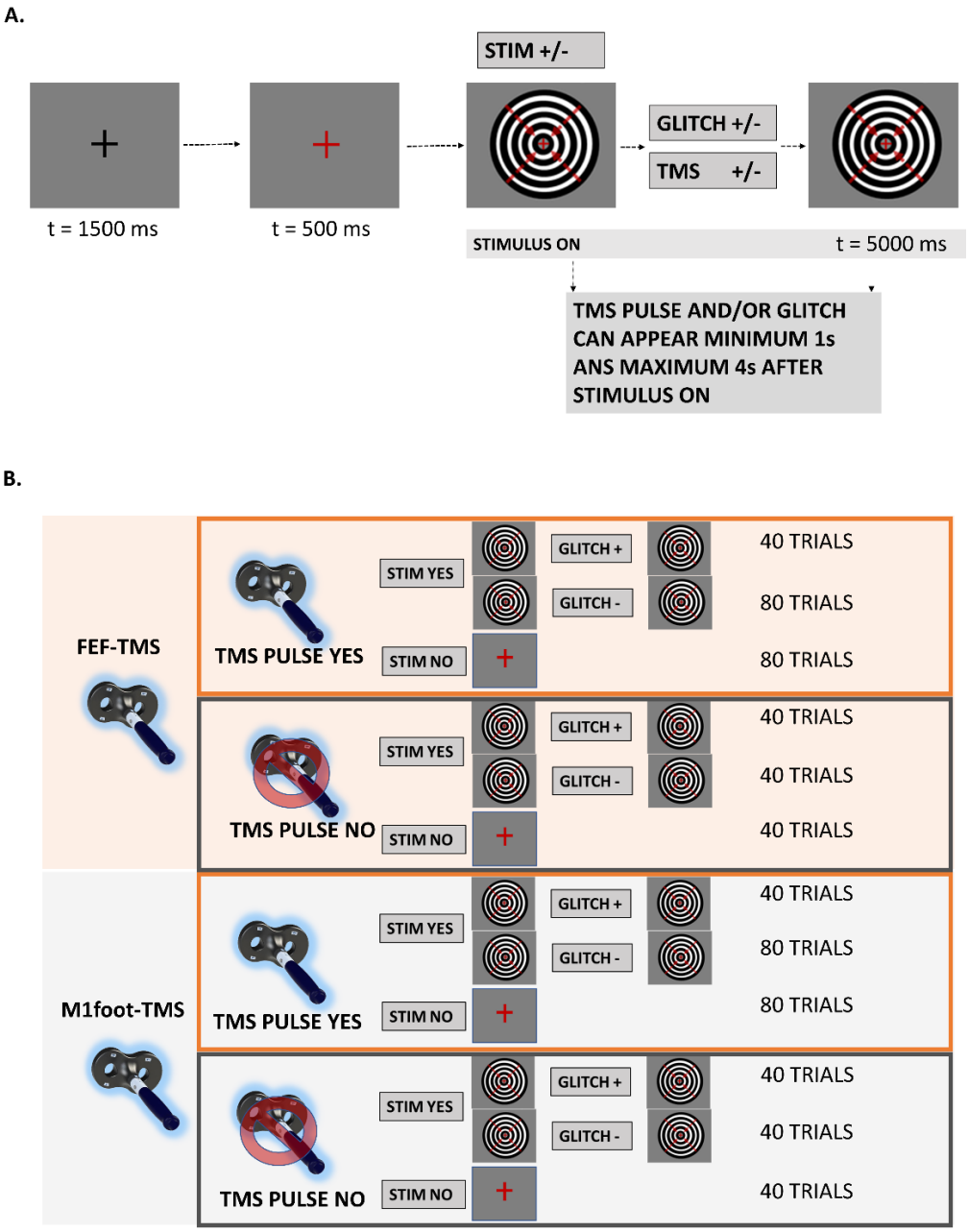

Figure 1. **Experimental and task design.**

A. Task Trial Sequence. Each trial began with a black fixation cross lasting 1500 ms. Afterwards the cross would become red indicating that the stimulus will arrive shortly (after 500 ms). Then the stimulus, in a form of a black and white sine-grating contracting inwards, could appear for 5 seconds. In stimulus absent condition, red fixation cross would be present for the same time. Some stimulus-present trials were followed by the target glitch in the stimulus movement, and participants had to respond with a button press whenever they would perceive the glitch. Moreover, some, both stimulus present and stimulus absent trials, could also contain a TMS pulse. Both TMS pulse and target glitch could appear from minimum 1 second and maximum 4 seconds after the stimulus appearance. **B. Experimental design.** Task conditions with respective number of trials per condition.

Titration Session. The duration of the glitch in the sine-grating movement, in terms of number of frames that the grating kept still, was individually threshold for each

participant via the blocked staircase procedure. Specifically, the session began with a supra-threshold glitch duration values (20 frames of 144 Hz, equal to 14ms) in an initial block (N = 10 trials), where half of them were target trials (sine grating with the glitch) and half of them catch trials (sine grating without the glitch). Subsequently, the percentage of the correct trials was calculated, and the glitch duration was tuned accordingly (100 % correct: glitch duration reduced for 6 frames; 95 - 86 % correct: glitch duration reduced for 4 frames; 85 - 76 % correct: glitch duration reduced for 2 frames; 75 - 56 % correct: same glitch duration; 55 - 46 % correct: glitch duration enhanced for 2 frames; 45 - 36 % correct: glitch duration enhanced for 4 frames; 35 - 26 % correct: glitch duration enhanced for 6 frames; 25 - 6 % correct: glitch duration enhanced for 8 frames; 5 – 0 % correct: glitch duration enhanced for 10 frames). The staircase procedure continued for 16 blocks in total (N_{total} = 160 trials), and glitch duration values for each block were fitted to the sigmoid function as to identify duration values corresponding to the 70 % of accuracy for each participant (M_{glitch} duration (SD) = 7.14 (2.12)).

TMS. TMS was applied by means of a high-power Magstim 200 machine (Magstim Company, Whitland, UK), whereas the stimulator was connected to a 70mm standard figure-of-eight coil, triggered remotely using Matlab. TMS intensity was kept constant for the two stimulated sites at 65 % maximal stimulator output (MSO), as shown to be an adequate intensity to effectively activate FEF (Grosbras & Paus, 2003; Veniero et al., 2021) and lead to behavioral changes (O'Shea et al., 2004). Likewise, the coil position was kept constant, placed tangentially with the handle of the coil pointing backward and laterally approximately 45 degrees to the interhemispheric line.

In order to locate the target area, T1-weighted structural magnetic resonance images (MRI) were acquired via a 3T Siemens Trio Tim scanner (Siemens, Erlangen, Germany). Subsequently, the stimulation site for the right FEF was identifies separately for

each participant, applying the Cortex-based Alignment (CBA) approach in Brain-Voyager QX 2.8 (Brain Innovation, Maastricht, Netherlands). Specifically, anatomical data was used to reconstruct the cortical surface of each participant, which was subsequently aligned to the functional probabilistic group maps of the right FEF. These group maps were then back-transformed to the individual brain anatomy (Duecker et al., 2014; Frost & Goebel, 2012; Veniero et al., 2021). FEF coordinates were on average (± SD) $x = 31.2 \pm 3.7$, $y = -9.7 \pm 2.9$, $z = 49.74 \pm 5.1$. On the other hand, the control area (M1-foot area) was localized using averaged Talaraich coordinated identified in the literature ($x = 6.8$, $y = -14.8$, $z = 69.8$)(Chainay et al., 2004). Finally, to target the FEF and M1-foot area, and to ensure that the coil orientation and position is stable, Talairach coordinates obtained with the CBA (and constant coordinates for the control area) were imported to a neuro-navigation system (Brainsight; Rogue solution).

TMS-EEG recordings – acquisition and processing

EEG activity was recorded using a TMS-compatible EEG system (BrainAmp MRplus, BrainProducts), by using 61 TMS-compatible electrodes (EasyCap GmbH, Herrsching, Germany) positioned according to the 10–10 International System. The signal was acquired at a sampling rate of 5000 Hz, and bandpass filtered at 0.1–1000 Hz, with the electrode impedence kept bellow 10 KΩ. Eye moveemnts were accounted for via electrode placed on the outer canthus of the left eye.

TMS artifacts were located and eliminated using the TMS-EEG signal analyser (TESA), an open-source EEGLab plugin (Rogasch et al., 2017). First, EEG data were epoched around sine-grating stimulus appearance or TMS pulse onset (between -1ms and 10ms). In trials where TMS-pulse was not present, an additional marker in the TMS-timing window was added in order to allow the epoching. Afterward, a baseline correction was applied by subtracting the average of the entire epoch from each data point. Then TMS

pulse artifacts and peaks of TMS-evoked scalp muscle activities were removed (-1ms +10ms), and sunsequently intorpolated prior to down-sampling the data (from 5000Hz to 1000Hz). At this point, data were visually inspected to remove noisy trials. Interpolated data was once more eliminated before performing an ICA. Specifically, a fastICA algorithm was used (pop_tesa_fastica function) to identify individual components representing artifacts, combined with automatic component classification (pop tesa compselect function), with manual verification and reclassification as required. Here, only components with large amplitude artifacts, such as rhythmic-TMS-evoked scalp muscle artifacts, were removed. Before using pass-band (between 1 and 100Hz) and stop-band (between 48 and 52Hz) Butterworth filters, the data were once again interpolated. Interpolated data were then one more eliminated before another ICA aimed at eliminating all additional artifacts. Then, the TMS-pulse period was interpolated, and data were re-referenced to the average of all electrodes. Last but not least, single trials were visually examined, and those that still had TMS artifacts were eliminated.. The described TMS artifact removal procedure was applied to all EEG data. On average, less than 15% of all epochs were removed (M = 14.19%, SD = 5.85%).

Time-Frequency Amplitude. As a first step, to ensure that the continuous sine grating did indeed lead to an increase of gamma activity, a time-frequency analysis was performed on the signal epoched around the stimulus appearance. Specifically, complex Morelet wavelet convolution was applied to the signal, with morlet wavelet peak frequencies ranging from 3 to 80 Hz in 60 logarithmic steps. The full width at half-maximum (FWHM) ranged from 500 to 200 ms with increasing wavelet peak frequency. Subsequently, alpha-power values were normalized by decibel conversion, with the baseline period from -500ms to -200ms before the stimulus appearance. Finally, time-frequency differences between the trials with and without the sine-grating in parieto-

occipital cluster (cluster electrodes: O2, PO4, PO8, Oz, POz, PO3, PO7, O1) were compared via cluster-based permutation testing. Specifically, the z-scores were obtained by comparing the time-frequency map differences with permuted (N=1000) random differences (obtained by randomizing the sign of difference map for every subject), with differences with z-values corresponding to $p<0.05$ were retained as significant. Subsequently, the results were cluster-corrected, whereas the cluster threshold was determined by the 5% biggest cluster size in the null distribution of permuted z-scores (thus $p<.05$).

ITPC. Next, the period around the TMS stimulation was investigated, with the aim of affirming higher fronto-posterior phase-realignment and connectivity induced by the pulse. One previously used measure of the influence of FEF stimulation on the posterior cortex is intertrial phase clustering (ITPC), which can give information on the frequency-specific phase-realignment of the posterior activity after the frontal TMS pulse. ITPC is the measure of the extent to which a distribution of phase angles at each time-frequency-electrode point across the trials is nonuniformly distributed in polar space (Cohen, 2014). Phase angles were obtained by the same wavelet convolution procedure as used for the time-frequency power analysis. Likewise, the same statistical permutation-based cluster analysis used for amplitude differences was used for ITPC-difference plots between the two stimulation protocols (FEF-TMS, M1-foot-TMS, separately when the stimulus was present or absent). Posterior electrodes used in time-frequency amplitude analysis were also used here, separately for the right (O2, PO4, PO8, Oz, POz) and left (Oz, POz, PO3, PO7, O1) electrode cluster.

WPLI. Phase connectivity was estimated in the sensor space via the weighted phase-lag index (wPLI) (Vinck et al., 2011), in the same manner as per Experiment 4. Here, once wPLI values were extracted for every frequency bin (3 to 30 Hz in 1 Hz steps)

and epoch, they were averaged to obtain distinct values for each of-interest experimental condition (FEF and M1-foot stimulation when sine-grating was present or absent) in higher alpha/lower beta frequency band identified as significant via ITPC (13-20 Hz). Subsequently, non-parametric permutation-based analysis (1000 iterations) was performed to compare the connectivity between two stimulation protocols, as already reported in Experiment 4. Here, the connectivity index of each condition was then estimated using the formula: CI = sig_pos/ sp_total, where sig_pos are connections that are significantly higher after FEF-TMS with respect to M1foot-TMS, and sp_tot are all possible connections. Furthermore, another permutation test was introduced to calculate the significance threshold for CI (for details, see Experiment 4; connectivity threshold= 0.055).

Phase-Amplitude Coupling. Finally, the hypothesized interaction between the feedback signal emulated by the pulse and feedforward sensory input was measured via phase-amplitude coupling, with the idea that the amplitude of high-frequency (gamma) oscillations should be modulated by the phase of low-frequency rhythms. Phase-amplitude coupling was quantified via modulation index (Tort et al., 2010). Briefly, the signal was first filtered at the two frequency ranges under analysis (low frequencies = 5-20Hz with 4Hz bandwidth; high frequencies = 30-80Hz with 10Hz bandwidth). Then, the Hilbert transform was applied to obtain the time series of the phases for the lower frequency range and the time series of the amplitude envelope for higher frequencies. Next, these phases were binned, and the mean of amplitude over each bin was calculated and normalized by the sum over all the bins, resulting in mean amplitude distribution over phase bins. Finally, the modulation index (MI) was calculated as the difference between the observed amplitude distribution and the uniform distribution. MI was calculated for every cross-frequency point for every electrode in time-window of interest (0- 200 ms) after the TMS pulse, concatenated between trials. Likewise, the same statistical permutation-based cluster

analysis used for ITPC and amplitude was used for CFC-difference maps between two stimulated sites, separately for stimulus-present and stimulus-absent conditions. The right parieto-occipital cluster (POZ, OZ, O2, PO4, PO8), identified as significant with wPLI and ITPC, was also used here.

Results

Sensory input induces higher gamma-band amplitude

The first analysis aimed at confirming that our experimental manipulation had expected consequences, i.e., that the sensory input in the form of a continuous sine grating would indeed enhance gamma activity over the posterior cortex. To do so, all the trials with and without stimulus were compared in a pre TMS-pulse period (first second of the stimulus duration). The permutation-based analysis confirmed that there is significantly higher gamma synchronization in a stimulus-present condition (compared to a no-stimulus condition), lasting for the whole post-stimulus time window (0-800 ms). These differences span between both low and higher gamma frequency bands (50-80 Hz). Importantly, topographic differences indicate that these effects were constrained to the posterior electrode cluster (see Figure 2B). As expected, the stimulus appearance was also followed by a desynchronization across the lower frequencies (10-20 Hz).

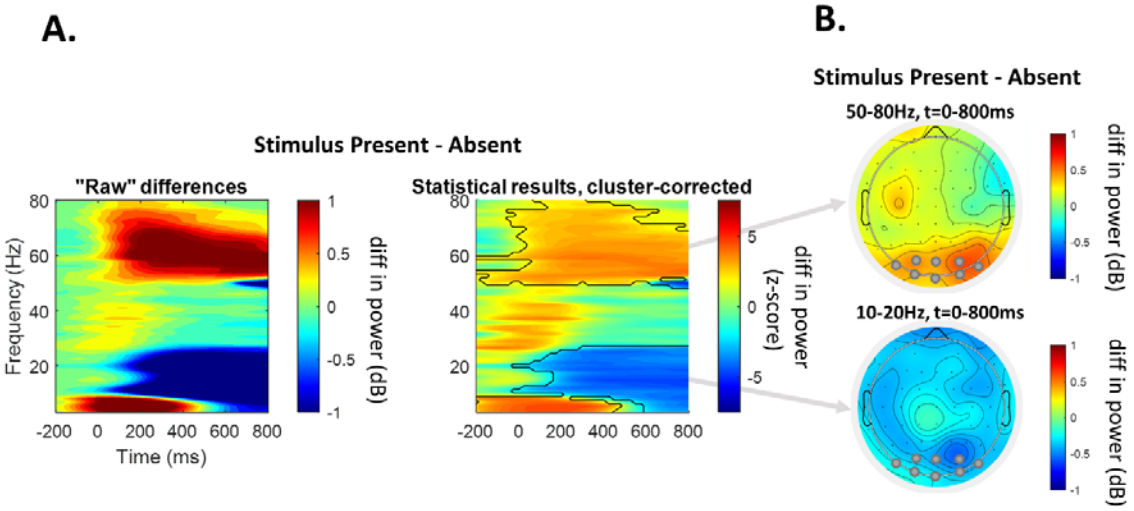

Figure 2. **Time-Frequency Analysis: Stimulus appearance**.

A. *Left panel:* Raw differences in time-frequency plots of the posterior cluster (electrodes: O2, O1, POz, Oz, PO8, PO7, PO4, PO3) between stimulus present and stimulus absent condition. Frequency range for the analysis (y-axis) is from 5-80 Hz. Time range for the analysis (x-axis) is from -200 to 800 ms, where 0 point is the stimulus appearance. *Right panel:* Z-scores of the permutation-based analysis between stimulus present and stimulus absent condition. Significant clusters are framed with the black line. **B.** Topographies of the significant clusters of the amplitude differences in the gamma (upper) and higher alpha/lower beta frequency (lower). Electrodes used for the time-frequency analysis are marked with grey circles. diff = difference; dB = decibel; Hz=herz; t=time.

FEF-stimulation excerpts feedback control over the posterior cortex through phase connectivity and realignment

The influence of FEF-TMS on the posterior cortex has been investigated via ITPC. As previously reported, FEF stimulation should lead to a phase-reset over the posterior cortex in the alpha/beta frequency band as part of the top-down mechanism that would shape the activity of the visual cortex through oscillatory re-alignment (Veniero et al., 2021). Here, we replicate these findings. When the visual stimulus was not present, there was a significantly higher ITPC for FEF-TMS vs. control stimulation in the lower beta frequency (13-20 Hz), for around 300ms after the TMS pulse (Figure 3A). Similar effects have also been noted for the stimulus-present condition, where however, differences were also evident in the higher alpha frequency range (11-19Hz) and mainly present in the first 200ms after the pulse (Figure 3B).

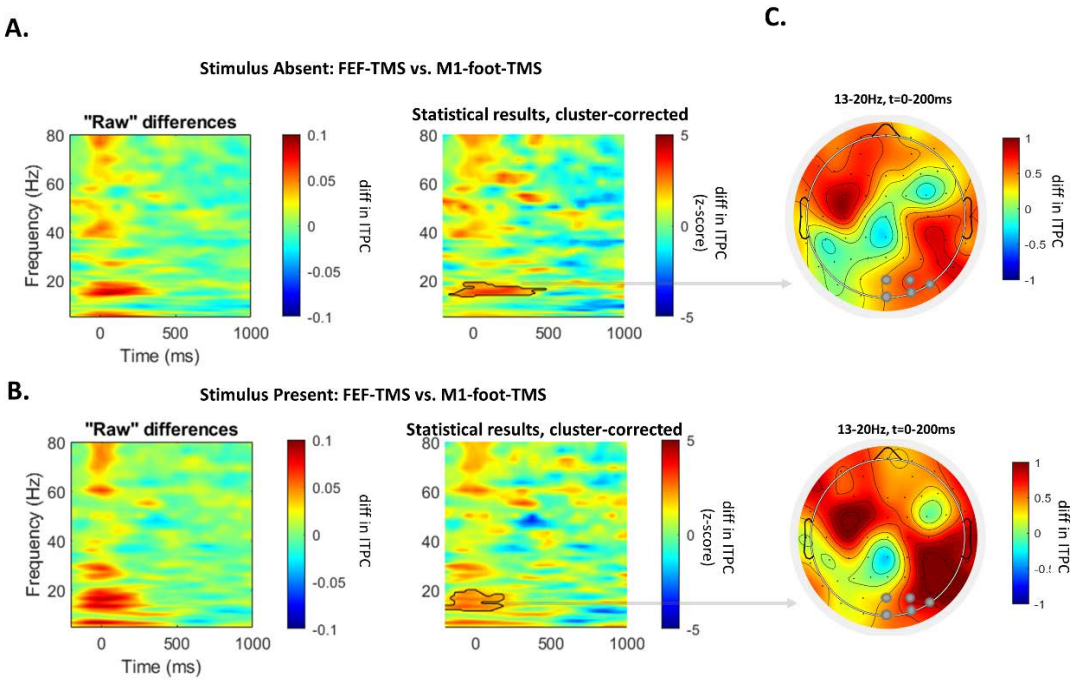

Figure 3. **ITPC Analysis: Differences between FEF-TMS and control stimulation (M1foot-TMS).**

A. Stimulus Absent condition. *Left panel*: Raw differences in ITPC plots of the posterior cluster in the stimulated (right) hemisphere (electrodes: O2, POz, Oz, PO8, PO4) between FEF-TMS and control stimulation (M1foot-TMS). Frequency range for the analysis (y-axis) is from 5-80 Hz. Time range for the analysis (x-axis) is from -200 to 1000 ms, where 0 point is the timing of the TMS-pulse. *Right panel:* Z-scores of the permutation-based analysis between FEF-TMS and control stimulation (M1foot-TMS). Significant clusters are framed with the black line. **B. Stimulus Present condition.** *Left panel:* Raw differences in ITPC plots of the posterior cluster in the stimulated (right) hemisphere (electrodes: O2, POz, Oz, PO8, PO4) between FEF-TMS and control stimulation (M1foot-TMS). Frequency range for the analysis (y-axis) is from 5-80 Hz. Time range for the analysis (x-axis) is from -200 to 1000 ms, where 0 point is the timing of the TMS-pulse. *Right panel:* Z-scores of the permutation-based analysis between FEF-TMS and control stimulation (M1foot-TMS). **C.** Topographies of the significant clusters of the identified ITPC differences in the stimulus absent (upper) and stimulus present condition (lower). Electrodes used for the ITPC analysis are marked with grey circles. diff = difference; ITPC = inter-trial phase coherence; Hz=herz; t=time.

To assess if the FEF-TMS (vs. control site) would enhance its inter-site phase coupling with the posterior cortex, we used the weighted phase lag index (wPLI): a phase lag-based measure not affected by volume conduction and not biased by the sample size. Subsequently, non-parametric permutation analysis was used to compare wPLI values across the two stimulation sites (FEF-TMS, M1-foot) in the two task conditions (stimulus present, stimulus absent). Connectivity was estimated in 300ms following sp-TMS, between frontal and parieto-occipital clusters, both in the stimulated and non-stimulated hemisphere, in the lower beta band identified as significant via ITPC. The results indicate

that there is enhanced fronto-posterior connectivity for the FEF-TMS with respect to the control site (Figure 4A). Importantly, these differences were only present in the right (stimulated) hemisphere. As expected, these differences were visible both in the stimulus present and absent condition (Figure 4B and 4C), as they represent a top-down control mechanism that should be present even in the absence of the sensory input.

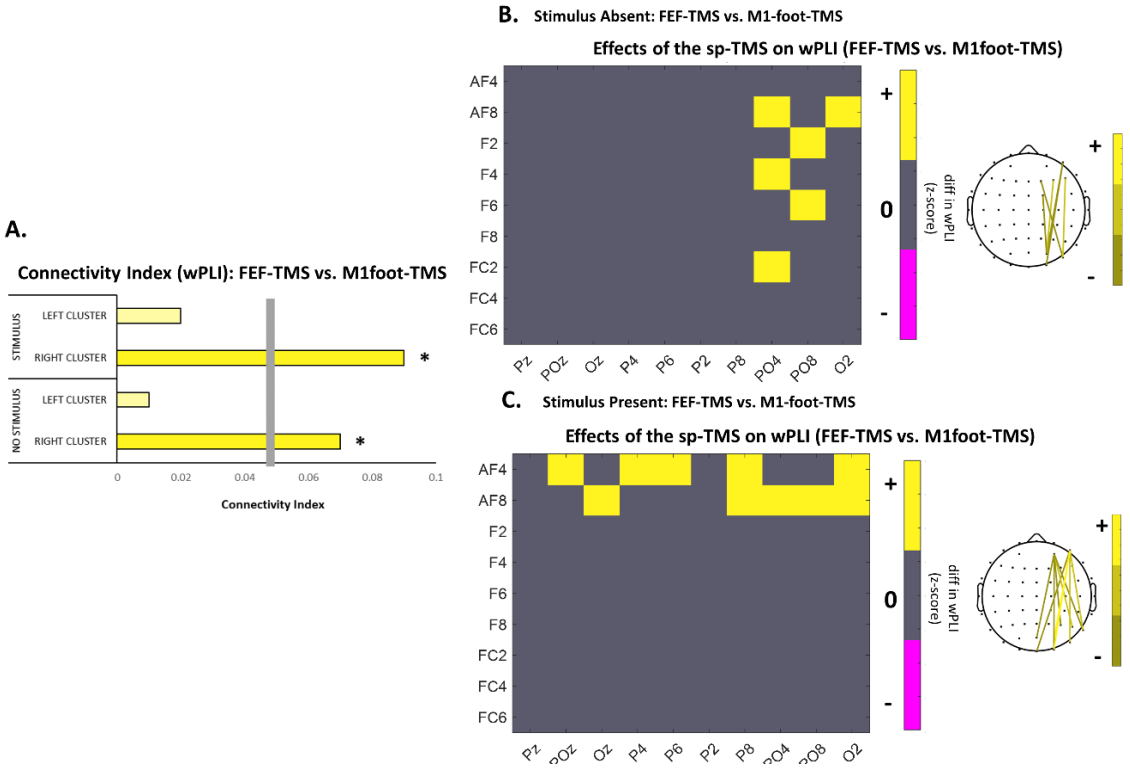

Figure 4. **Changes in interregional coupling between frontal and posterior ROIs when contrasting activity recorded during FEF-TMS and control stimulation (M1foot-TMS).**

A. Representation of the connectivity index for each of the experimental conditions (stimulus present vs absent) and the two hemispheres (right (stimulated) and the left hemisphere); grey vertical bar shows the statistical threshold. Yellow ink indicates increases in interregional coupling for the FEF-TMS vs, control stimulation. **B. Stimulus absent Condition.** *Left:* Connectivity matrix measured by the weighted phase lag index (wPLI) across all electrodes included in the regions of interest for the stimulus absent condition in higher alpha/lower beta range (13-20 Hz). Yellow ink indicates significant increases in interregional coupling for the FEF-TMS vs, control stimulation. *Right:* Topographical representations of the electrodes showing significant increased coupling for the FEF-TMS vs, control stimulation **C. Stimulus Present Condition.** *Left:* Connectivity matrix measured by the weighted phase lag index (wPLI) across all electrodes included in the regions of interest for the stimulus present condition in higher alpha/lower beta range (13-20 Hz), in the right (stimulated) hemisphere . Yellow ink indicates significant increases in interregional coupling for the FEF-TMS vs. control stimulation. *Right:* Topographical representations of the electrodes showing significant increased coupling for the FEF-TMS vs, control stimulation. wPLI = weighted phase-lag index.

Feedback control gets integrated with sensory input through cross-frequency coupling

In the previous paragraphs, we have demonstrated that the sensory input, in the form of a sine-grating moving inwards, would evoke gamma activity in the posterior cortex. Moreover, the FEF stimulation can excerpt top-down control over the posterior cortex through phase-realignment of the oscillatory activity in the posterior cortex, also evident in the higher fronto-parietooccipital phase-based connectivity. However, in order to have an efficient attentional selection and smooth and efficient perceptual experience, feedback mechanisms should constantly integrate incoming sensory input. What is then the mechanism underlying this integration? Here we hypothesize that this integration is made possible through phase-amplitude coupling, whereas the sensory input, related to high-frequency gamma amplitude, would be nested in certain phases of the lower frequency, that in turn, is controlled by a feedback route.

In order to test this hypothesis, the modulation index of phase-amplitude coupling was calculated for different experimental conditions in a time window of interest (0 - 200ms after TMS pulse), between a wide range of low- and -high frequencies, across the right parieto-occipital ROI. Results showed that the phase-amplitude coupling in the posterior cortex is indeed more clearly visible for the FEF-stimulation (vs. control M1-foot stimulation) only when the stimulus was presented. Specifically, the amplitude of the gamma frequency from 60 Hz – 90 Hz was coupled to the beta frequency phase (13-20 Hz). Crucially, these differences between the two stimulation protocols were not present in the absence of the sensor input, speaking in favor of the integration-through-coupling hypothesis (Figure 5).

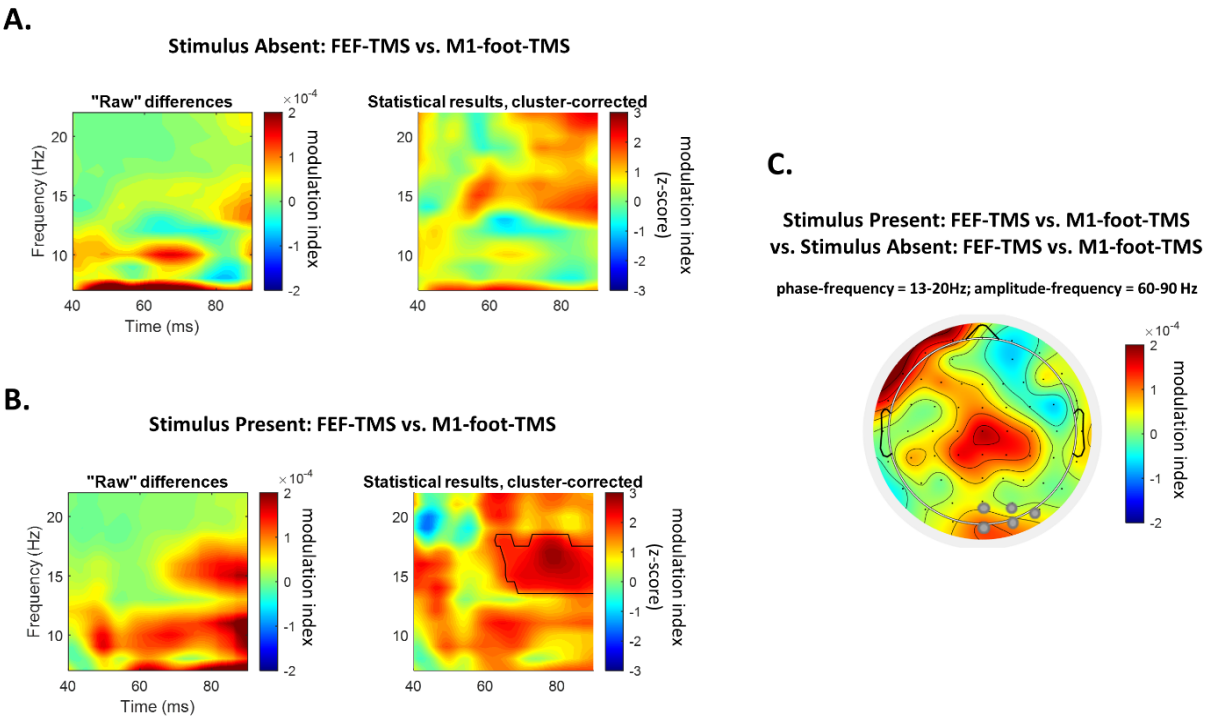

Figure 5. **Phase-to-amplitude Coupling (Modulation Index) after the TMS pulse (0-200 ms).**

A. Stimulus Absent condition. *Left panel:* Raw differences in modulation index (MI) plots of the posterior cluster in the stimulated (right) hemisphere (electrodes: O2, POz, Oz, PO8, PO4) between FEF-TMS and control stimulation (M1foot-TMS). Frequency range for the analysis for the lower phase-frequency (y-axis) is from 5-20 Hz. Frequency range for the analysis for the higher gamma amplitude-frequency (x-axis) is from 30-80 Hz. *Right panel:* Z-scores of the permutation-based analysis between FEF-TMS and control stimulation (M1foot-TMS). Significant clusters are framed with the black line. **B. Stimulus Present condition.** *Left panel*: Raw differences in modulation index (MI) plots of the posterior cluster in the stimulated (right) hemisphere (electrodes: O2, POz, Oz, PO8, PO4) between FEF-TMS and control stimulation (M1foot-TMS). Frequency range for the analysis for the lower phase-frequency (y-axis) is from 5-20 Hz. Frequency range for the analysis for the higher gamma amplitude-frequency (x-axis) is from 30-80 Hz. *Right panel:* Z-scores of the permutation-based analysis between FEF-TMS and control stimulation (M1foot-TMS). Significant clusters are framed with the black line**. *C.*** Topographies of the significant clusters of the identified MI differences in the stimulus present vs. stimulus absent condition. Electrodes used for the MI analysis are marked with grey circles. Hz=herz.

Discussion

Perception is much more than sensory input: it's an outcome of the complex interactions between our past experiences, expectations, and goals on the one hand and an incoming external sensory input on the other (Gregory et al., 1980; Neisser, 2014). This mechanism is at the core of the predictive coding theory, stating, in essence, that higher-order brain areas constantly generate predictions grounded on incoming sensory evidence and prior experience. Subsequently, those predictions are communicated back to lower-level brain areas, where they are subtracted from sensory evidence such that only prediction errors need to be forwarded to higher areas. Therefore, this constant interplay between priors and sensory evidence is what determines the efficiency of our conscious experience (Bastos et al., 2012).

In this interplay, brain oscillations may represent a neural mechanism implementing predictive coding (Alamia & VanRullen, 2019; Bastos et al., 2012). Indeed, both sensory processing and function communication between brain regions is accomplished via rhythmic modulation and coherence, speaking in favor of the feedback and feedforward processing enabled by slower and faster oscillatory activity, respectively. What remains largely unknown is how the feedforward route shapes the sensory input: or, in terms of predictive coding, the neural mechanism underlying the integration of prior expectations and sensory evidence. Here we hypothesize that the integration of the top-down control with sensory input in the posterior cortex is made possible by the nesting of the high-frequency amplitude evoked by the sensory input to the low-frequency phase, guided by top-down expectations. The aim of this study was to causally test the proposed model by emulating an attentional pulse via FEF-TMS during (or in the absence of) sensory processing.

First, we confirm that the continuous visual input, in the form of moving sine-

grating, results in higher synchronization in the gamma range across the posterior brain areas. In other words, there was a stimulus-driven increase in the gamma band, summing up to the converging evidence that the feedforward drive of sensory input is followed by gamma synchronization. This gamma increase is thought to enhance synaptic summation (Michalareas et al., 2016), thereby boosting the transfer of information at hand (Tiesinga et al., 2004).

Second, after emulating the attentional pulse over FEF (vs. control area), we observed a beta oscillatory re-alignment over the posterior brain areas, both in the presence and absence of the visual stimulus. Accordingly, we also observed higher phase-based connectivity at the same frequencies across both conditions but specific for the antero-posterior network of the stimulated hemisphere. These analyses confirm that the top-down feedback control within the fronto-occipital network is subtended by the beta oscillations: indeed, there are mounting evidence demonstrating that low beta oscillations in the fronto-parietal cortex reflects the activity of the dorsal attentional network, that in turn would guide perception along lower order visual areas (Battaglini et al., 2020; Capilla et al., 2022; Ronconi et al., 2018; Samaha, Gosseries, et al., 2017). Crucially, we observed the described phase-realignment and enhanced connectivity both with and without sensory input, confirming the notion that reorganization of the beta phase through long-range connectivity in the same frequency may represent a basic code for feedback communication (Veniero et al., 2021).

In terms of predictive coding, these feedforward and feedback influences are thought to attend to the signaling of prediction errors and predictions, respectively. Crucially, in this framework, predictions are updated through the gradual build-up of prediction errors, leading to the conclusion that predictions change more slowly than prediction errors. Therefore, if predictions and prediction errors are enabled via inter-areal

rhythmic coherence, the transmission of prediction errors would request higher frequencies than the transmission of predictions (Fontolan et al., 2014; Michalareas et al., 2016). This prediction is well in line with our findings, where the feedforward signaling is dominated by gamma and feedback signaling is dominated by beta rhythms.

Importantly, we affirm that the integration of the feedback signal, communicated to the visual cortex via beta frequency, and the sensory input, processed in the gamma range, is made possible through phase-to-amplitude cross-frequency coupling. Specifically, in the same posterior cluster identified in the previous analysis, there was higher locking of gamma activity to the beta-frequency phases for the FEF-TMS vs. control stimulation, only in the presence of the sensory input. Interestingly, the frequency ranges of the coupled oscillators exactly mirrored the gamma range identified as significant to sensory processing and the lower beta range identified via ITPC. This mechanism can be explained through the framework that posits that the communication between brain regions is based on nested oscillations (Bonnefond et al., 2017). The idea integrates the two most dominant theories of oscillatory communication. The first one is communication through coherence theory, where interregional communication is considered established when these regions oscillate at the same frequency with a stable phase difference (Fries, 2015). The second one is the gating through inhibition hypothesis, where slower oscillations are considered associated with pulses of inhibition and, as such, can aid communication between different regions through phase synchrony and release of inhibition (Jensen & Mazaheri, 2010; Klimesch et al., 2007). Finally, the unified framework based on nested oscillations posits that the communication between two areas is enabled via phase synchronization of oscillations at lower frequencies (<25 Hz), which serve as a temporal constrain for information carried by high-frequency activity (>40 Hz) (Bonnefond et al., 2017). Our results speak in favor of this theory, where top-down expectations carried from FEF are communicated through

oscillatory coherence to the posterior cortex, where they dictate sensory information flow through the nesting of the gamma oscillators.

In sum, the current experiment causally confirmed the proposed mechanism based on phase-to-power coupling between feedforward and feedback signals by carefully manipulating and timing the interaction between attention signaling and bottom-up processing. Importantly, these results represent a significant step forward toward a better understanding of the neural mechanisms underlying a failure to integrate external inputs into an internal representation of the world, present in some neurological and neuropsychiatric conditions.

GENERAL CONCLUSION

Current work aimed at advancing both theoretical and methodological state-of-the-art on the role of neural oscillations in visual perception, attention, and awareness. In order to meet this aim, the problem at hand was approached via three distinct pathways. First, through several studies and different experimental manipulations, the current thesis tried to double-dissociate oscillatory mechanisms of perceptual accuracy and subjective awareness but also to understand how they interact in order to ensure the optimal conscious experience of the external environment. In other words, what happens when the top-down control is implemented to guide the available resources towards the specific attentional focus, and in what manner do these top-down expectations, projected in a feedback manner, interact with the incoming sensory input. Second, current work is also interested in bridging the gap between research exploring oscillatory activity versus evoked components by trying to draw a link between them and establish if and how they could both present mutually dependent building blocks of the same mechanism underlying a given cognitive or sensory process. Third, across different studies, current work tried to overcome methodological limitations of available neuroimaging and neurostimulation tools by combining them, thus offering experimental answers from the approach that goes beyond correlative evidence, with a hope to further promoting the perks of multimodal methodologies (i.e., TMS-EEG approach). At the same time, current work tried to acknowledge potential difficulties and unknowns related to the TMS-EEG approach by further examining potential causes of the inter-individual differences in the stimulation outcome and seeking a way to predict them.

Dissociating oscillatory mechanisms of perceptual accuracy and awareness. The aim of Study 1 was to probe distinct oscillatory mechanisms underlying perceptual

accuracy, perceptual awareness, and metacognition. Specifically, here it was hypothesized that our capacity to accurately perceive visual stimuli, and our subjective perception of having correctly perceived them, are supported by different mechanisms in the brain. Crucially, the neural substrates of objective accuracy and subjective experience of that accuracy were empirically identified and demonstrated that they could be causally dissociated. This study builds on decades of electrophysiological research revealing a consistent correlational relationship linking alpha oscillations in the visual system to simple stimulus visibility (Dijk et al., 2008; Hanslmayr et al., 2007; Romei et al., 2008), a view that has, however been challenged by recent research (Benwell et al., 2017; Limbach & Corballis, 2016; Samaha, Iemi, et al., 2017). The latter highlights the need to dissociate between the processes that shape visual sensitivity and those influencing how an individual interprets a sensory event. Here, across three experiments, by means of combined EEG and rhythmic TMS (rhTMS) in human observers, correlational and then causal evidence was provided to show that the frequency of alpha oscillations is the best proxy of objective accuracy (with faster alpha frequency accounting for higher accuracy), whereas alpha amplitude best predicts the level of subjective conscious perception (with alpha amplitude being inversely related to subjective confidence). Moreover, alpha-amplitude continues having an important role even after stimulus appearance, whereas the initial bias in subjective awareness (measured via confidence levels) gets integrated with the information brought by the stimulus via further changes of the alpha-amplitude. Consequently, post-stimulus alpha-amplitude would shape metacognition, defined as a measure of accordance between the confidence levels and the actual perception. Mechanistically, this links alpha frequency to the neural pace of information sampling and alpha amplitude to the level of neural excitability and conscious access to both signal and noise. Thus, the current study directly demonstrated that the processing of visual information and its subjective

interpretation (i.e., subjective confidence), which are strongly inter-dependent in everyday life, have distinct oscillatory mechanisms and can be selectively modulated by non-invasive neurostimulation. Moreover, it gives us important insight about the mechanisms underlying metacognition, a process that integrates the awareness with objective performance, and that has been identified as dysfunctional in diverse psychopathologies (Sun et al., 2017). Therefore, understanting its neural fingerprint could subsequently aid the identification of the oscillatory abnormalities present in such pathologies. In sum, this work offers a significant advance in our understanding of the neural mechanisms that lead to conscious perceptual experience. Here it was demonstrated that objective accuracy and subjective perception are governed by independent neural mechanisms, explaining how and why, at times, we become confident of an event when, in fact, it did not occur and vice versa. This insight is pivotal for the way future research in diverse scientific communities (e.g., vision science, decision-making, consciousness, etc.) approach their core topics, interpret interindividual differences and explain pathological outcomes (e.g., failure in sensory processing, sub-optimal decision-making strategies, hallucinations, etc.).

Interacting oscillatory mechanisms of perceptual accuracy and awareness during selective attention. The aim of Study 4 was to understand how the mechanisms of perceptual accuracy and awareness, dissociated in Study 1, would interact under attentional demands in order to enhance the perceptual experience. Specifically, in Study 1, unpredictable lateralized stimuli were used, and, in this case, the frequency of pre-stimulus individual alpha oscillations (IAF) across both hemispheres could account for “objective” visual sensitivity such that faster IAF predicted higher accuracy, while the level of confidence on the response was accounted for by the amplitude of pre-stimulus alpha such that the higher the alpha amplitude across the hemispheres, the lower their “subjective” confidence. Moreover, it was found that contralateral alpha amplitude post-stimulus can

account for the level of metacognition, i.e., how accurate is the subjective representation of the individual about their objective performance.

Here these findings were further explored by testing the influence of a pre-stimulus informative attentional cue on the deployment of lateralized alpha activity. The results showed that the lateralized attentional cue modulated fronto-posterior connectivity in the alpha range, with higher synchronization for successful attentional deployment (i.e., for correct trials vs. error). Attentional cue also modulated pre-stimulus alpha amplitude as well as pre-stimulus IAF in the posterior cortex. Specifically, the informative cue desynchronizes alpha amplitude and speeds up IAF contralateral to the stimulus. Interestingly, the lateralized speed-up of IAF accounted for visual sensitivity (not confidence), while the modulation of pre-stimulus alpha power accounted specifically for individual confidence (not sensitivity) and, importantly, could account for metacognition, i.e., participants' subjective estimate is more accurate about their objective performance, even before they perform, speaking on the relevance of the informative cue in shaping individual anticipation towards stimulus presentation. By the use of signal detection theory and metacognitive measures, these findings offer a novel and up-to-date interpretation of classical findings, usually associating pre-stimulus alpha amplitude with modulations in visual accuracy and attention (Jensen & Mazaheri, 2010; Kelly et al., 2006; Romei et al., 2008; Thut et al., 2006). The study demonstrates the level of confound not considered by previous research and proposes a mechanistic principle by which top-down attentional cues shape internal predisposition towards attending vs. ignoring a given location via modulation of alpha amplitude lateralization. This allows for improved metacognitive ability before the stimulus is presented, i.e., enhancing the predictability of the individual to successfully anticipate the presence of the stimulus. However, the alpha amplitude is not responsible for the enhanced perceptual sensitivity per se. Alpha amplitude act as a top-

down control serving the allocation of sensory resources at the to-be-attended location by speeding up sensory sampling via faster IAF, ultimately enhancing perceptual sensitivity.

Dissociation and interaction via long-range feedforward and feedback oscillatory mechanism. While Study 1 and Study 4 mainly looked at posterior brain changes in distinct alpha parameters during conscious visual perception and how they work in unison under attentional deployment, Study 5 zoomed out to capture the long-range oscillatory mechanisms. In particular, the current study explored how prior expectations and attentional selection from anterior brain areas are transmitted to and integrated with the sensory input in the posterior cortex. Even in this case, an online TMS-EEG approach was implemented, where a single pulse TMS (sp-TMS) over FEF was applied to emulate a top-down attentional pulse during a continuous visual stimulation, in turn, aimed at evoking a bottom-up mechanism of visual processing (namely gamma activity). While sensory input processing was followed by an increase in the evoked gamma activity during the entire stimulus duration, top-down control, as approximated via sp-FEF, was followed by higher fronto-posterior connectivity in the lower frequency range (higher alpha/lower beta frequencies), resulting in a phase-realignment of the same-frequency oscillations over the posterior cortex. The interaction between the high-frequency feedforward and low-frequency feedback mechanism was visible through their cross-frequency coupling over the visual cortex, where gamma bursts were nested within specific phases of the slower oscillations. These results indicate that the top-down control in the fronto-parietal attentional network is exerted through long-range coherence across lower frequencies between anterior and posterior areas (Bonnefond et al., 2017; Fries, 2015). At the same time, these feedback expectations get integrated with the sensory input through cross-frequency coupling, where the amplitude of the faster oscillations is linked to the specific phases of the slower frequencies communicating expectations. In this way, by controlling

the phases of the slower frequencies, prior expectations can modulate the spatial and temporal coding of the visual processing. Although there was some preliminary understanding of how attentional control is transmitted to lower-level visual areas, little was known about how these areas interact with bottom-up sensory information to achieve the best possible balance between visual processing and resource allocation. The current experiment causally corroborated the suggested mechanism based on phase-to-power coupling between feedforward and feedback oscillatory signals.

Oscillatory model of conscious perception and attention. Based on the above-described results of Studies 1, 4, and 5, an oscillatory model of conscious perception and attention can be proposed.

One of the most common experimental observations regarding alpha activity is their sustained variability in terms of individual alpha frequency (Mierau et al., 2017), first considered as a highly heritable, stable trait reflecting anatomical properties of an individual brain, thus reflecting general cognitive capacities of the system (Grandy et al., 2013; Posthuma et al., 2001). However, alpha peak frequency shifts were also noted on a shorter timescale, according to the current state of the system. However, it remained unclear to which extent these frequency drifts represent shifts in neural processing or transitions in neural sampling strategies (Mierau et al., 2017). Considering recent literature and our own data, it can be concluded that these frequency drifts represent far more than random fluctuations. Instead, they can be better defined as an adaptive mechanism that mirrors neural activation levels, which can be self-regulated and tuned autonomously, adjusting to environmental demands by regulating input and information processing. Indeed, various studies identified IAF as a temporal sampling mechanism (Battaglini et al., 2020; Cecere et al., 2015; Minami & Amano, 2017; Ronconi et al., 2018; Sharp et al., 2022; Wutz et al., 2018), where higher alpha speed would transfer into better temporal

resolution in the visual domain or into a narrower temporal window of integration in the multisensory processing (Bastiaansen et al., 2020; Cecere et al., 2015; Migliorati et al., 2020). Moreover, here we demonstrate that the IAF causally modulates perceptual accuracy also in non-temporal tasks by dictating the amount of processing abilities even within a single alpha cycle. This finding goes well in hand with various studies pointing that faster IAF helps individuals adjust to higher task demands (Haegens et al., 2014; Mierau et al., 2017) due to the higher regional cerebral blood flow in regions related to attention control and readiness for sensory input (Jann et al., 2010).

On the other hand, spontaneous fluctuations in alpha-amplitude present changes in brain excitability levels (Romei et al., 2008, 2010), with low alpha levels reflecting high excitability that amplifies the representation of both signal and noise, thus driving decision confidence and perceptual awareness across different perceptual tasks, without being related to perceptual accuracy per se. Although here we demonstrated this relationship using low-level visual stimuli, the effect is also robust when higher-level visual areas are engaged, e.g., when using complex visual stimuli such as houses and faces (Samaha et al., 2022).

Although dissociable, both parameters of alpha activity are subject to attentional control, where both IAF and alpha-amplitude could be controlled by top-down factors. While in Study 4, the attentionally focused faster contralateral IAF was the best strategy leading to higher task accuracy, other studies demonstrated that IAF could be strategically modulated even in the opposite direction, e.g., slowed down if the task involved temporal integration (Sharp et al., 2022; Wutz et al., 2018). Likewise, the attentionally-controlled alpha amplitude can improve predictability and control the allocation of sensory resources, as well as shape post-perceptual strategies by integrating stimulus information, as shown in Study 4. Thus, both parameters of alpha activity are under top-down, internal control.

This top-down regulation is communicated from higher-order areas to the visual cortex in the alpha range (Bonnefond et al., 2017; Riddle et al., 2020; van Kerkoerle et al., 2014; von Stein et al., 2000), where alpha oscillations set up the communication within the fronto-parietal network depending on the task context. Indeed, in Study 4, succesfull attentional control was followed by the higher synchronization between frontal and parieto-occipital sensors in the alpha range. Similarly, in Study 5, it has been demonstrated that the activation of the FEF would communicate expectations towards the occipital areas via alpha/beta phase synchrony and re-alignment. It is probable that, during attentional control, alpha activity in the anterior cortex would entrain alpha oscillations over posterior regions, thus strengthening the functional connectivity and strategically tuning alpha parameters in the visual cortex– including both IAF and alpha-amplitude- according to task demands, and at least in some task contexts. Specifically, it is possible that different tasks would implement distinct frequency channels of the fronto-parietal network. For instance, lower beta frequency has been identified as an important mechanisms of the dorsal attentional network in discriminating different features of the visual input, as well as in local visual processing in the context of visual crowdeness (Battaglini et al., 2020; Ronconi et al., 2018). On the other hand, alpha activity becomes crucial in temporal and spatial sampling mechanisms, as demonstrated in Experiment 1 & 4.

This feedback information needs to be integrated with the feedforward input: Study 5 would indicate that this integration occurs via the coupling of slow and fast oscillations, where gamma oscillations are coupled to the specific phases of the slower oscillatory activity. Therefore, the gamma oscillations phase-modulated by the slower activity would represent the input that needs to be transferred in a feed-forward manner. In other words, prior expectations would shape the speed, amplitude, and timing of the posterior brain activity along slower frequencies, that in turn, would control the flow of the sensory input

carried by faster gamma activity nested within the specific phases of slower oscillations (Bonnefond et al., 2017; Jensen et al., 2014a).

In a practical example of our experimental paradigm in Study 4, an informative spatial cue would activate the attentional fronto-parietal network, where the alpha activity over frontal nodes would entrain local alpha activity in the visual cortex, with a desynchronized and faster alpha activity contralateral to the attended hemifield. In turn, sensory input carried by the attended stimulus would be communicated via faster gamma frequency, nested within the feedback-tuned alpha activity, thus enabling optimal perceptual and metacognitive performance in the indicated spatial position.

Although the experiments incuded in the current work did not include (or measure) eye movements, saccades are a crucial element of the more ecological visual perception and attention, and are known to be controlled by the FEFs. Therefore, the oscillatory model of perception should be able to incorporate their presence and mechanism. Indeed, the phase of ongoing high alpha/low beta (11–17 Hz) prestimulus activity at frontal locations has been associated with saccadic response latencies (Drewes & VanRullen, 2011). If we keep in mind that alpha phase is a mechanism regulating neuronal excitability and connectivity between cortical areas during cognitive processing, it may also offer a temporal frame for the oculomotor control, aiding where and how long to look at a given target, and when to move to the next one (Popov et al., 2021). Similarly, individual alpha frequency, which here we defined as a sampling mechanism, should dictate the speed of the saccadic switches, i.e., shape how fast one can perform saccadic sampling between different targets. This hypothesis should be tested in future research. Moreover, alpha amplitude has also been shown to vary with saccades, with high amplitude during intervals of fixation, and reduced amplitude following a saccade execution. In light of our experiments, pre-stimulus alpha-amplitude would index cortical excitability and criterion

shifts, while anticipating decision strategies during attentional task. These excitability variations and decision strategies could also reflect oculomotor control, with modulations of alpha amplitude deciding our proneness towards the external/internal input and aiding the decision process where to look next via oculomotor control (Popov et al., 2021).

Oscillatory model of evoked responses. Taken together, the results discussed thus far loudly speak in favor of the fact that the complex neural patterns present in the absence of the sensory input, aka spontaneous brain oscillations, have an important role in perception and cognition. However, if and mechanistically how these oscillatory patterns influence sensory processing, defined as brain-evoked responses, is largely unknown. My thesis also addresses this timely question. Specifically, during a visual discrimination task with a confidence prompt, the study looked at the pre-stimulus oscillatory activity and early and late evoked responses, together with their link to behavior. Crucially, a TMS-EEG approach was also used with the aim of estimating the impact of the entrained pre-stimulus oscillations on evoked activity. A direct link was established between the alpha-frequency and latency of the early (P1) evoked response, where faster IAF was followed by an earlier P1. Crucially both IAF and P1 latency were linked to higher perceptual accuracy. On the other hand, higher alpha-amplitude directly shaped the amplitude of later P3 evoked response. In turn, both alpha and P3 amplitude were linked to confidence ratings but not perceptual accuracy. These results clearly speak in favor of the oscillatory model of the ERP genesis, where different mechanisms could play a role in drawing the link between brain oscillations and evoked responses. Specifically, the relationship between IAF and P1 latency can be best described by phase-reset mechanisms, where the phase of ongoing alpha activity gets resetted by the stimulus, ultimately creating evoked response of the same polarity and similar frequency characteristics. On the other hand, the link between alpha amplitude and later ERPs can be attributed to the mechanisms of functional

inhibition, where lower excitability of the visual regions, resulting from an increased pre-stimulus alpha amplitude, would have an inhibitory impact and reduce the amplitude of the additive P3 component. The mechanism should hold even outside here-investigated task context, and could explain other neural-cognitive links. For instance, both low alpha amplitude and high P3 response have been linked to higher working memory performance (Bonnefond & Jensen, 2012; Hanslmayr et al., 2009; Klimesch et al., 1996; Polich & Kok, 1995). Similar to attentional mechanism, high vs. low alpha amplitude would track the strategy of sensory allocation: this time, not between different locations as it happens in spatial attention, but rather between external vs. internal resource allocation. In turn, these initial amplitude levels would shape the P3 amplitude, resulting in a close relationship also between WM performance and P3 component.

From a theoretical perspective, these results are important as they bridge the artificially-created gap between research focused on brain oscillations vs. evoked responses, demonstrating that both are the interdependent parts of the same mechanisms underlying perceptual accuracy and confidence. This gap was also present due to the methodological difficulties in detangling evoked vs. oscillatory model of ERP genesis by using EEG/MEG only. Therefore, the information-based TMS-EEG approach used here has proven to be an essential tool in providing clear scientific evidence contradicting the evoked model.

Predicting inter-individual differences in oscillatory entrainment outcome. Study 1 and Study 3 implemented different entrainment protocols to causally test how distinct parameters of alpha activity influence behavior and evoked responses. Although on a group level, different entrainment protocols led to expected electrophysiological and behavioral effects, there was a large between-participant variability in the entrainment outcome. Study 2 tried to explain this variability by looking at the resting-state individual power spectrum,

with a hypothesis that Gaussian fitting of the alpha power spectrum can present an individual approximation of the malleability of these brain oscillations towards changes induced by rhTMS. While the height of the curve could predict the changes in alpha oscillatory activity during at-peak entrainment, i.e., when alpha-amplitude changes are induced, the width of the Gaussian curve could best predict the outcome of off-peak entrainment, i.e., when oscillatory activity is tuned towards faster of a slower pace. Although rhTMS has been getting more attention in both basic and clinical research, little was known about the factors that would influence how the individual reacts to the stimulation. Study 2 addressed this question, demonstrating that we can predict entrainment outcomes based on the few-minute resting-state recording, which could be proven crucial in the way we design rhTMS experiments, select participants, and interpret the results in both research and clinical setting.

FINAL REMARKS

Taken together, the overarching aim of these studies was to investigate the oscillatory mechanisms of attention, perception, and consciousness while at the same time tackling current issues in the field. These timely issues include the difficulty of experimentally disentangling these processes, as they often work in close synchrony, looking at the relationship between oscillations and evoked responses and combining different methodological approaches to compensate for their drawbacks when used separately. First, the studies included here demonstrate that previous contradictory findings can be attributed to confounding effects when these distinct mechanisms are not carefully accounted for (Study 1, 3 & 4). In particular, here we demonstrate that the pre-stimulus alpha amplitude shapes subjective awareness but not perceptual accuracy, a finding that could be easily neglected if the perceptual sensitivity and confidence ratings are not dissociated. On the other hand, perceptual sensitivity was predicted by alpha-frequency drifts, acting as a spatial and temporal sampling mechanism. Second, not only the oscillatory correlates of distinct mechanisms of perception and awareness are identified, but also their interaction was describe, that ensures a coherent and meaningful perception (Studies 4 & 5). Briefly, prior beliefs from the anterior cortex would transmit these expectations to the posterior cortex via entrainment, phase coherence, and phase realignment in alpha/beta frequency. In turn, the resulting tuned posterior slower activity would control the timing and selection of the sensory input transmitted in the faster gamma frequency via oscillatory nesting. Third, these studies bridge the gap between research looking at oscillations and ERPs as predictors of behavior, as demonstrated to represent a part of the same mechanism (Study 3). Finally, these studies rely on a TMS-EEG approach, thus enabling active manipulation of oscillatory parameters while having a direct and time-precise overview of the TMS-induced effects on ongoing brain activity (Study 1, 2, 3 & 5).

REFERENCES

Aine, C. J., Supek, S., George, J. S., Ranken, D., Lewine, J., Sanders, J., Best, E., Tiee, W., Flynn, E. R., & Wood, C. C. (1996). Retinotopic organization of human visual cortex: Departures from the classical model. *Cerebral Cortex (New York, N.Y.: 1991)*, *6*(3), 354–361. https://doi.org/10.1093/cercor/6.3.354

Akam, T., & Kullmann, D. M. (2010). Oscillations and Filtering Networks Support Flexible Routing of Information. *Neuron*, *67*(2), 308–320. https://doi.org/10.1016/j.neuron.2010.06.019

Alamia, A., & VanRullen, R. (2019). Alpha oscillations and traveling waves: Signatures of predictive coding? *PLOS Biology*, *17*(10), e3000487. https://doi.org/10.1371/journal.pbio.3000487

Albouy, P., Weiss, A., Baillet, S., & Zatorre, R. J. (2017). Selective Entrainment of Theta Oscillations in the Dorsal Stream Causally Enhances Auditory Working Memory Performance. *Neuron*, *94*(1), 193-206.e5. https://doi.org/10.1016/j.neuron.2017.03.015

Astafiev, S. V., Shulman, G. L., Stanley, C. M., Snyder, A. Z., Essen, D. C. V., & Corbetta, M. (2003). Functional Organization of Human Intraparietal and Frontal Cortex for Attending, Looking, and Pointing. *Journal of Neuroscience*, *23*(11), 4689–4699. https://doi.org/10.1523/JNEUROSCI.23-11-04689.2003

Barceló, F., Suwazono, S., & Knight, R. T. (2000). Prefrontal modulation of visual processing in humans. *Nature Neuroscience*, *3*(4), 399–403. https://doi.org/10.1038/73975

Barrett, A. B., Dienes, Z., & Seth, A. K. (2013). Measures of metacognition on signal-detection theoretic models. *Psychological Methods*, *18*(4), 535–552. https://doi.org/10.1037/a0033268

Başar, E., Başar-Eroglu, C., Karakaş, S., & Schürmann, M. (2001). Gamma, alpha, delta, and theta oscillations govern cognitive processes. *International Journal of*

Psychophysiology: Official Journal of the International Organization of Psychophysiology, *39*(2–3), 241–248. https://doi.org/10.1016/s0167-8760(00)00145-8

Başar, E., Schürmann, M., Başar-Eroglu, C., & Karakaş, S. (1997). Alpha oscillations in brain functioning: An integrative theory. *International Journal of Psychophysiology*, *26*(1), 5–29. https://doi.org/10.1016/S0167-8760(97)00753-8

Bastiaansen, M., Berberyan, H., Stekelenburg, J. J., Schoffelen, J. M., & Vroomen, J. (2020). Are alpha oscillations instrumental in multisensory synchrony perception? *Brain Research*, *1734*, 146744. https://doi.org/10.1016/j.brainres.2020.146744

Bastos, A. M., Usrey, W. M., Adams, R. A., Mangun, G. R., Fries, P., & Friston, K. J. (2012). Canonical Microcircuits for Predictive Coding. *Neuron*, *76*(4), 695–711. https://doi.org/10.1016/j.neuron.2012.10.038

Battaglini, L., Mena, F., Ghiani, A., Casco, C., Melcher, D., & Ronconi, L. (2020). The Effect of Alpha tACS on the Temporal Resolution of Visual Perception. *Frontiers in Psychology*, *11*, 1765. https://doi.org/10.3389/fpsyg.2020.01765

Benwell, C. S. Y., London, R. E., Tagliabue, C. F., Veniero, D., Gross, J., Keitel, C., & Thut, G. (2019). Frequency and power of human alpha oscillations drift systematically with time-on-task. *NeuroImage*, *192*, 101–114. https://doi.org/10.1016/j.neuroimage.2019.02.067

Benwell, C. S. Y., Tagliabue, C. F., Veniero, D., Cecere, R., Savazzi, S., & Thut, G. (2017). Prestimulus EEG Power Predicts Conscious Awareness But Not Objective Visual Performance. *ENeuro*, *4*(6), ENEURO.0182-17.2017. https://doi.org/10.1523/ENEURO.0182-17.2017

Berger, H. (1929). Über das Elektrenkephalogramm des Menschen. *Archiv für Psychiatrie und Nervenkrankheiten*, *87*(1), 527–570. https://doi.org/10.1007/BF01797193

Bestmann, S., Ruff, C. C., Blakemore, C., Driver, J., & Thilo, K. V. (2007). Spatial

Attention Changes Excitability of Human Visual Cortex to Direct Stimulation. *Current Biology*, *17*(2), 134–139. https://doi.org/10.1016/j.cub.2006.11.063

Bichot, N. P., Rossi, A. F., & Desimone, R. (2005). Parallel and serial neural mechanisms for visual search in macaque area V4. *Science*, *308*(5721), 529–535. https://doi.org/10.1126/science.1109676

Bisley, J. W., & Goldberg, M. E. (2003). Neuronal Activity in the Lateral Intraparietal Area and Spatial Attention. *Science*, *299*(5603), 81–86. https://doi.org/10.1126/science.1077395

Block, N. (2010). Attention and Mental Paint. *Philosophical Issues*, *20*(1), 23–63. https://doi.org/10.1111/j.1533-6077.2010.00177.x

Bodenmann, S., Rusterholz, T., Dürr, R., Stoll, C., Bachmann, V., Geissler, E., Jaggi-Schwarz, K., & Landolt, H.-P. (2009). The functional Val158Met polymorphism of COMT predicts interindividual differences in brain alpha oscillations in young men. *The Journal of Neuroscience: The Official Journal of the Society for Neuroscience*, *29*(35), 10855–10862. https://doi.org/10.1523/JNEUROSCI.1427-09.2009

Bolognini, N., Senna, I., Maravita, A., Pascual-Leone, A., & Merabet, L. B. (2010). Auditory enhancement of visual phosphene perception: The effect of temporal and spatial factors and of stimulus intensity. *Neuroscience Letters*, *477*(3), 109–114. https://doi.org/10.1016/j.neulet.2010.04.044

Bonnefond, M., & Jensen, O. (2012). Alpha Oscillations Serve to Protect Working Memory Maintenance against Anticipated Distracters. *Current Biology*, *22*(20), 1969–1974. https://doi.org/10.1016/j.cub.2012.08.029

Bonnefond, M., Kastner, S., & Jensen, O. (2017). Communication between Brain Areas Based on Nested Oscillations. *ENeuro*, *4*(2), ENEURO.0153-16.2017. https://doi.org/10.1523/ENEURO.0153-16.2017

Bornkessel, I. D., Fiebach, C. J., Friederici, A. D., & Schlesewsky, M. (2004). ‘Capacity’ Reconsidered: Interindividual Differences in Language Comprehension and Individual Alpha Frequency. *Experimental Psychology*, *51*, 279–289. https://doi.org/10.1027/1618-3169.51.4.279

Braboszcz, C., & Delorme, A. (2011). Lost in thoughts: Neural markers of low alertness during mind wandering. *NeuroImage*, *54*(4), 3040–3047. https://doi.org/10.1016/j.neuroimage.2010.10.008

Brignani, D., Manganotti, P., Rossini, P. M., & Miniussi, C. (2008). Modulation of cortical oscillatory activity during transcranial magnetic stimulation. *Human Brain Mapping*, *29*(5), 603–612. https://doi.org/10.1002/hbm.20423

Brunet, N., Vinck, M., Bosman, C. A., Singer, W., & Fries, P. (2014). Gamma or no gamma, that is the question. *Trends in Cognitive Sciences*, *18*(10), 507–509. https://doi.org/10.1016/j.tics.2014.08.006

Busch, N. A., Dubois, J., & VanRullen, R. (2009). The Phase of Ongoing EEG Oscillations Predicts Visual Perception. *Journal of Neuroscience*, *29*(24), 7869–7876. https://doi.org/10.1523/JNEUROSCI.0113-09.2009

Busch, N. A., & VanRullen, R. (2010). Spontaneous EEG oscillations reveal periodic sampling of visual attention. *Proceedings of the National Academy of Sciences*, *107*(37), 16048–16053. https://doi.org/10.1073/pnas.1004801107

Buschman, T. J., & Miller, E. K. (2007). Top-down versus bottom-up control of attention in the prefrontal and posterior parietal cortices. *Science (New York, N.Y.)*, *315*(5820), 1860–1862. https://doi.org/10.1126/science.1138071

Buzsáki, G. (2006). *Rhythms of the Brain*. Oxford University Press. https://doi.org/10.1093/acprof:oso/9780195301069.001.0001

Buzsáki, G., Anastassiou, C. A., & Koch, C. (2012). The origin of extracellular

fields and currents—EEG, ECoG, LFP and spikes. *Nature Reviews Neuroscience*, *13*(6), Article 6. https://doi.org/10.1038/nrn3241

Buzsáki, G., & Draguhn, A. (2004). Neuronal oscillations in cortical networks. *Science (New York, N.Y.)*, *304*(5679), 1926–1929. https://doi.org/10.1126/science.1099745

Buzsáki, G., Logothetis, N., & Singer, W. (2013). Scaling Brain Size, Keeping Timing: Evolutionary Preservation of Brain Rhythms. *Neuron*, *80*(3), 751–764. https://doi.org/10.1016/j.neuron.2013.10.002

Canolty, R. T., Edwards, E., Dalal, S. S., Soltani, M., Nagarajan, S. S., Kirsch, H. E., Berger, M. S., Barbaro, N. M., & Knight, R. T. (2006). High Gamma Power Is Phase-Locked to Theta Oscillations in Human Neocortex. *Science*, *313*(5793), 1626–1628. https://doi.org/10.1126/science.1128115

Capilla, A., Arana, L., García-Huéscar, M., Melcón, M., Gross, J., & Campo, P. (2022). The natural frequencies of the resting human brain: An MEG-based atlas. *NeuroImage*, *258*, 119373. https://doi.org/10.1016/j.neuroimage.2022.119373

Capotosto, P., Babiloni, C., Romani, G. L., & Corbetta, M. (2012). Differential Contribution of Right and Left Parietal Cortex to the Control of Spatial Attention: A Simultaneous EEG–rTMS Study. *Cerebral Cortex (New York, NY)*, *22*(2), 446–454. https://doi.org/10.1093/cercor/bhr127

Carrasco, M. (2011). Visual attention: The past 25 years. *Vision Research*, *51*(13), 1484–1525. https://doi.org/10.1016/j.visres.2011.04.012

Cattaneo, Z., Silvanto, J., Battelli, L., & Pascual-Leone, A. (2009). The mental number line modulates visual cortical excitability. *Neuroscience Letters*, *462*(3), 253–256. https://doi.org/10.1016/j.neulet.2009.07.027

Cecere, R., Rees, G., & Romei, V. (2015). Individual differences in alpha frequency drive crossmodal illusory perception. *Current Biology: CB*, *25*(2), 231–235.

https://doi.org/10.1016/j.cub.2014.11.034

Chainay, H., Krainik, A., Tanguy, M.-L., Gerardin, E., Le Bihan, D., & Lehéricy, S. (2004). Foot, face and hand representation in the human supplementary motor area. *NeuroReport*, *15*(5), 765–769.

Chica, A. B., Valero-Cabré, A., Paz-Alonso, P. M., & Bartolomeo, P. (2014). Causal Contributions of the Left Frontal Eye Field to Conscious Perception. *Cerebral Cortex*, *24*(3), 745–753. https://doi.org/10.1093/cercor/bhs357

Clark, A. (2013). Whatever next? Predictive brains, situated agents, and the future of cognitive science. *The Behavioral and Brain Sciences*, *36*(3), 181–204. https://doi.org/10.1017/S0140525X12000477

Cohen, D. (1968). Magnetoencephalography: Evidence of Magnetic Fields Produced by Alpha-Rhythm Currents. *Science*, *161*(3843), 784–786. https://doi.org/10.1126/science.161.3843.784

Cohen, M. (2011). It's about Time. *Frontiers in Human Neuroscience*, *5*. https://www.frontiersin.org/articles/10.3389/fnhum.2011.00002

Cohen, M. (2014). *Analyzing Neural Time Series Data: Theory and Practice*. MIT Press. https://lib.hpu.edu.vn/handle/123456789/33192

Cohen, M. (2015a). Effects of time lag and frequency matching on phase-based connectivity. *Journal of Neuroscience Methods*, *250*, 137–146. https://doi.org/10.1016/j.jneumeth.2014.09.005

Cohen, M. (2015b). *Cycles in mind: How brain rhythms control perception and action*. Sinc(x) press.

Coldea, A., Veniero, D., Morand, S., Trajkovic, J., Romei, V., Harvey, M., & Thut, G. (2022). Effects of Rhythmic Transcranial Magnetic Stimulation in the Alpha-Band on Visual Perception Depend on Deviation From Alpha-Peak Frequency: Faster Relative

Transcranial Magnetic Stimulation Alpha-Pace Improves Performance. *Frontiers in Neuroscience*, *16*, 886342. https://doi.org/10.3389/fnins.2022.886342

Cooke, J., Poch, C., Gillmeister, H., Costantini, M., & Romei, V. (2019). Oscillatory Properties of Functional Connections Between Sensory Areas Mediate Cross-Modal Illusory Perception. *Journal of Neuroscience*, *39*(29), 5711–5718. https://doi.org/10.1523/JNEUROSCI.3184-18.2019

Corbetta, M., & Shulman, G. L. (2002). Control of goal-directed and stimulus-driven attention in the brain. *Nature Reviews Neuroscience*, *3*(3), Article 3. https://doi.org/10.1038/nrn755

Corlier, J., Carpenter, L. L., Wilson, A. C., Tirrell, E., Gobin, A. P., Kavanaugh, B., & Leuchter, A. F. (2019). The relationship between individual alpha peak frequency and clinical outcome with repetitive Transcranial Magnetic Stimulation (rTMS) treatment of Major Depressive Disorder (MDD). *Brain Stimulation*, *12*(6), 1572–1578. https://doi.org/10.1016/j.brs.2019.07.018

Daunizeau, J., Ouden, H. E. M. den, Pessiglione, M., Kiebel, S. J., Stephan, K. E., & Friston, K. J. (2010). Observing the Observer (I): Meta-Bayesian Models of Learning and Decision-Making. *PLOS ONE*, *5*(12), e15554. https://doi.org/10.1371/journal.pone.0015554

Daw, N. W. (2014). Functional Organization of the Visual System. In N. W. Daw (Ed.), *Visual Development* (pp. 7–24). Springer US. https://doi.org/10.1007/978-1-4614-9059-3_2

de Lange, F. P., Rahnev, D. A., Donner, T. H., & Lau, H. (2013). Prestimulus oscillatory activity over motor cortex reflects perceptual expectations. *The Journal of Neuroscience: The Official Journal of the Society for Neuroscience*, *33*(4), 1400–1410. https://doi.org/10.1523/JNEUROSCI.1094-12.2013

Dehaene, S., & Changeux, J.-P. (2011). Experimental and Theoretical Approaches to Conscious Processing. *Neuron*, *70*(2), 200–227. https://doi.org/10.1016/j.neuron.2011.03.018

Dehaene, S., Changeux, J.-P., Naccache, L., Sackur, J., & Sergent, C. (2006). Conscious, preconscious, and subliminal processing: A testable taxonomy. *Trends in Cognitive Sciences*, *10*(5), 204–211. https://doi.org/10.1016/j.tics.2006.03.007

Delorme, A., & Makeig, S. (2004). EEGLAB: An open source toolbox for analysis of single-trial EEG dynamics including independent component analysis. *Journal of Neuroscience Methods*, *134*(1), 9–21. https://doi.org/10.1016/j.jneumeth.2003.10.009

Demertzi, A., Tagliazucchi, E., Dehaene, S., Deco, G., Barttfeld, P., Raimondo, F., Martial, C., Fernández-Espejo, D., Rohaut, B., Voss, H. U., Schiff, N. D., Owen, A. M., Laureys, S., Naccache, L., & Sitt, J. D. (2019). Human consciousness is supported by dynamic complex patterns of brain signal coordination. *Science Advances*, *5*(2), eaat7603. https://doi.org/10.1126/sciadv.aat7603

Destexhe, A., & Sejnowski, T. J. (2003). Interactions Between Membrane Conductances Underlying Thalamocortical Slow-Wave Oscillations. *Physiological Reviews*, *83*(4), 1401–1453. https://doi.org/10.1152/physrev.00012.2003

Di Gregorio, F., Trajkovic, J., Roperti, C., Marcantoni, E., Di Luzio, P., Avenanti, A., Thut, G., & Romei, V. (2022a). Tuning alpha rhythms to shape conscious visual perception. *Current Biology*. https://doi.org/10.1016/j.cub.2022.01.003

Di Gregorio, F., Trajkovic, J., Roperti, C., Marcantoni, E., Di Luzio, P., Avenanti, A., Thut, G., & Romei, V. (2022b). Tuning alpha rhythms to shape conscious visual perception. *Current Biology*, *32*(5), 988-998.e6. https://doi.org/10.1016/j.cub.2022.01.003

Di Russo, F., Martínez, A., Sereno, M. I., Pitzalis, S., & Hillyard, S. A. (2002). Cortical sources of the early components of the visual evoked potential. *Human Brain*

Mapping, *15*(2), 95–111. https://doi.org/10.1002/hbm.10010

Dickinson, A., DiStefano, C., Senturk, D., & Jeste, S. S. (2018). Peak alpha frequency is a neural marker of cognitive function across the autism spectrum. *The European Journal of Neuroscience*, *47*(6), 643–651. https://doi.org/10.1111/ejn.13645

Dijk, H. van, Schoffelen, J.-M., Oostenveld, R., & Jensen, O. (2008). Prestimulus Oscillatory Activity in the Alpha Band Predicts Visual Discrimination Ability. *Journal of Neuroscience*, *28*(8), 1816–1823. https://doi.org/10.1523/JNEUROSCI.1853-07.2008

Duecker, F., Frost, M. A., de Graaf, T. A., Graewe, B., Jacobs, C., Goebel, R., & Sack, A. T. (2014). The cortex-based alignment approach to TMS coil positioning. *Journal of Cognitive Neuroscience*, *26*(10), 2321–2329. https://doi.org/10.1162/jocn_a_00635

Dujardin, K., Derambure, P., Defebvre, L., Bourriez, J. L., Jacquesson, J. M., & Guieu, J. D. (1993). Evaluation of event-related desynchronization (ERD) during a recognition task: Effect of attention. *Electroencephalography and Clinical Neurophysiology*, *86*(5), 353–356. https://doi.org/10.1016/0013-4694(93)90049-2

Eimer, M., & Mazza, V. (2005). Electrophysiological correlates of change detection. *Psychophysiology*, *42*(3), 328–342. https://doi.org/10.1111/j.1469-8986.2005.00285.x

Engel, A. K., & Fries, P. (2010). Beta-band oscillations—Signalling the status quo? *Current Opinion in Neurobiology*, *20*(2), 156–165. https://doi.org/10.1016/j.conb.2010.02.015

Engel, A. K., Fries, P., & Singer, W. (2001). Dynamic predictions: Oscillations and synchrony in top-down processing. *Nature Reviews. Neuroscience*, *2*(10), 704–716. https://doi.org/10.1038/35094565

Ergenoglu, T., Demiralp, T., Bayraktaroglu, Z., Ergen, M., Beydagi, H., & Uresin, Y. (2004). Alpha rhythm of the EEG modulates visual detection performance in humans.

Cognitive Brain Research, *20*(3), 376–383. https://doi.org/10.1016/j.cogbrainres.2004.03.009

Fan, J., McCandliss, B. D., Sommer, T., Raz, A., & Posner, M. I. (2002). Testing the efficiency and independence of attentional networks. *Journal of Cognitive Neuroscience*, *14*(3), 340–347. https://doi.org/10.1162/089892902317361886

Fenner, B., Cooper, N., Romei, V., & Hughes, G. (2020). Individual differences in sensory integration predict differences in time perception and individual levels of schizotypy. *Consciousness and Cognition*, *84*, 102979. https://doi.org/10.1016/j.concog.2020.102979

Fernández, T., Harmony, T., Silva, J., Galín, L., Díaz-Comas, L., Bosch, J., Rodríguez, M., Fernández-Bouzas, A., Yáñez, G., Otero, G., & Marosi, E. (1998). Relationship of specific EEG frequencies at specific brain areas with performance. *NeuroReport*, *9*(16), 3680–3687. https://doi.org/10.1097/00001756-199811160-00021

Ferri, F., Venskus, A., Fotia, F., Cooke, J., & Romei, V. (2018). Higher proneness to multisensory illusions is driven by reduced temporal sensitivity in people with high schizotypal traits. *Consciousness and Cognition*, *65*, 263–270. https://doi.org/10.1016/j.concog.2018.09.006

Fleming, S. M., & Daw, N. D. (2017). Self-evaluation of decision-making: A general bayesian framework for metacognitive computation. *Psychological Review*, *124*(1), 91–114. https://doi.org/10.1037/rev0000045

Fontolan, L., Morillon, B., Liegeois-Chauvel, C., & Giraud, A.-L. (2014). The contribution of frequency-specific activity to hierarchical information processing in the human auditory cortex. *Nature Communications*, *5*(1), Article 1. https://doi.org/10.1038/ncomms5694

Förster, J., Koivisto, M., & Revonsuo, A. (2020). ERP and MEG correlates of

visual consciousness: The second decade. *Consciousness and Cognition, 80*, 102917. https://doi.org/10.1016/j.concog.2020.102917

Foxe, J. J., Simpson, G. V., & Ahlfors, S. P. (1998). Parieto-occipital approximately 10 Hz activity reflects anticipatory state of visual attention mechanisms. *Neuroreport, 9*(17), 3929–3933. https://doi.org/10.1097/00001756-199812010-00030

Fries, P. (2005). A mechanism for cognitive dynamics: Neuronal communication through neuronal coherence. *Trends in Cognitive Sciences, 9*(10), 474–480. https://doi.org/10.1016/j.tics.2005.08.011

Fries, P. (2015). Rhythms For Cognition: Communication Through Coherence. *Neuron, 88*(1), 220–235. https://doi.org/10.1016/j.neuron.2015.09.034

Fries, P., Reynolds, J. H., Rorie, A. E., & Desimone, R. (2001). Modulation of oscillatory neuronal synchronization by selective visual attention. *Science (New York, N.Y.), 291*(5508), 1560–1563. https://doi.org/10.1126/science.1055465

Fries, P., Womelsdorf, T., Oostenveld, R., & Desimone, R. (2008). The Effects of Visual Stimulation and Selective Visual Attention on Rhythmic Neuronal Synchronization in Macaque Area V4. *Journal of Neuroscience*, *28*(18), 4823–4835. https://doi.org/10.1523/JNEUROSCI.4499-07.2008

Friston, K. (2009). The free-energy principle: A rough guide to the brain? *Trends in Cognitive Sciences, 13*(7), 293–301. https://doi.org/10.1016/j.tics.2009.04.005

Friston, K. (2010). The free-energy principle: A unified brain theory? *Nature Reviews Neuroscience*, *11*(2), Article 2. https://doi.org/10.1038/nrn2787

Friston, K. (2019). Waves of prediction. *PLOS Biology*, *17*(10), e3000426. https://doi.org/10.1371/journal.pbio.3000426

Friston, K., & Kiebel, S. (2009). Predictive coding under the free-energy principle. *Philosophical Transactions of the Royal Society B: Biological Sciences*, *364*(1521), 1211–

1221. https://doi.org/10.1098/rstb.2008.0300

Frost, M. A., & Goebel, R. (2012). Measuring structural-functional correspondence: Spatial variability of specialised brain regions after macro-anatomical alignment. *NeuroImage*, *59*(2), 1369–1381. https://doi.org/10.1016/j.neuroimage.2011.08.035

Fu, K.-M. G., Foxe, J. J., Murray, M. M., Higgins, B. A., Javitt, D. C., & Schroeder, C. E. (2001). Attention-dependent suppression of distracter visual input can be cross-modally cued as indexed by anticipatory parieto–occipital alpha-band oscillations. *Cognitive Brain Research*, *12*(1), 145–152. https://doi.org/10.1016/S0926-6410(01)00034-9

Fuentemilla, L., Marco-Pallarés, J., & Grau, C. (2006). Modulation of spectral power and of phase resetting of EEG contributes differentially to the generation of auditory event-related potentials. *NeuroImage*, *30*(3), 909–916. https://doi.org/10.1016/j.neuroimage.2005.10.036

Garry, M., Manning, C. G., Loftus, E. F., & Sherman, S. J. (1996). Imagination inflation: Imagining a childhood event inflates confidence that it occurred. *Psychonomic Bulletin & Review*, *3*(2), 208–214. https://doi.org/10.3758/BF03212420

Gerwig, M., Kastrup, O., Meyer, B.-U., & Niehaus, L. (2003). Evaluation of cortical excitability by motor and phosphene thresholds in transcranial magnetic stimulation. *Journal of the Neurological Sciences*, *215*(1–2), 75–78. https://doi.org/10.1016/s0022-510x(03)00228-4

Grandy, T. H., Werkle-Bergner, M., Chicherio, C., Lövdén, M., Schmiedek, F., & Lindenberger, U. (2013). Individual alpha peak frequency is related to latent factors of general cognitive abilities. *NeuroImage*, *79*, 10–18. https://doi.org/10.1016/j.neuroimage.2013.04.059

Grandy, T. H., Werkle-Bergner, M., Chicherio, C., Schmiedek, F., Lövdén, M., & Lindenberger, U. (2013). Peak individual alpha frequency qualifies as a stable neurophysiological trait marker in healthy younger and older adults. *Psychophysiology*, *50*(6), 570–582. https://doi.org/10.1111/psyp.12043

Gratton, G., Coles, M. G., & Donchin, E. (1983). A new method for off-line removal of ocular artifact. *Electroencephalography and Clinical Neurophysiology*, *55*(4), 468–484. https://doi.org/10.1016/0013-4694(83)90135-9

Green, D. M., & Swets, J. A. (1966). *Signal detection theory and psychophysics.* (John Wiley, Ed.). Oxford, England. https://doi.org/10.1901/jeab.1969.12-475

Green, D. M., & Swets, J. A. (1974). *Signal detection theory and psychophysics* (pp. xiii, 479). Robert E. Krieger.

Greenhouse, S. W., & Geisser, S. (1959). On methods in the analysis of profile data. In *Psychometrika* (Vol. 24, pp. 95–112). https://doi.org/citeulike-article-id:6139128

Gregoriou, G. G., Gotts, S. J., & Desimone, R. (2012). Cell-type-specific synchronization of neural activity in FEF with V4 during attention. *Neuron*, *73*(3), 581–594. https://doi.org/10.1016/j.neuron.2011.12.019

Gregoriou, G. G., Gotts, S. J., Zhou, H., & Desimone, R. (2009). High-frequency, long-range coupling between prefrontal and visual cortex during attention. *Science (New York, N.Y.)*, *324*(5931), 1207–1210. https://doi.org/10.1126/science.1171402

Gregory, R. L., Longuet-Higgins, H. C., & Sutherland, N. S. (1980). Perceptions as hypotheses. *Philosophical Transactions of the Royal Society of London. B, Biological Sciences*, *290*(1038), 181–197. https://doi.org/10.1098/rstb.1980.0090

Grosbras, M.-H., & Paus, T. (2002). Transcranial Magnetic Stimulation of the Human Frontal Eye Field: Effects on Visual Perception and Attention. *Journal of Cognitive Neuroscience*, *14*(7), 1109–1120. https://doi.org/10.1162/089892902320474553

Grosbras, M.-H., & Paus, T. (2003). Transcranial magnetic stimulation of the human frontal eye field facilitates visual awareness. *The European Journal of Neuroscience*, *18*(11), 3121–3126. https://doi.org/10.1111/j.1460-9568.2003.03055.x

Gruber, W. R., Klimesch, W., Sauseng, P., & Doppelmayr, M. (2005). Alpha phase synchronization predicts P1 and N1 latency and amplitude size. *Cerebral Cortex (New York, N.Y.: 1991)*, *15*(4), 371–377. https://doi.org/10.1093/cercor/bhh139

Haegens, S., Cousijn, H., Wallis, G., Harrison, P. J., & Nobre, A. C. (2014). Inter- and intra-individual variability in alpha peak frequency. *NeuroImage*, *92*(100), 46–55. https://doi.org/10.1016/j.neuroimage.2014.01.049

Hanslmayr, S., Aslan, A., Staudigl, T., Klimesch, W., Herrmann, C. S., & Bäuml, K.-H. (2007). Prestimulus oscillations predict visual perception performance between and within subjects. *NeuroImage*, *37*(4), 1465–1473. https://doi.org/10.1016/j.neuroimage.2007.07.011

Hanslmayr, S., Klimesch, W., Sauseng, P., Gruber, W., Doppelmayr, M., Freunberger, R., Pecherstorfer, T., & Birbaumer, N. (2007). Alpha phase reset contributes to the generation of ERPs. *Cerebral Cortex (New York, N.Y.: 1991)*, *17*(1), 1–8. https://doi.org/10.1093/cercor/bhj129

Hanslmayr, S., Spitzer, B., & Bäuml, K.-H. (2009). Brain oscillations dissociate between semantic and nonsemantic encoding of episodic memories. *Cerebral Cortex (New York, N.Y.: 1991)*, *19*(7), 1631–1640. https://doi.org/10.1093/cercor/bhn197

Hasselmo, M. E., Bodelón, C., & Wyble, B. P. (2002). A Proposed Function for Hippocampal Theta Rhythm: Separate Phases of Encoding and Retrieval Enhance Reversal of Prior Learning. *Neural Computation*, *14*(4), 793–817. https://doi.org/10.1162/089976602317318965

Herweg, N. A., Solomon, E. A., & Kahana, M. J. (2020). Theta oscillations in

human memory. *Trends in Cognitive Sciences*, *24*(3), 208–227. https://doi.org/10.1016/j.tics.2019.12.006

Hirst, W., Phelps, E. A., Meksin, R., Vaidya, C. J., Johnson, M. K., Mitchell, K. J., Buckner, R. L., Budson, A. E., Gabrieli, J. D. E., Lustig, C., Mather, M., Ochsner, K. N., Schacter, D., Simons, J. S., Lyle, K. B., Cuc, A. F., & Olsson, A. (2015). A ten-year follow-up of a study of memory for the attack of September 11, 2001: Flashbulb memories and memories for flashbulb events. *Journal of Experimental Psychology. General*, *144*(3), 604–623. https://doi.org/10.1037/xge0000055

Ho, H. T., Burr, D. C., Alais, D., & Morrone, M. C. (2019). Auditory Perceptual History Is Propagated through Alpha Oscillations. *Current Biology*, *29*(24), 4208-4217.e3. https://doi.org/10.1016/j.cub.2019.10.041

Hubel, D. H., & Wiesel, T. N. (1962). Receptive fields, binocular interaction and functional architecture in the cat's visual cortex. *The Journal of Physiology*, *160*(1), 106-154.2.

Hubel, D. H., & Wiesel, T. N. (1965). Receptive fields and functional architecture in two nonstriate visual areas (18 and 19) of the cat. *Journal of Neurophysiology*, *28*(2), 229–289. https://doi.org/10.1152/jn.1965.28.2.229

Iemi, L., & Busch, N. A. (2018). Moment-to-Moment Fluctuations in Neuronal Excitability Bias Subjective Perception Rather than Strategic Decision-Making. *ENeuro*, *5*(3), ENEURO.0430-17.2018. https://doi.org/10.1523/ENEURO.0430-17.2018

Iemi, L., Busch, N. A., Laudini, A., Haegens, S., Samaha, J., Villringer, A., & Nikulin, V. V. (2019). Multiple mechanisms link prestimulus neural oscillations to sensory responses. *ELife*, *8*. https://doi.org/10.7554/eLife.43620

Iemi, L., Chaumon, M., Crouzet, S. M., & Busch, N. A. (2017). Spontaneous Neural Oscillations Bias Perception by Modulating Baseline Excitability. *The Journal of*

Neuroscience: The Official Journal of the Society for Neuroscience, *37*(4), 807–819. https://doi.org/10.1523/JNEUROSCI.1432-16.2016

Jacobs, J., Kahana, M. J., Ekstrom, A. D., & Fried, I. (2007). Brain oscillations control timing of single-neuron activity in humans. *The Journal of Neuroscience: The Official Journal of the Society for Neuroscience*, *27*(14), 3839–3844. https://doi.org/10.1523/JNEUROSCI.4636-06.2007

Jann, K., Koenig, T., Dierks, T., Boesch, C., & Federspiel, A. (2010). Association of individual resting state EEG alpha frequency and cerebral blood flow. *NeuroImage*, *51*(1), 365–372. https://doi.org/10.1016/j.neuroimage.2010.02.024

Janssens, S. E. W., Sack, A. T., Ten Oever, S., & de Graaf, T. A. (2022). Calibrating rhythmic stimulation parameters to individual electroencephalography markers: The consistency of individual alpha frequency in practical lab settings. *The European Journal of Neuroscience*, *55*(11–12), 3418–3437. https://doi.org/10.1111/ejn.15418

Jensen, O., Gips, B., Bergmann, T. O., & Bonnefond, M. (2014a). Temporal coding organized by coupled alpha and gamma oscillations prioritize visual processing. *Trends in Neurosciences*, *37*(7), 357–369. https://doi.org/10.1016/j.tins.2014.04.001

Jensen, O., Gips, B., Bergmann, T. O., & Bonnefond, M. (2014b). Temporal coding organized by coupled alpha and gamma oscillations prioritize visual processing. *Trends in Neurosciences*, *37*(7), 357–369. https://doi.org/10.1016/j.tins.2014.04.001

Jensen, O., & Mazaheri, A. (2010). Shaping Functional Architecture by Oscillatory Alpha Activity: Gating by Inhibition. *Frontiers in Human Neuroscience*, *4*. https://www.frontiersin.org/articles/10.3389/fnhum.2010.00186

Jiménez, A., Lu, Y., Jambhekar, A., & Lahav, G. (2022). Principles, mechanisms and functions of entrainment in biological oscillators. *Interface Focus*, *12*(3), 20210088. https://doi.org/10.1098/rsfs.2021.0088

Keitel, C., Ruzzoli, M., Dugué, L., Busch, N. A., & Benwell, C. S. Y. (2022). Rhythms in cognition: The evidence revisited. *European Journal of Neuroscience*, *55*(11–12), 2991–3009. https://doi.org/10.1111/ejn.15740

Kelly, S. P., Lalor, E. C., Reilly, R. B., & Foxe, J. J. (2006). Increases in alpha oscillatory power reflect an active retinotopic mechanism for distracter suppression during sustained visuospatial attention. *Journal of Neurophysiology*, *95*(6), 3844–3851. https://doi.org/10.1152/jn.01234.2005

Kemmerer, S. K., Sack, A. T., de Graaf, T. A., ten Oever, S., De Weerd, P., & Schuhmann, T. (2022). Frequency-specific transcranial neuromodulation of alpha power alters visuospatial attention performance. *Brain Research, 1782*, 147834. https://doi.org/10.1016/j.brainres.2022.147834

Kersten, D., Mamassian, P., & Yuille, A. (2004). Object perception as Bayesian inference. *Annual Review of Psychology*, *55*, 271–304. https://doi.org/10.1146/annurev.psych.55.090902.142005

Klimesch, W. (1997). EEG-alpha rhythms and memory processes. *International Journal of Psychophysiology: Official Journal of the International Organization of Psychophysiology*, *26*(1–3), 319–340. https://doi.org/10.1016/s0167-8760(97)00773-3

Klimesch, W. (1999). EEG alpha and theta oscillations reflect cognitive and memory performance: A review and analysis. *Brain Research Reviews*, *29*(2), 169–195. https://doi.org/10.1016/S0165-0173(98)00056-3

Klimesch, W., Sauseng, P., & Hanslmayr, S. (2007). EEG alpha oscillations: The inhibition-timing hypothesis. *Brain Research Reviews*, *53*(1), 63–88. https://doi.org/10.1016/j.brainresrev.2006.06.003

Klimesch, W., Sauseng, P., Hanslmayr, S., Gruber, W., & Freunberger, R. (2007). Event-related phase reorganization may explain evoked neural dynamics. *Neuroscience &*

Biobehavioral Reviews, *31*(7), 1003–1016. https://doi.org/10.1016/j.neubiorev.2007.03.005

Klimesch, W., Schack, B., Schabus, M., Doppelmayr, M., Gruber, W., & Sauseng, P. (2004). Phase-locked alpha and theta oscillations generate the P1-N1 complex and are related to memory performance. *Brain Research. Cognitive Brain Research*, *19*(3), 302–316. https://doi.org/10.1016/j.cogbrainres.2003.11.016

Klimesch, W., Schimke, H., Doppelmayr, M., Ripper, B., Schwaiger, J., & Pfurtscheller, G. (1996). Event-related desynchronization (ERD) and the Dm effect: Does alpha desynchronization during encoding predict later recall performance? *International Journal of Psychophysiology*, *24*(1), 47–60. https://doi.org/10.1016/S0167-8760(96)00054-2

Kogo, N., & Wagemans, J. (2013). The emergent property of border-ownership and the perception of illusory surfaces in a dynamic hierarchical system. *Cognitive Neuroscience*, *4*(1), 54–61. https://doi.org/10.1080/17588928.2012.754750

Koivisto, M., & Revonsuo, A. (2008). The role of selective attention in visual awareness of stimulus features: Electrophysiological studies. *Cognitive, Affective & Behavioral Neuroscience*, *8*(2), 195–210. https://doi.org/10.3758/cabn.8.2.195

Koivisto, M., Revonsuo, A., & Lehtonen, M. (2006). Independence of Visual Awareness from the Scope of Attention: An Electrophysiological Study. *Cerebral Cortex*, *16*(3), 415–424. https://doi.org/10.1093/cercor/bhi121

Köther, U., Lincoln, T. M., & Moritz, S. (2018). Emotion perception and overconfidence in errors under stress in psychosis. *Psychiatry Research*, *270*, 981–991. https://doi.org/10.1016/j.psychres.2018.03.044

Lamy, D., Salti, M., & Bar-Haim, Y. (2009). Neural correlates of subjective awareness and unconscious processing: An ERP study. *Journal of Cognitive Neuroscience*, *21*(7), 1435–1446. https://doi.org/10.1162/jocn.2009.21064

Landau, A. N. (2018). Neuroscience: A Mechanism for Rhythmic Sampling in Vision. *Current Biology*, *28*(15), R830–R832. https://doi.org/10.1016/j.cub.2018.05.081

Landau, A. N., & Fries, P. (2012). Attention samples stimuli rhythmically. *Current Biology: CB*, *22*(11), 1000–1004. https://doi.org/10.1016/j.cub.2012.03.054

Le Van Quyen, M. (2011). The brainweb of cross-scale interactions. *New Ideas in Psychology*, *29*(2), 57–63. https://doi.org/10.1016/j.newideapsych.2010.11.001

Li, K., & Malhotra, P. A. (2015). Spatial neglect. *Practical Neurology*, *15*(5), 333–339. https://doi.org/10.1136/practneurol-2015-001115

Limbach, K., & Corballis, P. M. (2016). Prestimulus alpha power influences response criterion in a detection task. *Psychophysiology*, *53*(8), 1154–1164. https://doi.org/10.1111/psyp.12666

Lin, Y.-J., Shukla, L., Dugué, L., Valero-Cabré, A., & Carrasco, M. (2021). *TMS entrains occipital alpha activity: Individual alpha frequency predicts the strength of entrained phase-locking.* https://doi.org/10.21203/rs.3.rs-574152/v1

Linkenkaer-Hansen, K., Nikulin, V. V., Palva, S., Ilmoniemi, R. J., & Palva, J. M. (2004). Prestimulus oscillations enhance psychophysical performance in humans. *The Journal of Neuroscience: The Official Journal of the Society for Neuroscience*, *24*(45), 10186–10190. https://doi.org/10.1523/JNEUROSCI.2584-04.2004

Llinás, R. R. (1988). The Intrinsic Electrophysiological Properties of Mammalian Neurons: Insights into Central Nervous System Function. *Science*, *242*(4886), 1654–1664. https://doi.org/10.1126/science.3059497

Lobier, M., Palva, J. M., & Palva, S. (2018). High-alpha band synchronization across frontal, parietal and visual cortex mediates behavioral and neuronal effects of visuospatial attention. *NeuroImage*, *165*, 222–237. https://doi.org/10.1016/j.neuroimage.2017.10.044

Ma, W. J., Beck, J. M., Latham, P. E., & Pouget, A. (2006). Bayesian inference with probabilistic population codes. *Nature Neuroscience*, *9*(11), Article 11. https://doi.org/10.1038/nn1790

Makeig, S., Westerfield, M., Jung, T.-P., Enghoff, S., Townsend, J., Courchesne, E., & Sejnowski, T. J. (2002). Dynamic Brain Sources of Visual Evoked Responses. *Science*, *295*(5555), 690–694. https://doi.org/10.1126/science.1066168

Mäkinen, V., Tiitinen, H., & May, P. (2005). Auditory event-related responses are generated independently of ongoing brain activity. *NeuroImage*, *24*(4), 961–968. https://doi.org/10.1016/j.neuroimage.2004.10.020

Maniscalco, B., & Lau, H. (2012). A signal detection theoretic approach for estimating metacognitive sensitivity from confidence ratings. *Consciousness and Cognition*, *21*(1), 422–430. https://doi.org/10.1016/j.concog.2011.09.021

Marshall, T. R., O'Shea, J., Jensen, O., & Bergmann, T. O. (2015). Frontal eye fields control attentional modulation of alpha and gamma oscillations in contralateral occipitoparietal cortex. *The Journal of Neuroscience: The Official Journal of the Society for Neuroscience*, *35*(4), 1638–1647. https://doi.org/10.1523/JNEUROSCI.3116-14.2015

Martinovic, J., & Busch, N. A. (2011). High frequency oscillations as a correlate of visual perception. *International Journal of Psychophysiology*, *79*(1), 32–38. https://doi.org/10.1016/j.ijpsycho.2010.07.004

Mathewson, K. E., Gratton, G., Fabiani, M., Beck, D. M., & Ro, T. (2009). To See or Not to See: Prestimulus α Phase Predicts Visual Awareness. *Journal of Neuroscience*, *29*(9), 2725–2732. https://doi.org/10.1523/JNEUROSCI.3963-08.2009

Mayer, A., Schwiedrzik, C. M., Wibral, M., Singer, W., & Melloni, L. (2016). Expecting to See a Letter: Alpha Oscillations as Carriers of Top-Down Sensory Predictions. *Cerebral Cortex*, *26*(7), 3146–3160. https://doi.org/10.1093/cercor/bhv146

Mazaheri, A., & Jensen, O. (2006). Posterior α activity is not phase-reset by visual stimuli. *Proceedings of the National Academy of Sciences*, *103*(8), 2948–2952. https://doi.org/10.1073/pnas.0505785103

Mazaheri, A., & Jensen, O. (2010). Rhythmic Pulsing: Linking Ongoing Brain Activity with Evoked Responses. *Frontiers in Human Neuroscience*, *4*. https://www.frontiersin.org/articles/10.3389/fnhum.2010.00177

Mevorach, C., Humphreys, G. W., & Shalev, L. (2006). Opposite biases in salience-based selection for the left and right posterior parietal cortex. *Nature Neuroscience*, *9*(6), 740–742. https://doi.org/10.1038/nn1709

Michalareas, G., Vezoli, J., van Pelt, S., Schoffelen, J.-M., Kennedy, H., & Fries, P. (2016). Alpha-beta and gamma rhythms subserve feedback and feedforward influences among human visual cortical areas. *Neuron*, *89*(2), 384–397. https://doi.org/10.1016/j.neuron.2015.12.018

Mierau, A., Klimesch, W., & Lefebvre, J. (2017). State-dependent alpha peak frequency shifts: Experimental evidence, potential mechanisms and functional implications. *Neuroscience*, *360*, 146–154. https://doi.org/10.1016/j.neuroscience.2017.07.037

Migliorati, D., Zappasodi, F., Perrucci, M. G., Donno, B., Northoff, G., Romei, V., & Costantini, M. (2020). Individual Alpha Frequency Predicts Perceived Visuotactile Simultaneity. *Journal of Cognitive Neuroscience*, *32*(1), 1–11. https://doi.org/10.1162/jocn_a_01464

Miller, E. K., & Buschman, T. J. (2013). Cortical circuits for the control of attention. *Current Opinion in Neurobiology*, *23*(2), 216–222. https://doi.org/10.1016/j.conb.2012.11.011

Min, B.-K., & Herrmann, C. S. (2007). Prestimulus EEG alpha activity reflects

prestimulus top-down processing. *Neuroscience Letters*, *422*(2), 131–135. https://doi.org/10.1016/j.neulet.2007.06.013

Minami, S., & Amano, K. (2017). Illusory Jitter Perceived at the Frequency of Alpha Oscillations. *Current Biology*, *27*(15), 2344-2351.e4. https://doi.org/10.1016/j.cub.2017.06.033

Miniussi, C., & Thut, G. (2010). Combining TMS and EEG offers new prospects in cognitive neuroscience. *Brain Topography*, *22*(4), 249–256. https://doi.org/10.1007/s10548-009-0083-8

Moore, T., & Fallah, M. (2004). Microstimulation of the Frontal Eye Field and Its Effects on Covert Spatial Attention. *J Neurophysiol*, *91*, 152–162. https://doi.org/10.1152/jn.00741.2002

Moore, T., Nature, K. A.-, & 2003, undefined. (n.d.). Selective gating of visual signals by microstimulation of frontal cortex. *Nature.Com*.

Moran, L. V., & Hong, L. E. (2011). High vs Low Frequency Neural Oscillations in Schizophrenia. *Schizophrenia Bulletin*, *37*(4), 659–663. https://doi.org/10.1093/schbul/sbr056

Moran, R. J., Campo, P., Maestu, F., Reilly, R. B., Dolan, R. J., & Strange, B. A. (2010). Peak Frequency in the Theta and Alpha Bands Correlates with Human Working Memory Capacity. *Frontiers in Human Neuroscience*, *4*. https://doi.org/10.3389/fnhum.2010.00200

Murphy, P. R., Robertson, I. H., Harty, S., & O'Connell, R. G. (2015). Neural evidence accumulation persists after choice to inform metacognitive judgments. *ELife*, *4*, e11946. https://doi.org/10.7554/eLife.11946

Navajas, J., Bahrami, B., & Latham, P. E. (2016). Post-decisional accounts of biases in confidence. *Current Opinion in Behavioral Sciences*, *11*, 55–60.

https://doi.org/10.1016/j.cobeha.2016.05.005

Neisser, U. (2014). *Cognitive Psychology: Classic Edition*. Psychology Press. https://doi.org/10.4324/9781315736174

Nyhus, E., & Curran, T. (2010). Functional role of gamma and theta oscillations in episodic memory. *Neuroscience & Biobehavioral Reviews*, *34*(7), 1023–1035. https://doi.org/10.1016/j.neubiorev.2009.12.014

O'Connell, R. G., Dockree, P. M., & Kelly, S. P. (2012). A supramodal accumulation-to-bound signal that determines perceptual decisions in humans. *Nature Neuroscience*, *15*(12), 1729–1735. https://doi.org/10.1038/nn.3248

O'Shea, J., Muggleton, N. G., Cowey, A., & Walsh, V. (2004). Timing of target discrimination in human frontal eye fields. *Journal of Cognitive Neuroscience*, *16*(6), 1060–1067. https://doi.org/10.1162/0898929041502634

Owen, A. M., Coleman, M. R., Boly, M., Davis, M. H., Laureys, S., & Pickard, J. D. (2006). Detecting awareness in the vegetative state. *Science (New York, N.Y.)*, *313*(5792), 1402. https://doi.org/10.1126/science.1130197

Palva, J. M., Palva, S., & Kaila, K. (2005). Phase Synchrony among Neuronal Oscillations in the Human Cortex. *Journal of Neuroscience*, *25*(15), 3962–3972. https://doi.org/10.1523/JNEUROSCI.4250-04.2005

Palva, S., & Palva, J. M. (2007). New vistas for alpha-frequency band oscillations. *Trends in Neurosciences*, *30*(4), 150–158. https://doi.org/10.1016/j.tins.2007.02.001

Palva, S., & Palva, J. M. (2012). Discovering oscillatory interaction networks with M/EEG: Challenges and breakthroughs. *Trends in Cognitive Sciences*, *16*(4), 219–230. https://doi.org/10.1016/j.tics.2012.02.004

Pernet, C., Wilcox, R., & Rousselet, G. (2013). Robust Correlation Analyses: False Positive and Power Validation Using a New Open Source Matlab Toolbox. *Frontiers in*

Psychology, *3*. https://www.frontiersin.org/articles/10.3389/fpsyg.2012.00606

Pfurtscheller, G. (1992). Event-related synchronization (ERS): An electrophysiological correlate of cortical areas at rest. *Electroencephalography and Clinical Neurophysiology*, *83*(1), 62–69. https://doi.org/10.1016/0013-4694(92)90133-3

Pfurtscheller, G., & Klimesch, W. (1992). Functional topography during a visuoverbal judgment task studied with event-related desynchronization mapping. *Journal of Clinical Neurophysiology*, *9*(1), 120–131. https://doi.org/10.1097/00004691-199201000-00013

Pfurtscheller, G., Stancák, A., & Neuper, Ch. (1996). Event-related synchronization (ERS) in the alpha band — an electrophysiological correlate of cortical idling: A review. *International Journal of Psychophysiology*, *24*(1), 39–46. https://doi.org/10.1016/S0167-8760(96)00066-9

Pitcher, D., Walsh, V., Yovel, G., & Duchaine, B. (2007). TMS Evidence for the Involvement of the Right Occipital Face Area in Early Face Processing. *Current Biology*, *17*(18), 1568–1573. https://doi.org/10.1016/j.cub.2007.07.063

Pitts, M. A., Metzler, S., & Hillyard, S. A. (2014). Isolating neural correlates of conscious perception from neural correlates of reporting one's perception. *Frontiers in Psychology*, *5*, 1078. https://doi.org/10.3389/fpsyg.2014.01078

Pleskac, T. J., & Busemeyer, J. R. (2010). Two-stage dynamic signal detection: A theory of choice, decision time, and confidence. *Psychological Review*, *117*, 864–901. https://doi.org/10.1037/a0019737

Polich, J. (2007). Updating P300: An integrative theory of P3a and P3b. *Clinical Neurophysiology: Official Journal of the International Federation of Clinical Neurophysiology*, *118*(10), 2128–2148. https://doi.org/10.1016/j.clinph.2007.04.019

Polich, J., & Kok, A. (1995). Cognitive and biological determinants of P300: An

integrative review. *Biological Psychology*, *41*(2), 103–146. https://doi.org/10.1016/0301-0511(95)05130-9

Popov, T., Miller, G., Rockstroh, B., Jensen, O., & Langer, N. (2021). *Alpha oscillations link action to cognition: An oculomotor account of the brain's dominant rhyth*. https://doi.org/10.1101/2021.09.24.461634

Posner, M. I. (1995). Attention in cognitive neuroscience: An overview. In *The cognitive neurosciences* (pp. 615–624). The MIT Press.

Posthuma, D., Neale, M. C., Boomsma, D. I., & de Geus, E. J. (2001). Are smarter brains running faster? Heritability of alpha peak frequency, IQ, and their interrelation. *Behavior Genetics*, *31*(6), 567–579. https://doi.org/10.1023/a:1013345411774

Postle, B. R. (2020, February 5). *Essentials of Cognitive Neuroscience*. Wiley. https://www.wiley.com/en-us/Essentials+of+Cognitive+Neuroscience%2C+2nd+Edition-p-9781119674153

Rajagovindan, R., & Ding, M. (2011). From prestimulus alpha oscillation to visual-evoked response: An inverted-U function and its attentional modulation. *Journal of Cognitive Neuroscience*, *23*(6), 1379–1394. https://doi.org/10.1162/jocn.2010.21478

Re, D., Inbar, M., Richter, C. G., & Landau, A. N. (2019). Feature-Based Attention Samples Stimuli Rhythmically. *Current Biology*, *29*(4), 693-699.e4. https://doi.org/10.1016/j.cub.2019.01.010

Rees, G., & Lavie, N. (2001). What can functional imaging reveal about the role of attention in visual awareness? *Neuropsychologia*, *39*, 1343–1353. https://doi.org/10.1016/S0028-3932(01)00122-1

Riddle, J., Hwang, K., Cellier, D., Dhanani, S., & D'Esposito, M. (2019). Causal Evidence for the Role of Neuronal Oscillations in Top–Down and Bottom–Up Attention. *Journal of Cognitive Neuroscience*, *31*(5), 768–779. https://doi.org/10.1162/jocn_a_01376

Riddle, J., Scimeca, J. M., Cellier, D., Dhanani, S., & D'Esposito, M. (2020). Causal Evidence for a Role of Theta and Alpha Oscillations in the Control of Working Memory. *Current Biology*, *30*(9), 1748-1754.e4. https://doi.org/10.1016/j.cub.2020.02.065

Rihs, T. A., Michel, C. M., & Thut, G. (2007). Mechanisms of selective inhibition in visual spatial attention are indexed by alpha-band EEG synchronization. *The European Journal of Neuroscience*, *25*(2), 603–610. https://doi.org/10.1111/j.1460-9568.2007.05278.x

Rihs, T. A., Michel, C. M., & Thut, G. (2009). A bias for posterior alpha-band power suppression versus enhancement during shifting versus maintenance of spatial attention. *NeuroImage*, *44*(1), 190–199. https://doi.org/10.1016/j.neuroimage.2008.08.022

Rodriguez, E., George, N., Lachaux, J.-P., Martinerie, J., Renault, B., & Varela, F. J. (1999). Perception's shadow: Long-distance synchronization of human brain activity. *Nature*, *397*(6718), Article 6718. https://doi.org/10.1038/17120

Rogasch, N. C., Sullivan, C., Thomson, R. H., Rose, N. S., Bailey, N. W., Fitzgerald, P. B., Farzan, F., & Hernandez-Pavon, J. C. (2017). Analysing concurrent transcranial magnetic stimulation and electroencephalographic data: A review and introduction to the open-source TESA software. *NeuroImage*, *147*, 934–951. https://doi.org/10.1016/j.neuroimage.2016.10.031

Romei, V., Bauer, M., Brooks, J. L., Economides, M., Penny, W., Thut, G., Driver, J., & Bestmann, S. (2016). Causal evidence that intrinsic beta-frequency is relevant for enhanced signal propagation in the motor system as shown through rhythmic TMS. *NeuroImage*, *126*, 120–130. https://doi.org/10.1016/j.neuroimage.2015.11.020

Romei, V., Brodbeck, V., Michel, C., Amedi, A., Pascual-Leone, A., & Thut, G. (2008). Spontaneous fluctuations in posterior alpha-band EEG activity reflect variability in excitability of human visual areas. *Cerebral Cortex (New York, N.Y.: 1991)*, *18*(9), 2010–

2018. https://doi.org/10.1093/cercor/bhm229

Romei, V., Gross, J., & Thut, G. (2010). On the Role of Prestimulus Alpha Rhythms over Occipito-Parietal Areas in Visual Input Regulation: Correlation or Causation? *Journal of Neuroscience*, *30*(25), 8692–8697. https://doi.org/10.1523/JNEUROSCI.0160-10.2010

Romei, V., Murray, M. M., Cappe, C., & Thut, G. (2009). Preperceptual and Stimulus-Selective Enhancement of Low-Level Human Visual Cortex Excitability by Sounds. *Current Biology*, *19*(21), 1799–1805. https://doi.org/10.1016/j.cub.2009.09.027

Romei, V., Murray, M. M., Merabet, L. B., & Thut, G. (2007). Occipital transcranial magnetic stimulation has opposing effects on visual and auditory stimulus detection: Implications for multisensory interactions. *The Journal of Neuroscience: The Official Journal of the Society for Neuroscience*, *27*(43), 11465–11472. https://doi.org/10.1523/JNEUROSCI.2827-07.2007

Ronconi, L., Busch, N. A., & Melcher, D. (2018). Alpha-band sensory entrainment alters the duration of temporal windows in visual perception. *Scientific Reports*, *8*(1), Article 1. https://doi.org/10.1038/s41598-018-29671-5

Rosanova, M., Casali, A., Bellina, V., Resta, F., Mariotti, M., & Massimini, M. (2009). Natural Frequencies of Human Corticothalamic Circuits. *Journal of Neuroscience*, *29*(24), 7679–7685. https://doi.org/10.1523/JNEUROSCI.0445-09.2009

Rossi, S., Antal, A., Bestmann, S., Bikson, M., Brewer, C., Brockmöller, J., Carpenter, L. L., Cincotta, M., Chen, R., Daskalakis, J. D., Di Lazzaro, V., Fox, M. D., George, M. S., Gilbert, D., Kimiskidis, V. K., Koch, G., Ilmoniemi, R. J., Lefaucheur, J. P., Leocani, L., … Hallett, M. (2021). Safety and recommendations for TMS use in healthy subjects and patient populations, with updates on training, ethical and regulatory issues: Expert Guidelines. *Clinical Neurophysiology*, *132*(1), 269–306.

https://doi.org/10.1016/j.clinph.2020.10.003

Rossi, S., Hallett, M., Rossini, P. M., & Pascual-Leone, A. (2011). Screening questionnaire before TMS: An update. *Clinical Neurophysiology: Official Journal of the International Federation of Clinical Neurophysiology*, *122*(8), 1686. https://doi.org/10.1016/j.clinph.2010.12.037

Ruff, C. C., Blankenburg, F., Bjoertomt, O., Bestmann, S., Freeman, E., Haynes, J.-D., Rees, G., Josephs, O., Deichmann, R., & Driver, J. (2006). Concurrent TMS-fMRI and Psychophysics Reveal Frontal Influences on Human Retinotopic Visual Cortex. *Current Biology*, *16*(15), 1479–1488. https://doi.org/10.1016/j.cub.2006.06.057

Rutiku, R., Martin, M., Bachmann, T., & Aru, J. (2015). Does the P300 reflect conscious perception or its consequences? *Neuroscience*, *298*, 180–189. https://doi.org/10.1016/j.neuroscience.2015.04.029

Salinas, E., & Sejnowski, T. J. (2001). Correlated neuronal activity and the flow of neural information. *Nature Reviews Neuroscience*, *2*(8), Article 8. https://doi.org/10.1038/35086012

Salti, M., Bar-Haim, Y., & Lamy, D. (2012). The P3 component of the ERP reflects conscious perception, not confidence. *Consciousness and Cognition*, *21*(2), 961–968. https://doi.org/10.1016/j.concog.2012.01.012

Samaha, J., Gosseries, O., & Postle, B. R. (2017). Distinct Oscillatory Frequencies Underlie Excitability of Human Occipital and Parietal Cortex. *Journal of Neuroscience*, *37*(11), 2824–2833. https://doi.org/10.1523/JNEUROSCI.3413-16.2017

Samaha, J., Iemi, L., Haegens, S., & Busch, N. A. (2020). Spontaneous Brain Oscillations and Perceptual Decision-Making. *Trends in Cognitive Sciences*, *24*(8), 639–653. https://doi.org/10.1016/j.tics.2020.05.004

Samaha, J., Iemi, L., & Postle, B. R. (2017). Prestimulus alpha-band power biases

visual discrimination confidence, but not accuracy. *Consciousness and Cognition, 54*, 47–55. https://doi.org/10.1016/j.concog.2017.02.005

Samaha, J., LaRocque, J. J., & Postle, B. R. (2022). Spontaneous alpha-band amplitude predicts subjective visibility but not discrimination accuracy during high-level perception. *Consciousness and Cognition, 102*, 103337. https://doi.org/10.1016/j.concog.2022.103337

Samaha, J., & Postle, B. R. (2015). The Speed of Alpha-Band Oscillations Predicts the Temporal Resolution of Visual Perception. *Current Biology, 25*(22), 2985–2990. https://doi.org/10.1016/j.cub.2015.10.007

Sanchez, G., Hartmann, T., Fuscà, M., Demarchi, G., & Weisz, N. (2020). Decoding across sensory modalities reveals common supramodal signatures of conscious perception. *Proceedings of the National Academy of Sciences, 117*(13), 7437–7446. https://doi.org/10.1073/pnas.1912584117

Sannita, W. G., Bandini, F., Beelke, M., De Carli, F., Carozzo, S., Gesino, D., Mazzella, L., Ogliastro, C., & Narici, L. (2001). Time dynamics of stimulus- and event-related gamma band activity: Contrast-VEPs and the visual P300 in man. *Clinical Neurophysiology, 112*(12), 2241–2249. https://doi.org/10.1016/S1388-2457(01)00700-3

Sauseng, P., Klimesch, W., Gruber, W. R., Hanslmayr, S., Freunberger, R., & Doppelmayr, M. (2007). Are event-related potential components generated by phase resetting of brain oscillations? A critical discussion. *Neuroscience, 146*(4), 1435–1444. https://doi.org/10.1016/j.neuroscience.2007.03.014

Sauseng, P., Klimesch, W., Stadler, W., Schabus, M., Doppelmayr, M., Hanslmayr, S., Gruber, W. R., & Birbaumer, N. (2005). A shift of visual spatial attention is selectively associated with human EEG alpha activity. *European Journal of Neuroscience, 22*(11), 2917–2926. https://doi.org/10.1111/j.1460-9568.2005.04482.x

Sayers, B. McA., Beagley, H. A., & Henshall, W. R. (1974). The mechanism of auditory evoked EEG responses. *Nature, 247*, 481–483. https://doi.org/10.1038/247481a0

Schelonka, K., Graulty, C., Canseco-Gonzalez, E., & Pitts, M. A. (2017). ERP signatures of conscious and unconscious word and letter perception in an inattentional blindness paradigm. *Consciousness and Cognition*, *54*, 56–71. https://doi.org/10.1016/j.concog.2017.04.009

Schnitzler, A., & Gross, J. (2005). Normal and pathological oscillatory communication in the brain. *Nature Reviews Neuroscience*, *6*(4), Article 4. https://doi.org/10.1038/nrn1650

Senior, C., Russell, T., & Gazzaniga, M. S. (Eds.). (2006). *Methods in mind*. MIT Press.

Shafto, J. P., & Pitts, M. A. (2015). Neural Signatures of Conscious Face Perception in an Inattentional Blindness Paradigm. *The Journal of Neuroscience: The Official Journal of the Society for Neuroscience*, *35*(31), 10940–10948. https://doi.org/10.1523/JNEUROSCI.0145-15.2015

Shah, A. S., Bressler, S. L., Knuth, K. H., Ding, M., Mehta, A. D., Ulbert, I., & Schroeder, C. E. (2004). Neural Dynamics and the Fundamental Mechanisms of Event-related Brain Potentials. *Cerebral Cortex*, *14*(5), 476–483. https://doi.org/10.1093/cercor/bhh009

Sharp, P., Gutteling, T., Melcher, D., & Hickey, C. (2022). Spatial Attention Tunes Temporal Processing in Early Visual Cortex by Speeding and Slowing Alpha Oscillations. *Journal of Neuroscience*, *42*(41), 7824–7832. https://doi.org/10.1523/JNEUROSCI.0509-22.2022

Siclari, F., Baird, B., Perogamvros, L., Bernardi, G., LaRocque, J. J., Riedner, B., Boly, M., Postle, B. R., & Tononi, G. (2017). The neural correlates of dreaming. *Nature*

Neuroscience, *20*(6), Article 6. https://doi.org/10.1038/nn.4545

Siegel, M., Donner, T. H., Oostenveld, R., Fries, P., & Engel, A. K. (2007). High-Frequency Activity in Human Visual Cortex Is Modulated by Visual Motion Strength. *Cerebral Cortex*, *17*(3), 732–741. https://doi.org/10.1093/cercor/bhk025

Siegel, M., Donner, T. H., Oostenveld, R., Fries, P., & Engel, A. K. (2008). Neuronal Synchronization along the Dorsal Visual Pathway Reflects the Focus of Spatial Attention. *Neuron*, *60*(4), 709–719. https://doi.org/10.1016/j.neuron.2008.09.010

Silvanto, J., Lavie, N., & Walsh, V. (2005). Double dissociation of V1 and V5/MT activity in visual awareness. *Cerebral Cortex*, *15*(11), 1736–1741. https://doi.org/10.1093/cercor/bhi050

Silvanto, J., Lavie, N., & Walsh, V. (2006). Stimulation of the Human Frontal Eye Fields Modulates Sensitivity of Extrastriate Visual Cortex. *Journal of Neurophysiology*, *96*(2), 941–945. https://doi.org/10.1152/jn.00015.2006

Silvanto, J., & Muggleton, N. G. (2008). A novel approach for enhancing the functional specificity of TMS: Revealing the properties of distinct neural populations within the stimulated region. *Clinical Neurophysiology*, *119*(3), 724–726. https://doi.org/10.1016/j.clinph.2007.10.022

Smit, C. M., Wright, M. J., Hansell, N. K., Geffen, G. M., & Martin, N. G. (2006). Genetic variation of individual alpha frequency (IAF) and alpha power in a large adolescent twin sample. *International Journal of Psychophysiology: Official Journal of the International Organization of Psychophysiology*, *61*(2), 235–243. https://doi.org/10.1016/j.ijpsycho.2005.10.004

Snyder, A. C., & Foxe, J. J. (2010). Anticipatory Attentional Suppression of Visual Features Indexed by Oscillatory Alpha-Band Power Increases:A High-Density Electrical Mapping Study. *Journal of Neuroscience*, *30*(11), 4024–4032.

https://doi.org/10.1523/JNEUROSCI.5684-09.2010

Staudigl, T., Hanslmayr, S., & Bäuml, K.-H. T. (2010). Theta Oscillations Reflect the Dynamics of Interference in Episodic Memory Retrieval. *Journal of Neuroscience*, *30*(34), 11356–11362. https://doi.org/10.1523/JNEUROSCI.0637-10.2010

Stecher, H. I., & Herrmann, C. S. (2018). Absence of Alpha-tACS Aftereffects in Darkness Reveals Importance of Taking Derivations of Stimulation Frequency and Individual Alpha Variability Into Account. *Frontiers in Psychology*, *9*. https://www.frontiersin.org/articles/10.3389/fpsyg.2018.00984

Steriade, M., Gloor, P., Llinás, R. R., Lopes da Silva, F. H., & Mesulam, M.-M. (1990). Basic mechanisms of cerebral rhythmic activities. *Electroencephalography and Clinical Neurophysiology*, *76*(6), 481–508. https://doi.org/10.1016/0013-4694(90)90001-Z

Sun, X., Zhu, C., & So, S. H. W. (2017). Dysfunctional metacognition across psychopathologies: A meta-analytic review. *European Psychiatry*, *45*, 139–153. https://doi.org/10.1016/j.eurpsy.2017.05.029

Tagliabue, C. F., Veniero, D., Benwell, C. S. Y., Cecere, R., Savazzi, S., & Thut, G. (2019). The EEG signature of sensory evidence accumulation during decision formation closely tracks subjective perceptual experience. *Scientific Reports*, *9*(1), Article 1. https://doi.org/10.1038/s41598-019-41024-4

Taylor, P. C. J., Nobre, A. C., & Rushworth, M. F. S. (2007). FEF TMS Affects Visual Cortical Activity. *Cerebral Cortex*, *17*(2), 391–399. https://doi.org/10.1093/cercor/bhj156

Thut, G., Nietzel, A., Brandt, S. A., & Pascual-Leone, A. (2006). α-Band Electroencephalographic Activity over Occipital Cortex Indexes Visuospatial Attention Bias and Predicts Visual Target Detection. *The Journal of Neuroscience*, *26*(37), 9494–9502. https://doi.org/10.1523/JNEUROSCI.0875-06.2006

Thut, G., Veniero, D., Romei, V., Miniussi, C., Schyns, P., & Gross, J. (2011). Rhythmic TMS Causes Local Entrainment of Natural Oscillatory Signatures. *Current Biology*, *21*(14), 1176–1185. https://doi.org/10.1016/j.cub.2011.05.049

Tiesinga, P. H. E., Fellous, J.-M., Salinas, E., José, J. V., & Sejnowski, T. J. (2004). Synchronization as a mechanism for attentional gain modulation. *Neurocomputing*, *58–60*, 641–646. https://doi.org/10.1016/j.neucom.2004.01.108

Tort, A. B. L., Komorowski, R., Eichenbaum, H., & Kopell, N. (2010). Measuring Phase-Amplitude Coupling Between Neuronal Oscillations of Different Frequencies. *Journal of Neurophysiology*, *104*(2), 1195–1210. https://doi.org/10.1152/jn.00106.2010

Toscani, M., Marzi, T., Righi, S., Viggiano, M. P., & Baldassi, S. (2010). Alpha waves: A neural signature of visual suppression. *Experimental Brain Research*, *207*(3), 213–219. https://doi.org/10.1007/s00221-010-2444-7

Trajkovic, J., Di Gregorio, F., Marcantoni, E., Thut, G., & Romei, V. (2022). A TMS/EEG protocol for the causal assessment of the functions of the oscillatory brain rhythms in perceptual and cognitive processes. *STAR Protocols*, *3*(2), 101435. https://doi.org/10.1016/j.xpro.2022.101435

Traub, R. D., Bibbig, A., LeBeau, F. E. N., Buhl, E. H., & Whittington, M. A. (2004). Cellular mechanisms of neuronal population oscillations in the hippocampus in vitro. *Annual Review of Neuroscience*, *27*, 247–278. https://doi.org/10.1146/annurev.neuro.27.070203.144303

Tremblay, S., Rogasch, N. C., Premoli, I., Blumberger, D. M., Casarotto, S., Chen, R., Di Lazzaro, V., Farzan, F., Ferrarelli, F., Fitzgerald, P. B., Hui, J., Ilmoniemi, R. J., Kimiskidis, V. K., Kugiumtzis, D., Lioumis, P., Pascual-Leone, A., Pellicciari, M. C., Rajji, T., Thut, G., … Daskalakis, Z. J. (2019). Clinical utility and prospective of TMS–EEG. *Clinical Neurophysiology*, *130*(5), 802–844.

https://doi.org/10.1016/j.clinph.2019.01.001

Valera, F. J., Toro, A., Roy John, E., & Schwartz, E. L. (1981). Perceptual framing and cortical alpha rhythm. *Neuropsychologia*, *19*(5), 675–686. https://doi.org/10.1016/0028-3932(81)90005-1

Van Albada, S., & Robinson, P. (2013). Relationships between Electroencephalographic Spectral Peaks Across Frequency Bands. *Frontiers in Human Neuroscience*, *7*. https://www.frontiersin.org/articles/10.3389/fnhum.2013.00056

van Kerkoerle, T., Self, M. W., Dagnino, B., Gariel-Mathis, M.-A., Poort, J., van der Togt, C., & Roelfsema, P. R. (2014). Alpha and gamma oscillations characterize feedback and feedforward processing in monkey visual cortex. *Proceedings of the National Academy of Sciences*, *111*(40), 14332–14341. https://doi.org/10.1073/pnas.1402773111

VanRullen, R. (2016). Perceptual Cycles. *Trends in Cognitive Sciences*, *20*(10), 723–735. https://doi.org/10.1016/j.tics.2016.07.006

Varela, F., Lachaux, J. P., Rodriguez, E., & Martinerie, J. (2001). The brainweb: Phase synchronization and large-scale integration. *Nature Reviews. Neuroscience*, *2*(4), 229–239. https://doi.org/10.1038/35067550

Veniero, D., Bortoletto, M., & Miniussi, C. (2009). TMS-EEG co-registration: On TMS-induced artifact. *Clinical Neurophysiology*, *120*(7), 1392–1399. https://doi.org/10.1016/j.clinph.2009.04.023

Veniero, D., Gross, J., Morand, S., Duecker, F., Sack, A. T., & Thut, G. (2021). Top-down control of visual cortex by the frontal eye fields through oscillatory realignment. *Nature Communications*, *12*(1), Article 1. https://doi.org/10.1038/s41467-021-21979-7

Verleger, R., Jaśkowski, P., & Wascher, E. (2005). Evidence for an Integrative Role of P3b in Linking Reaction to Perception. *Journal of Psychophysiology*, *19*, 165–181. https://doi.org/10.1027/0269-8803.19.3.165

Vinck, M., Oostenveld, R., van Wingerden, M., Battaglia, F., & Pennartz, C. M. A. (2011). An improved index of phase-synchronization for electrophysiological data in the presence of volume-conduction, noise and sample-size bias. *NeuroImage*, *55*(4), 1548–1565. https://doi.org/10.1016/j.neuroimage.2011.01.055

Volpe, U., Mucci, A., Bucci, P., Merlotti, E., Galderisi, S., & Maj, M. (2007). The cortical generators of P3a and P3b: A LORETA study. *Brain Research Bulletin*, *73*(4–6), 220–230. https://doi.org/10.1016/j.brainresbull.2007.03.003

von Stein, A., Chiang, C., & König, P. (2000). Top-down processing mediated by interareal synchronization. *Proceedings of the National Academy of Sciences of the United States of America*, *97*(26), 14748–14753.

von Stein, A., & Sarnthein, J. (2000). Different frequencies for different scales of cortical integration: From local gamma to long range alpha/theta synchronization. *International Journal of Psychophysiology*, *38*(3), 301–313. https://doi.org/10.1016/S0167-8760(00)00172-0

Wang, X.-J. (2010). Neurophysiological and computational principles of cortical rhythms in cognition. *Physiological Reviews*, *90*(3), 1195–1268. https://doi.org/10.1152/physrev.00035.2008

Ward, J. (2015). *The Student's Guide to Cognitive Neuroscience*. https://www.routledge.com/go/students-guide-to-cognitive-neuroscience

Weiskrantz, L. (1996). Blindsight revisited. *Current Opinion in Neurobiology*, *6*(2), 215–220. https://doi.org/10.1016/S0959-4388(96)80075-4

Weisz, N., Lüchinger, C., Thut, G., & Müller, N. (2014). Effects of individual alpha rTMS applied to the auditory cortex and its implications for the treatment of chronic tinnitus. *Human Brain Mapping*, *35*(1), 14–29. https://doi.org/10.1002/hbm.22152

Whittington, M. A., & Traub, R. D. (2003). Interneuron Diversity series: Inhibitory

interneurons and network oscillations in vitro. *Trends in Neurosciences*, *26*(12), 676–682. https://doi.org/10.1016/j.tins.2003.09.016

Wilson, M. A., & McNaughton, B. L. (1994). Reactivation of Hippocampal Ensemble Memories During Sleep. *Science*, *265*(5172), 676–679. https://doi.org/10.1126/science.8036517

Wolinski, N., Cooper, N. R., Sauseng, P., & Romei, V. (2018). The speed of parietal theta frequency drives visuospatial working memory capacity. *PLoS Biology*, *16*(3), e2005348. https://doi.org/10.1371/journal.pbio.2005348

Worden, M. S., Foxe, J. J., Wang, N., & Simpson, G. V. (2000). Anticipatory biasing of visuospatial attention indexed by retinotopically specific alpha-band electroencephalography increases over occipital cortex. *The Journal of Neuroscience: The Official Journal of the Society for Neuroscience*, *20*(6), RC63.

Wutz, A., Melcher, D., & Samaha, J. (2018). Frequency modulation of neural oscillations according to visual task demands. *Proceedings of the National Academy of Sciences*, *115*(6), 1346–1351. https://doi.org/10.1073/pnas.1713318115

Yeung, N., & Summerfield, C. (2012). Metacognition in human decision-making: Confidence and error monitoring. *Philosophical Transactions of the Royal Society B: Biological Sciences*, *367*, 1310–1321. https://doi.org/10.1098/rstb.2011.0416

Zaehle, T., Fründ, I., Schadow, J., Thärig, S., Schoenfeld, M., & Herrmann, C. (2009). Inter- and intra-individual covariations of hemodynamic and oscillatory gamma responses in the human cortex. *Frontiers in Human Neuroscience*, *3*. https://www.frontiersin.org/articles/10.3389/neuro.09.008.2009

Zazio, A., Ruhnau, P., Weisz, N., & Wutz, A. (2022). Pre-stimulus alpha-band power and phase fluctuations originate from different neural sources and exert distinct impact on stimulus-evoked responses. *European Journal of Neuroscience*, *55*(11–12),

3178–3190. https://doi.org/10.1111/ejn.15138

Zeki, S. (1993). *A vision of the brain* (pp. xi, 366). Blackwell Scientific Publications.

Zoefel, B., & VanRullen, R. (2017). Oscillatory Mechanisms of Stimulus Processing and Selection in the Visual and Auditory Systems: State-of-the-Art, Speculations and Suggestions. *Frontiers in Neuroscience*, *11*, 296. https://doi.org/10.3389/fnins.2017.00296